UNIVERSITY OF BIRMINGHAM

Processing Optimisation, Conductivity Enhancement & Adhesion Improvement of PEDOT:PSS Films

By

Joseph Lewis Carter

A thesis submitted to the University of Birmingham for the degree of DOCTOR OF PHILOSOPHY

School of Metallurgy and Materials

Collage of Engineering and Physical Sciences

University of Birmingham

March 2022

Abstract

The use of aqueous poly(3,4-ethylene dioxythiophene):poly(styrene sulfonate) (PEDOT:PSS) as a replacement for indium tin oxide (ITO) in optoelectronic devices has gathered a large degree of interest in the last 40 years. This is due to reduced costs, improved mechanical flexibility and solution processibility (e.g., roll-2-roll, ink jet printing) of PEDOT:PSS. However, pristine PEDOT:PSS conductivity is approximately 1 Scm^{-1}, which is considerably lower than that of ITO (4500 Scm^{-1}). Current conductivity enhancing methods mainly employ volatile and harmful substances, such as concentrated acids (e.g., H_2SO_4). Additionally, the adhesion of PEDOT:PSS to polymeric substrates commonly used in flexible optoelectronic devices or during bulk manufacturing processes is weak and, therefore, needs to be addressed.

The aim of this study is to increase the conductivity of PEDOT:PSS with the addition of the environmentally safe, non-ionic surfactant Tween 80. Processing and surfactant concentration were optimised to provide the best conductivity, while solution properties were analysed to indicate the suitability of this system in common bulk processing methods. Other conductivity enhancement methods were also explored, such as multiple layer application, methyl ethyl ketone (MEK) addition, and solvent washing. Mechanisms of conductivity enhancement were assessed using atomic force microscopy (AFM), x-ray diffraction (XRD) and Raman spectroscopy. Finally, investigation was carried out into the use of polydopamine (PDA) as a primer layer for PEDOT:PSS adhesion improvement on polymeric substrates.

The lowest sheet resistivity obtained in this study was 16.75 $\Omega\square^{-1}$ for a 5 layered pristine PEDOT:PSS sample, whereas the greatest conductivity was achieved by washing pristine PEDOT:PSS with methanol (74.4 Scm^{-1}). However, both methods were deemed impractical approaches to improving conductivity on a bulk manufacturing scale. Therefore, Tween 80 was found to be promising alternative to enhance the electrical properties of PEDOT:PSS. At a concentration of 1 wt% Tween 80, sheet resistivity improved from approximately 1000 to 130 $\Omega\square^{-1}$, corresponding to a conductivity increase from 3 to 20 Scm^{-1}. The greatest conductivity achieved due to surfactant addition was 26.8 Scm^{-1} at 1.40 wt%, however, film quality began to deteriorate at this concentration. It was established, via AFM, that phase separation of the PEDOT and PSS regions occurred when Tween 80 was added, and alignment was detected with XRD. Conductivity enhancement was attributed to both of these mechanisms, and it was suspected that a benzoid to quinoid structural change within PEDOT was occurring, although this was not detected by the Raman analysis in this study.

Solution properties of PEDOT:PSS were also improved when using Tween 80 as an additive. Wettability on polypropene (PP) and poly(ethylene terephthalate) (PET) was shown to increase with greater surfactant concentrations. This led to a corresponding improvement in adhesion and film quality on both substrates. Finally, the use of a PDA primer was also shown to have a positive effect on wettability and adhesion. This was shown to be the case across all substrates for PEDOT:PSS/Tween 80 films. Adhesion improvement was greatest for pristine PEDOT:PSS films, however, there is scope to further expand on the work presented in this study.

This thesis is dedicated to my Dad, Nelson Paul Carter, who always encouraged and inspired me to pursue my dreams and believe in myself.

"Take life one cup of coffee at a time"

Acknowledgments

I would like to express my deepest appreciation to all who have supported me throughout my PhD. I am extremely grateful to my supervisors, Dr Mike Jenkins, Dr Catherine Kelly, and Dr Stephen Kukureka, for their invaluable guidance, patience, and support. I wish to extend my appreciation to Mr Frank Biddlestone for his excellent technical assistance and ability to solve any practical problem I approached him with. Thanks should also go to the EPSRC and UKRI (Grant number: EP/N509590/1) for providing the funding needed to make this project possible.

Acknowledgements for specific contributions go to: Dr Jean Marshall (Warwick Manufacturing Group) for her knowledge and expertise in performing XRD and Raman analysis; Mrs Vicki Hammond for her work on drop cast PEDOT:PSS/Tween 80 films; Dr Naomi Bennett-Steele for her contribution regarding PDA and PEDOT:PSS adhesion; and Mr Marc Bruggeman for his knowledge and assistance in collecting AFM images.

I cannot begin to express my gratitude for the unwavering belief in my abilities shown by my family. In particular, I am extremely thankful for the support of my Mom, whose confidence in me has never wavered and without whom I would not have achieved so much. I also have to thank my partner, Ellie, for her endless encouragement and reassurance, especially during the long evenings as I finished my write up.

A final thanks goes to my friends who have been there throughout it all (despite my complaining) and have never failed to make me laugh when I have needed it. A shout out goes to the original 1B20 crowd for creating an amazing office environment and making the first two years of my PhD so enjoyable. Our regular trips to Starbucks, lunches at The Plough and Friday club will certainly be missed.

Table of Contents

List of Figures

List of Tables

List of Abbreviations

AFM	- Atomic force microscopy
BF_4^-	- Tetrafluoroborate
CS	- Sulphated cellulose
DBSA	- 4-dodecylbenzenesulfonic acid
DDAPS	- Ndodecyl-N,N-dimethyl-3-ammonio-1-propanesulfonate
DEG	- Diethylene glycol
DETA	- Dielectric thermal analysis
DMF	- Dimethylformamide
DMSO	- Dimethylsulfoxide
DOPA	- 2,4-dihydroxyphenylalanine
DSC	- Differential scanning calorimetry
DTG	- Derivative thermogravimetry
EDOT	- Ethylenedioxythiophene
EDS	- Energy dispersive x-ray spectroscopy
E_g	- Bandgap
EG	- Ethylene glycol
EGBE	- Ethylene glycol butyl ether
FDSC	- Flash differential scanning calorimetry
FTIR	- Fourier transform infrared spectroscopy
GLY	- Glycerol
GO	- Graphene oxide
HOMO	- Highest occupied molecular orbital
ICP	- Intrinsically conducting polymer
IJP	- Inkjet printing
ITO	- Indium tin oxide
LCD	- Liquid crystal display
LUMO	- Lowest unoccupied molecular orbital
MEK	- Methyl ethyl ketone
Mw	- Molecular weight
NMP	- N-mythyl-2-pyrrolidone / N-mehtylpyrrolidone
OLED	- Organic light emitting diode
PANi	- Polyaniline
PDA	- Polydopamine
PE	- Polyethylene
PEDOT	- Poly(3,4-ethylene dioxythiophene)
PEG	- Poly(ethylene glycol)
PET	- Poly(ethylene terephthalate)
PF_6^-	- Hexafluorophosphate
PP	- Polypropylene
PPy	- Polypyrrole

PSS	- Poly(styrene sulfonate)
PTFE	- Polytetrafluoroethylene
PTh	- Polythiophene
Ra	- Roughness average
R2R	- Roll-to-roll
SDBA	- Sodium dodecyl benzenesulfonic acid
SDBS	- Sodium dodecylbenzene sulfonate
SDS	- Sodium dodecyl sulphate
SEM	- Scanning electron microscopy
Si	- Silicon
SSA	- Salicylsulfonic acid
T_c	- Crystallisation temperature
TDE	- 2,2'-thiodiethanol
TEM	- Tunnelling electron microscope
TFMS	- Trifluoromethanesulfonic acid
T_g	- Glass – liquid transition temperature
TGA	- Thermal gravimetric analysis
T_m	- Melting temperature
Tos	- Tosylate
Tris	- Tris(hydroxymethyl)aminomethane
Tween 80	- Polysorbate 80
VPP	- Vapor phase polymerisation
XPS	- X-ray photoelectron spectroscopy
XRD	- X-ray diffraction

Chapter 1: Introduction and Literature Review

This chapter provides a background into the field of conductivity within polymeric materials, focusing primarily on intrinsically conducting polymers (ICPs), their development, mechanisms of conductivity, applications and issues associated with their use. Some of the key conducting polymers will be highlighted with the main focus being on poly(3,4-ethylene dioxythiophene) (PEDOT) and poly(3,4-ethylene dioxythiophene):poly(styrene sulfonate) (PEDOT:PSS). The literature exploring the structure, properties, benefits, and limitations of PEDOT:PSS will be reviewed. This will include discussions about the effect of moisture in the material, comparison to indium tin oxide (ITO), its suitability in bulk manufacturing, solution properties and thermal characteristics of the dried material. An evaluation of factors that effect PEDOT:PSS conductivity and current conductivity enhancing methods, focusing on conductivity enhancing agents, is presented. The agents used in this study and their previous use with PEDOT:PSS is also summarized. The issues surrounding PEDOT:PSS adhesion to polymeric substrates is considered and the use of polydopamine (PDA) as a surface modification layer to address this issue is investigated. Finally, the scope of this project is outlined.

1.1 Intrinsically Conducting Polymers (ICPs)

1.1.1 Brief History

ICPs have been a source of great interest in the last 40 years, especially within the field of optoelectronics. Polymer conductivity in a broader sense has been said to be traceable as far back as the 1860's when the effect of electricity on aniline dissolved in dilute H_2SO_4 was investigated.[1] The more relevant and crucial discovery occurred in 1977 when halogen doped polyacetylene was found to be conductive.[2-4] Despite the films being considered unsuitable in

any application due to long term instability,[2,5] this discovery breached the field of ICPs. Since then, there have been studies into the use of alternative conjugated polymers such as polyanilines (PANi), polypyrroles (PPy) and polyphenylenes all of which have varying levels of conductivity, stability, and optical properties.[4-9] Shortly after the discovery by Chiang, *et al.* (1977)[2], it was found that polythiophenes (PTh) could be made to conduct when oxidised.[10,11] This lead to research into various PTh derivatives[6] eventually leading to the discovery of PEDOT in 1988 by Bayer AG.[5,6] PEDOT is generally considered to have superior conductivity, long term stability and enhanced optical properties over other ICPs (section 1.2).[5,6,12-16] However, it is difficult to polymerise and insoluble in most solvents which limits applications (section 1.2).[5,6,15,17,18] A solution to this was discovered in 1990 when PEDOT was polymerised with the counterion poly(styrene sulfonate) (PSS) to give PEDOT:PSS, which is water soluble, improving processability (section 1.2.1).[5,6,15,17-19] One of the main reasons PEDOT:PSS, and other ICPs, have gathered considerable interest is due to its potential to replace ITO in optoelectronic devices such as organic light emitting diodes (OLEDs), liquid crystal displays (LCDs) and flexible electronic displays (section 1.3.3).[5-7,9,15,20-27]

1.1.2 Conductivity Mechanisms of ICPs

ICPs act as semi-conductors and are sometimes describes as 'semi-metallic'.[4,5,28] The conductivity of conjugated polymers can be as low as 10^{-8} Scm^{-1}, boarding on electronic insulators, and reach as high as 10^{4} Scm^{-1}, which is in the region of metallic conductivity.[4,5] However, they exhibit an increase in conductivity when temperature increases, which defines ICPs as semi-conductors, since the opposite is true of metallic conductivity.[5] It is also the case that these semi-conductors would not show any measurable conductivity at absolute zero.[5,29]

The mechanisms by which ICPs can conduct are electron hopping and π – π (pi – pi) stacking.[4,18,30-32] Electron hopping involves the movement of either an extra free electron or a hole (lack of electron) along the polymer chain.[4,18,33] However, both of these rely on a chemical structure which can facilitate this movement, such as a conjugated double bond system, enabling the delocalisation of electrons and their movement along the polymer chain (Figure 1-1).[4,5,18] Alternatively, π – π stacking occurs through alignment of the benzene rings within the chains.[34-37] When aligned, the benzene rings will share electrons,[17,18,37,38] creating a 'sea' of delocalised electrons and an easy pathway for electron flow.[17,18,33] Therefore, greater chain alignment within the polymer leads to better π – π stacking and subsequent conductivity improvement.[18,28,39]

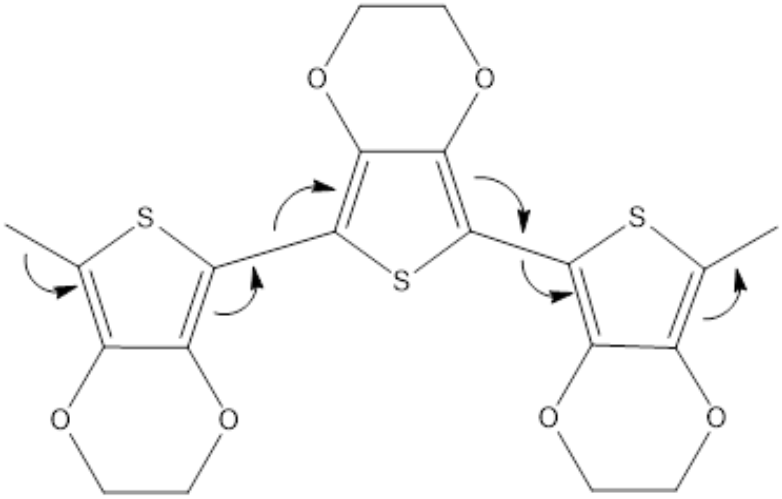

Figure 1-1: Diagram illustrating the mechanism of electron hopping within PEDOT. Arrows indicate the movement of electrons along the conjugated chain structure

The degree of conductivity these materials exhibit is determined by the bandgap (E_g) which establishes the energy required to move an electron from the valance to the conductive band.[18,29,40] These bands are bordered by the highest occupied molecular orbital (HOMO) and

lowest unoccupied molecular orbital (LUMO), respectively.[5,18,28,29] Therefore, it is often considered that the E_g is defined by the HOMO/LUMO energy gap.[28,29,40] Intrinsic semi-conductors (e.g., silicon) are defined by having a filled valence band and empty conduction band, normally with a E_g of less than 2 eV, when in a pure state.[29]

Conductivity of these materials can be improved by doping, making the material an extrinsic semi-conductor.[18,29,41] Doping is the addition of an impurity that alters the overall charge of the material.[29,42] To illustrate this, silicon (Si) in a pure state is considered an intrinsic semi-conductor with no charge.[29] Si atoms have four electrons and are covalently bonded with four other Si atoms.[29] If an impurity with a valency of 5 was substituted for one Si atom, there would now be an extra electron not covalently bonded with another atom.[29] This renders silicon an n-type extrinsic semi-conductor with an overall negative charge due to the extra electron.[29,42] When a current is then applied, this electron moves more freely, improving conductivity. The opposite is true if an atom was introduced with a valency of 3. In this case, a hole (or lack of electron) is produced causing the overall charge to be positive, making the material a p-type extrinsic semi-conductor.[29,42] This hole can then be filled by adjacent electrons when a current is applied, leaving another free hole. Effectively, the hole moves through the material increasing conductivity.[18] In both cases, there is a reduction in E_g between the HOMO and LUMO making it easier for electrons to transfer from the valence band to the conductive band, improving conductivity.[18,28,30,43,44] As with silicon, ICPs can be doped to improve their conductivity (sections 1.2.1 & 1.5.2).

1.2 Poly (3,4-ethylene dioxythiophene) (PEDOT) Structure and Properties

PEDOT (Figure 1-2) is a conjugated polymer where the backbone consists of alternating single and double bonds.[4,5,18,33,45] The position of the double bond, or π-bond, in the structure is thought to be able to dynamically interchange between two positions, which is a contributing element of the conductivity of this material.[8,17,40] These bond positions create two structural configurations known as benzoid (Figure 1-3a) and quinoid (Figure 1-3b).[13,18,46] Despite some suggestions to the contrary,[46] it is generally considered that PEDOT alone is in a benzoid configuration, in which the carbon-carbon bond between thiophene rings is a single bond.[5,6,15,18,43] This is due to it being the more stable, lower energy configuration and represents the HOMO state.[18,35,46] Conversely, un-altered PEDOT in a quinoidal configuration (Figure 1-3a) is considered to be the higher energy LUMO state making it unstable.[18,46] The conductivity of pure PEDOT is normally between 200 – 550 Scm^{-1} depending on the polymerisation route.[6,12-14] Due to the regularity of the chain structure, π – π stacking of the aromatic rings can readily occur[17,37] creating a 'sea' of electrons through which charge can be carried.[37] When the polymer is more ordered through differing polymerisation mechanisms, there will be more of these aligned regions which can lead to higher conductivity.[5,47,48]

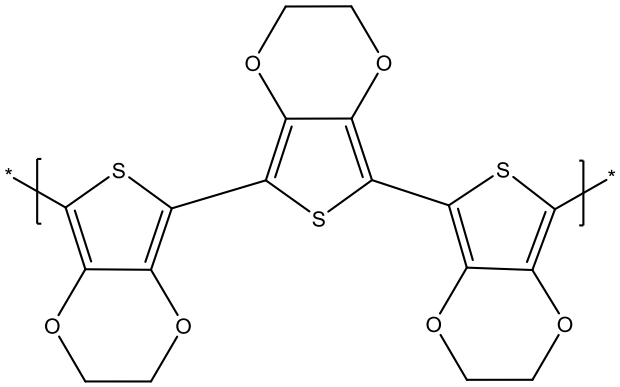

Figure 1-2: Chemical structure of PEDOT. Replicated from Groenendaal, et al. (2000)[6]

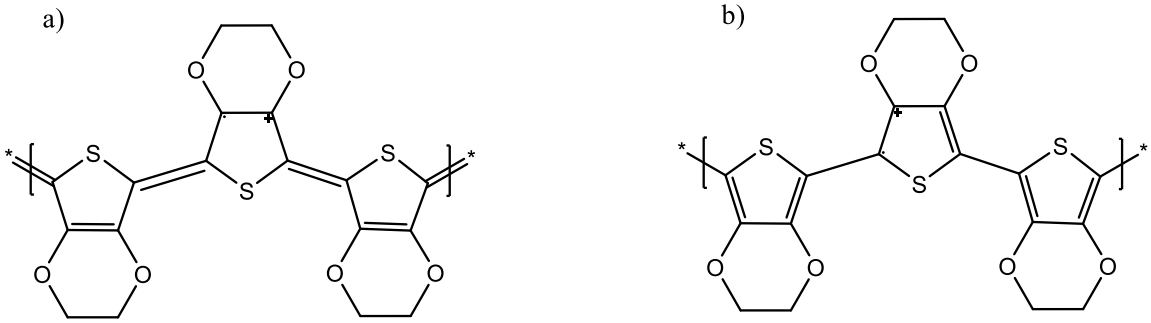

Figure 1-3: Two PEDOT form structures a) quinoid and b) benzoid. Replicated from Ouyang (2013)[13]

Despite there being many other ICPs, such as PPy, PANi and PTh,[4,7-9] PEDOT is considered to be superior for a number of reasons, the first being the relatively high conductivity of the material. When compared to the 5 – 30 Scm^{-1} shown by PANi[5,49] or 0.01 – 8 Scm^{-1} of PPy,[5,50,51] PEDOT conductivity is significantly greater. This is mainly attributed to PEDOT having a smaller E_g between the HOMO and LUMO (section 1.1.2).[6,9,15,18,43] For comparison, the E_g of PEDOT is approximately 1.6 eV,[6,15] whereas PTh has a bandgap of 2.3 eV.[15] PEDOT is also considered to be superior with regards to stability, transparency, optical/electrical properties, and biocompatibility.[5,6,15,16]

However, despite these superiorities, PEDOT has some major drawbacks. The main issue is processibility limitation due to it being insoluble in most solvents.[5,6,15] Additionally, polymerisation of PEDOT is usually oxidative chemical or electrochemical producing either a PEDOT powder or requiring direct application to a substrate, respectively.[5,15,17,18] Vapor phase polymerisation (VPP) has also been used to polymerise PEDOT, resulting in higher conductivities of around 1000 Scm^{-1}.[5,13,52] However, this higher conductivity was largely achieved due to PEDOT becoming doped with Tosylate (Tos) (section 1.2.1) during VPP.[52] The main issue with all of these methods is that they are very restrictive in regard to their ability to be scaled up to a bulk manufacturing process. Furthermore, despite suggestions of a glass – liquid transition temperature (T_g) of 102 °C, PEDOT does not melt[53] and there have been no reports of PEDOT being used in classic thermal processing methods. Finally, without the use of alteration or doping (section 1.2.1) the upper conductivity of PEDOT is limited, even with the advancement in VPP, it does not compare with the 4500 Scm^{-1} obtained by ITO.[8]

1.2.1 PEDOT and Counterions

To overcome processing and conductivity limitations, the PEDOT monomer (EDOT) is often polymerised with a counterion. This can be done during both chemical and electrochemical polymerisation and a summary of the main counterions has been reported by Elschner, *et al.* (2011)[5]. One counterion that has already been mentioned is Tos which was used during the VPP of PEDOT.[52] However, most counterions can be used during chemical polymerisation of EDOT to produce PEDOT:counterion combinations, often with a lower conductivity than achieved with VPP. Examples include Tos,[5,12,28] sulphated cellulose (CS),[54] hexafluorophosphate (PF_6^-),[5,55] and tetrafluoroborate (BF_4^-)[5,55] which yield conductivities of 450, 576, 200 and 50 Scm^{-1}, respectively.

The main use of counterions is to dope the polymer, which improves the conductivity potential.[5,18,28,40] The term ‘doped’, or ‘doping’ normally refers to the introduction of an impurity into a semiconducting material, altering the overall charge and improving conductivity (section 1.1.2).[29,42] However, counterions do not necessarily dope PEDOT in the traditional sense.[5] Rather, the oxidative reaction during polymerisation allows ionic bonding of the counterion with an electron deficient site in PEDOT.[4,5,18] This bond could then be considered to maintain the doped state of PEDOT.[5,17,18,40] To keep consistent with the literature, the term ‘doped’ will continue to be used with regard to the use of counterions.

Despite conductivity improvements, the counterions previously mentioned still have issues with regards to the processability of the polymer. However, in 1990 poly(styrene sulfonic) acid (PPS(H)) (Figure 1-4a) was used as a counterion in the polymerisation of EDOT to give poly(3,4-ethylene dioxythiophene):poly (styrene sulfonate), or PEDOT:PSS (section 1.3).[5,19] Studies have also shown that polymerising EDOT with the salt form of PSS (PSS(Na)) (Figure 1-4b) also produces PEDOT:PSS with good conductivity (section 1.5.1.1).[12,56,57]

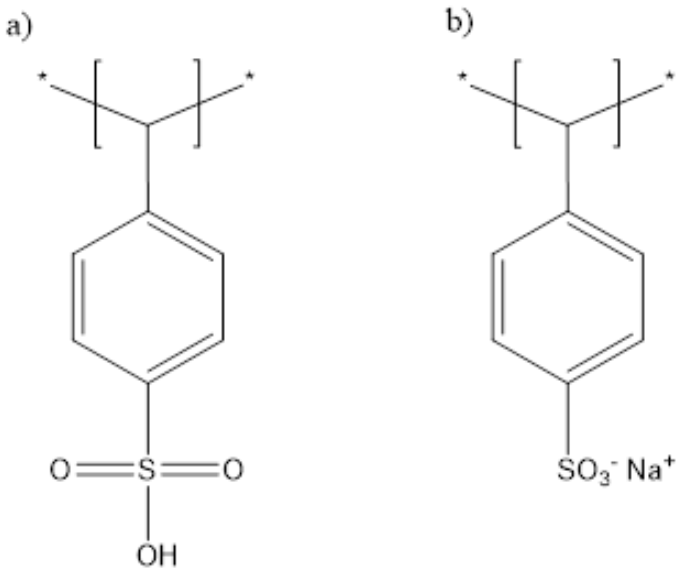

Figure 1-4: Chemical structure of PSS showing both a) acid form (PSS(H)), replicated from Groenendaal, et al. (2000)[6], and b) salt form (PSS(Na)), replicated from Yılmaztürk, et al. (2009)[56]

The greatest advantage of PSS is it allows PEDOT:PSS to be water soluble whilst providing high conductivity potentials and acceptable optical properties for use in optoelectric devices.[5,6,15,17,18] Furthermore, since PEDOT:PSS comes in aqueous solution, it can be used in many bulk processing techniques such as spray coating, inkjet printing (IJP) and roll-to-roll (R2R) manufacturing (section 1.3.4).[15,17,41] However, when polymerised there is often an excess of PSS and, due to it being an insulator,[17] the conductivity of pristine[a] PEDOT:PSS is relatively low at 0.001 – 120 Scm^{-1} (Table 1-1), which varies depending on polymerisation route (section 1.5.1.1).[12,13,22,58-60] Despite this, the conductivity can be dramatically improved by using conductivity enhancement methods (section 1.5).

[a] The use of 'pristine' is a term consistent with the literature to indicate that the PEDOT:PSS has undergone no treatments, either to the solution or film, to enhance properties of the material.

Table 1-1: Example conductivity values of various material. Note, these values do not take into consideration variation of processing route, measurement techniques, or other factors that contribute to conductivity differences

Material	Approximate Conductivity (Scm^{-1})	
Polystyrene	6.7×10^{-14}	[61]
PEDOT	200 – 550	[6,12-14]
Pristine PEDOT:PSS	0.001 – 120	[12,22,58,60,62]
PEDOT:Tos	400 – 500	[12,28]
PEDOT:PSS with H_2SO_4 post treatment	4200	[58]
ITO	3000 – 4500	[8,20]
Copper	580000	[63]

1.3 Poly(3,4-ethylene dioxythiophene):Poly(styrene sulfonate) (PEDOT:PSS)

1.3.1 PEDOT:PSS Structure

PEDOT:PSS can be synthesised using a variety of techniques.[5,6,17] The most common process is to polymerise EDOT in an aqueous polyelectrolyte solution of PSS(H) with the use of an oxidising agent.[5,6] The most successful oxidising agents, developed by Bayer AG, are peroxodisulfates, such as sodium peroxodisulfate ($Na_2S_2O_8$).[5,6,19] The use of an oxidising agent removes electrons from PEDOT and, therefore, PEDOT:PSS it is considered a p-type semi-conductor.[5,6,29] This results in PSS ionically bonding to either the benzoid (Figure 1-5) or quinoid (Figure 1-6) forms of PEDOT.[6,64] Due to the removal of electrons in the oxidative reaction, the quinoidal form of PEDOT becomes the more stable, lower energy state, which is further stabilised by PSS (Figure 1-6).[18,40,44,64] It is also well established that the ionic interaction only occurs every three to four thiophene rings.[5,12,32]

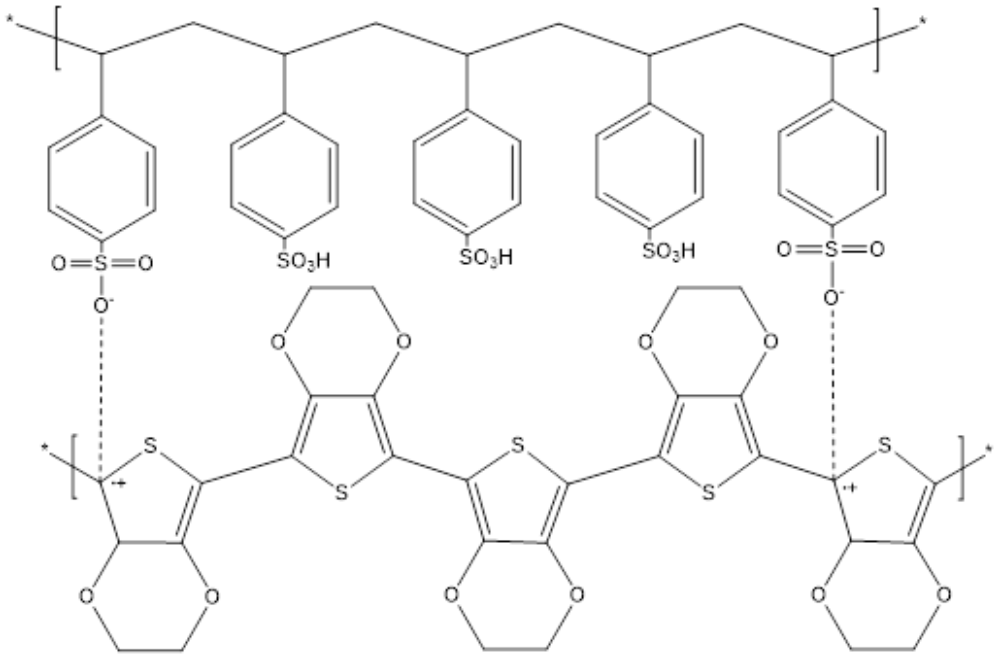

Figure 1-5: Ionic bonding of benzoid PEDOT and PSS. Replicated from Groenendaal, et al. (2000)[6]

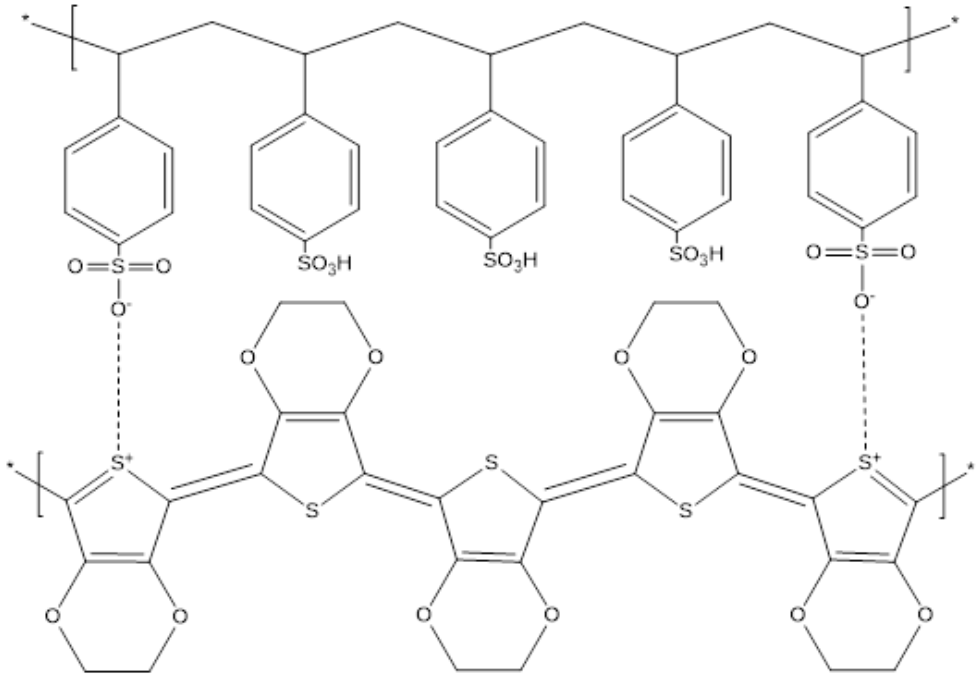

Figure 1-6: Ionic bonding of quinoidal PEDOT and PSS. Replicated from Dimitriev, et al. (2011)[64]

The secondary PEDOT:PSS structure shows multiple 5-mer to 18-mer PEDOT oligomers bonded to a longer PSS chain (Figure 1-7).[22,27,40,64] Due to repulsive forces between the PSS chains and the interaction of the PEDOT oligomers, a partially coiled or helical PEDOT:PSS structure is formed, despite the more linear quinoid PEDOT configuration.[40] This is because the longer PSS chains dominate the overall PEDOT:PSS structure.[28,40,55,65-67]

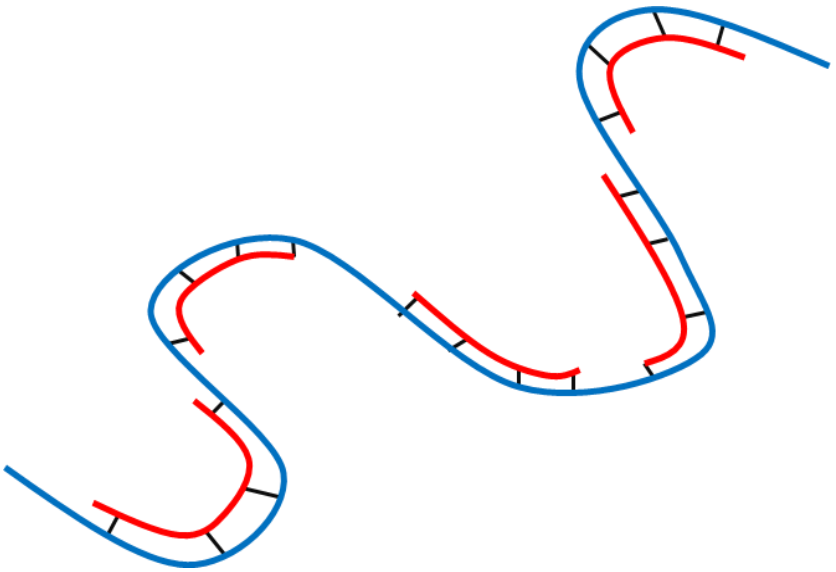

Figure 1-7: PEDOT:PSS structure showing PEDOT oligomers (red) ionically bonded to PSS backbone (blue). Image reproduced from Mengistie, et al. (2013)[22]

In solution, PEDOT:PSS chains aggregate together to form particles that, due to the hydrophobic and hydrophilic nature of PEDOT and PSS respectively, consist of a PEDOT-rich core and PSS-rich shell (Figure 1-8).[18,64,68] The particles are considered to be a gel and are composed of approximately 90 – 95% water.[5,21,27,69] Furthermore, tunnelling electron microscopy (TEM) and scanning electron microscopy (SEM) analyses have shown them to be rectangular or triangular in shape, rather than spherical, and fall into distinct size ranges after sonication: 25 – 80 nm and 350 – 460 nm.[40,70-72] These PEDOT:PSS gel particles are suspended

in a PSS-rich water medium caused by the excess PSS present during the polymerisation process.[27,40,70] Although bonding to PSS causes a reduction in the E_g of PEDOT, the excess PSS creates an insulating effect and a large decrease in the conductivity. This is exacerbated by the excess PSS between the PEDOT:PSS particles since it increases the hopping distance[b] between PEDOT-rich phases.[21,31,67]

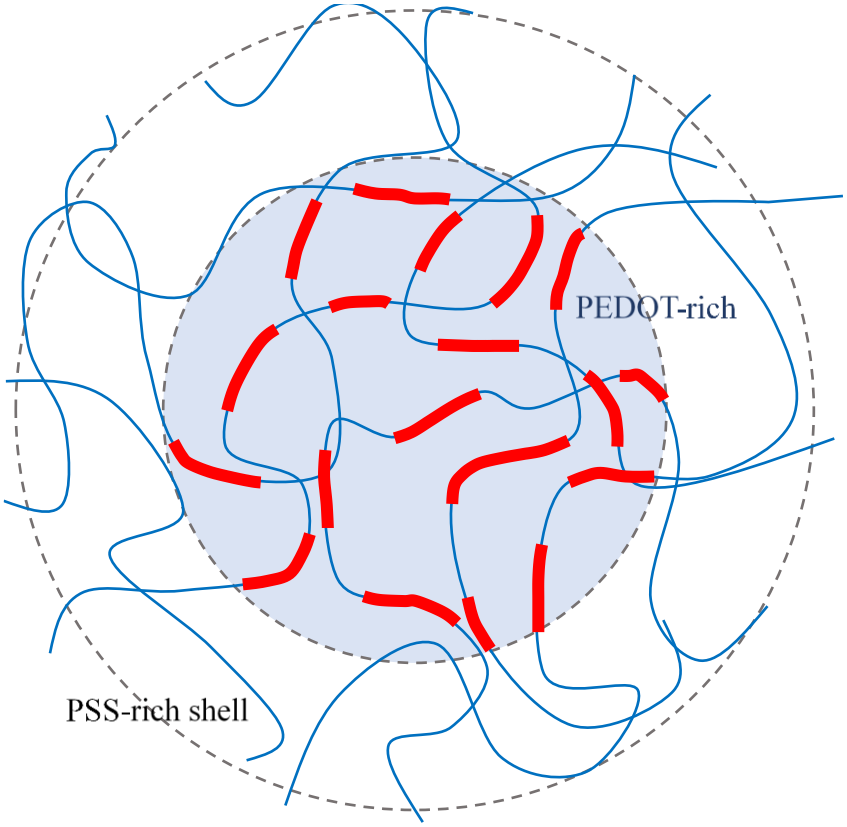

Figure 1-8: In solution PEDOT:PSS particle structure showing PEDOT-rich core (inner blue shaded circle) and PSS-rich shell (outer circle). Long, thin lines (blue) represent PSS backbone chains while short, thick sections (red) represent the PEDOT oligomers attach to the PSS chains. Replicated from Kroon, et al. (2016)[18]

[b] Hopping distance reference to the distance electrons have to move between conductive regions. In this case, that will be the distance between PEDOT-rich sites or PEDOT chains.

In a dry state, pristine PEDOT:PSS is considered to be amorphous with only some short range ordering.[28,55,65-67] This has been confirmed with SEM,[67] thermal analysis (section 1.4.2.1)[69,71] and x-ray diffraction (XRD).[58,65,67,73] XRD directly assesses the degree of alignment and orientation of polymer chains i.e., the polymer crystallinity.[29,73-75] Pristine PEDOT:PSS displays no sharp peaks, indicative of order, in the diffraction pattern.[58,65,67,73] Instead, only broad peaks around 4, 7, 18 and 26 ° have been reported which were attributed to the amorphous nature of the material.[36,54,58,66,76-78] However, the ratio of PEDOT to PSS has been reported to alter the diffraction pattern with an increase in PSS marginally increasing the measured alignment.[79] This would suggest that the chain order is being dominated by PSS, which is expected due to the greater ratio of PSS to PEDOT.[79] Other counterions have also been shown to alter the crystallinity of the dry film in varying ways. For example, when doped with PF_6^-, the films were reported to be amorphous by XRD.[55] However, Tos doped PEDOT displayed regions of crystallinity with sharp peaks at 6, 12 and 26 °.[80] The peak at 26 ° is common when doping with either PSS and Tos since it represents the stacking of PEDOT rings.[58] However, the variation in the other peaks shows that the counterion is the dominating factor to the alignment.

1.3.2 PEDOT:PSS and Water

The hydrophilic nature of PSS, due to the presence of hydroxyl (OH^-) groups on the sulfonate moiety,[71,76] results in moisture from the atmosphere readily being absorbed by PEDOT:PSS films following drying.[5,22,71,81,82] This moisture uptake has been studied utilising mass measurements, differential scanning calorimetry (DSC) and thermal gravimetric analysis (TGA) (section 1.4.2.1).[5,39,69,71,76,83-85] It has been shown that when left in air at 24 °C with a relative humidity of 70 %, oven dried PEDOT:PSS will exhibit a 10 % mass increase in 3 minutes due to moisture uptake.[5] It is generally considered that approximately 10 – 25 % of

PEDOT:PSS film mass is bound water[5,39,69,71,76,83,84] dependant on sample geometry, atmospheric conditions[86] and PSS content.[5,86-88] The variation in chemical treatment (section 1.5.2) can also alter moisture uptake.[5,22] For example, the addition of poly(ethylene glycol) (PEG) increases absorption of the film due to it also having an affinity to water.[22] On the other hand, PEDOT:PSS with the addition of sorbitol absorbs less moisture.[84]

This affinity to water has subsequent effects on the materials properties. For example, it has been shown that PEDOT:PSS films exposed to higher humidity environments are less brittle due to the increase in the moisture content of the film.[5,68,71] This was attributed to water swelling the PSS phase, and weakening the hydrogen bonds[68,71] allowing the chains to more easily slide past each other upon loading.[71] The presence of moisture can also exacerbate PEDOT:PSS degradation.[82] Changes in water content in PEDOT:PSS films have been shown alter film thickness,[5,60,69,89] with around a 10 – 20 % thickness reduction after drying being reported.[60,69] The other key property influenced by moisture content is conductivity, with an increase in water content reducing the conductivity of PEDOT:PSS.[22,69,71,78,82,88,90] This is potentially due to two reasons. Firstly, water has a lower conductivity than dry PEDOT:PSS therefore any moisture in the film will negatively impact the conductivity.[71,91] Secondly, the PSS-rich phase swells when moisture is absorbed, creating a greater insulating barrier between PEDOT-rich phases, and leading to a greater electron hopping distance.[60,69,71,78,90]

The effect of water can be reduced by encapsulation of dried PEDOT:PSS films in an inert, moisture free environment,[5,17,82,92] however, this adds to the cost of production.[17,92] Alternatively, it has been suggested that stabilisation of PEDOT:PSS moisture content occurs after 2 – 4 months, with small degrees of chain reorganisation taking place.[93] While this negates the need for encapsulation neither option is practical for all applications and manufacturing processes.[17]

1.3.3 PEDOT:PSS Comparison to Indium Tin Oxide (ITO)

One of the main reasons PEDOT:PSS has gathered interest is due to its potential to replace ITO in optoelectronic devices.[5,6,15,20-25] PEDOT:PSS has already been used as a conductive film coating or layer for applications such as OLEDs, LCDs and flexible electronic displays, or for use as an antistatic coating.[7,9,22,26,27] The use of PEDOT:PSS in these devices has some important benefits. Firstly, indium is expensive due to decreasing availability[25,94,95] and, therefore, PEDOT:PSS provides a cheaper option.[24,25,92] Additionally, there is a reduction in production costs as PEDOT:PSS components can more easily be produced via R2R manufacturing (section 1.3.4).[24,92]

More importantly, the mechanical properties of PEDOT:PSS are greatly suited for use in flexible devices due to reduce susceptibility to mechanical fatigue compared to ITO.[9,26,96] Cairns, *et al.* (2005)[26] demonstrated this by investigating the change in electrical resistance of ITO and PEDOT:PSS coated poly(ethylene terephthalate) (PET) under tensile loading. It was found that, while an increase in strain caused resistance to increase in both cases, the PEDOT:PSS coating was able to conduct up to 60 % strain whereas no measurements could be taken after 3 % strain for ITO.[26] It is important to note that even though resistivity of PEDOT:PSS could still be measured at a 60 % strain, increased resistance was observed from as low as 4 %.[26,65] Despite this, the advantage of PEDOT:PSS and the short comings of ITO cause by the brittle nature of the ceramic are highlighted.[26]

PEDOT:PSS was also found to be superior during bend testing. The resistivity of PEDOT:PSS films on PET was shown to be unaffected by an outer (tensile) and inner (compressive) bend radius of approximately 10 mm.[65] Whilst the resistance of ITO films on the same substrate was also unaffected by compressive bending to the same radius (and in some cases showing an

decrease in resistance), there was an increase of approximately 10 – 20 % for tensile bending.[97] Furthermore, PEDOT:PSS could be tested to a radius of 5 mm in both compressive and tensile bending with only an approximate 8 % increase in resistance.[65] It was also reported that at this radius no cracks were present during the outer bend condition, however, delamination of the film occurred on the inside bend at a 7 mm radius.[65] The resistance of ITO at a tensile bend of 5 mm increased 50,000 % due to the damage caused during testing.[97]

Finally, ITO also shows a greater susceptibility to failure during cyclic bend loading, with 1000 cycles causing an 8 % increase in resistance of ITO coated PET compared to less than 2 % increase for PEDOT:PSS coated PET.[26] The durability of PEDOT:PSS during cyclic loading has been shown for inner and outer bending as well as through a twisting cycle.[65] These properties were enhanced further with additions of surfactants, such as the Triton X series, to the PEDOT:PSS solution prior to film forming.[47,98] Pristine PEDOT:PSS showed a significant decrease in conductivity at a bending strain of 2 %, compared to 11 % when Triton X-100 was present.[47] It has also been shown that addition of Triton X-405 allows for a bend radius up to 1.5 mm with minimal sheet resistivity reduction.[98] It is thought this improvement is due to a plasticising effect caused by the surfactant.[78]

However, despite the benefits, the conductivity of pristine PEDOT:PSS is currently much lower than that of ITO (Table 1-1). Even in the best processing conditions, pristine PEDOT:PSS conductivity is only 120 Scm^{-1} (section 1.5.1.1),[60] compared to 4500 Scm^{-1} for ITO.[8] However, as discussed later, this issue can be overcome with the use of conductivity enhancing methods (section 1.5).

1.3.4 Bulk Manufacturing of PEDOT:PSS

As already mentioned, PEDOT:PSS has a large advantage due to its water soluble nature, enabling processing via cost and time effective bulk manufacturing.[5,15,17,18,24,92,99] This is particularly true when considering commonly used lab techniques such as VPP or, dip, drop and spin casing which are more attuned to single batch outputs.[15,100] The use of PEDOT:PSS in bulk manufacturing processes such as R2R, IJP and other methods (E.g., slot casting, spray coating) has already been well established and reviewed in depth by Wen, *et al.* (2017)[15], Kirchmeyer, *et al.* (2007)[17] and Søndergaard, *et al.* (2012)[100].

The area of R2R processing is particularly versatile with varying techniques such as gravure, flexographic, screen printing and knife coating all of which require an 'ink' to be deposited onto a flexible substrate to create a specific pattern (Figure 1-9).[100] Arguably the greatest advantage of R2R is the high processing speeds, which can reach 15 ms^{-1} for gravure printing.[100] Although, the use of gravure printing with PEDOT:PSS solution on PET has been shown to successfully produce coherent films with desirable optical properties,[15,60,65,100] research in this area seems limited.[100]

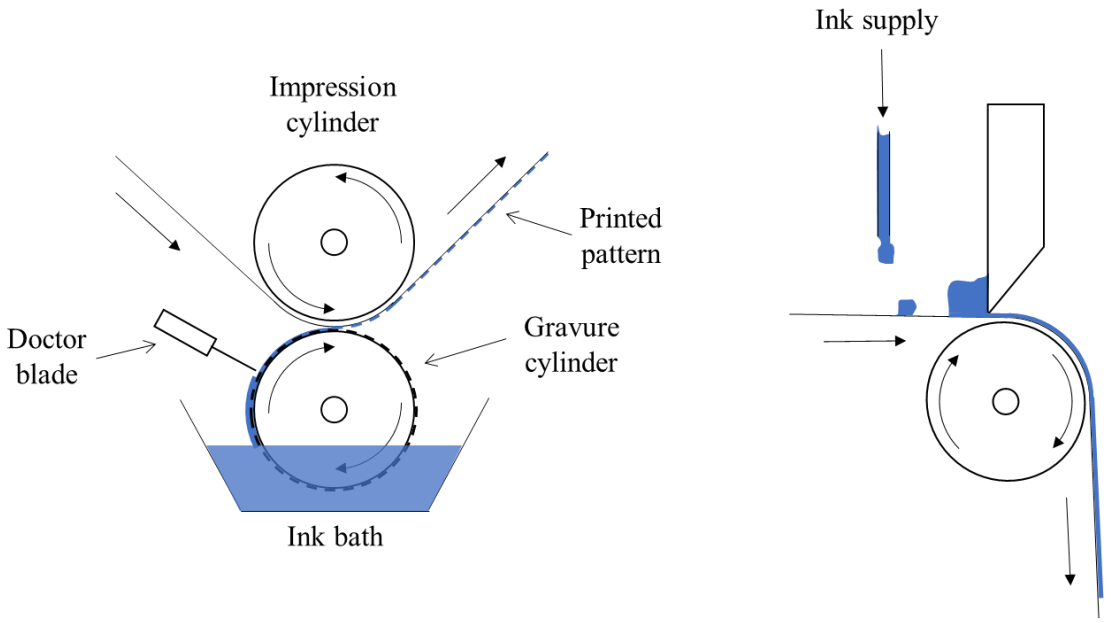

Figure 1-9: Schematic of two R2R processing examples with main components labelled. Left: gravure printing, right: knife coating. Replicated from Søndergaard, et al. (2012)[100]

Similarly with R2R, IJP is another common form of solution processing requiring an 'ink' to be loaded into cartridge and deposited in a specific pattern onto a substrate (Figure 1-10).[15,17,41,100] The use of PEDOT:PSS solution as an ink in IJP is more established and has been successfully printed onto a variety of substrates.[89,101-107] While the output of IJP may be slower than some R2R methods, the greatest advantage is the ability to produce more complex patterns that are easier to modify on non-speciality software.[100,107]

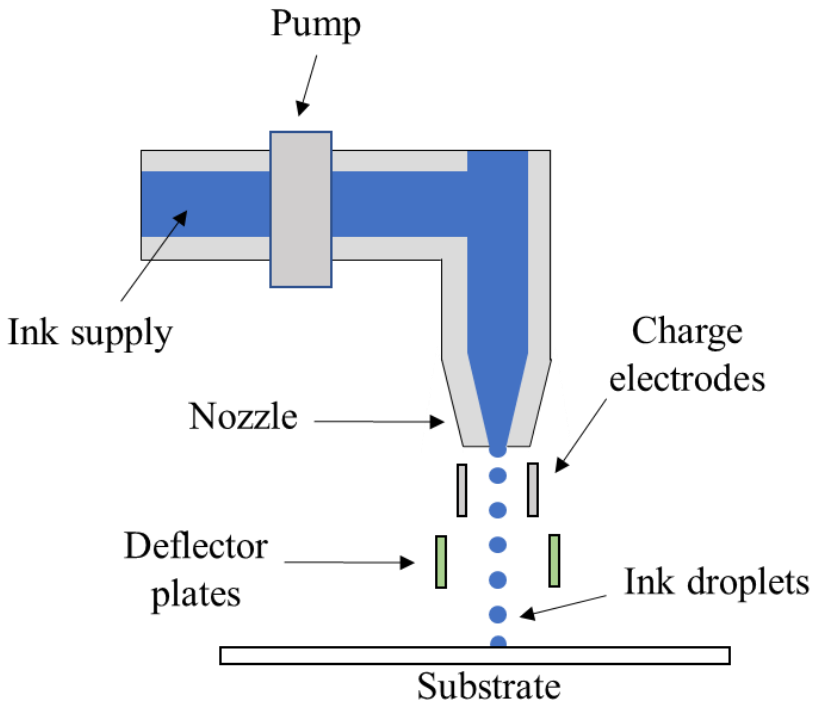

Figure 1-10: Schematic of an IJP process with main components labelled. Replicated from Wen, et al. (2017)[15]

Whilst PEDOT:PSS has been shown to be suitable for these processes, there are some factors that have to be considered. First, flexible substrates tend to be polymeric in nature and the affinity of pristine PEDOT:PSS solution to these materials is weak.[47,108] One solution is modification of the surface of the substrate, such as the use of corona treatment.[60,109] An alternative option is to treat the PEDOT:PSS solution with additives, such as surfactants, to better match the surface energies and improve wettability (section 1.4.1).[47,65,102-104,107] However, the solution properties, such as viscosity, surface tension and wettability, also need to be carefully considered and optimised for each process.[100] For example, R2R processes are more suited to lower viscosity inks.[100] In the case of, IJP pattern resolution is heavy reliant on solution viscosity and wettability.[15,17,99] Therefore, additions made not only need to aid wettability, but also need to be appropriate for the manufacturing process being used.

1.4 Characterisation of PEDOT:PSS

1.4.1 PEDOT:PSS Solutions

The properties of PEDOT:PSS solution, such as viscosity, wettability, and surface tension, are important to consider due to their effect on substrate coverage, solution flow and film quality during bulk manufacturing (section 1.3.4).[100-104,107,108] The fluid properties of pristine PEDOT:PSS solution are often described as exhibiting non-Newtonian, shear thinning behaviour, with an increase in shear rate resulting in a decrease in viscosity.[76,103,110] However, the main constituent of PEDOT:PSS solution is water[69] which has a relatively high surface tension of 72 – 73 mNm^{-1} at 20 °C.[60,103,111-113] The viscosity of water at 20 °C was quoted as 1 mPa.s when measuring via U-tube glass viscometer[112] and 1.2 mPa.s via oscillating drop testing.[103] However, the surface tension of water has been shown to skew rheology results at lower shear rates, with viscosity appearing to be double those quoted in other studies.[103,112,114] Therefore, it is likely a similar effect is occurring when measuring PEDOT:PSS solution via rheometry, which could be causing a higher viscosity at lower shear rates and showing a false shear thinning effect.

The concentration of PEDOT:PSS in solution can impact the viscosity with 0.5, 1 and 1.1 wt% PEDOT:PSS displaying viscosities of 10, 60 and 63 mPa.s, respectively at a shear rate of 1 s^{-1}.[103,110] However, Giuri, *et al.* (2017)[76] found that for the same shear rate the viscosity was 20 mPa.s with a 1.3 wt% PEDOT:PSS in solution which does not fit this trend. Even though both results were obtained with a rheometer, the variation could have come about from differences in the cone and plate geometry or PEDOT:PSS grades. In all cases, the viscosity of PEDOT:PSS solution is greater than that of water which is to be expected due to the presence of the polymer gel particles.[103,115]

Furthermore, additives have been shown to effect the rheological properties with graphene oxide (GO) nanocomposite significant increasing the viscosity of PEDOT:PSS solution.[76] Hoath, *et al.* (2015)[103] showed that, similar to GO, the combined addition of 0.23 wt% Dynol 607 and 0.27 wt% Zonyl FSO-100 surfactants increases the viscosity of PEDOT:PSS solutions. This behaviour would be expected since the viscosity of these surfactants is likely to be greater than the PEDOT:PSS solution. Additives are also effective in changing the surface tension of the PEDOT:PSS solution. The surface tension of pristine PEDOT:PSS is deemed to be comparable to water at 70 – 73 mNm^{-1},[47,103,104,110] but has been quoted as low as 44 mNm-[1].[116] This has been shown to reduce to 30, 21 and 18 mNm^{-1} for additions of 1 wt% Triton X-100, 0.23 wt% Dynol 607 and 0.27 wt% Zonyl FSO-100 combined, and 0.1 wt% Capstone.[47,103,104] Other surfactant and alcohol additions, such as 4-dodecylbenzenesulfonic acid (DBSA), Ndodecyl-N,N-dimethyl-3-ammonio-1-propanesulfonate (DDAPS), ethanol and 1-pentanol, were also studied by Kommeren, *et al.* (2018)[104] showing smaller decreases in the surface tension.

As already mentioned, the ability to control PEDOT:PSS solution properties is of importance when considering IJP and R2R manufacturing (section 1.3.4).[100-104,107,108] Reducing surface tension is especially significant since it improves wettability on polymeric materials by better matching solution and substrate surface energies, leading to superior film quality.[47,65,102-104,107] The addition of Triton X-100 has been used as a wettability enhancer in IJP.[107] Furthermore, at a 1 wt% concentration it has been shown to substantially reduce the contact angle on Teflon, poly(dimethylsiloxane) and PET substrates by 45, 45 and 50 °, respectively.[47] Similar results have been shown on PET, with additions of ethylene glycol (EG), sodium dodecyl sulphate (SDS) and sodium dodecylbenzene sulfonate (SDBS) decreasing PEDOT:PSS contact angle from 40 ° by 5, 20 and 35 °, respectively.[108] However, not all additives will improve the

wettability for all substrates. For example, the introduction of dimethylsulfoxide (DMSO) to PEDOT:PSS increased the contact angle on PET from 40 to 90 ° and the presence of SDS on glass raised measurements by 10 °.[108] It is clear that additions, such as surfactant, can change the wettability of PEDOT:PSS solution which occurs through surface energy alteration.[47,103,104,110] Therefore, it is crucial to understand whether the addition will increase or decrease solution surface tension, and match that change to the substrate surface energy in order to improve wetting properties.[47,65,102-104,107] Furthermore, the importance of matching the solution properties to the manufacturing technique has been highlighted.

1.4.2 PEDOT:PSS Films

1.4.2.1 Thermal Analysis and Degradation

DSC is commonly used to assess thermal transitions, such as melting (T_m), crystallisation (T_c) and T_g, of polymers.[29] However, in the case of PEDOT:PSS, DSC analysis is relatively limited as the first heating run is often dominated by a large exothermic peak, spanning a range of 75 – 160 °C, due to the loss of water (section 1.3.2).[5,71,76,85] Since temperatures significantly above the boiling point of water are required to fully remove it, this indicates the presence of bound moisture.[71] Furthermore, the water loss peak is not seen on subsequent runs.[71] A moisture loss of 10 – 25 % has also been reported with TGA up to 250 °C.[5,39,69,71,76,83,84] Other thermal transitions, including T_m, T_c, and T_g, are not seen for PEDOT:PSS between 25 – 220 °C,[69,71] which was not altered with the presence of solvents such as 2,2'-thiodiethanol (TDE) or glycerol (GLY).[66]

Despite indication that PEDOT can become more crystalline when heated to 200 °C,[32] XRD and SEM has shown pristine PEDOT:PSS to be amorphous, with no crystalline regions except for short range order (section 1.3.1).[28,55,65-67] The amorphous nature of the material suggests

that a T_g should be identifiable by thermal analysis, and a range could be estimated from the T_g values of PEDOT and PSS(H) at 102[53] and 152 °C,[117,118] respectively. This would indicate that PEDOT:PSS T_g would fall between 102 –152 °C, with a similar range being suggested by Yu, *et al.* (2016)[119] between 120 – 140 °C. However, it is thought that, due to strong ionic interaction between the PEDOT and the PSS, a T_g will not present itself via thermal analysis.[17,71,119] One source quotes a PEDOT:PSS T_g as 75 °C,[85] but this seems unlikely since it has not been reported elsewhere and does not fall within the expected T_g range. It is more likely that this was either caused by degradation, since samples were heated to 220 °C which is close to PEDOT:PSS degradation temperature,[69] or contamination by the PET substrate, which has a T_g of 70 °C.[29]

A second significant mass loss between 220 – 320 °C was observed by TGA and attributed to degradation.[5,69,71,83] This was shown in both air and an inert nitrogen atmosphere[71] implying that the degradation is not oxidative. However, there has been some evidence to suggest that the presence of oxygen can accelerate the this process.[87] PEDOT:PSS degradation can present as a reduction in film thickness and is known to be detrimental to conductivity.[22,69,87,119,120] It is generally accepted that PSS degrades first at 250 °C through the breakdown of the sulfonate groups as observed by Fourier transform infrared spectroscopy (FTIR) (section 1.4.2.2)[69,76,121] and x-ray photoelectron spectroscopy (XPS).[120,122] This is followed by PEDOT degradation at 300 °C,[53] showing the presence of PSS is the limiting constituent to PEDOT:PSS thermal stability. A similar case was observed with DSC analysis by Kiebooms, *et al.* (1999)[55], in which PEDOT:PF_6^- began degradation at 150 °C with a maximum exotherm at 300 – 350 °C with DSC analysis. It was not stated in the paper if an inert purge gas was used and there was little discussion into the degrading mechanisms. However, it is reasonable to assume that the initial degradation at 150 °C is linked to the breakdown of PF_6^- with the maximum endotherm at 300 °C being attributed to PEDOT degradation.[53,55] The degradation properties of PEDOT:PSS

do not seem to be improved by chemical additions such as PEG[22] or various surfactants.[83] Furthermore, it was found that some surfactants, such as DDAPS and sodium dodecyl benzenesulfonic acid (SDBA), caused degradation onset 10 to 15 °C lower than pristine PEDOT:PSS.[83]

Generally, it its accepted that PEDOT:PSS is thermally stable up to 220 °C,[5,69,71,83] however, 200 °C has been recommended as a more suitable upper processing temperature to ensure no degradation is occurring.[5]

1.4.2.2 Fourier Transform Infrared Spectroscopy (FTIR) Analysis

FTIR is used to identify the chemical bonds within a polymeric material. Typically, FTIR analysis of PEDOT:PSS has been used to identify degradation[69,76,121] and assess the effect of additives[22,66,106] and processing conditions.[69]

PEDOT is identifiable by the C-O-C stretching in the ethylenedioxy group which appears at 1230, 1150 and a main peak at 1065 cm^{-1}.[69,123-126] Other peaks between 1350 – 1600 cm^{-1}, mainly a peak at 1530 cm^{-1}, have also been suggested as the thiophene / phenyl ring of PEDOT.[69,124-126] In PSS, the sulfonate group containing S=O and S-O bonds, at 1200 and 1120 – 1160 cm^{-1}, respectively, tends to be the main identifying peaks. The S-phenyl or C-S bonds are identified between 700 – 1000 cm^{-1} but can be harder to distinguish compared to the S=O and S-O groups, due to the presence of C-S bonds in the PEDOT thiophane ring.[69,106,123,124,126,127] A summary of identifying bonds and wavenumbers from the literature are given in Table 1-2.

Table 1-2: Wavenumber identification of common bonds within PEDOT:PSS, as found in the literature

Author	Bond	Wavenumber (cm^{-1})
Sriprachuabwong, *et al.* (2012)[106]	S-O	1157, 1121
	S-phenyl	1012
	C=C	1532
	C-C	1356
	C-S	952, 845, 704
Kvarnström, *et al.* (1999)[123]	Ethylenedioxy ring	1147, 1058, 1014
	C-S	944
Han, *et al.* (2004)[124]	C-O-C	1234, 1068
	C-C, C=C (quinoidal structure)	1357
	C-S	989, 856, 700
Friedel, *et al.* (2009)[69]	Thiophene / phenyl rings	1350 - 1600
	C-O-C	1240, 1070
	S=O	1180
	O-S-O	1030
	Sulfonic acid	<600

As mentioned above, FTIR has been used to assess the effect of additives on the PEDOT:PSS structure. The use of TDE was shown to produce a shift in the SO_3 band to 1230 cm^{-1} which was attributed to the removal of an H^+ ion from the group, increasing the PEDOT and PSS interaction.[66] In another case, FTIR showed that when dissolved polycarbonate in dichloromethane was mixed with PEDOT:PSS, hydrogen bonding was detected between the two polymers through movement of the carbonyl peak from 1770 to 1766 cm^{-1}.[121] However, it appears that many additives such as, GLY, graphene, or PEG, do not cause structural changes detectable by FTIR, despite showing improvements in film conductivity (section 1.5.2.1).[22,66,106,128] Despite this, FTIR can be used to identify whether a substance

remains in the film after processing. For example, PEG was shown to remain in PEDOT:PSS after annealing at 130 °C, and was identifiable by peaks appearing at 2875 and 1645 cm^{-1}.[22] On the other hand, it was also reported that EG was not present after annealing due to the lower boiling point.[22] Similarly, the removal of PSS can also be detected when the film has been treated with a solvent wash (section 1.5.2.4).[127]

Finally, FTIR has been used to identify the degradation mechanisms of PEDOT:PSS. As discussed in section 1.4.2.1, it is well known that degradation will occur above 220 °C.[5,69,71,83] This degradation has been shown to be due to the breakdown of the sulfonate group in PSS[69,76,121] with the peaks at 1300, 1000 – 700 and below 600 cm^{-1}, no longer present or having a significantly reduced absorbance.[5,69,121] However, peaks commonly used to identify PEDOT remain present after heating to 250 °C, confirming PEDOT is not degrading due to its thermally stability up to 300 °C.[53]

1.5 PEDOT:PSS Conductivity Enhancement

As already mentioned, conductivity is one of the main limiting factors of PEDOT:PSS when compared to ITO and other PEDOT counterion combinations (section 1.2.1). However, there are a variety of factors that can influence the conductivity such as polymerisation route, PEDOT to PSS ratio, processing factors, annealing, film thickness and environmental conditions. Improvements can also be made through the use of conductivity enhancing agents (section 1.5.2). These normally fall into either ‘pre-treatment’ or ‘post-treatment’ categories depending on whether the agent is added to the PEDOT:PSS solution prior to film casting, or if the substance is used to treat an already cast film in the form of a wash, respectively. In some cases, a combination of these enhancement methods is used to provide an even greater improvement by utilising differing effects caused by the separate treatment methods.

Many of these factors, especially the use of conductivity enhancing agents, have already been widely reviewed in the literature.[6,13,15,17,18,25,59] However, this section aims to highlight the key factors relevant to this work.

1.5.1 Factors that Alter the Conductivity of Pristine PEDOT:PSS

1.5.1.1 Polymerisation Route and Associated Factors

As already stated, the conductivity of pristine PEDOT:PSS can vary greatly from 0.001 to 120 Scm^{-1} (section 1.2.1).[12,22,58,60,62] The polymerisation route has an effect on the conductivity of PEDOT:PSS with chemical synthesis giving a conductivity of approximately 3 Scm^{-1}, whereas electrochemical polymerisation yielded 80 Scm^{-1}.[12] This is caused by reduced PSS – PEDOT interaction during chemical polymerisation, leading to excess PSS in the resultant solution, whereas synthesising electrochemically causes PEDOT to interact with the required quantity of PSS, causing little to no excess insulating material.[12]

Variation can also come from the ratio of PEDOT to PSS within the film,[5,21,62,79,129] due to the presence of excess PSS creating a greater insulating barrier between PEDOT-rich sites and, therefore, increasing the electron hopping distances.[12,17,62] This was demonstrated by Stöcker, *et al.* (2012)[62] in which the ratios of PEDOT to PSS were varied from 1:1 through to 1:30, resulting in conductivities of 2.3 Scm^{-1} and 0.001 Scm^{-1}, respectively. A similar trend has been reported for PEDOT:PSS films containing EG which show that the PSS concentration is still a determining factor of conductivity, even after treatment.[79]

PEDOT:PSS conductivity has also been shown to vary with different forms of the PSS counterion.[12,31,57] Zotti, *et al.* (2003)[12] showed that synthesis with the salt, PSS(Na), or acid, PSS(H), forms provided conductivities of 1 Scm^{-1} and 80 Scm^{-1}, respectively. XPS found that electrochemically synthesising PEDOT:PSS with PSS(Na) resulted in reduced PSS – PEDOT

interaction, therefore, having higher qualities of excess insulating material compared to polymerising with PSS(H).[12,31] It was further suggested that PSS(H) provided greater doping than PSS(Na).[12] It is also likely that the differences seen by Zotti, *et al.* (2003)[12] are influenced by the pH changes when using either the acid or base form of PSS. Research has shown that with an increase in pH, there is a rapid decrease in the conductivity until pH 7 at which point it plateaus.[64,67] The enhancement at low pH was attributed to the interaction of the protons with the SO_3^- group within the PSS. This leads to a weakened interaction between the PEDOT and PSS components, allowing the PEDOT chains to uncoil and provide an easier pathway for electron movement and improved $\pi - \pi$ stacking.[64] The pH of the solution can also be altered by additions to PEDOT:PSS solution (section 1.5.2.1).

The final factor which has been shown to alter pristine PEDOT:PSS is the size of the PEDOT:PSS particles.[21,83,87,122] While there is conflict within the literature, larger particles are generally considered to increase conductivity.[21,87] Kirchmeyer, *et al.* (2005)[21] demonstrated that average PEDOT:PSS particle sizes of 58 and 25 nm produced resistivities of 1.96 and 12.6 kΩcm, respectively, due to larger particles reducing the number of insulating PSS barriers between PEDOT-rich sites.[21,87] However, Friedel, *et al.* (2011)[122] found the opposite, with smaller PEDOT:PSS particles causing conductivity to increase due to closer packing decreasing hopping distance between areas of PEDOT. However, in the latter case, particle size was altered by heating the PEDOT:PSS solution, whereas other studies did not use this method.[21,87] It is possible the heating process influenced other aspects, such as chain reorganisation, leading to a conductivity increase.[81]

1.5.1.2 Annealing

The annealing[c] of PEDOT:PSS films is known to be of great importance due to the increase in conductivity achieved after heat treatment.[5,60,69,78,81,120] It is generally accepted that the reason for this conductivity enhancement is partially due to the removal of excess, or bound, water (section 1.3.2).[22,60,69,71,88,90] There has also been indication that the annealing process causes structural rearrangement through the softening of the PSS region and PEDOT re-alignment.[32,69,81]

In most instances within the literature an annealing temperature and time is stated with little to no reasoning as to why those conditions were selected. Furthermore, parameters can vary greatly such as: 110 °C for 2 hours;[107] 140 °C for 20 seconds;[60] 150 °C for 10 minutes;[125] 200 °C for 2 minutes.[84] It can be seen from these cases that there is little consistency between annealing conditions other than higher temperatures often being employed for shorter times. Annealing is normally performed over 100 °C to ensure the removal of water, although, based on the literature surrounding thermal analysis, temperatures as high as 160 °C could be needed to fully remove all moisture (section 1.4.2.1).[5,71,76,85] There have been exceptions to this in which lower temperatures, around 40 °C, have been used to anneal samples for several days in a vacuum oven.[86] However, there was no comparison to high temperature annealing and whilst moisture will be removed, structural rearrangement is unlikely to occur at lower temperatures.

[c] In most cases, the term 'annealing' is used to describe when the material is already set as a film and then taken to high temperatures. In some cases, this is termed 'baking' or 'drying'. In all situations the main effect is the removal of bound water from the material. However, sometimes this process is done at lower temperatures and performed in a vacuum oven but still termed 'annealing'. Occasionally a 'setting' phase is also referred to which takes the material from solution to film (confusingly also sometimes termed 'drying'). To maintain consistency, 'annealing' will be used to describe heating the film while 'setting' refers to the solution to film phase.

There have been limited and somewhat conflicting findings about the variation of annealing temperature on the conductivity of PEDOT:PSS films. For instance, Friedel, *et al.* (2009)[69] found that resistivity dropped from 1.3 MΩcm to 0.15 MΩcm after annealing for 30 minutes at 120 °C and 250 °C, respectively. It was suggested that the effect of water removal was the main factor for this change up to 160 °C above which the segregation of the PSS phase caused resistivity to decrease further.[69] Comparably, Lombardo, *et al.* (2018)[90] showed annealing for 10 minutes at 100, 150 and 200 °C produced progressively lower sheet resistivity. Similar trends have been seen elsewhere in the literature,[58,60,87] however, measurements often plateau around 150 °C.[60,87] Koidis, *et al.* (2011)[60] concluded that 140 °C was the optimum annealing temperature, with higher temperatures not providing significant benefits to conductivity. In some cases it has even been suggested that annealed samples left to fully equilibrate to atmospheric conditions show no difference in conductivity to samples that had not been annealed.[81] However, it is possible other factors, such as PEDOT:PSS grade, substrate material, coating method and equilibration period contributed to the differences in these findings.

PEDOT:PSS treatments have also been shown to affect the optimal annealing conditions needed. For example, conductivity was not significantly influenced by annealing up to 200 °C when either EG[130] or H_2SO_4[90] was added to PEDOT:PSS solution prior to film formation. However, alteration of annealing temperature does affect conductivity after using 100 % concentrated H_2SO_4 to wash PEDOT:PSS films.[58] It was found that the optimum annealing temperature was 120 °C, producing a conductivity of approximately 4100 Scm^{-1}, which decreased to 3300 Scm^{-1} when increasing the temperature to 160 °C.[58] These cases show that the annealing effect can vary depending on the treatment method and it cannot be assumed that results seen for pristine PEDOT:PSS will apply to other scenarios.

Annealing time variation shows similar inconsistency within the literature. As seen above, times can vary from 20 seconds to 2 hours for temperatures ranging from 110 – 200 °C.[60,84,107,125] Whilst it could be assumed that the sample would be fully annealed over longer times, there was no indication that the shorter time of 20 seconds was insufficient.[60] No literature was found that accurately evaluated annealing time whist keeping all other parameters consistent. Comparisons between different studies is also difficult. For example Koidis, *et al.* (2011)[60] annealed at 140 °C for 20 seconds to give a conductivity of 120 Scm^{-1} whereas Eom, *et al.* (2009)[102] annealed at the same temperature for 20 minutes and obtained a conductivity of 0.8 Scm^{-1}. This result is unexpected since it could be assumed that the longer annealing time would provide the higher conductivity. However, this highlights the issue of comparisons between research groups since two different coating techniques were implemented, gravure R2R versus IJP respectively, as well as different grades of PEDOT:PSS.[60,102]

There have been some studies into longer annealing times which could potentially be considered ageing. However, they still provide insight into how the conductivity can be affected by longer heating periods and highlights the risks of prolonged annealing. This was shown to be the case in a study by Vitoratos, *et al.* (2009)[120] in which samples of pristine PEDOT:PSS were held at 120 °C for up to 55 hours. Data showed that room temperature conductivity decreased from 1.85 to 1.60 to 0.90 Scm^{-1} for samples held for 20 minutes, 3 hours and 55 hours, respectively.[120] This was attributed to a degradation effect caused by thermal ageing, seen at a much lower temperature compared to the previously discussed degradation temperature of 220 °C (section 1.4.2.1).[5,69,71,83] It was reasoned that breakdown of the ionic PEDOT – PSS interaction caused an increase in the insulating barrier between conductive PEDOT sites.[120]

It is clear that optimisation of the processing conditions is needed in order to provide the best conductivity of pristine PEDOT:PSS. Both the temperature and time have been shown to have

a significant effect, and with the optimum temperature of 140 °C quoted by Koidis, *et al.* (2011)[60] being conflicted by other literature, more research is required. Equally, the uncertainly about annealing time needs resolving. Whilst it is assumed that a shorter annealing time does not fully anneal PEDOT:PSS, there is clear evidence that annealing for too long can have irreversible detrimental effects on the conductivity.[120] Finally, it is important to consider these parameters alongside any treatments performed to PEDOT:PSS as is evident from studies using EG addition or and H_2SO_4 wash.[58,130]

1.5.1.3 Thickness

As previously mentioned, the thickness of PEDOT:PSS films is influenced by the water content, with greater moisture leading to an increase in thickness (section 1.3.2).[60,69] The film thickness has also been shown to vary with conductivity enhancing agents.[22,88] In the case of PEG addition, PEDOT:PSS films were shown to be 30 nm thicker with a 6 vol% concentration compared to 1 vol%.[22] On the other hand, the addition of EG caused a decrease in film thickness from 40 nm, with no EG, to 27 nm at 7.5 vol%.[88] These differences likely come from whether evaporation of the additive occurs during annealing and their effect on water uptake by PEDOT:PSS. A thickness decrease has also been shown for samples that undergo a post-treatment wash, which is more intuitive since the wash will remove part of the PSS from the film (section 1.5.2.4).[58,88,127,131] Resistivity has been shown to vary with film thickness for pristine PEDOT:PSS,[66] and films containing Triton X-100,[47] EG,[88] formic acid,[132] and methanol.[127] In general, an increase in the thickness leads to a decrease in sheet resistivity.[66,88,107,127,132] This trend appears to be non-linear with values tending towards a plateau at greater thicknesses.[88,127,132]

However, the validity of some of these results is in question for varying reasons. Firstly, in most cases the sheet resistivity is measured with the use of the 4-point probe which relies on the use

of three geometrical correctional factors (section 2.6).[133] One of these factors indicates that for thicker samples, the measured resistivity is multiplied by a factor between 0 and 1.[133] Problematically, there is little reference to whether these factors are accounted for as the thickness is varied. Secondly, the coating method may also affect the results. For example, Martin, *et al.* (2004)[66] showed a decrease in the sheet resistivity from 4300 $\Omega\square^{-1}$ to 1800 $\Omega\square^{-1}$, with a change in thickness from 0.17 µm to 0.53 µm. To manufacture these thickness the films were spin coated at different spin speeds of 2000 and 500 rpm, respectively.[66] It could be argued that the spinning process induces orientation into the sample which would result in the electrical properties being directionally superior.[134] Therefore, although the trend would remain, the measured sheet resistivities seen by Martin, *et al.* (2004)[66] for thinner samples may be lower than expected due to the induced orientation at a higher spin speed.

In some cases, thickening was achieved by casting multiple layers of PEDOT:PSS at constant spin conditions with an annealing and treatment phase between each applied layer.[88,105,127,132] The trend showed a decrease in sheet resistivity for an increase in the film thickness, and by extension the number of applied layers, with results tending towards a plateau.[88,105,127,132] Alemu, *et al.* (2012)[127] saw a resistivity decrease from 140 $\Omega\square^{-1}$ at 50 nm (1 layer) to 70 $\Omega\square^{-1}$ at 90 nm (2 layers) with a minimum of 25 $\Omega\square^{-1}$ being reached at 300 nm (6 layers). Similarly, Mengistie, *et al.* (2014)[132] saw a decrease from 145 $\Omega\square^{-1}$ at 35 nm (1 layer) to 68 $\Omega\square^{-1}$ at 75 nm (2 layers) with a minimum of 23 $\Omega\square^{-1}$ being reached at 225 nm (6 layers). Finally, Kim, *et al.* (2011)[88] utilised both increasing spin speed and multiple layering to build thicker films. It was reported that resistivity dropped from 450 $\Omega\square^{-1}$ at 20 nm (5000 rpm, 1 layer) to 50 $\Omega\square^{-1}$ at 140 nm (2500 rpm, 4 layers).[88] A comparable trend was also seen with the use of IJP multiple layers of PEDOT:PSS, with sheet resistivity in the region of 10^4 $k\Omega\square^{-1}$ for 2 layers dropping by over three orders of magnitude at 30 layers.[105] While thickness is not directly discussed, it can

be assumed that it is increasing with each layer.[105] However, despite these findings there were no suggestions as to why the thickness reduces sheet resistivity. The main issue is that it is unclear how the PEDOT:PSS solution will interact with a layer of itself compared to the substrate material. This may be causing PEDOT-rich regions to preferentially sit closer to the surface of the film which would decrease sheet resistivity.

Despite this, it is clear that thickness significantly affects resistivity.[66,88] However, none of these papers quote conductivity which would factor in the thickness and substantiate the changes seen. For example, in the situation presented by Martin, *et al.* (2004)[66], the sheet resistivity, as measured by 4-point probe, and thickness measurements of 4300 $\Omega\square^{-1}$ at 0.17 µm and 1800 $\Omega\square^{-1}$ at 0.53 µm would equate to conductivity values of 13.7 and 10.5 Scm^{-1}, respectively (based on Equation 2-10, section 2.6). What these results then suggest is that a thicker film reduces conductivity. These results seem more logical since the thinner films were manufacture using a higher spin speed which induced orientation into the films, leading to improved conductivity.[66,134] If the same is done for data obtained by Alemu, *et al.* (2012)[127] and Mengistie, *et al.* (2014)[132], then conductivities of 1429, 1587 & 1333 Scm^{-1} are found for thicknesses of 50, 90 & 300 nm, and 1970, 1961 & 1932 Scm^{-1} for 35, 75 & 225 nm, respectively. However, this conversion may not be an accurate representation of the properties of films containing multiple layers, since it is unknown how each layer of PEDOT:PSS will interact with one another. Furthermore, the 4-point probe only measures the surface layer and not the bulk electrical properties[133] demonstrating the potential for error in converting to conductivity. Despite this, these examples still indicate that large differences in thickness do not affect the conductivity as significantly, or in the same way, as resistivity. Therefore, there might not actually be a change in the bulk electrical properties caused by thickness variation.

1.5.1.4 Temperature Dependence

The conductivity of PEDOT:PSS has widely been shown to vary with regards to temperature, with a rise in temperature leading to an increase in the conductivity of the material.[67,71,80,87,120,130] Huang, *et al.* (2005)[87] found that increasing temperature from 25 to 200 °C resulted in an increase from 6 x 10^{-4} to 4 x 10^{-3} Scm^{-1}. Similarly, Zhou, *et al.* (2014)[71] saw when increasing temperature from 21 to 200 °C, conductivity increased from 0.25 to approximately 2.5 Scm^{-1}. Whilst the actual results vary greatly between the two studies (likely caused by different grades of PEDOT:PSS) the increase in conductivity is to the order of one magnitude. When cooling below room temperature, there is a significant drop in conductivity, however, not on the same magnitude as reported above.[67,80,120]

The reason for the increase in conductivity with temperature is two-fold. Firstly, it has already been established that PEDOT:PSS is a p-type semi-conductor (section 1.3.1).[5,6,29] Unlike metallic conductivity, in which an increase in temperature leads to a decrease in conductivity, the semi-conducting nature of this material causes the opposite to occur.[28,29] Raising the temperature causes the electrons to have an increased energy, improving their mobility and increasing the availability of electrons within the conducting band.[29] Secondly, the increased temperature removes moisture from the sample, causing the PSS-rich phase to shrink, reducing barriers to electron flow (section 1.3.2).[60,69,78] However, this would mostly occur at higher temperatures since water removal does not start to become a factor until about 80 °C.[5,71,76,85] Even though this trend is well established for pristine PEDOT:PSS, the research into the temperature effect following conductivity enhancing treatment is limited. It is possible that alteration of the HOMO/LUMO energy gaps could lead to less energy being required to move electrons into the conductive band.[5]

1.5.2 Conductivity Enhancing Agents and PEDOT:PSS

Throughout the literature a large variety of conductivity enhancement agents[d] have been used including high boiling point solvents, organic co-solvents, alcohols, surfactants, non-volatile wetting agents, polymeric binders, plasticisers, silanes, and fibres. Whilst many of these have already been reviewed in the literature,[5,13,15,18,24,25,59] this section aims to highlight the some of the key treatment methods, their effect on PEDOT:PSS conductivity and the primary mechanisms that facilitate this. The degree of conductivity enhancement can vary depending on the agent, the quantity and whether it is used as a pre- or post-treatment method. There are also situations where multiple treatments result in further improvements seen when chemical additions and washes were used in conjunction. Finally, the treatments utilised in this study are discussed with regards to previous applications and justification for use. Due to the large number of factors that can influence conductivity, making comparisons between literature sources is difficult. Table 1-3 shows an overview of some of the treatments reported in the literature and their associated conductivity effects.

[d] The term 'conductivity enhancing agent' describes any substance used to treat PEDOT:PSS as either a pre- or post-treatment. Commonly, the terms 'secondary doping' or 'secondary dopant' are used as an alternative (with PSS being the primary dopant to PEDOT). Occasionally, 'conductivity enhancing additive' is also used. However, these normally refer to substances that are added to PEDOT:PSS solution, therefore, excluding post-treatments. It is also often the case that the substance added is not 'doping' the PEDOT:PSS again but is causing improvement through other mechanisms. Therefore, it was deemed that 'conductivity enhancing agents' was a more accurate term and is used throughout this work.

Table 1-3: Literature summary of conductivity (Scm^{-1}) increase for treated PEDOT:PSS films caused by conductivity enhancing agents. Chemical agents grouped by treatment method and weight percentage (wt%) of additives are shown (if known). NB: This table is a guide to illustrate the potential for conductivity enhancement and does not cover all variable

Treatment Type	Chemical Agent	Weight Percentage (wt%) Addition	Conductivity Increase (Scm^{-1})	Ref.
Pre-treatment	DMSO	-	0.4 to 143	130
		5	1.5 to 350	27
		5	0.7 to 880	77
		10	2.5 to 1233	135
	Diethylene glycol (DEG)	0.3	0.006 to 10	34
		5	0.007 to 10	28
	EG	5	1.5 to 200	27
		6	0.3 to 640	22
		6	1 to 735	88
	PEG	2	0.3 to 805	22
	Dimethylformamide (DMF)	-	0.4 to 37	130
		5	1.5 to 200	27
	N-mythyl-2-pyrrolidone (NMP)	-	0.4 to 46	130
		5	1.5 to 200	27
		20	0.03 to 30	12
	TDE	5	15 to 98	66
	GLY	5	15 to 57	66
		6	0.792 to 152	102
	SDS	10	0.16 to 70	108
	SDBS	10	0.16 to 224	108
	Triton X-100	1	0.24 to 100	47
		5	0.21 to 67	98
	DBSA	2	1 to 500	131
	HCl	-	6 to 20	67
Post-treatment	H_2SO_4	N/A	1 to 4380	58
	Trifluoromethanesulfonic acid (TFMS)	N/A	1 to 3600	58
	Methanol	N/A	0.3 to 1015	127
		N/A	0.21 to 71	98
		N/A	0.24 to 350	47
		N/A	0.7 to 920	77
	Ethanol	N/A	0.3 to 672	127
		N/A	0.24 to 200	47
	Isopropanol	N/A	0.3 to 468	127
	EG	N/A	0.4 to 200	130
	DMSO	N/A	2.5 to 2124	135

1.5.2.1 Pre-treatments

The primary objective of chemical addition is to improve the conductivity of PEDOT:PSS, with a large number of successful pre-treatments agents reported in the literature (Table 1-3). One effect additives can have is alteration of the PEDOT:PSS solution pH, which has been shown to impact the film conductivity.[12,64,67,136] Aleshin, *et al.* (1998)[67] decreased or increased pH by adding HCl and NaOH, respectively, then measured conductivity of the resultant film. The highest conductivity was 20 Scm^{-1} at pH 1.2, which decreased with increasing pH, until a plateau of 0.1 Scm^{-1} was reached at pH 7.[67] In the case of Zotti, *et al.* (2003)[12], the differences in conductivity seen between polymerisation with either PSS(Na) (1 Scm^{-1}) or PSS(H) (80 Scm^{-1}) can partially be explained by the variation of solution pH, even though this is not directly discussed.

However, it can be seen that the effect of pH is relatively small and, therefore, this alone is not the most effective method to improve conductivity. Additions of high boiling point solvents, such as DMSO, EG, DMF or NMP caused conductivity increased from 1.5 to 200 – 350 Scm^{-1}.[27] This is a much greater improvement than achieved through pH alone, suggesting other mechanisms factor into conductivity enhancement. The difference between enhancement agents is also highlighted with 5 wt% EG, DMF and NMP yielding improvements to 200 Scm^{-1} whilst DMSO gave a conductivity of 350 Scm^{-1}.[27] Other agents added at 5 wt% have shown to produce much lower improvements, such as GLY and TDE improving conductivity from 15 to 57 and 98 Scm^{-1}, respectively.[66]

While this demonstrates the effect of various pre-treatments, Table 1-3 shows variation can occur when using the same addition. For example, conductivity increase caused by DMSO was reported by Lingstedt, *et al.* (2019)[135] to be 2.5 to 1233 Scm^{-1} at 10 wt%, Wang, *et al.* (2018)[77] as 0.7 to 800 Scm^{-1} at 5 wt%, and Ouyang, *et al.* (2004)[130] from 0.4 to 143 Scm^{-1}. Although

Lingstedt, *et al.* (2019)[135] reported the largest maximum value for conductivity with DMSO treatment, the greatest percentage increase was seen by Wang, *et al.* (2018)[77]. Similarly, conductivity enhancements caused by EG were reported as 10 to 550 Scm^{-1} by Lubianez, *et al.* (2008)[27], 1 to 735 by Kim, *et al.* (2011)[88] and 0.3 to 640 Scm^{-1} by Mengistie, *et al.* (2014)[132]. Comparable variations for NMP[12,27,130] and DMF[27,130] have also been seen.

The additive concentration in PEDOT:PSS can also effect conductivity as shown by both Mengistie, *et al.* (2013)[22] and Kim, *et al.* (2011)[88] in which increasing the concentration of EG resulted in improvements to 640 and 735 Scm^{-1}, respectively. In both cases, a plateau occurred at 6 wt% EG showing good consistency between studies. However, maximum conductivity can occur at different concentrations for alternative pre-treatments and do not always show the same consistency between studies. For example, DEG has been shown to increase conductivity from 0.007 to 10 Scm^{-1} at 5 wt%,[28] and 0.006 to 10 Scm^{-1} at 0.03 wt%.[34] Here it can be seen that, whilst the conductivity increases are similar, the concentration of DEG needed to achieve this varies greatly.

It is common that an increase in conductivity will only be evident over a small range of concentrations with high quantities decreasing conductivity due to the insulating nature of the additive.[22,83] This is likely the reason why Ouyang, *et al.* (2005)[23] only saw an increase from 0.4 to 160 Scm^{-1} when 50 wt% EG was added to PEDOT:PSS. Issues can also arise, with high additive concentrations, relating to film quality[66,85] which plays a key role within certain applications.[8,9,41] This was demonstrated by Martin, *et al.* (2004)[66] when salicylsulfonic acid (SSA) was used as pre-treatment for PEDOT:PSS. Whilst the sheet resistance decreased from 2600 $\Omega\square^{-1}$ to 375 $\Omega\square^{-1}$, SSA caused a decrease in the transparency of the film,[66] reducing its potential in applications that require good optical properties such as flexible flat panel displays.[8,9,66]

The molecular weight (Mw) of an additive can also influence conductivity. Mengistie, *et al.* (2013)[22] investigated this by pre-treating PEDOT:PSS with 2 wt% PEG with Mw of 200 to 6000. It was reported that for Mws of 200, 300 and 400 the conductivity improved from 0.3 to 805 Scm^{-1}. However, once the Mw increased to 600, the maximum conductivity achieved was 350 Scm^{-1}.[22] It was proposed that this was due to the reduced chain mobility of the higher Mw PEG hindering PEDOT:PSS re-organisation (section 1.5.3) and leading to lower conductivity.

1.5.2.2 Surfactant Pre-Treatments

The use of surfactants to improve conductivity has been explored less in the literature but is of interest due to their effect on the solution and mechanical properties (sections 1.4.1 & 1.3.3, respectively) and, therefore, potential benefits with regards to bulk manufacture. Anionic surfactants have been reported to significantly improve the conductivity when added to PEDOT:PSS solution. Changes from 0.61 to 70 and 224 Scm^{-1} have been achieved with 10 wt% SDS and SDBS, respectively. An even greater improvement was seen by Zhang, *et al.* (2015)[131] when 2 wt% of DBSA surfactant produced an increase from 1 to 500 Scm^{-1}.

The Triton X series of non-ionic surfactants are a group of particular interest. As already discussed, they show excellent improvements in the mechanical properties of PEDOT:PSS films (section 1.3.3). Additionally, the Triton X surfactants also provide significant increases in the conductivity of PEDOT:PSS. Kim, *et al.* (2017)[98] found that Triton X-405 at a concentration of 3 wt% provided the greatest increase in conductivity, from 0.21 to 206 Scm^{-1}, when compared to other Triton X surfactants. A high level of transmittance was also maintained through the film (92 %) showing suitability for optoelectronic devices.[98] However, there were issues regarding the miscibility of this Triton X grade at concentrations above 1.5 wt%.[98] On the other hand, these issues were not present for Triton X grades with fewer repeat units. For example, Triton X-100 showed no separation, even at concentrations above 10 wt%, but only

showed a maximum conductivity increase to 67 Scm^{-1} at 5 wt%.[98] Other studies have shown slightly larger improvements in conductivity with the use of Triton X-100. For example, Oh, *et al.* (2014)[47] found an increase from 0.24 to 100 Scm^{-1} which plateaued at 1 wt%. Noticeably, the concentrations at which the conductivity plateau varies between the two studies. However, this is likely due to the different grades of PEDOT:PSS having differing availability of material to interact with (section 1.5.3).

1.5.2.3 Pre-Treatment Combinations

In some cases, a combination of additives resulted in further conductivity enhancement. This was demonstrated with the use of DBSA surfactant which, at 2 wt% concentration, increased conductivity from 1 to 500 Scm^{-1}.[131] However, when 0.5 wt% DBSA was combined with either 5 wt% GLY or 2.5 wt% sorbitol, conductivities of 650 Scm^{-1} were achieved in both cases.[131] This is a larger increase in both percentage and absolute values to the previously discussed 6 wt% GLY and 2.5 wt% sorbitol additions, showing increases of 0.78 to 152 Scm^{-1},[102] and 1 to 200 Scm^{-1},[137] respectively.

However, it is not always the case that combinations of additives attain greater conductivities. For example, a third addition of 5 wt% 3-glycidoxypropyltrimethoxysilane to the DBSA/GLY mix described, decreased conductivity back to near the pristine PEDOT:PSS value of approximately 1 Scm^{-1}.[131] Combinations of 0.5 wt% DBSA with 5 wt% DMSO or EG did improve conductivity from 1 to 650 Scm^{-1} and 450 Scm^{-1}, respectively.[131] However, neither of these are close to results obtained when adding DMSO[77,135] or EG[22,88] alone. Similarly, Jönsson, *et al.* (2003)[129] increased PEDOT:PSS conductivity from 0.37 to 48 Scm^{-1} with a combination of 1.4 wt% sorbitol, 2.4 wt% NMP and 48 wt% isopropanol. Again, this increase is relatively low compared to the addition of either sorbitol[137] or NMP[27]. However, this lower conductivity could be partially caused by the large quantity of isopropanol diluting the PEDOT:PSS solution

meaning the charge hopping distance increases.[62,122] Care is similarly needed regarding the concentration when mixing additions. This was best demonstrated by Eom, *et al.* (2009)[102] where the addition of 6 wt% GLY and 0.2 wt% ethylene glycol butyl ether (EGBE) resulted in an increase from 0.78 to 164 Scm^{-1}. However, once the EGBE concentration was increased to 0.4 wt%, the conductivity fell to near pristine PEDOT:PSS values.[102]

It clear that there are a broad range of possible chemical agents that can be used as a pre-treatment for conductivity enhancement of PEDOT:PSS. The use of surfactants has been established as one method for improving these properties. They have the additional advantage of improvements to film mechanical properties (section 1.3.3) as well as being more environmentally friendly and less volatile than high boiling point solvents. In some cases, such as Triton X-100, the conductivity enhancement was lower than high boiling point solvents (e.g., DMSO). However, Triton X-405 show comparable conductivity improvements to these solvents. This gives rise to the question as to whether there are other, more suitable non-ionic surfactant that could induce this kind of conductivity improvement.

1.5.2.4 Post-treatments

Post-treatment of PEDOT:PSS refers to implementing a wash of the film once the sample has been annealed. This method has been shown to effectively enhance conductivity for PEDOT:PSS films without any prior pre-treatment (Table 1-3). One method is to use concentrated acids, such as formic acid increasing conductivity from 0.3 to 1950 Scm^{-1},[132] and TFMS from 1 to 3600 Scm^{-1}.[58] The most significant conductivity enhancement of PEDOT:PSS to date was achieved by Kim, *et al.* (2014)[58] in which concentrated H_2SO_4 was used as a wash, yielding a conductivity of 4380 Scm^{-1}. This conductivity rivals that of ITO[8,20] and does not require any additives in the PEDOT:PSS solution prior to film formation. However, this

treatment method is not suitable for bulk manufacturing processes due to the volatility and environmentally hazardous nature of these acids.

It has been found that pre-treatment additives (section 1.5.2.1) can also be used as a post-treatment, with comparable changes in conductivity. For example, an EG wash has been found to improve conductivity from 0.4 to 200 Scm^{-1},[130] with increases as high as 600 Scm^{-1} and 960 Scm^{-1} also being reported.[48,119] Similarly, DMSO has been used effectively as a pre-treatment,[119,135] with the greatest improvement of 2.5 to 2120 Scm^{-1} reported by Lingstedt, *et al.* (2019)[135]. Not only is this a greater improvement than that achieved by adding it to PEDOT:PSS solution,[77,135] it also rivals the conductivity seen by some concentrated acids.[58,132] However, it is not always the case that treatments are effective as both an addition and a wash. For example, when methanol was implemented as a pre-treatment, an insignificant change from 0.3 to 0.5 Scm^{-1} at 10 wt% was induced.[127] On the other hand, methanol is a well-established wash substance with results varying from 350 to 1015 Scm^{-1}.[47,77,98,119,127] The variation in these results is likely due to differences in either the PEDOT:PSS grade or the washing method, with conductivity variation depending on whether the sample was fully submerged or rinsed with the solvent.[127] In other cases, chemicals will only cause improvement when implemented as a pre-treatment. In the case of DMF, conductivity significantly increases when used as an addition to PEDOT:PSS.[27] However, when utilised as a wash there is only a minor increase in conductivity from 0.2 to 1.2 Scm^{-1}.[119]

While alternative solvents have been shown to increase PEDOT:PSS conductivity as a post-treatment, many do not result in the same level of improvement as methanol. For example, despite PEDOT:PSS being water soluble,[5,6,15,17,18] utilising water as a wash only increases conductivity between 3 to 10 Scm^{-1}.[48,119] Ethanol, isopropyl and i-butanol have all shown relatively large improvements to 350,[47,48,127] 468,[127] and 286 Scm^{-1},[127] respectively. Octanol,

γ-butyrolactone and acetone have also be explored but produce relatively weak increases to 50, 0.87 and 0.24 Scm^{-1}, respectively.[47,119] Unlike with pre-treatments, there are limited studies where mixed solvents washes were utilised. One study demonstrated that a methanol/TFMS wash improved conductivity from 0.7 to 2980 Scm^{-1}.[77] However, this is lower than the increase seen by using TFMS alone.[58]

1.5.2.5 Pre- and Post-Treatment Combinations

There are also situations where a pre-treatment addition followed by a post-treatment wash improves conductivity further than either individual treatment. This was explored in depth by Oh, *et al.* (2014)[47] with the addition of Triton X-100 surfactant initially improving conductivity to 100 Scm^{-1}. This was then further increased to 350, 650 and 900 Scm^{-1} by washing with butanol, ethanol, or methanol, respectively.[47] These are all greater improvements than implementing the wash without the initial surfactant addition. Yoon, *et al.* (2016)[78] found a 20 % reduction in sheet resistivity when washing PEDOT:PSS films containing 0.1 and 2 wt% Triton-X 100 with methanol.[78] Similarly, Mengistie, *et al.* (2013)[22] post-treated PEDOT:PSS films containing PEG200 and EG, with methanol. Treatment was either done by immersion in methanol or dropping methanol onto the film and, in both cases, the conductivity was improved to over 1100 Scm^{-1}.[22] The same effect with this combination of additives and wash has been seen elsewhere in the literature.[130] Furthermore, there was one situation where the pre- and post-treatment were performed with the same solvent. This was done by Kim, *et al.* (2011)[88] where EG was first added to PEDOT:PSS, then the resulting film was washed with EG. The increase after the solvent addition was 1 to 735 Scm^{-1} which improved further to 1420 Scm^{-1} after washing.[88] However, it is not always the case that there will be any further improvement when a combination of treatments in implemented. This was found when Triton X-100 was added to PEDOT:PSS to give a conductivity of 100 Scm^{-1} which was not further improved by

washing with octanol.[47] This highlights the important of trying new treatment combinations to assess whether further conductivity increases can be achieved.

1.5.3 Mechanisms of Conductivity Enhancement

As demonstrated, there are a great deal of methods that have been used to enhance the conductivity of PEDOT:PSS to varying degrees by either pre- or post-treatment. However, the reasons for these improvements often encompass a couple of key structural changes and mechanisms that are explored here. The main effect crucial to conductivity enhancement is disruption of the ionic interaction between PEDOT and PSS which causes the two components to separate and segregate.[22,119,137] This effect has been analysed through techniques such as scanning tunnelling microscopy and atomic force microscopy (AFM), with greater distinction between PEDOT-rich and PSS-rich areas observed after pre-treatments with NMP, EG, PEG and sorbitol.[12,22,137] It is considered that this change in the PEDOT:PSS particle structure occurs whilst in solution, and reduces the energy barrier between the PEDOT-rich phases, subsequently increasing film conductivity.[27] XPS has also shown a greater amount of PEDOT residing at the surface following such treatments,[12,22,129] possibly resulting in higher conductivity at the film surface. However, it was suggested by Jönsson, *et al.* (2003)[129] that this occurred due to more uniform mixing of the PEDOT and PSS components after treatment, due to the shell/core breakdown of the pristine PEDOT:PSS structure (section 1.3.1), which resulted in a higher ratio of PEDOT being recorded at the sample surface.

Disruption of the ionic bond also allows PEDOT to 'uncoil' into a more linear structure with greater orientation and increased $\pi - \pi$ stacking, providing better conduction pathways for electron flow.[5,13,15,18,22,24,25,59,64,67] In the case of pH alterations, this disruption is linked to the availability of H^+ ions within solution.[64,67] It is thought that the protons interact with the SO_3^-

group of the PSS, weakening the PEDOT and PSS ionic bond.[64,67] Therefore, the lower the pH, the more readily available these protons are and the more they can interact with PSS weakening the ionic bond. However, as discussed pH only creates relatively small variations in the conductivity. For other pre-treatments, (e.g., high boiling point solvents, surfactants) it has been proposed that the additive requires two polar groups in order to cause this disruption and lead to a significant increase in the conductivity.[130] This is why EG, DMSO, and Triton X-405 all induce large increases in conductivity,[12,22,27,98,130] whereas acetonitrile, cyclohexone and methanol do not.[130] Furthermore, these additives often have a threshold quantity, below which no conductivity increase is observed, since it is thought that the additives initially interact with the excess PSS within the solution before interacting with the PSS bonded to the PEDOT.[98] There is also a maximum amount of additive that can be used before the solution becomes saturated and there is no further PSS to interact with. This is why a plateau was seen in conductivity above a concentration of 6 wt% EG[22] and is most likely the reason why insulating effects of additives become dominant after a given point.[83]

It is been suggested that a main driving force for the 'uncoiling' process is caused by the change in the resonance structure of the PEDOT from benzoid to quinoid (section 1.3.1).[22,31,40,127,130] The latter is known to be more linear, due to the position of the double bond within the backbone structure, creating more orientation and refinement of the PEDOT chains.[13,22,40,130] This reasoning is commonly seen within the literature and is not limited to pre-treatment methods, with solvent washes reportedly inducing the same structural changes.[13,22,127] However, there is a degree of conflict in the literature about this benzoid/quinoid change and which techniques can be used to observe it. It has been suggested that the addition of Triton X-100 or washing with EG causes this resonance structural shift, as seen with Raman spectroscopy by a red-shift of the 1400 – 1500 cm^{-1} band correlating to the $C_\alpha=C_\beta$ bond in the thiophene ring in

PEDOT.[78,125,130] However, there has also been speculation that, while the addition of surfactants does causes a benzoid/quinoid change, the effect is not significant enough to be seen through Raman analysis.[108] Similarly for FTIR, there is reference to 'quinoidal structure' that is associated with bands around 1400 cm^{-1},[53,124] with some claiming a difference between the resonance structures can be seen.[125] However, there are FTIR studies which make no reference either to this structure or any observable benzoid/quinoid change.[22] Other techniques, such as electron spin resonance and electrochemical characterisation, have been used to strengthen evidence for this benzoid to quinoid change.[130] Furthermore, molecular modelling of the PEDOT resonance structures has shown that in an undoped state (i.e. without PSS) the benzoid form is dominant, whereas a more quinoidal like structure appears when bonded to PSS.[40] This would suggest no change would occur with treatments since the quinoidal form is already present. However, this modelling was only done for 8-mer oligomers and is not necessarily representative of larger PEDOT:PSS structures.[40]

While the evidence for the benzoid/quinoid change is somewhat uncertain, the improvement in alignment and re-organisation caused by certain treatments is widely reported throughout the literature.[22,34,58,78,98,127] This improved alignment has been primarily seen through the use of higher magnification AFM.[58,72,98,127,132] Additives such as DEG, Triton X-100, EG and PEG have all shown a refinement of the microstructure, with more defined separation between PEDOT and PSS chains demonstrating a clear inter-connected network, or 'nanofibril' structure, of PEDOT.[22,34,78,98,127] In the case of Triton X-100 addition, this refined structure was not altered when further treated with a methanol wash.[78] However, it has also been found that the same structural refinement is achieved when washing is utilised as a sole treatment method. This was seen with both methanol and H_2SO_4 in which AFM analysis showed the same 'nanofibril' microstructure.[58,127] While a large number of studies utilise AFM to show this

structural change, XRD has also been used to assess the degree of alignment and orientation of the polymer chains.[29] Although pristine PEDOT:PSS is known to be amorphous,[58,65,67] Triton X-100 addition and washing with H_2SO_4 cause sharper peaks to appear on the XRD trace, suggesting chain alignment and structural refinement.[58,77,78]

As discussed, the use of washes can create similar structural changes as additives, with evidence of a benzoid/quinoid change occurring with a TFMS-Methanol wash[77] and chain alignment being reported in other studies.[58,77,127] However, there appear to be two key differences in the mechanisms of conductivity enhancement between pre- and post-treatments. The first is that, whilst structural refinement and alignment can occur with washing,[58,77,127] a segregation effect has not been reported in the literature. This is likely because the segregation caused by an additive will occur when in solution since the two components have more freedom to move.

The second mechanism of conductivity enhancement is that solvent washing removes PSS from the film.[13,22,59,127] Depending on the solvent used, this can be just the excess PSS (i.e., PSS not bonded to PEDOT) or it can also remove some of the bound PSS.[13,22,59,127] In either case, the act of removing the PSS in itself will improve conductivity since less insulating material will be present in the film.[17,127,129] This removal has been identified through the use of techniques such as XPS and FTIR analysis, with a reduction in associated PSS peak size.[127,129,138] Furthermore, PSS removal has added benefits including improved thermal stability[127] and reduced moisture uptake.[78] It has also been reported that when a surfactant, such as Triton X-100, was added as a pre-treatment and the resultant film was washed with methanol, both PSS and surfactant were removed from the film.[22,47,78,98] It was reasoned that the presence of Triton X-100 created PEDOT – surfactant and PSS – surfactant complexes, allowing for preferential removal of the PSS and surfactant when washed.[47,78,98]

1.5.4 Conductivity Enhancing Agents in this Study

Analysis of the literature found that surfactants, specifically non-ionic surfactants, show potential as a superior additive to enhance PEDOT:PSS properties. This is due to an improvement in solution characteristics, the higher conductivity achieved without negatively affecting film quality, improvement in PEDOT:PSS mechanical properties, and the reduced impact on the environment compared to other additives. They also have the potential to be used alongside other treatment methods in order to further improve PEDOT:PSS conductivity.

Therefore, in this study, focus will be on addition of the non-ionic surfactant polysorbate 80 (Tween 80) (Figure 1-11) as a conductivity enhancing agent. Given the volatility of the solvents more commonly used in other studies, this provides a more environmentally friendly and less hazardous alternative.[139] Furthermore, as shown in section 1.5.2.1, surfactants are a less commonly used pre-treatment, with the non-ionic Triton X series being the most researched.[47,78,98] It is likely Tween 80 will act in a similar way to these surfactants, resulting in comparable findings.

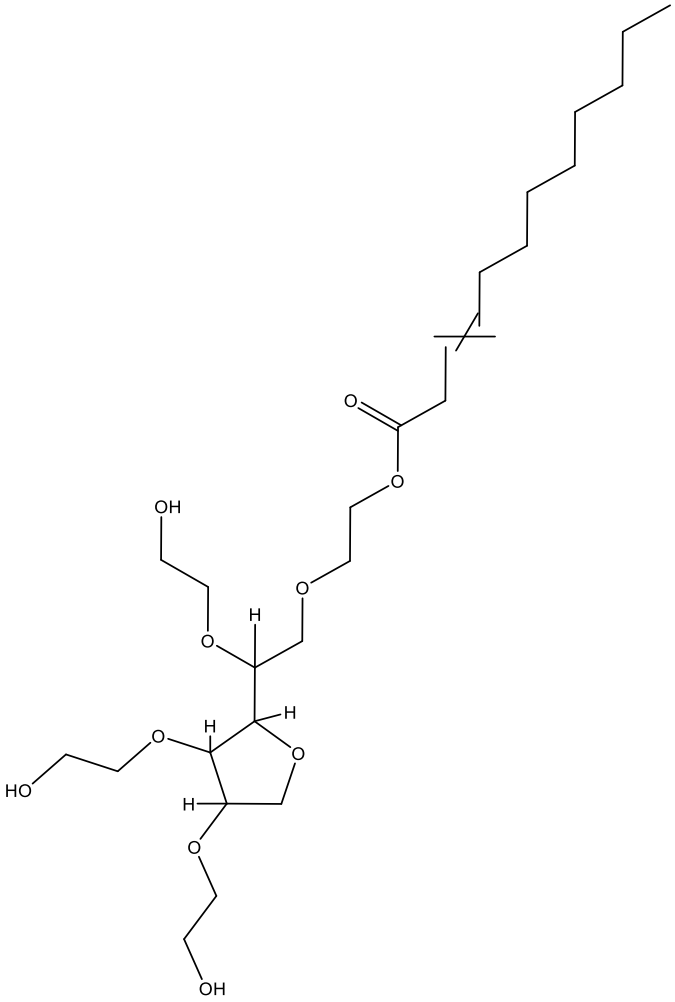

Figure 1-11: Chemical structure of Tween 80. Replicated from Pubchem (2018)[140]

Whilst Tween 80 addition has been previously explored as a route for conductivity enhancement, this was in conjunction with the solvent methyl ethyl ketone (MEK).[85] Results showed that low concentrations of the additives caused resistivity to initially increase to a maximum of 10^4 $\Omega\square^{-1}$ at 1 wt% however, further additions caused resistivity to drop to approximately 1200 $\Omega\square^{-1}$ at 2 wt% at which point it plateaued.[85] It is unclear from this study how Tween 80 alone will affect conductivity since this study was conducted with a Tween 80/MEK mix and did not assess the effect of each component individually. Furthermore, while conductivity results were quoted, these measurements were taken as readings directly

from the 4-point probe with no reference to the thickness measurements which are crucial when calculating conductivity.[133] In a similar case, Tween 80 was added to PEDOT:PSS solution to improve the wettability and film quality for gravure printed OLED's,[116] however, no comments were made relating to conductivity improvement or variation of the additive. Tween 80 has also been used as a solubilizing agent in the electrochemical deposition of PEDOT[141] but, while the effectiveness in this situation is commented on, it does not inform the use of this surfactant as a conductivity enhancing agent. There are other cases where Tween 80 has been mentioned in conjunction with PEDOT:PSS, however, it is mainly used to alter the wettability and surface tension of the solution, commonly alongside other additives, with no mention of the effect on conductivity.[142-144] Further study into Tween 80 as a pre-treatment for PEDOT:PSS would, therefore, provide insight into its viability to improve conductivity.

This study will also employ the use of MEK (Figure 1-12) as both a pre- and post-treatment method. Again, whilst MEK has been previously added to PEDOT:PSS,[85] the use of this solvent in isolation has not been reported. MEK will also be used as a post-treatment to wash pristine PEDOT:PSS films and PEDOT:PSS films containing Tween 80. While no benzoid to quinoid change is likely to occur when washing with this solvent, it is likely excess PSS will be removed from the film.

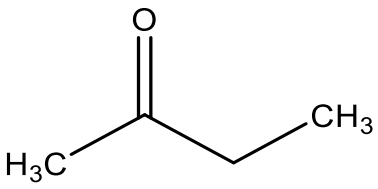

Figure 1-12: Chemical structure of MEK. Replicated from Sigma-Aldrich (2018)[145]

Both ethanol and methanol washes will also be tested on these films for comparison. While the latter two are more established choices for solvent washing (section 1.5.2.4), MEK has not previously been reported as a post-treatment method. It could be argued that MEK would be a more favourable option given it is less volatile than both ethanol and methanol. Using these washes in conjunction with a Tween 80 pre-treatment will also determine whether the effects of both treatments result in a conductivity enhancement greater than either individual method, such as that seen with Triton X-100 addition by Yoon, *et al.* (2016)[78].

1.6 Adhesion of PEDOT:PSS

The adhesion of PEDOT:PSS to various substrates is of importance, especially in bulk manufacturing processes (section 1.3.4). This is because polymeric material are often used in methods such as R2R processing, or in applications where flexibility is needed, such as flexible optoelectronic devices.[8,9,15,17,66,100] However, the affinity of PEDOT:PSS to polymers is known to be weak,[47,105,108] likely due to polymer substrates being hydrophobic and exhibiting poor adhesive properties.[47,146] There are a number of variables that contribute to adhesion which have been reviewed in the literature.[146-148] In the case of PEDOT:PSS, adhesion is complicated since there are two states of the polymer that need to be considered: how it interacts as a liquid, that is primarily water, and then as a solid film. The presence of excess PSS in solution also needs to be considered since it may alter wetting properties (section 1.4.1). Therefore, the factors most likely to affect the adhesion of PEDOT:PSS are substrate roughness, wettability, and electrostatic interactions.[29,146,147]

It is thought that a rougher material will allow for greater mechanical interlocking and increase the surface area of interaction between the two materials.[146-148] However, this is not always the case and it has often been shown that good adhesion can be achieved on smooth substrates

(e.g., glass),[147,148] but when polymer substrates have been roughened, adhesion has decreased.[149] It has also been argued that roughness it not enough to create strong adhesive bonds, with good molecular bonding being a greater priority.[146] Electrostatic interaction relates to the charge transfer (such as van der Waals or dipole-dipole interaction) that takes place when two materials are brought into contact.[29,146,147] This relies on polar groups that can lead to these interactions, as well as close contact between materials that is free of defects and air bubbles.[146,149-151] However, wettability will affect both of these parameters since it will determine how much of the PEDOT:PSS solution will be in contact with the surface of the substrate.[29,146,147] On hydrophobic surfaces, hydrophilic PEDOT:PSS solution will show poor wetting properties due to a large gap between substrate surface energy and solution surface tension (section 1.4.1).[47,104] This will cause the solution to bead on the surface rather than spread. Therefore, even if the surface has been roughened, the solution will not flow into the gaps created to utilise an increased surface contact.[29,146,147] Additionally, this will also affect electrostatic interactions since a reduced surface contact decreases the possibility for molecular bonds to form.[29,146,147] This shows that wetting is the most important parameter to consider since it will determine the ability of the other adhesion mechanisms to perform.

1.6.1 Polydopamine (PDA)

PDA (Figure 1-13a) is a biopolymer from the melanin family which is formed via the oxidative polymerisation of dopamine (Figure 1-13b) to create a black powered substance.[152,153] A PDA derivative, 2,4-dihydroxyphenylalanine (DOPA) (Figure 1-13c), has been found to be synthesised by mussels, allowing them to attach to rocks and boats in harsh conditions.[152,154,155] Much like DOPA, PDA has a number of functional groups with which other molecules can strongly interact.[152,153,156] PDA has gathered interest as a surface modifier or primer layer due to the ability to adhere to almost any substrate such as noble metals, metal oxides, ceramics, and

polymers (including PET, polyethylene (PE), and polytetrafluoroethylene (PTFE)).[152,153,157,158] It has also been shown to alter the surface energy of these substrates, causing wettability to improve.[155] This could provide better conditions for PEDOT:PSS solution to spread, therefore, increasing surface contact and allowing for more electrostatic interaction to take place. Furthermore, once the PEDOT:PSS is dry, the PDA will provide more functional groups to form molecular bonds, improving adhesive potential.[152,153,156]

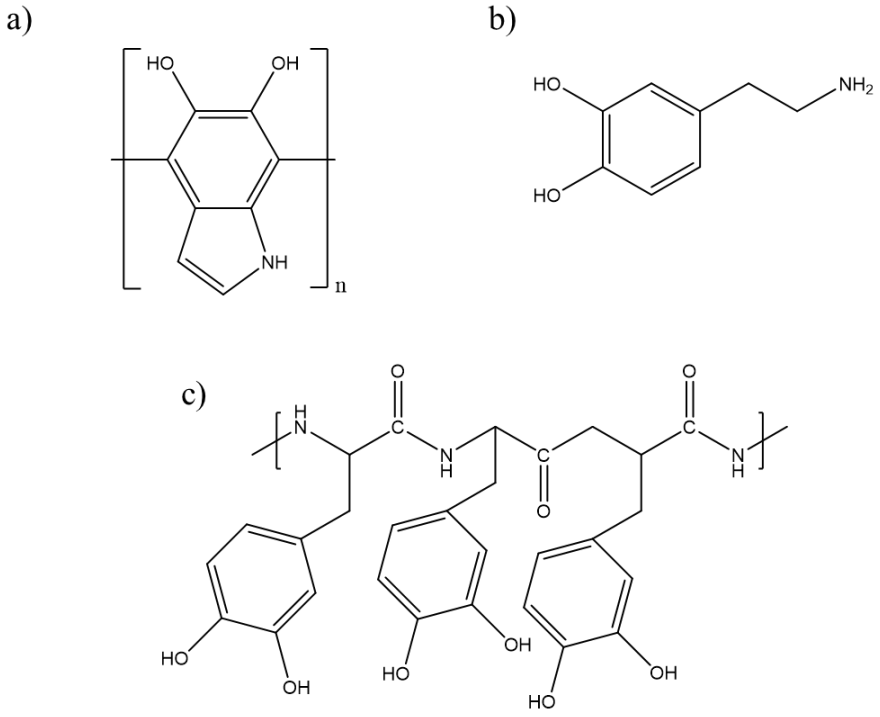

Figure 1-13: Chemical structures of a) PDA, b) dopamine, c) DOPA. Replicated from Kwon, et al. (2018)[159] and Jia, et al. (2019)[155]

The synthesis of PDA in this study is detailed in section 2.1.1 following the method used by Lee, *et al.* (2007)[152]. Typically, an aqueous dopamine HCl solution is prepared where the concentration of dopamine has been shown to affect the PDA produced.[153,160,161] For example, greater dopamine concentrations lead to larger PDA particles,[161] however, a concentration

greater than 2 mg/ml is recommended to form PDA films.[162] When PDA is synthesised via oxidation, the pH of the solution needs to be greater than pH 7.5.[163,164] This is primarily done through the use of buffers such as bicarbonate, phosphate, and tris(hydroxymethyl)aminomethane (Tris) (Figure 1-14),[152,161,164] the latter of which was used in this study (section 2.1.1). The type of buffer can also affect the properties of the PDA films produced, such as film thickness and adhesive properties.[152,161,164] When polymerised in the presence of a substrate, PDA synthesised with Tris buffer forms as a coating on the substrate material.[152,156,161] The submersion time of the substrate during PDA polymerisation can also affect coating thickness, which increases rapidly after initial submersion but plateaus at approximately 50 nm thick after 24 hrs.[152,156,161]

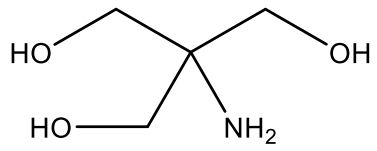

Figure 1-14: Chemical structure of Tris buffer. Replicated from Della Vecchia, et al. (2014)[161]

Although PDA has been used in conjunction with PEDOT:PSS previously, the two polymers were combined in solution, along with other additives, and electrical properties were assessed.[165] However, PDA has not been previously used as a substrate surface modifier to improve PEDOT:PSS application. Given the improvements seen for wettability and adhesion when a PDA primer is applied,[152,153,155,156] its presence will likely benefit PEDOT:PSS application to polymer substrates. PDA is also known to form semi-conducting films,[166-168] and, therefore, it is unlikely to interfere with the conductive properties of PEDOT:PSS.

1.7 Project Scope

The initial focus of this project will be investigation into the properties of pristine PEDOT:PSS. Specifically, thermal analysis via DSC and TGA will identify any thermal transitions and establish the stability of the material at elevated temperatures, as well as inform the upper temperature limits to processing. Degradation analysis using FTIR will also allow for clarification of the decomposition route of PEDOT:PSS. Moisture kinetics will be explored providing insight into the affinity of water and how this might affect electrical properties. Annealing temperature and time studies will also be used to find the optimal processing conditions for pristine PEDOT:PSS.

Similar analyses will be performed on PEDOT:PSS samples containing Tween 80 surfactant, initially examining how it alters the thermal properties and optimal processing conditions. The effect of varying surfactant concentration on film conductivity for dip and drop cast film will be explored using sheet and bulk resistivity measurements. Mechanisms of conductivity enhancement will be assessed via structural analysis using AFM, XRD and Raman spectroscopy. The effect of Tween 80 concentration in PEDOT:PSS solution on viscosity and wettability will also be examined.

Alternative conductivity enhancement methods including film thickness via increased layering using multiple dip castings, the addition of MEK solvent, and the use of solvent washing with MEK, ethanol and methanol will be analysed. These will be employed on pristine PEDOT:PSS as well as PEDOT:PSS containing Tween 80. The effects of each treatment will be analysed with XRD and Raman analysis to establish microstructural changes in the films to explain findings.

Lastly, the use of PDA as a primer on glass and polymeric substrates (polypropylene (PP) and PET) to improve PEDOT:PSS wettability and adhesion will be explored. This will be done through contact angle measurements, film quality assessment, tape scratch testing and force pull-off analysis. Tests will initially be performed on pristine PEDOT:PSS for all substrates with and without the PDA primer. Varying Tween 80 concentration will also be assessed to determine the effect of the surfactant on wettability and adhesion. This will be done without and in conjunction with the PDA primer. A final analysis will be performed on the sheet resistivity of PEDOT:PSS films containing Tween 80 on all substrates with and without PDA. This will inform any effect the primer has on the conducting properties of PEDOT:PSS films.

1.8 References

1. Letheby, H. 1862. On the production of a blue substance by the electrolysis of sulphate of aniline. *Journal of the Chemical Society,* 15**,** 161-163.
2. Chiang, C. K., Fincher, C. R., Park, Y. W., Heeger, A. J., Shirakawa, H., Louis, E. J., Gau, S. C. & MacDiarmid, A. G. 1977. Electrical conductivity in doped polyacetylene. *Physical Review Letters,* 39**,** 1098-1101.
3. Shirakawa, H., Louis, E. J., Macdiarmid, A. G., Chiang, C. K. & Heeger, A. J. 1977. Synthesis of electrically conducting organic polymers: halogen derivatives of polyacetylene, (CH) x. *Journal of the Chemical Society, Chemical Communications***,** 578-580.
4. Salaneck, W., R., Lundstrom, I. & Ranby, B. 1993. *Conjugated Polymers and Related Materials : The Interconnection of Chemical and Electronic Structure : Proceedings of the Eighty-first Nobel Symposium,* New York, United States, Oxford University Press Inc.
5. Elschner, A., Kirchmeyer, S., Lövenich, W., Merker, U. & Reuter, K. 2011. *PEDOT; principals and applications of an intrinsically conductive polymer*, CRC Press.
6. Groenendaal, L., Jonas, F., Freitag, D., Pielartzik, H. & Reynolds, J. R. 2000. Poly(3,4- ethylenedioxythiophene) and Its Derivatives: Past, Present, and Future. *Advanced Materials,* 12**,** 481-494.
7. Gupta, S. K., Jha, P., Singh, A., Chehimi, M. M. & Aswal, D. K. 2015. Flexible organic semiconductor thin films. *Journal of Materials Chemistry C,* 3**,** 8468-8479.
8. Crawford, G. P. 2005. *Flexible flat panel displays,* Chichester, John Wiley & Sons, Ltd.
9. Lee, J.-H., Liu, D. N. & Wu, S.-T. 2008. *Introduction to flat panel displays,* Chichester, Wiley.
10. Street, G. B. & Clarke, T. C. 1981. Conducting polymers: A review of recent work. *IBM Journal of Research and Development,* 25**,** 51-57.
11. Tourillon, G. & Garnier, F. 1982. New electrochemically generated organic conducting polymers. *Journal of Electroanalytical Chemistry,* 135**,** 173-178.
12. Zotti, G., Zecchin, S., Schiavon, G., Louwet, F., Groenendaal, L., Crispin, X., Osikowicz, W., Salaneck, W. & Fahlman, M. 2003. Electrochemical and XPS studies toward the role of monomeric and polymeric sulfonate counterions in the synthesis, composition, and properties of poly(3,4- ethylenedioxythiophene). *Macromolecules,* 36**,** 3337-3344.
13. Ouyang, J. 2013. "Secondary doping" methods to significantly enhance the conductivity of PEDOT:PSS for its application as transparent electrode of optoelectronic devices. *Displays,* 34**,** 423-436.
14. Jonas, F. & Schrader, L. 1991. Conductive modifications of polymers with polypyrroles and polythiophenes. *Synthetic Metals,* 41**,** 831-836.
15. Wen, Y. & Xu, J. 2017. Scientific Importance of Water-Processable PEDOT–PSS and Preparation, Challenge and New Application in Sensors of Its Film Electrode: A Review. 55**,** 1121-1150.
16. Rozlosnik, N. 2009. New directions in medical biosensors employing poly(3,4-ethylenedioxy thiophene) derivative-based electrodes. *Analytical and Bioanalytical Chemistry,* 395**,** 637-645.
17. Kirchmeyer, S., Reuter, K. & Simpson, J. 2007. Poly(3,4-ethylene dioxythiophene) scientific importance, remarkable properties, and applications. *In:* Skotheim, T. & Reynolds, J. (eds.) *Handbook of conducting polymers.* 3rd ed. Boca Raton, London and New York: CRC press.

18. Kroon, R., Mengistie, D. A., Kiefer, D., Hynynen, J., Ryan, J. D., Yu, L. & Mller, C. 2016. Thermoelectric plastics: from design to synthesis, processing and structureproperty relationships. *Chemical Society Reviews,* 45**,** 6147-6164.
19. Jonas, F. & Krafft, W. EP 440 957 (Bayer AG). Prior: December 20, 1990.
20. Cui, J., Wang, A., Edleman, N. L., Ni, J., Lee, P., Armstrong, N. R. & Marks, T. J. 2001. Indium Tin Oxide Alternatives—High Work Function Transparent Conducting Oxides as Anodes for Organic Light-Emitting Diodes. *Advanced Materials,* 13**,** 1476-1480.
21. Kirchmeyer, S. & Reuter, K. 2005. Scientific importance, properties and growing applications of poly(3,4-ethylenedioxythiophene). *Journal of Materials Chemistry,* 15**,** 2077-2088.
22. Mengistie, D. A., Wang, P.-c. & Chu, C.-w. 2013. Effect of molecular weight of additives on the conductivity of PEDOT:PSS and efficiency for ITO-free organic solar cells. *Journal of Materials Chemistry A,* 1**,** 9907-9915.
23. Ouyang, J., Chu, C. W., Chen, F. C., Xu, Q. & Yang, Y. 2005. High-Conductivity Poly(3,4-ethylenedioxythiophene):Poly(styrene sulfonate) Film and Its Application in Polymer Optoelectronic Devices. *Advanced Functional Materials,* 15**,** 203-208.
24. Po, R., Carbonera, C., Bernardi, A., Tinti, F. & Camaioni, N. 2012. Polymer- and carbon-based electrodes for polymer solar cells: Toward low-cost, continuous fabrication over large area. *Solar Energy Materials and Solar Cells,* 100**,** 97-114.
25. Sun, K., Zhang, S., Li, P., Xia, Y., Zhang, X., Du, D., Isikgor, F. & Ouyang, J. 2015. Review on application of PEDOTs and PEDOT:PSS in energy conversion and storage devices. *Journal of Materials Science: Materials in Electronics,* 26**,** 4438-4462.
26. Cairns, D. R. & Crawford, G. P. 2005. Electromechanical Properties of Transparent Conducting Substrates for Flexible Electronic Displays. *Proceedings of the IEEE,* 93**,** 1451-1458.
27. Lubianez, R. P., Kirchmeyer, S. & Gaiser, D. 2008. Advances in PEDOT: PSS conductive polymer dispersions.
28. Bubnova, O., Khan, Z. U., Wang, H., Braun, S., Evans, D. R., Fabretto, M., Hojati-Talemi, P., Dagnelund, D., Arlin, J.-B., Geerts, Y. H., Desbief, S., Breiby, D. W., Andreasen, J. W., Lazzaroni, R., Chen, W. M., Zozoulenko, I., Fahlman, M., Murphy, P. J., Berggren, M. & Crispin, X. 2013. Semi-metallic polymers. *Nature Materials,* 13**,** 190.
29. Callister, W. D. 2000. Materials science and engineering: an introduction. 5th ed. New York; Chichester: Wiley.
30. Bredas, J. L., Themans, B., Andre, J. M., Chance, R. R. & Silbey, R. 1984. The role of mobile organic radicals and ions (solitons, polarons and bipolarons) in the transport properties of doped conjugated polymers. *Synthetic Metals,* 9**,** 265-274.
31. Crispin, X., Marciniak, S., Osikowicz, W., Zotti, G., van der Gon, A. W. D., Louwet, F., Fahlman, M., Groenendaal, L., De Schryver, F. & Salaneck, W. R. 2003. Conductivity, morphology, interfacial chemistry, and stability of poly(3,4-ethylene dioxythiophene)–poly(styrene sulfonate): A photoelectron spectroscopy study. *Journal of polymer science. Part B, Polymer physics,* 41**,** 2561-2583.
32. Aasmundtveit, K. E., Samuelsen, E. J., Pettersson, L. A. A., Inganäs, O., Johansson, T. & Feidenhans, R. 1999. Structure of thin films of poly(3,4-ethylenedioxythiophene). *Synthetic Metals,* 101**,** 561-564.
33. Clayden, J. 2012. *Organic chemistry*, Oxford : Oxford University Press, c2012.
34. Crispin, X., Jakobsson, F. L. E., Crispin, A., Grim, P. C. M., Andersson, P., Volodin, A., Van Haesendonck, C., Van Der Auweraer, M., Salaneck, W. R. & Berggren, M. 2006. The origin of the high conductivity of poly(3,4-ethylenedioxythiophene)-

poly(styrenesulfonate) (PEDOT-PSS) plastic electrodes. *Chemistry of Materials,* 18**,** 4354-4360.
35. Geskin, V. M. & Brédas, J. L. 2003. Polaron Pair versus Bipolaron on Oligothiophene Chains: A Theoretical Study of the Singlet and Triplet States. *Chemphyschem,* 4**,** 498-505.
36. Kim, N., Lee, B. H., Choi, D., Kim, G., Kim, H., Kim, J.-R., Lee, J., Kahng, Y. H. & Lee, K. 2012. Role of interchain coupling in the metallic state of conducting polymers. *Physics Review Letters,* 109**,** 106405-106405.
37. Martinez, C., R. & Iverson, B., L. 2012. Rethinking the term "pi-stacking". *Chemical Science,* 3**,** 2191-2201.
38. Sinnokrot, M. O., Valeev, E. F. & Sherrill, C. D. 2002. Estimates of the ab initio limit for pi-pi interactions: the benzene dimer. *Journal of the American Chemical Society,* 124**,** 10887-10893.
39. Kim, S.-M., Kim, C.-H., Kim, Y., Kim, N., Lee, W.-J., Lee, E.-H., Kim, D., Park, S., Lee, K., Rivnay, J. & Yoon, M.-H. 2018. Influence of PEDOT:PSS crystallinity and composition on electrochemical transistor performance and long-term stability. *Nature communications,* 9**,** 3858-3858.
40. Gangopadhyay, R., Das, B. & Molla, M. R. 2014. How does PEDOT combine with PSS? Insights from structural studies. *RSC Advances,* 4**,** 43912-43920.
41. Forrest, S. R. 2004. The path to ubiquitous and low-cost organic electronic appliances on plastic. *Nature,* 428**,** 911.
42. Atkins, P. W. 2017. Elements of physical chemistry. *In:* De Paula, J. & Smith, D. (eds.) 7th edition. ed. Oxford: Oxford University Press.
43. Cornil, J., Beljonne, D. & Brédas, J. L. 1995. Nature of optical transitions in conjugated oligomers. I. Theoretical characterization of neutral and doped oligo(phenylenevinylene)s. *The Journal of chemical physics,* 103**,** 834-841.
44. Brédas, J. L., Wudl, F. & Heeger, A. J. 1987. Polarons and bipolarons in doped polythiophene: A theoretical investigation. *Solid state communications,* 63**,** 577-580.
45. McMurry, J. 2000. *Organic Chemistry,* Pacific Grove, CA, Brooks/Cole.
46. Zykwinska, A., Domagala, W., Czardybon, A., Pilawa, B. & Lapkowski, M. 2003. In situ EPR spectroelectrochemical studies of paramagnetic centres in poly(3,4-ethylenedioxythiophene) (PEDOT) and poly(3,4-butylenedioxythiophene) (PBuDOT) films. *Chemical physics,* 292**,** 31-45.
47. Oh, J. Y., Shin, M., Lee, J. B., Ahn, J. H., Baik, H. K. & Jeong, U. 2014. Effect of PEDOT nanofibril networks on the conductivity, flexibility, and coatability of PEDOT:PSS films. *ACS Applied Materials and Interfaces,* 6**,** 6954-6961.
48. Takano, T., Masunaga, H., Fujiwara, A., Okuzaki, H. & Sasaki, T. 2012. PEDOT nanocrystal in highly conductive PEDOT:PSS polymer films. *Macromolecules,* 45**,** 3859-3865.
49. Mamadou, I., Yu, L.-T. & Buvet, R. 1974. Conductivity of polyaniline and polypyrrole composites under point-plane geometry electronic injection. *Comptes Rendus C (Sciences Chimiques),* 279**,** 931-934.
50. Dall'Olio, A., Dascola, G., Varacca, V. & Bocchi, V. 1968. Resonance paramagnetique electronique et conductivite d'un noir d'oxypyrrol electrolytique. *Comptes Rendus C (Sciences Chimiques),* 267**,** 433-435.
51. Jonas, F. & Heywang, G. 1994. Technical applications for conductive polymers. *Electrochimica acta,* 39**,** 1345-1347.

52. Winther-Jensen, B. & West, K. 2004. Vapor-Phase Polymerization of 3,4-Ethylenedioxythiophene: A Route to Highly Conducting Polymer Surface Layers. *Macromolecules,* 37**,** 4538-4543.
53. Lakshmi, K. 2007. *Development of thermoplastic conducting polymer composites based on polyaniline and polythiophenes for microwave and electrical applications.* Doctor of Philosophy, Cochin University of Science and Technology.
54. Horikawa, M., Fujiki, T., Shirosaki, T., Ryu, N., Sakurai, H., Nagaoka, S. & Ihara, H. 2015. The development of a highly conductive PEDOT system by doping with partially crystalline sulfated cellulose and its electric conductivity. *J. Mater. Chem. C,* 3**,** 8881-8887.
55. Kiebooms, R., Aleshin, A., Hutchison, K., Wudl, F. & Heeger, A. 1999. Doped poly(3,4- ethylenedioxythiophene) films: Thermal, electromagnetical and morphological analysis. *Synthetic Metals,* 101**,** 436-437.
56. Yılmaztürk, S., Deligöz, H., Yılmazoğlu, M., Damyan, H., Öksüzömer, F., Koç, S. N., Durmuş, A. & Gürkaynak, M. A. 2009. A novel approach for highly proton conductive electrolyte membranes with improved methanol barrier properties: Layer-by- Layer assembly of salt containing polyelectrolytes. *Journal of Membrane Science,* 343**,** 137-146.
57. Lefebvre, M., Qi, Z., Rana, D. & Pickup, P. G. 1999. Chemical synthesis, characterization, and electrochemical studies of poly(3,4- ethylenedioxythiophene)/ Poly(styrene- 4- sulfonate) composites. *Chemistry of Materials,* 11**,** 262-268.
58. Kim, N., Kee, S., Lee, S. H., Lee, B. H., Kahng, Y. H., Jo, Y. R., Kim, B. J. & Lee, K. 2014. Highly Conductive PEDOT:PSS Nanofibrils Induced by Solution- Processed Crystallization. *Advanced Materials,* 26**,** 2268-2272.
59. Shi, H., Liu, C., Jiang, Q. & Xu, J. 2015. Effective Approaches to Improve the Electrical Conductivity of PEDOT:PSS: A Review. *Advanced Electronic Materials,* 1**,** 1-16.
60. Koidis, C., Logothetidis, S., Kapnopoulos, C., Karagiannidis, P. G., Laskarakis, A. & Hastas, N. A. 2011. Substrate treatment and drying conditions effect on the properties of roll-to-roll gravure printed PEDOT:PSS thin films. *Materials Science & Engineering B,* 176**,** 1556-1561.
61. Qi, X.-Y., Yan, D., Jiang, Z., Cao, Y.-K., Yu, Z.-Z., Yavari, F. & Koratkar, N. 2011. Enhanced electrical conductivity in polystyrene nanocomposites at ultra- low graphene content. *ACS Applied Materials and Interfaces,* 3**,** 3130-3133.
62. Stöcker, T., Moos, R. & Köhler, A. 2012. Why does the electrical conductivity in PEDOT:PSS decrease with PSS content? A study combining thermoelectric measurements with impedance spectroscopy. *Journal of Polymer Science, Part B: Polymer Physics,* 50**,** 976-983.
63. Blue Sea Systems. 2002. *Electrical Conductivity of Materials* [Online]. Available: https://www.bluesea.com/resources/108/Electrical_Conductivity_of_Materials [Accessed 08/11/17].
64. Dimitriev, O. P., Piryatinski, Y. P. & Pud, A. A. 2011. Evidence of the controlled interaction between PEDOT and PSS in the PEDOT:PSS complex via concentration changes of the complex solution. *The Journal of Physical Chemistry. B,* 115**,** 1357.
65. Cho, C.-K., Hwang, W.-J., Eun, K., Choa, S.-H., Na, S.-I. & Kim, H.-K. 2011. Mechanical flexibility of transparent PEDOT:PSS electrodes prepared by gravure printing for flexible organic solar cells. *Solar Energy Materials & Solar Cells,* 95**,** 3269-3276.
66. Martin, B. D., Nikolov, N., Pollack, S. K., Saprigin, A., Shashidhar, R., Zhang, F. & Heiney, P. A. 2004. Hydroxylated secondary dopants for surface resistance enhancement in transparent poly(3,4- ethylenedioxythiophene)– poly(styrenesulfonate) thin films. *Synthetic Metals,* 142**,** 187-193.

67. Aleshin, A. N., Williams, S. R. & Heeger, A. J. 1998. Transport properties of poly(3,4- ethylenedioxythiophene)/ poly(styrenesulfonate). *Synthetic Metals,* 94**,** 173-177.
68. Lang, U., Naujoks, N. & Dual, J. 2009. Mechanical characterization of PEDOT:PSS thin films. *Synthetic metals,* 159**,** 473-479.
69. Friedel, B., Keivanidis, P. E., Brenner, T. J. K., Abrusci, A., McNeill, C. R., Friend, R. H. & Greenham, N. C. 2009. Effects of layer thickness and annealing of PEDOT:PSS layers in organic photodetectors. *Macromolecules,* 42**,** 6741-6747.
70. Lang, U., Müller, E., Naujoks, N. & Dual, J. 2009. Microscopical Investigations of PEDOT:PSS Thin Films. *Advanced Functional Materials,* 19**,** 1215-1220.
71. Zhou, J., Anjum, D. H., Chen, L., Xu, X., Ventura, I. A., Jiang, L. & Lubineau, G. 2014. The temperature- dependent microstructure of PEDOT/ PSS films: insights from morphological, mechanical and electrical analyses. *J. Mater. Chem. C,* 2**,** 9903-9910.
72. Kemerink, M., Timpanaro, S., De Kok, M. M., Meulenkamp, E. A., Touwslager, F. J. & Timpanaro, F. J. 2004. Three-dimensional inhomogeneities in PEDOT:PSS films. *Journal of Physical Chemistry B,* 108**,** 18820-18825.
73. Murthy, N. S. & Minor, H. 1995. Analysis of poorly crystallized polymers using resolution enhanced X-ray diffraction scans. *Polymer,* 36**,** 2499-2504.
74. Cullity, B. D. 1956. *Elements of x-ray diffraction,* Reading, Mass. ; London, Addison-Wesley Publishing Company.
75. Murthy, N. S. 2016. X-ray Diffraction from Polymers. *In:* Guo, Q. (ed.) *Polymer Morphology: Principles, Characterization, and Processing.* Hoboken, NJ, USA: John Wiley & Sons, Inc.
76. Giuri, A., Masi, S., Colella, S., Listorti, A., Rizzo, A., Kovtun, A., Dell'Elce, S., Liscio, A. & Corcione, C. E. 2017. Rheological and physical characterization of PEDOT:PSS/Graphine Oxide nanocomposites for perovskite solar cells. *Polymer Engineering & Science,* 57**,** 546-552.
77. Wang, X., Kyaw, A. K. K., Yin, C., Wang, F., Zhu, Q., Tang, T., Yee, P. I. & Xu, J. 2018. Enhancement of thermoelectric performance of PEDOT:PSS films by post-treatment with a superacid. *RSC Adv.,* 8**,** 18334-18340.
78. Yoon, S. S. & Khang, D. 2016. Roles of Nonionic Surfactant Additives in PEDOT:PSS Thin Films. *J. Phys. Chem. C,* 120**,** 29525-29532.
79. Horii, T., Hikawa, H., Katsunuma, M. & Okuzaki, H. 2018. Synthesis of highly conductive PEDOT:PSS and correlation with hierarchical structure. *Polymer,* 140**,** 33-38.
80. Kim, T. Y., Park, C. M., Kim, J. E. & Suh, K. S. 2005. Electronic, chemical and structural change induced by organic solvents in tosylate-doped poly(3,4-ethylenedioxythiophene) (PEDOT-OTs). *Synthetic Metals,* 149**,** 169-174.
81. Huang, J., Miller, P. F., de Mello, J. C., de Mello, A. J. & Bradley, D. D. C. 2003. Influence of thermal treatment on the conductivity and morphology of PEDOT/PSS films. *Synthetic Metals,* 139**,** 569-572.
82. Kawano, K., Pacios, R., Poplavskyy, D., Nelson, J., Bradley, D. D. C. & Durrant, J. R. 2006. Degradation of organic solar cells due to air exposure. *Solar Energy Materials & Solar Cells,* 90**,** 3520-3531.
83. Romyen, N., Thongyai, S., Praserthdam, P. & Wacharawichanant, S. 2017. Effect of Surfactant Addition During Polymerization on Properties of PEDOT:PSS for Electronic Applications. *Journal of Electronic Materials,* 46**,** 6709-6716.
84. Nardes, A. M., Kemerink, M., de Kok, M. M., Vinken, E., Maturova, K. & Janssen, R. A. J. 2008. Conductivity, work function, and environmental stability of PEDOT:PSS thin films treated with sorbitol. *Organic Electronics,* 9**,** 727-734.

85. Thompson, B. T. 2017. *Enhancing the conductivity of PEDOT:PSS on bulk substrates.* Doctor of Philosophy, University of Warwick.
86. Peters, K., Braun, J., Schmidt-Hansberg, B., Scharfer, P. & Schabel, W. 2011. Phase equilibrium of water in different types of PEDOT:PSS. *Chemical Engineering & Processing: Process Intensification,* 50**,** 555-557.
87. Huang, J., Miller, P. F., Wilson, J. S., De Mello, A. J., De Mello, J. C. & Bradley, D. D. C. 2005. Investigation of the Effects of Doping and Post-Deposition Treatments on the Conductivity, Morphology, and Work Function of Poly(3,4-ethylenedioxythiophene)/Poly(styrene sulfonate) Films. *Advanced Functional Materials,* 15**,** 290-296.
88. Kim, Y. H., Sachse, C., Machala, M. L., May, C., Müller-Meskamp, L. & Leo, K. 2011. Highly Conductive PEDOT:PSS Electrode with Optimized Solvent and Thermal Post-Treatment for ITO-Free Organic Solar Cells. *Advanced Functional Materials,* 21**,** 1076-1081.
89. Nitta, A., Imamura, Y., Kawahara, K. & Takeda, K. 2017. Examination of Treatment Methods for a PEDOT:PSS Transparent Conductive Film Produced Using an Inkjet Method. *Advances in Materials Physics and Chemistry,* 07**,** 311-322.
90. Lombardo, V., Apos, Urso, L., Mannino, G., Scalese, S., Spucches, D., La Magna, A., Terrasi, A. & Puglisi, R. A. 2018. Transparent conductive polymer obtained by in-solution doping of PEDOT:PSS. *Polymer,* 155**,** 199-207.
91. Lenntech. 2018. *Water Conductivity* [Online]. Available: https://www.lenntech.com/applications/ultrapure/conductivity/water-conductivity.htm [Accessed 24/05/18].
92. Azzopardi, B., Emmott, C. J. M., Urbina, A., Krebs, F. C., Mutale, J. & Nelson, J. 2011. Economic assessment of solar electricity production from organic-based photovoltaic modules in a domestic environment. *Energy Environmental Science,* 4**,** 3741-3753.
93. Duc, C., Malliaras, G. G., Senez, V. & Vlandas, A. 2018. Long-term ageing of PEDOT:PSS: wettability Study. *Synthetic Metals,* 238**,** 14-21.
94. Tao, C. S., Jiang, J. & Tao, M. 2011. Natural resource limitations to terawatt-scale solar cells. *Solar Energy Materials & Solar Cells,* 95**,** 3176-3181.
95. Chipman, A. 2007. A commodity no more. *Nature,* 449**,** 131.
96. Paetzold, R., Heuser, K., Henseler, D., Roeger, S., Wittmann, G. & Winnacker, A. 2003. Performance of flexible polymeric light-emitting diodes under bending conditions. *Applied physics letters,* 82**,** 3342-3344.
97. Tran, D.-P., Tran, Lu, H.-I. & Lin, C.-K. 2018. Conductive Characteristics of Indium Tin Oxide Thin Film on Polymeric Substrate under Long-Term Static Deformation. *Coatings,* 8**,** 212.
98. Kim, S., Cho, S., Lee, S. J., Lee, G., Kong, M., Moon, S., Myoung, J.-M. & Jeong, U. 2017. Boosting up the electrical performance of low-grade PEDOT:PSS by optimizing non-ionic surfactants. *Nanoscale,* 9**,** 16079-16085.
99. Palavesam, N., Marin, S., Hemmetzberger, D., Landesberger, C., Bock, K. & Kutter, C. 2018. Roll-to-roll processing of film substrates for hybrid integrated flexible electronics. *Flexible and Printed Electronics,* 3**,** 014002-014019.
100. Søndergaard, R., Hösel, M., Angmo, D., Larsen-Olsen, T. T. & Krebs, F. C. 2012. Roll-to-roll fabrication of polymer solar cells. *Materials Today,* 15**,** 36-49.
101. Sirringhaus, H., Kawase, T., Friend, R. H., Shimoda, T., Inbasekaran, M., Wu, W. & Woo, E. P. 2000. High-resolution inkjet printing of all-polymer transistor circuits. *Science (New York, N.Y.),* 290**,** 2123-2126.

102. Eom, S. H., Senthilarasu, S., Uthirakumar, P., Yoon, S. C., Lim, J., Lee, C., Lim, H. S., Lee, J. & Lee, S.-H. 2009. Polymer solar cells based on inkjet-printed PEDOT:PSS layer. *Organic Electronics,* 10**,** 536-542.
103. Hoath, S. D., Hsiao, W.-K., Martin, G. D., Jung, S., Butler, S. A., Morrison, N. F., Harlen, O. G., Yang, L. S., Bain, C. D. & Hutchings, I. M. 2015. Oscillations of aqueous PEDOT:PSS fluid droplets and the properties of complex fluids in drop-on-demand inkjet printing. *Journal of Non-Newtonian Fluid Mechanics,* 223**,** 28-36.
104. Kommeren, S., Coenen, M. J. J., Eggenhuisen, T. M., Slaats, T. W. L., Gorter, H. & Groen, P. 2018. Combining solvents and surfactants for inkjet printing PEDOT:PSS on P3HT/PCBM in organic solar cells. *Organic Electronics,* 61**,** 282-288.
105. Mustonen, T., Kordás, K., Saukko, S., Tóth, G., Penttilä, J. S., Helistö, P., Seppä, H. & Jantunen, H. 2007. Inkjet printing of transparent and conductive patterns of single-walled carbon nanotubes and PEDOT-PSS composites. *Physica Status Solidi (b),* 244**,** 4336-4340.
106. Sriprachuabwong, C., Karuwan, C., Wisitsorrat, A., Phokharatkul, D., Lomas, T., Sritongkham, P. & Tuantranont, A. 2012. Inkjet- printed graphene- PEDOT:PSS modified screen printed carbon electrode for biochemical sensing. *Journal of Materials Chemistry,* 22**,** 5478-5485.
107. Yoshioka, Y. & Jabbour, G. 2006. Desktop inkjet printer as a tool to print conducting polymers. *Synth. Met.,* 156**,** 779-783.
108. Kishi, N., Kondo, Y., Kunieda, H., Hibi, S. & Sawada, Y. 2018. Enhancement of thermoelectric properties of PEDOT:PSS thin films by addition of anionic surfactants. *Journal of Materials Science: Materials in Electronics,* 29**,** 4030-4034.
109. Leclercq, B., Sotton, M., Baszkin, A. & Ter-Minassian-Saraga, L. 1977. Surface modification of corona treated poly(ethylene terephthalate) film: adsorption and wettability studies. *Polymer,* 18**,** 675-680.
110. Hoath, S. D., Jung, S., Hsiao, W.-K. & Hutchings, I. M. 2012. How PEDOT:PSS solutions produce satellite- free inkjets. *Organic Electronics,* 13**,** 3259-3262.
111. Claussen, W. F. 1967. Surface Tension and Surface Structure of Water. *Science,* 156**,** 1226-1227.
112. Khattab, I. S., Bandarkar, F., Fakhree, M. A. A. & Jouyban, A. 2012. Density, viscosity, and surface tension of water+ethanol mixtures from 293 to 323K. *The Korean Journal of Chemical Engineering,* 29**,** 812-817.
113. Kamusewitz, H., Possart, W. & Paul, D. 1993. Measurements of solid-water contact angles in the presence of different vapours. *International Journal of Adhesion and Adhesives,* 13**,** 243-249.
114. Johnston, M. T. & Ewoldt, R. H. 2013. Precision rheometry: Surface tension effects on low-torque measurements in rotational rheometers. *Journal of Rheology,* 57**,** 1515-1532.
115. Wei, R., Chen, J.-H. & Huizinga, J. D. 2014. On the Relationship Between Viscosity and Surface Tension. *Journal of Emerging Investigators*.
116. Kopola, P., Tuomikoski, M., Suhonen, R. & Maaninen, A. 2009. Gravure printed organic light emitting diodes for lighting applications. *Thin Solid Films,* 517**,** 5757-5762.
117. polymersource.com 2010. Poly(4-styrene sulfonic acid) or poly(styrene sulfonic acid) in dialysed form or undialysed form. Sample #: P4998-USSO3H-Undialysed form.
118. Weiss, R. A., Turner, S. R. & Lundberg, R. D. 1985. Sulfonated polystyrene ionomers prepared by emulsion copolymerization of styrene and sodium styrene sulfonate. *Journal of Polymer Science,* 23**,** 525-533.
119. Yu, Z., Xia, Y., Du, D. & Ouyang, J. 2016. PEDOT:PSS Films with Metallic Conductivity through a Treatment with Common Organic Solutions of Organic Salts and

Their Application as a Transparent Electrode of Polymer Solar Cells. *ACS Appl. Mater. Interfaces,* 8**,** 11629-11638.
120. Vitoratos, E., Sakkopoulos, S., Dalas, E., Paliatsas, N., Karageorgopoulos, D., Petraki, F., Kennou, S. & Choulis, S. A. 2009. Thermal degradation mechanisms of PEDOT:PSS. *Organic Electronics: physics, materials, applications,* 10**,** 61-66.
121. Zhou, J., Ventura, I. & Lubineau, G. 2014. Probing the Role of Poly(3,4-ethylenedioxythiophene)/ Poly(styrenesulfonate)-Coated Multiwalled Carbon Nanotubes in the Thermal and Mechanical Properties of Polycarbonate Nanocomposites. *Industrial & Engineering Chemistry Research,* 53**,** 3539-3549.
122. Friedel, B., Brenner, T. J. K., McNeill, C. R., Steiner, U. & Greenham, N. C. 2011. Influence of solution heating on the properties of PEDOT:PSS colloidal solutions and impact on the device performance of polymer solar cells. *Organic Electronics,* 12**,** 1736-1745.
123. Kvarnström, C., Neugebauer, H., Blomquist, S., Ahonen, H. J., Kankare, J. & Ivaska, A. 1999. In situ spectroelectrochemical characterization of poly(3,4-ethylenedioxythiophene). *Electrochimica Acta,* 44**,** 2739-2750.
124. Han, M. G. & Foulger, S. H. 2004. Crystalline Colloidal Arrays Composed of Poly(3,4- ethylenedioxythiophene)-Coated Polystyrene Particles with a Stop Band in the Visible Regime. *Advanced Materials,* 16**,** 231-234.
125. Rutledge, S. A. & Helmy, A. S. 2015. Etch-free patterning of poly(3,4-ethylenedioxythiophene)-poly(styrenesulfonate) for optoelectronics. *ACS applied materials & interfaces,* 7**,** 3940-3948.
126. Glagovich, N. 2005. *IR Absorptions for Representative Functional Groups* [Online]. Available: http://www.instruction.greenriver.edu/kmarr/chem%20162/Chem162%20Labs/Interpreting%20IR%20Spectra/IR%20Absorptions%20for%20Functional%20Groups.htm [Accessed 08/03/2018].
127. Alemu, D., Wei, H.-y., Ho, K.-c. & Chu, C.-w. 2012. Highly conductive PEDOT:PSS electrode by simple film treatment with methanol for ITO-free polymer solar cells. *Energy Environ. Sci.,* 5**,** 9662-9671.
128. Yoon, D. H., Yoon, S. H., Ryu, K.-S. & Park, Y. J. 2016. PEDOT:PSS as multi-functional composite material for enhanced Li-air-battery air electrodes. *Scientific reports,* 6**,** 19962-19962.
129. Jönsson, S. K. M., Birgerson, J., Crispin, X., Greczynski, G., Osikowicz, W., Denier van Der Gon, A. W., Salaneck, W. R. & Fahlman, M. 2003. The effects of solvents on the morphology and sheet resistance in poly(3,4-ethylenedioxythiophene)–polystyrenesulfonic acid (PEDOT–PSS) films. *Synthetic Metals,* 139**,** 1-10.
130. Ouyang, J., Xu, Q., Chu, C.-W., Yang, Y., Li, G. & Shinar, J. 2004. On the mechanism of conductivity enhancement in poly(3,4- ethylenedioxythiophene): poly(styrene sulfonate) film through solvent treatment. *Polymer,* 45**,** 8443-8450.
131. Zhang, S., Kumar, P., Nouas, A., Fontaine, L., Tang, H. & Cicoira, F. 2015. Solvent-induced changes in PEDOT: PSS films for organic electrochemical transistors. *APL Mater.,* 3.
132. Mengistie, D. A., Ibrahem, M. A., Wang, P.-C. & Chu, C.-W. 2014. Highly conductive PEDOT:PSS treated with formic acid for ITO-free polymer solar cells. *ACS applied materials & interfaces,* 6**,** 2292-2299.
133. Miccoli, I., Edler, F., Pfnur, H. & Tegenkamp, C. 2015. The 100th anniversary of the four-point probe technique: the role of probe geometries in isotropic and anisotropic systems. *Journal of Physics-Condensed Matter,* 27.

134. Nardes, A. M., Kemerink, M., Janssen, R. A. J., Bastiaansen, J. A. M., Kiggen, N. M. M., Langeveld, B. M. W., van Breemen, A. J. J. M. & de Kok, M. M. 2007. Microscopic Understanding of the Anisotropic Conductivity of PEDOT:PSS Thin Films. *Advanced Materials,* 19**,** 1196-1200.
135. Lingstedt, L. V., Ghittorelli, M., Lu, H., Koutsouras, D. A., Marszalek, T., Torricelli, F., Crăciun, N. I., Gkoupidenis, P. & Blom, P. W. M. 2019. Effect of DMSO Solvent Treatments on the Performance of PEDOT:PSS Based Organic Electrochemical Transistors. *Advanced Electronic Materials,* 5**,** 1800804.
136. Xia, Y. & Ouyang, J. 2010. Significant Conductivity Enhancement of Conductive Poly(3,4-ethylenedioxythiophene): Poly(styrenesulfonate) Films through a Treatment with Organic Carboxylic Acids and Inorganic Acids. *ACS Applied0 Materials & Interfaces,* 2**,** 474-483.
137. Timpanaro, S., Kemerink, M., Touwslager, F. J., De Kok, M. M. & Schrader, S. 2004. Morphology and conductivity of PEDOT/PSS films studied by scanning–tunneling microscopy. *Chemical Physics Letters,* 394**,** 339-343.
138. Greczynski, G., Kugler, T. & Salaneck, W. R. 1999. Characterization of the PEDOT-PSS system by means of X-ray and ultraviolet photoelectron spectroscopy. *Thin Solid Films,* 354**,** 129-135.
139. Goff, H. D. 1997. Colloidal aspects of ice cream—A review. *International Dairy Journal,* 7**,** 363-373.
140. Pubchem. 2018. *Compound summary for CID 443315, Tween 80* [Online]. National Center for Biotechnology Information. Available: https://pubchem.ncbi.nlm.nih.gov/compound/443315 [Accessed 21/06/2018].
141. Nasybulin, E., Wei, S., Kymissis, I. & Levon, K. 2012. Effect of solubilizing agent on properties of poly(3,4- ethylenedioxythiophene) (PEDOT) electrodeposited from aqueous solution. *Electrochimica Acta,* 78**,** 638-643.
142. Kopola, P. 2010. High efficient plastic solar cells fabricated with a high-throughput gravure printing method. *Solar Energy Materials & Solar Cells,* 94**,** 1673-1681.
143. Setti, L., Fraleoni-Morgera, A., Ballarin, B., Filippini, A., Frascaro, D. & Piana, C. 2005. An amperometric glucose biosensor prototype fabricated by thermal inkjet printing. *Biosensors and Bioelectronics,* 20**,** 2019-2026.
144. Hrehorova, E., Pekarovicova, A. & Fleming, P. D. 2006. Gravure Printability of Conducting Polymer Inks. *Proceedings of IS&T Digital Fabrication, Denver*.
145. Sigma-Aldrich 2018. Product specification: 2-Butanone.
146. Awaja, F., Gilbert, M., Kelly, G., Fox, B. & Pigram, P. J. 2009. Adhesion of polymers. *Progress in polymer science,* 34**,** 948-968.
147. Mittal, K. L. 1977. The role of the interface in adhesion phenomena. *Polymer Engineering and Science,* 17**,** 467-473.
148. Mittal, K. L. 2018. *Advances in contact angle, wettability and adhesion,* Hoboken, New Jersey ; Beverly, Massachusetts, John Wiley & Sons, Incorporated.
149. Basin, V. E. 1984. Advances in understanding the adhesion between solid substrates and organic coatings. *Progress in Organic Coatings,* 12**,** 213-250.
150. Kinloch, A. J. 1980. The science of adhesion - Part 1 Surface and interfacial aspects. *Journal of Materials Science,* 15**,** 2141-2166.
151. Sharpe, L. H. 1993. Interfaces, Interphases and "Adhesion": A Perspective. *The Interfacial Interactions in Polymeric Composites,* 230**,** 1-20.
152. Lee, H., Dellatore, S. M., Miller, W. M. & Messersmith, P. B. 2007. Mussel-inspired surface chemistry for multifunctional coatings. *Science (New York, N.Y.),* 318**,** 426-430.

153. Della Vecchia, N. F., Avolio, R., Alfè, M., Errico, M. E., Napolitano, A. & d'Ischia, M. 2013. Building-Block Diversity in Polydopamine Underpins a Multifunctional Eumelanin-Type Platform Tunable Through a Quinone Control Point. *Advanced Functional Materials,* 23**,** 1331-1340.
154. Waite, J. H. & Tanzer, M. L. 1981. Polyphenolic substance of Mytilus edulis: novel adhesive containing L-dopa and hydroxyproline. *Science,* 212**,** 1038-1040.
155. Jia, L., Han, F., Wang, H., Zhu, C., Guo, Q., Li, J., Zhao, Z., Zhang, Q., Zhu, X. & Li, B. 2019. Polydopamine-assisted surface modification for orthopaedic implants. *Journal of Orthopaedic Translation,* 17**,** 82-95.
156. Tyo, A., Welch, S., Hennenfent, M., Fooroshani, P. K., Lee, B. P. & Rajachar, R. 2019. Development and Characterization of an Antimicrobial Polydopamine Coating for Conservation of Humpback Whales. *Frontiers in Chemistry,* 7**,** 618-618.
157. Jia, Z., Li, H., Zhao, Y., Frazer, L., Qian, B., Borguet, E., Ren, F. & Dikin, D. A. 2017. Electrical and mechanical properties of poly(dopamine)-modified copper/reduced graphene oxide composites. *Journal of Materials Science,* 52**,** 11620-11629.
158. Ou, J., Pan, B., Chen, Y., Xie, C., Xue, M., Wang, F. & Li, W. 2015. Substrate-independent sequential deposition process to obtain the lotus effect based on mussel-inspired polydopamine. *Applied surface science,* 327**,** 149-153.
159. Kwon, I. S. & Bettinger, C. J. 2018. Polydopamine nanostructures as biomaterials for medical applications. *J. Mater. Chem. B,* 6**,** 6895-6903.
160. Del Frari, D., Bour, J., Ball, V., Toniazzo, V. & Ruch, D. 2012. Degradation of polydopamine coatings by sodium hypochlorite: A process depending on the substrate and the film synthesis method. *Polymer degradation and stability,* 97**,** 1844-1849.
161. Della Vecchia, N. F., Luchini, A., Napolitano, A., D'Errico, G., Vitiello, G., Szekely, N., d'Ischia, M. & Paduano, L. 2014. Tris Buffer Modulates Polydopamine Growth, Aggregation, and Paramagnetic Properties. *Langmuir,* 30**,** 9811-9818.
162. Ball, V., Frari, D. D., Toniazzo, V. & Ruch, D. 2012. Kinetics of polydopamine film deposition as a function of pH and dopamine concentration: Insights in the polydopamine deposition mechanism. *Journal of Colloid Interface Science,* 386**,** 366-372.
163. Du, X., Li, L., Li, J., Yang, C., Frenkel, N., Welle, A., Heissler, S., Nefedov, A., Grunze, M. & Levkin, P. A. 2014. UV-Triggered Dopamine Polymerization: Control of Polymerization, Surface Coating, and Photopatterning. *Advanced Materials,* 26**,** 8029-8033.
164. Bernsmann, F., Ball, V., Addiego, F. d. r., Ponche, A., Michel, M., Gracio, J. J. d. A., Toniazzo, V. r. & Ruch, D. 2011. Dopamine−Melanin Film Deposition Depends on the Used Oxidant and Buffer Solution. *Langmuir,* 27**,** 2819-2825.
165. Kanyong, P., Krampa, F. D., Aniweh, Y. & Awandare, G. A. 2018. Polydopamine-functionalized graphene nanoplatelet smart conducting electrode for bio- sensing applications. *Arabian Journal of Chemistry*.
166. Gao, A., Wang, Y.-R., He, X.-W. & Yin, X.-B. 2013. An Electrochemical Hydrogen Peroxide Biosensor Based on Polydopamine-Entrapped G-Quadruplex-Hemin DNAzyme. *Chinese Journal of Analytical Chemistry,* 40**,** 1471-1476.
167. Huang, K.-J., Liu, Y.-J., Wang, H.-B. & Wang, Y.-Y. 2014. A sensitive electrochemical DNA biosensor based on silver nanoparticles-polydopamine@graphene composite. *Electrochimica Acta,* 118**,** 130-137.
168. Liu, P., Bai, F.-Q., Lin, D.-W., Peng, H.-P., Hu, Y., Zheng, Y.-J., Chen, W., Liu, A.-L. & Lin, X.-H. 2016. One-pot green synthesis of mussel-inspired myoglobin–gold nanoparticles–polydopamine–graphene polymeric bionanocomposite for biosensor application. *Journal of Electroanalytical Chemistry,* 764**,** 104-109.

Chapter 2: Experimental

This chapter contains a detailed summary of the methods and experimental procedures used throughout this study including materials, sample preparation, solution, and film characterisation methods. Thermal and Infra-red analysis, sheet resistivity and adhesion testing are also described.

2.1 Materials

In this study, a high conductivity, surfactant free grade of poly(3,4-ethylene dioxythiophene):poly(styrene sulfonate) (PEDOT:PSS) solution with solid content approximately 1.2 % (w/v) in H_2O, density 999 kgm^{-3},[1] was obtained from Sigma-Aldrich (Gillingham, UK). Additives to the PEDOT:PSS solution were the non-ionic surfactant, Tween 80, with density 1064 kgm^{-3},[2] and methyl ethyl ketone (MEK), density 805 kgm^{-3}.[3] Solvent treatments were performed with either MEK, methanol or ethanol. 98% pure dopamine hydrochloride, tris(hydroxymethyl)aminomethane (Tris) buffered saline tablets and 98% pure, 0.1 $molL^{-1}$ NaOH were used for the synthesis of polydopamine (PDA). Polymer sheets were made from PP (Sabic, UK) (T_m=145 °C at 10 °$Cmin^{-1}$) and Melinar laser plus PET (DuPont, UK) (T_g=79 °C, T_m=240 °C at 10 °$Cmin^{-1}$). All materials were supplied by Sigma-Aldrich (Gillingham, UK), unless otherwise specified, and were used as received with no further purification.

2.1.1 Polydopamine (PDA) Synthesis

PDA was synthesised following the method used by Lee, *et al.* (2007)[4]. A Tris buffered saline was made using distilled water to a concentration of 0.05 $molL^{-1}$. The solution pH was measured using a Hanna Instruments HI2211 pH meter (Leighton Buzzard, UK) and adjusted to pH 8.5 with 0.1 $molL^{-1}$ NaOH. Dopamine hydrochloride (2 $mgmL^{-1}$) was added to the tris buffered

saline solution and magnetically stirred (IKA, Germany) for 24 hours to allow for full polymerisation of PDA.

2.1.2 PP and PET Sheet Processing

PP and PET sheets (1 mm) were formed using a Moore E1127 hydraulic hot press (Birmingham, UK) at 190 °C and 280 °C, respectively. The polymer pellets were dried in an oven for 2 hours at 70 °C before forming. Samples (30 g PP, 40 g PET) were placed inside a 1 mm thick, 155 x 175 mm PTFE mould and heated in the press, without pressure, for 3 minutes. A pressure of 10 tonnes was then applied for 5 minutes. Once pressed, the sheets were allowed to air cool.

2.2 Sample Preparation

The samples used in this study were primarily tested as either a solution or in the form of a film (unless otherwise specified). The following outlines the major sample preparation methods used, including the solvent wash method and application of the PDA coating to substrates.

2.2.1 Solution Samples

Solutions of PEDOT:PSS with varying Tween 80 concentrations from 0.00 – 3.50 % by weight (wt%), referred to as PEDOT:PSS/Tween 80, were produced. Mixtures of PEDOT:PSS/MEK and PEDOT:PSS/Tween 80/MEK were also created, with quantities of MEK added based on a 3:1 ratio with Tween 80.[5] PEDOT:PSS solution was measured using a 3 mL graduated plastic pipette while quantities of Tween 80 and MEK were measured using a 10 – 100 µL Eppendorf micropipette (Stevenage, UK). All solutions were magnetically stirred (IKA, Germany) and sonicated (Elma, Germany) for 10 minutes to ensure sufficient mixing and break down any agglomerates prior to film formation or solution testing. Solutions were made in small sample bottles which were stoppered to prevent evaporation throughout preparation and storage.

The high viscosity of Tween 80 caused it to stick to the sides of the pipet tips, resulting in inaccuracies in volume measurements, therefore, the weight percentage (%wt) of Tween 80 and/or MEK was adopted (Equation 2-1), to give a more accurate representation of the additive concentration in solution.

Equation 2-1

$$\%\, Addition = \frac{weight_{Addition}}{weight_{Total}} \times 100$$

Note: the concentrations of early experiments were initially measured by volume and converted to approximate wt% (as highlighted throughout). This was done using individual component densities to calculate the mass of the constituent based on the volume added. These mass values were then used in Equation 2-1 as before.

All concentrations are quoted in terms of the additive quantities in solution. Ratios of Tween 80 and MEK to PEDOT:PSS are not equivalent after drying since the water is removed.

2.2.2 Film Samples

Various substrate materials, geometries and casting methods were used to create films of PEDOT:PSS with and without Tween 80 and/or MEK. Prior to casting, the glass substrates were washed with hot water and detergent and then cleaned with acetone before being rinsed with distilled water and dried. PP and PET were rinsed with distilled water and dried. The two main casting methods used, drop casting (section 2.2.2.1) and dip casting (section 2.2.2.2), were employed in an attempt to mimic the application conditions of bulk manufacturing by R2R and IJP processing, respectively (section 1.3.4). Films were annealed at 140 °C for 1 hour in a Memmert Universal Digital Oven (Schwabach, Germany) following casting and allowed to equilibrate in atmospheric conditions for at least 12 hours prior to testing (unless otherwise specified).

2.2.2.1 Drop Casting

Solutions were drop cast onto substrates of varying materials and geometries, as summarised in Table 2-1. Solution quantities above 1 mL were measured using a 3 mL graduated plastic pipette and quantities below 1 mL using a 100 – 1000 µL Eppendorf micropipette.

Table 2-1: Summary of film preparation showing for drop cast films showing substrate material and geometry, quantity of solutions and film size produced

Substrate Material	Substrate Shape/Size (mm)	Solution Quantity Used (mL)	Sample Shape/Size (mm)
Glass (petri dish)	60 Ø	4.0	60 Ø
		2.0	
Glass (slide)	25 x 25	0.4	25 x 25
	20 x 10	0.2	10 x 10
Glass (slide)/PDA	20 x 10	0.2	10 x 10
PP			
PP/PDA			
PET			
PET/PDA			

2.2.2.2 Dip Casting and Multiple Dip Cast Samples

Dip casting was performed on various substrate materials following a similar preparation route to Alemu, *et al.* (2012)[6] (Table 2-2). Substrates were submerged into solution for 30 seconds. Excess solution was removed from the base of the substrate before annealing at 140 °C for 1 hour (unless otherwise stated). For samples that were dipped cast multiple times, the film was annealed, in the same conditions, and allowed to cool between each layer applied. Multiple dip samples were formed on glass substates only.

Table 2-2: Summary of film preparation for dip cast films showing substrate material and geometry and film size produced

Substrate Material	Substrate Shape/Size (mm)	Sample Shape/Size (mm)
Glass (slide)	20 x 10	10 x 10
Glass (slide)/PDA		
PP		
PP/PDA		
PET		
PET/PDA		

2.2.3 PDA Substrate Coating

Substrates of glass, PP and PET were coated in PDA (Table 2-1& 2-2) to assess its effect on the adhesion and sheet resistivity of PEDOT:PSS/Tween 80 films. Coating was achieved by fully submerging the substrates in PDA solution during polymerisation (section 2.1.1) for at least 24 hours. After submersion, samples were washed with distilled water and dried in the oven at 40 °C for 8 hours before film casting.

2.2.4 Solvent Wash Samples

Solvent washing of film samples was performed using three solvents: MEK, ethanol and methanol. These treatments were only performed on films that had been dip cast with a single layer onto a glass substrate following annealing. Washing was performed by completely submerging the film into a solvent bath and holding for 30 seconds. After treatment, films were re-annealed at 140 °C for 1 hour.

2.3 Solution Characterisation

To assess the suitability of solutions for bulk processing methods, such as IJP and R2R, the properties of the PEDOT:PSS solution and the effect of Tween 80 and/or MEK must be understood. Namely, solution viscosity and surface tension play a key role in both manufacturing processes as they determine the flow of the solution as well as indicating the affinity of the solution for a substrate.

2.3.1 Rheology

Rheology is a common analytical technique to study the resistance to flow of a solution under a given rotational force, i.e., shear rate. The rheometer applies a known shear rate to the solution across a specific area and geometry. By incrementally increasing the shear rate on a log scale, a range of data can be obtained regarding the changing viscosity of the solution under varying stress.

2.3.1.1 Methodology

Rheology was performed on a Kinexus Pro+ Rheometer (Netzsch) with a 4 °, 40 mm diameter cone and plate geometry. PEDOT:PSS/Tween 80 solution (approximately 1.2 mL) was pipetted onto the lower plate. The upper plate was then lowered to give a measuring gap of 1 mm. The shear rate was incrementally increased from 0.01 – 100 s^{-1} under a constant temperature of 25 °C.

2.3.2 Surface Tension

2.3.2.1 Contact Angles

Contact angle was used to assess the wettability of PEDOT:PSS/Tween 80 solutions on various substrates. A lower contact angle indicates better wetting properties whilst a high contact angle

shows the opposite. A single droplet of each PEDOT:PSS/Tween 80 solution was pipetted onto substrates of glass, PP and PET either uncoated or coated in PDA. An image of the droplet was taken and the contact angle of both sides of the droplet measured using ImageJ software (LOCI, University of Wisconsin) (Figure 2-1).

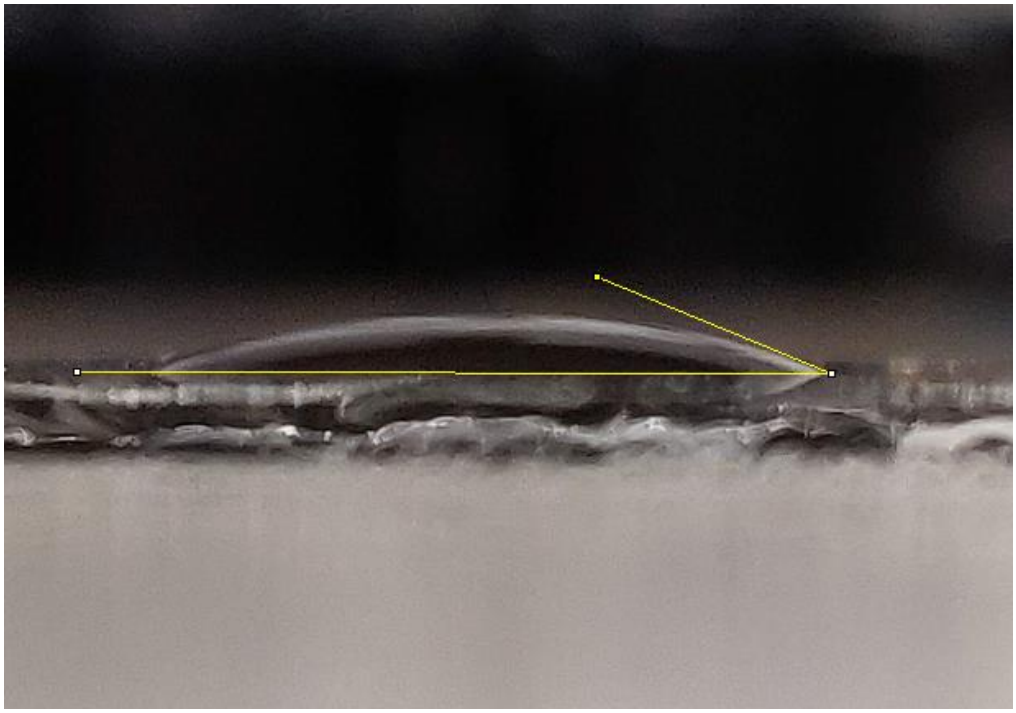

Figure 2-1: Example of solution droplet contact angle measurement using ImageJ software on a glass substrate

2.3.2.2 Capillary Measurements

The height climbed by each PEDOT:PSS/Tween 80 solution up a 0.8 mm diameter glass capillary at room temperature under atmospheric conditions was measured using the set up depicted in Figure 2-2. 10 minutes were allowed before measurements were taken to ensure maximum capillary climb by the solution.

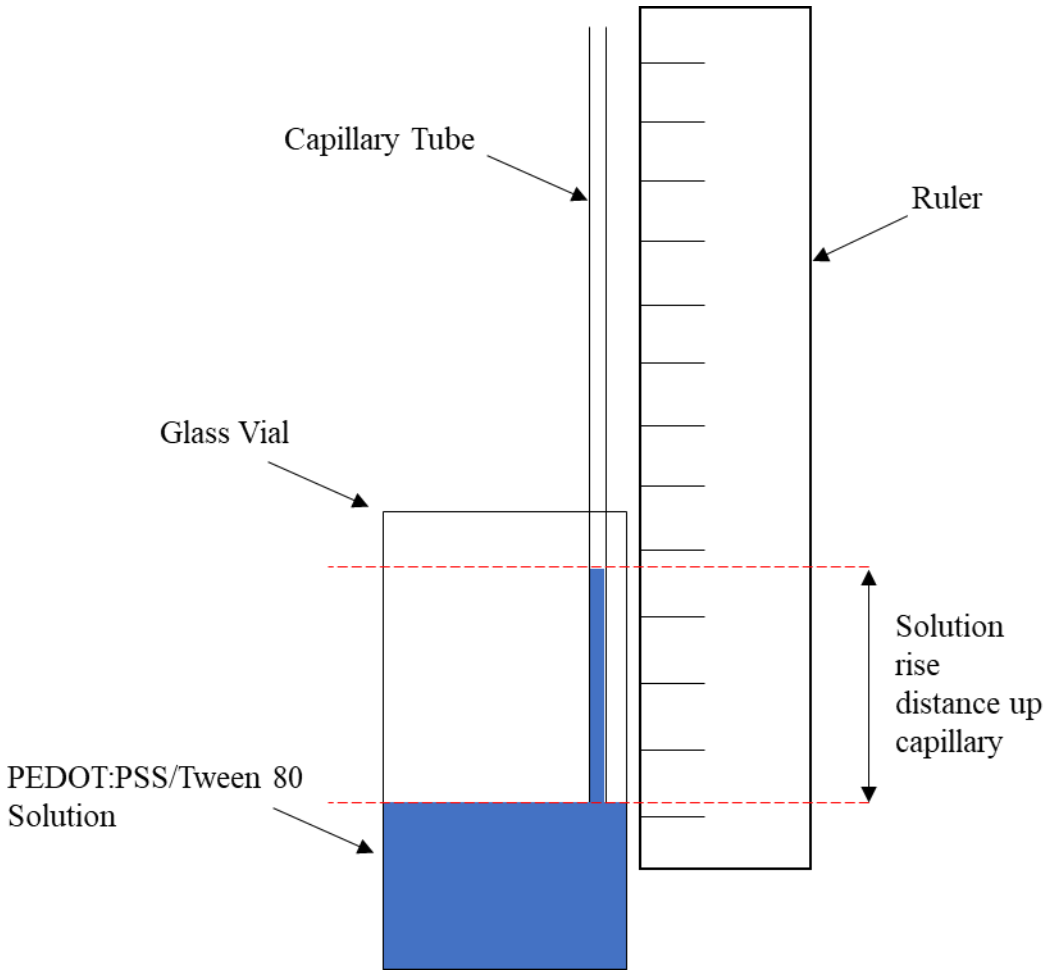

Figure 2-2: Schematic diagram showing the experimental set up for the capillary rise measurements

2.3.2.3 Surface Tension Calculation

Surface tensions of PEDOT:PSS/Tween 80 solutions were calculated using a similar method to Li, *et al.* (2018)[7], with the exception that the contact angle was measured and not assumed to be 0 ° (Equation 2-2).

Equation 2-2

$$Surface\ tension = \frac{\rho g r}{2} x \frac{h}{cos\theta}$$

where ρ is the solution density, g is the acceleration due to gravity (taken as 9.8 ms^{-1}), r is the radius of the capillary tube, h is the height the solution climbed up the capillary, and θ is the measured contact angle in radians.

Solutions densities (ρ) were calculated using Equation 2-3. Volumes (Vol) of PEDOT:PSS and Tween 80 were calculated using measured mass (m) of individual components and respective densities. The calculated volumes and measured masses were then used to recalculate overall density.

Equation 2-3

$$\rho = \frac{m_{PEDOT:PSS} + m_{Tween\,80}}{Vol_{PEDOT:PSS} + Vol_{Tween\,80}}$$

2.4 Thermal, Degradation and Infrared Analysis

Common thermal analytical techniques were used to assess the water kinetics of pristine PEDOT:PSS (also see section 2.5.1). The degradation of pristine PEDOT:PSS, PEDOT:PSS/Tween 80 and PEDOT:PSS/Tween 80/MEK were evaluated through thermal analysis and FTIR. The degradation properties of pristine Tween 80 were also assessed through thermal, FTIR and visual analysis.

2.4.1 Thermal Gravimetric Analysis (TGA)

TGA measures the loss of mass from a sample through a ramp heating run. The mass losses present as ‘drops’ or ‘dips’ on the TGA trace and are attributed to processes such as water loss or mechanisms of degradation. By associating these processes with the corresponding temperature at which they occur, upper temperature limits can be set on further thermal analysis and processing conditions. A derivative thermogravimetry (DTG) trace can also be obtained from the TGA experiment to show the rate of mass loss throughout the heating run. This was

used with pristine PEDOT:PSS samples to establish temperatures where rate of mass loss was greatest.

2.4.1.1 Methodology

TGA was performed on a Netzsch STA 449 C TGA controlled by Proteus analysis software (Berlin, Germany). Before each run a buoyancy correction was carried out with an empty pan as a background. Analysis was performed on a range of solution mixes in differing processing and testing conditions (Table 2-3) but all heating rates remained constant at 10 °Cmin^{-1}. For all samples (except pristine Tween 80), a dry mass of 5 – 15 mg in the crucible was used. This was achieved by repeatedly filling the crucible with solution, then setting the sample at the specified temperature (Table 2-3) for 1 hour. Samples were then left in atmospheric conditions to equilibrate for a minimum of 12 hours prior to TGA. For the sample of pristine Tween 80, the crucible was filled, and the liquid was tested without a setting or equilibration stage.

Table 2-3: Solution mixes and corresponding setting temperature, crucible and testing conditions used in TGA analysis

Solution Composition		Setting Temp. (°C)	Crucible Material	Purge Gas	Max. Temp. (°C)
PEDOT:PSS		95	Aluminium	Argon	450
		95	Aluminium	Air	450
PEDOT:PSS	0.37 wt% Tween 80	100	Alumina	Air	400
	0.93 wt% Tween 80	100	Alumina	Air	400
	1.32 wt% Tween 80	100	Alumina	Air	400
	0.52 wt% Tween 80, 1.19 wt% MEK	90	Aluminium	Air	400
Tween 80		N/a	Aluminium	Air	400

2.4.2 Differential Scanning Calorimetry (DSC)

DSC measures the difference in heat flow between a pan containing a sample and an empty reference pan as they are heated at a specific rate. Temperature differences, due to either thermal transitions or loss of water from the sample, are measured by the DSC. This change is then outputted as a difference in heat flow as a function of temperature. In this study, the DSC was used for two main purposes: to thoroughly investigate any potential thermal transitions in dry, pristine PEDOT:PSS; and to assess the water absorption kinetics of pristine PEDOT:PSS in atmospheric conditions.

2.4.2.1 Methodology

DSC was performed on a Mettler Toledo DSC 1 (Greifensee, Switzerland) under nitrogen (50 $mLmin^{-1}$), with a Huber TC100 cooling system (Offenburg, Germany). Heating and cooling control, as well as data analysis was conducted through the 'STARe' software (Mettler Toledo, Switzerland). Dry PEDOT:PSS samples (5 – 15 mg) were created in aluminium pans, by repeatedly filling the crucible and setting at 100 °C for 1 hour. Samples were weighed on an Ohaus Analytical Plus balance (Nänikon, Switzerland).

Thermal transitions of dry PEDOT:PSS were assessed over the temperature range 25 – 220 °C at a heating rate of 50 $°Cmin^{-1}$ and cooling rate of 20 $°Cmin^{-1}$. This was repeated for 11 cycles.

The water kinetics of pristine PEDOT:PSS were evaluated by heating and cooling a sample from 25 – 200 °C at 20 $°Cmin^{-1}$. After each DSC run, the sample was held in atmospheric conditions for 15 – 1440 minutes to allow for moisture uptake. Sample mass was taken before and immediately after each DSC run to measure the water absorbed.

2.4.3 Flash DSC (FDSC)

Similar to the DSC, the FDSC measures the heat flow to the sample as it goes through different thermal transitions. However, sample mass is on the scale of nanograms and instead of a crucible or pan, samples are placed directly onto the thermal sensor on the FDSC chip. The FDSC has the capability to achieve much greater heating and cooling rates which could exaggerate any possible transitions that otherwise cannot be seen by conventional DSC.[8]

2.4.3.1 Methodology

A Mettler Toledo FDSC 1 (Greifensee, Switzerland) with nitrogen purge gas (20 – 30 $mLmin^{-1}$) and a Huber TC100 cooling system (Offenburg, Germany) was used. The use of nitrogen and the Huber TC100 intracooler's two-step gas compression system allows for rapid cooling down to -90 °C. Heating, cooling, and data analysis was conducted through the 'STARe' software (Mettler Toledo, Switzerland).

A nanogram flake of pristine PEDOT:PSS film was paced onto the FDSC chip, and the sample heated and cooled from -90 – 200 °C with two differing heating and cooling rates. Experiment 1 heating and cooling rates were 1000 and 500 $°Cs^{-1}$ respectively, and experiment 2 had rates of 5000 and 1000 $°Cs^{-1}$, respectively. Each experiment consisted of eleven heat/cool cycles.

2.4.4 Bulk Resistivity Temperature Dependence

The resistance[e] of PEDOT:PSS/Tween 80 samples for varying surfactant concentrations was assessed employing a set up commonly used for dielectric thermal analysis (DETA)

[e] Note: Resistance and resistivity are two different terms. Resistance is a relatively arbitrary value which is not material specific and is affected by sample thickness and cross sectional area. Resistivity is a property of the material at a known temperature, therefore, independent of area and thickness.

(Figure 2-3). In this experiment, a constant DC voltage (V) was applied to the sample and the measured current (I) was used to calculate resistance (R) (Equation 2-4).

Equation 2-4

$$R = \frac{V}{I}$$

The whole DETA unit was contained within a furnace which enabled temperature control of the surrounding atmosphere and sample. This allowed for the effect of varying sample temperature on the measured resistance to be analysed. By knowing the sample geometry, bulk resistivity could be calculated as outlined in section 2.4.4.2.

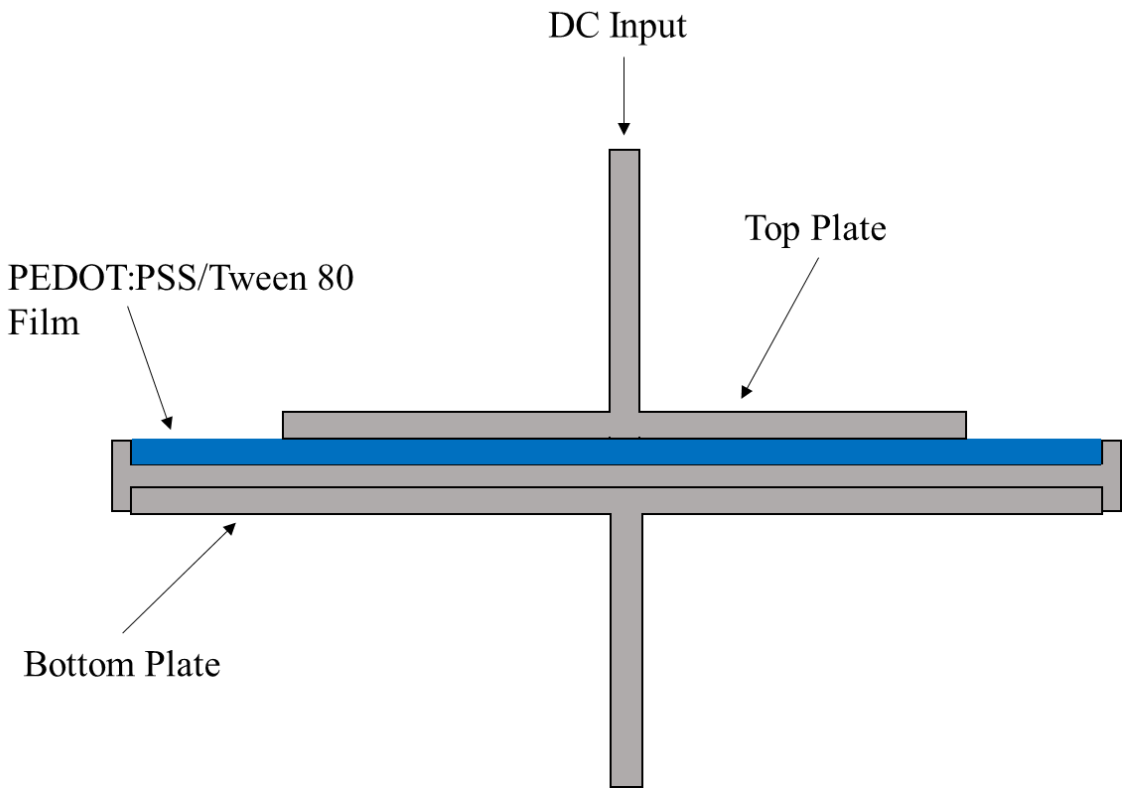

Figure 2-3: Diagram representing the DETA set up to measure PEDOT:PSS/Tween 80 film resistance for bulk resistivity calculation

2.4.4.1 Methodology

Resistance measurement of PEDOT:PSS/Tween 80 samples, containing 0.00 – 1.60 wt% surfactant, were obtained using a Polymer Laboratories dielectric thermal analyser (Church Stretton, UK). PEDOT:PSS/Tween 80 solutions (1 mL) were cast onto an aluminium bottom plate, with an inner ring diameter 32 mm, and allowed to set in atmospheric conditions for 12 hours. A 20 mm diameter top plate was used for measurements to ensure it was only in contact with the film. Resistance was measured throughout a temperature ramp from 25 – 140 °C at a heating rate of 1 °Cmin^{-1}, which was controlled by an A-M temperature programmer (Rheometric Scientific, London). Each sample was measured twice and underwent a 12 hour equilibration period in atmospheric conditions between runs. The sample was considered to be 'annealed' after the first run. Data was measured on a PC through National Instruments LabVIEW 2012 (National Instruments, Austin). Film thickness was obtained by measuring the bottom plate thickness with and without the PEDOT:PSS/Tween 80 film present, using a Mitutoyo IP65 digital micrometre (Andover, UK).

2.4.4.2 Bulk Resistivity and Bulk Conductivity Calculations

Using resistance on its own is not an informative or relevant way of comparing the samples, or with findings in the literature. By knowing both the area across which measurements were taken, and the thickness of the samples, it is possible to account for these geometric factors. Bulk resistivity (Ωm) can be calculated using Equation 2-5. Consequently, the bulk conductivity[f] can then be calculated using Equation 2-6.

[f] To allow for differentiation between conductivity that was calculated from bulk resistivity, the term 'bulk conductivity' is used in this study. This is opposed to when sheet resistivity is used in which case 'conductivity' is used. While the values should theoretically be the same, it was deemed necessary to make this distinction.

Equation 2-5

$$Bulk\ Resistivity = \frac{R \times A}{t}$$

where R is the measured resistance (Ω), A is the area (m^2) of the top plate, and t is the thickness (m) of the PEDOT:PSS/Tween 80 sample.

Equation 2-6

$$\sigma_b = \frac{1}{Bulk\ Resistivity}$$

where σ_b is the bulk conductivity (Sm^{-1}).

2.4.5 Fourier Transform Infrared Spectroscopy (FTIR)

In FTIR analysis, an infrared beam is directed at a sample of material. The bonds within the sample will vibrate at a specific associated frequency. This will cause light of that wavenumber to be absorbed and appears as a peak on the FTIR trace. This allows for identification of the material through the bonds that appear in the absorbance spectra. In this study, the main use of FTIR is to identify a reduction in the peak heights after thermal degradation, which will indicate which bonds have been broken. Degradation analysis was performed on PEDOT:PSS with and without the additions of Tween 80 and MEK, as well as pristine Tween 80. Non-degraded PEDOT:PSS/Tween 80 samples with and without MEK were also analysed to examine the structural effects of these additions. Finally, the solvents used to wash PEDOT:PSS/Tween 80 samples (section 2.2.4) were analysed to search for traces of PSS within the solvent.

2.4.5.1 Methodology

FTIR analysis was performed on a Thermo Fisher Scientific Nicolet 8700 FTIR (Massachusetts, US) with parameter control and data analysis being done on 'OMNIC' software (Thermo Fisher Scientific, Massachusetts). Samples were produced by mixing dried IR invisible potassium

bromide (KBr)[9] with three drops of each solution (Table 2-4), and dried/degraded as required in a Memmert Universal Digital Oven (Schwabach, Germany). The dry KBr – solution mix was then ground and pressed into 8 mm diameter discs. These were scanned in transmission for 100 scans over an IR range of 400 – 4000 cm^{-1} and at a resolution of 4 cm^{-1}. A 'blank' KBr disc was run as a background and subtracted from the sample traces. Samples of pristine PEDOT:PSS, pristine Tween 80, PEDOT:PSS/Tween 80 (0.00 – 3.50 wt% Tween 80), and PEDOT:PSS/Tween 80/MEK (0.52 wt% Tween 80, 1.19 wt% MEK) were created. For degradation comparison, two samples of each surfactant concentration were made and treated as follows: one sample was measured after drying (non-degraded); the other was measured after degradation (degraded). All degradation was induced at 250 °C. Degradation times and drying times/temperatures are summarised in Table 2-4. Spectra were normalised to the largest peak to allow comparison between samples.

Table 2-4: Solution composition and drying conditions used for FTIR analysis

Solution Composition	Drying Temp. (°C)	Drying Time (hrs)	Degradation Time (hrs)
PEDOT:PSS	125	5	5
	140	1	1
PEDOT:PSS/Tween 80	140	1	1
PEDOT:PSS/Tween 80/MEK	110	5	N/a
Tween 80	120	1	1
	140		

The solvents used for the washing of PEDOT:PSS/Tween 80 films (section 2.2.4) were analysed with a liquid crystal ATR set up with a mirror angle of 45 °. These were scanned

100 times over an IR range of 700 – 4000 cm^{-1} and at a resolution of 4 cm^{-1}. A background was run with no sample which was subtracted from the sample trace . The liquid crystal 'trough' was filled with a solvent wash for each run. The cell was rinsed with warm water and detergent, cleaned with acetone and distilled water then dried prior to any testing.

2.4.6 Tween 80 Degradation Visual Analysis

Samples of Tween 80 (2 mL) were heated from 60 – 220 °C in a Memmert Universal Digital Oven (Schwabach, Germany) for 1 hour. Images of the samples were taken on a Sony IMX 519, 16 megapixel camera to observe any colour changes caused by degradation.

2.5 Film Characterisation

2.5.1 Water Absorption Kinetics

The water absorption kinetics of pristine PEDOT:PSS films were explored to compliment the DSC results. Three samples of PEDOT:PSS solution (4 mL) were drop cast into 60 mm diameter petri dishes. Films were set at 95 °C for 2 hours before being annealed at 200 °C for 12 hours to remove all the moisture from the samples. Once dry, sample mass was recorded, and films were placed in a humidity chamber at 22 °C in 54 % humidity with a saturated salt solution of magnesium nitrate. Film mass was recorded at incremental time periods between 0 – 48 hours to determine the rate of moisture uptake.

2.5.2 X-Ray Diffraction (XRD)

XRD was used to analyse chain alignment within PEDOT:PSS/Tween 80 films. In XRD, X-rays are emitted at the sample through a range of angles and the reflective rays detected after interacting with the material. The intensity of X-rays detected at differing incident angles provides information on the alignment of the polymer chains.[10,11] At most angles and in

amorphous polymer, this causes destructive interference causing the intensity detected by the sensor to be low, leading to broad and undefined peaks.[11,12] However, in crystallised samples, certain angles will cause a reflection from the polymer chains which leads to constructive interference.[11,12] This then appears as a large, well defined peak on the XRD trace, from which information on chain spacing and orientation can be inferred.[10-12]

2.5.2.1 Methodology

XRD analysis[g] was performed on a 3rd generation Malvern Panalytical Empyrean XRD (Malvern, UK) equipped with multicore (iCore/dCore) optics and a Pixel3D detector operating in 1D scanning mode. A Cu tube was used giving Cu $K_{\alpha 1/2}$ radiation (1.5419 Å). Scans were performed in the range 1.5 – 50 ° 2θ with a step size of 0.0263 ° and a count time of ~ 147 s/step. XRD was performed on: single dip PEDOT:PSS/Tween 80 samples containing 0.00, 0.47 & 1.32 wt% surfactant; 2 and 5 dip samples containing 0.00 & 1.32 wt% surfactant; methanol wash samples containing 0.00 & 1.32 wt% surfactant; and an ethanol wash sample of pristine PEDOT:PSS. Data was corrected by removing a background trace of the glass substrate.

2.5.3 Atomic Force Microscopy (AFM)

AFM provides topographic images of a sample through a needle attached at a cantilever scanning the sample surface. A laser is reflected off a mirror on the cantilever which allows deflections of the needle to be detected by a sensor.[13] This deflection is then accounted for by a feedback system which adjusts the position of the needle accordingly to maintain a specified height above the sample. In most cases, this means that the feedback is a direct output of surface roughness.[13] In this study , the AFM was used in 'non-contact' mode meaning the needle never

[g] XRD data was collected by Dr Jean Marshall, University of Warwick. Analysis was performed by the author of this study.

comes into contact with the sample surface (as opposed to tapping and contact modes). In this mode, adhesion force mapping can be used to measure the attractive forces between the needle and the sample surface caused by intramolecular attraction and repulsion.[14] For PEDOT:PSS, the forces differ depending on the concentration of each polymer as PEDOT is more conductive than PSS. This will indicate which regions contain higher and lower concentrations of each polymer.

2.5.3.1 Methodology

AFM was performed using a NanoWizard II Atomic Force Microscope (JPK, Berlin) in non-contact mode. An SD-Sphere-CONT-M-10 silicon/silicon oxide sphere tip with a 2 µm diameter and a height of 10-15 µm was used. A 50 x 50 µm area was measured to a resolution of 64 * 64 pixels. Samples of pristine PEDOT:PSS and PEDOT:PSS/Tween 80 with 1.40 wt% surfactant were analysed.

2.5.4 Raman Spectroscopy

Raman spectroscopy is another method that allows analysis of the chemical bonds of a material. A light beam of known wavelength is directed at the sample which causes the bonds to vibrate. These vibrations cause scattering of the light beam which can be detected, the degree of which is termed a 'Raman shift'. Each bond will have an associated Raman shift and a large peak in the spectra suggests a greater concentration of a particular bond. Much like the FTIR, this will give an overall impression of the bonds present within the material.

2.5.4.1 Methodology

Raman spectroscopy was performed[h] on a Renishaw inVia Raman microscope (Wotton-under-Edge, UK) and was operated at wavelength 532 nm. Spectra were normalised to the largest peak to allow for comparison between samples. Raman analysis was performed on: single dip PEDOT:PSS/Tween 80 samples containing 0.00, 0.47 & 1.32 wt% surfactant; 2 and 5 dip samples containing 0.00 & 1.32 wt% surfactant; methanol wash samples containing 0.00 & 1.32 wt% surfactant; and ethanol wash sample of pristine PEDOT:PSS.

2.5.5 Stylus Surface Profiling

Dip cast (including multiple dip), drop cast and solvent washed samples of PEDOT:PSS/Tween 80 were surface profiled to determine the thickness of the films, as well as analysing the roughness. Surface profiling was performed using an Ambios XP200 Stylus Profilometer (Ambios Technology, Santa Cruz). Five measurements were performed on each sample at a spacing of 1.5 mm (Figure 2-4) at a scan speed of 0.10 mms^{-1}, scan length of 10 mm and a stylus force of 10 mg. Data was analysed on XP-Plus Stylus Profilometer software (Ambios Technology, Santa Cruz) and OriginPro 8 (Origin Lab Corporation, Northampton MA). Thickness was measured across a smaller sample area of the film to account for thinner sections at the edges of the films. Therefore, the outer runs (1 & 5) were removed and only data points 5 – 10 mm into the film were taken in the film average. This same data was then used to calculate roughness average (Ra) to assess film quality using Equation 2-7.

[h] Raman data was collected by Dr Jean Marshall, University of Warwick. Analysis was performed by the author of this study.

Equation 2-7

$$Ra = \frac{1}{n}\sum_{n}^{1}|Z_i - Z_{mean}|$$

where n is the number of data points, Z_i is the measured height displacement and Z_{mean} is the average height displacement. In this study, Z_{mean} was calculated as a moving average across 500 data points to account for the curvature of the film.

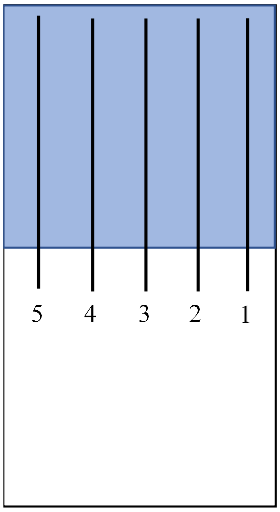

Figure 2-4: Schematic diagram showing the surface profiling scanning paths for each sample

2.6 Sheet Resistivity

The sheet resistivity of the films was measured using an in line 4-point probe. This method measures the changes in voltage between outer and inner probes, all spaced at equal distance, for a constant current (Figure 2-5).[15]

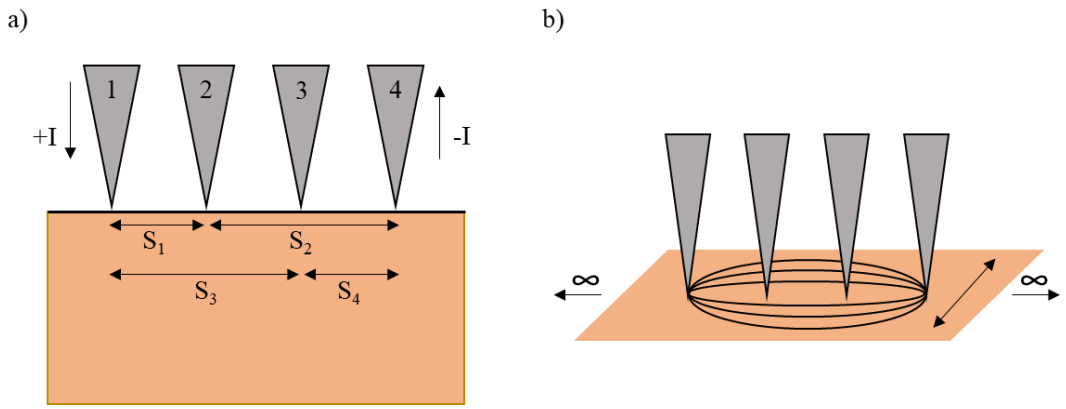

Figure 2-5: Schematic of the 4-point probe method showing a) the probe head set up with S_1=S_4 and S_3=S_2, b) the theoretical flow of electrons for an infinite 2D sheet with no depth. Adapted from Miccoli, et al. (2015)[15]

The ratio of voltage to current is a direct measure of sample resistance, and therefore resistivity. There are also 3 geometric correctional factor that have to be considered which relate to: Sample thickness (F_1); proximity to a single sample edge (F_2); the finite lateral boundaries of the sample (F_3).[15] In the case of F_1, if Equation 2-8 is satisfied (where t is thickness and s is probe spacing) then F_1 can be considered to be equal to 1.[15]

Equation 2-8

$$\frac{t}{s} \leq \frac{1}{5}$$

For F_2 to be equal to 1, then Equation 2-9 must be true (where d is the distance between probe head and edge of sample).[15]

Equation 2-9

$$d \geq s \times 4$$

F_3 can be considered equal to 1 when the sample width is one order of magnitude bigger than half the probe spacing.[15]

In this study, the probe spacing was equal to 1.27 mm and the thickest samples measured were 20 µm. This satisfies the conditions for F_1=1 since $\frac{0.02}{1.27} = 0.015$. For F_2=1 the distance from the edge would need to equal $4 \times 1.27 = 5.08\,mm$. The smallest samples created were 10 x 10 mm and the total probe head width was 3.81 mm which would give a distance to sample edge of 3.095 mm when the probe is placed in the centre of the film. Whilst this does not satisfy the requirements for F_2=1, the correctional factor would still be very close to 1 (F_2 > 0.98).[15] Similarly, the conditions for F_3=1 are not satisfied since one order of magnitude greater than half the probe spacing would be 12.7 mm. Again, this correctional factor would be very close to 1 (F_3 > 0.95). Despite the correctional factors not being implemented in this study, it was assumed that all factors would be greater than 0.95 resulting in only small variations in sheet resistivity measurement caused by differing sample geometries.

Knowing both sheet resistivity and film thickness (section 2.5.5) then allows for calculation of sample conductivity using Equation 2-10.

Equation 2-10

$$\sigma_s = \frac{1}{R_s \times t}$$

where σ_s is the conductivity (Scm^{-1}) calculated using sheet resistivity, R_s is sheet resistivity ($\Omega\square^{-1}$) (pronounced 'ohms per square') and t is film thickness (cm).

2.6.1 Pristine PEDOT:PSS Sheet Resistivity Measurements

Preliminary sheet resistivity measurements were performed on a Jandel Model RM3000 4-point probe (Leighton Buzard, UK), calibrated using an ITO standard with known sheet resistivity. Ten measurements were taken across each sample (Figure 2-6) at a current of 10 µA. Sheet resistivity values were stable within 1 $\Omega\square^{-1}$ before the reading was taken. All films were produced using pristine PEDOT:PSS solution (2 mL) drop cast into a petri dish. Unless

otherwise specified, samples were left for a 12 hour equilibration period in atmospheric conditions prior to any resistivity testing. These preliminary experiments focused on the effects of moisture and varying processing parameters on the sheet resistivity of pristine PEDOT:PSS.

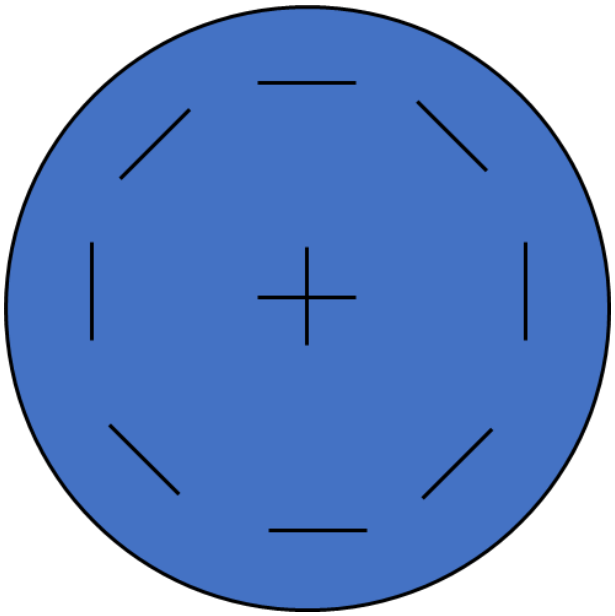

Figure 2-6: Schematic showing the sheet resistivity measurement pattern for films cast into a petri dish. The lines represent the placement and orientation of the 4-point probe head

2.6.1.1 Moisture and Sheet Resistivity

The effect of moisture absorbed on resistivity was investigated by obtaining measurements on the same samples described in section 2.5.1. Sheet resistivity was measured at the same time intervals as sample mass measurements.

2.6.1.2 Initial Setting Temperature

Pristine PEDOT:PSS solution was paced into an oven for 4 hours, whilst still liquid, at varying temperatures between 20 – 125 °C. Sheet resistivity was measured for each sample after equilibration.

2.6.1.3 Setting and Annealing Temperature Variation

PEDOT:PSS solution was set from a liquid at 20, 40 and 60 °C for 4 hours. Films set at each temperature were then annealed over a range of temperatures between 80 – 160 °C for 4 hours. Sheet resistivity was measured after both the setting and annealing stages.

2.6.1.4 Annealing Time Variation

PEDOT:PSS solution set at room temperature in atmospheric conditions for 12 hours. Films were then annealed at 140 °C for annealing times between 10 – 120 minutes, and sheet resistivity was measured after equilibration. Single factor ANOVA analysis was performed on this data to establish statistical differences between annealing times.

2.6.1.5 Vacuum vs Regular Oven

Pristine PEDOT:PSS films were set in atmospheric conditions for 12 hours. Annealing was then performed for 4 hours in the standard oven (section 2.2.2) and/or in a 30L S/S Gallenkamp vacuum oven (London, UK), evacuated using an Edwards nXDS-10iR scroll pump (Crawley, UK), at high (140 °C) and/or low (25 °C) temperatures as listed below:

- Vacuum oven at low temperature
- Vacuum oven at high temperature
- Standard oven at high temperature
- Vacuum oven at low temperature then standard oven at high temperature

Sheet resistivity was measured before and after annealing conditions for each sample.

2.6.2 Initial PEDOT:PSS/Tween 80 Film Resistivity Measurements

For the initial testing of PEDOT:PSS/Tween 80 films, the surfactant concentration was measured as a volume and the approximate wt% was calculated to be 0.53 wt% (section 2.2.1).

Solution (2 mL) was drop cast into a petri dish and all samples were set in atmospheric conditions before annealing.

2.6.2.1 Annealing Temperature Variation

PEDOT:PSS/Tween 80 films for concentration as above were annealed at 100, 120 and 140 °C for 4 hours to compare the optimal annealing conditions to those of pristine PEDOT:PSS. Sheet resistivity was measured after atmospheric equilibration of 12 hours for each annealing temperature. Single factor ANOVA analysis was performed on this data to establish statistical differences between annealing temperatures.

2.6.2.2 Annealing Time Variation

PEDOT:PSS/Tween 80 films for concentration as above were annealed at 140 °C for times between 0 – 120 minutes to assess the optimal annealing time. Sheet resistivity of each sample was measured after atmospheric equilibration for 12 hours. Single factor ANOVA analysis was performed on this data to establish statistical differences between annealing times.

2.6.3 PEDOT:PSS/Tween 80 Resistivity for Varying Surfactant Concentrations

From this point on (unless otherwise specified), sheet resistivity was measured with an Ossila 4-point probe (Ossila, Sheffield) at a maximum voltage of 1 V and a current of 100 µA. Six points were measured on each film to remove orientation bias (Figure 2-7) and 10 repeats were taken at each measurement point.

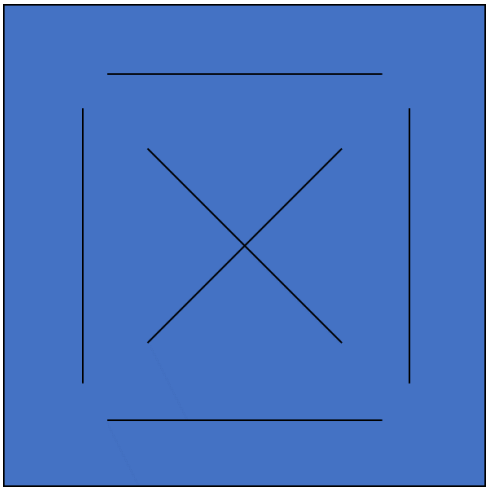

Figure 2-7: Diagram showing the sheet resistivity measurement pattern across for samples measured on the Ossila 4-point probe

2.6.3.1 Drop Cast Samples

PEDOT:PSS/Tween 80 solutions (0.4 mL), containing 0.00 – 2.67 wt% surfactant, were drop cast on to 25 x 25 mm glass substrates. Films were allowed to set in atmospheric conditions for 12 hours prior to annealing at 140 °C for 1 hour. Equilibration was performed as normal prior to resistivity testing.

2.6.3.2 Dip Cast Samples

Films were formed via dip casting onto glass, PP and PET substrates (10 x 20 mm) with and without a PDA coating. Three sets of PEDOT:PSS/Tween 80 solutions were produced for dip casting with surfactant concentration between 0.00 – 3.50 wt%. Samples were then: set and annealed; set with no annealing; annealed with no setting. Setting was carried out for 12 hours in atmospheric conditions and annealing was performed for 1 hour at 140 °C. Sheet resistivity was measured after equilibration.

2.6.4 Further Conductivity Enhancement Treatments

2.6.4.1 MEK Addition

Solutions of PEDOT:PSS containing Tween 80, MEK and both were created. For these sample, the concentrations of each additive were initially measured by volume and then converted into approximate wt% (section 2.2.1). The concentrations of each additive in solution were as follows:

- PEDOT:PSS/Tween 80 – 0.53 wt% Tween 80
- PEDOT:PSS/MEK – 1.19 wt% MEK
- PEDOT:PSS/Tween 80/MEK – 0.52 wt% Tween 80, 1.19 wt% MEK

Each solution (2 mL) was drop cast into 60 mmØ petri dishes, set in atmospheric conditions and annealed at 100 °C for 4 hours. After equilibration, sheet resistivity was measured using the Jandel 4-point probe.

A set of PEDOT:PSS/Tween 80/MEK solutions were created using a Tween 80:MEK ratio of 1:3 by volume, with a range of surfactant concentrations between 0.00 – 2.67 wt%. Films were created via drop casting on 25 x 25 mm glass substrates using 0.4 mL of solution. Samples were left to set in atmospheric conditions for 12 hours prior to annealing at 140 °C for 1 hour. Equilibration was performed as normal before resistivity analysis using the Ossila 4-point probe.

2.6.4.2 Solvent Washed Samples

Films of PEDOT:PSS/Tween 80 with surfactant concentration 0.00 – 3.50 wt% were washed using 3 solvents: MEK, ethanol and methanol. Sheet resistivity was measured before and after washing, with the appropriate equilibration period being allowed before testing.

2.6.4.3 Multiple Dip Cast Samples

Solutions of PEDOT:PSS/Tween 80, containing 0.00 – 3.50 wt% surfactant, were also used to assess the effect of applying multiple layers of the solution to the substrate. Samples were produced using 2 – 5 dips (see section 2.2.2.2 for details) for all Tween 80 concentrations. After the final anneal, films were left to equilibrate as normal before testing.

2.7 Adhesion Testing

Adhesion testing was performed on films of PEDOT:PSS/Tween 80 with surfactant concentration 0.00 – 3.50 wt%. Samples were created using both drop and dip casting methods onto substrates of glass, PP and PET (10 x 20 mm) with and without a PDA coating to create 10 x 10 mm films.

2.7.1 Scratch Tape Test

Adhesion was also measured via a tape test on dip cast samples following the ASTM Standard D3359-17 (2019)[16], adapted for the samples used in this study. Samples were scored in a cross hatching pattern with a spacing of 1 mm between each cut. Elcometer 99 adhesive tape (Manchester, UK) was applied to the film and left for 90 seconds before being removed. Adhesion was assessed visually using the standard classification system from 5B (0% film removal) to 0B (greater than 65% film removal) (Table 2-5).[16]

Table 2-5: Classification of scratch tape test and associated percentages of film remaining on substrate

Classification	Percentage Removal
5B	0 %
4B	< 5 %
3B	5 – 15 %
2B	15 – 35 %
1B	35 – 65 %
0B	> 65 %

2.7.2 Force Pull-Off Test

The pull of strength was analysed on drop cast samples following the ASTM Standard D4541-17 (2019)[17], adapted for the samples in this study. Force was measured on an Instron 5566 mechanical tester (Norwood, US) interfaced with a PC running Bluehill version 2 software (Instron, Norwood). An aluminium stub of 10 x 10 mm was attached to the films using Loctite Power Flex super glue and allowed to set for 24 hours before testing. The force measured was then normalised by dividing by the cross sectional area of the stub to give force per area. (Note: These samples were sheet resistivity tested as outlined in section 2.6.3.2 prior to adhesion testing).

2.8 Statistical Analysis

Where appropriate and as highlighted throughout this work, a one sided ANOVA analysis was performed on the data using Microsoft 365 Excel (Washington, U.S). This determines the statistical significance between the means of multiple data sets, determining whether they can be considered different or not to a given level of confidence. In this study, the confidence interval was set at 95 % and results were considered significantly different if the calculated p-value was less than 0.05.

2.9 References

1. Sigma-Aldrich 2015. Certificate of Analysis: Poly(3,4 ethylene dioxythiophene)-poly(styrene sulfonate).
2. Sigma-Aldrich 2018. Product Specifaction: Tween 80.
3. Sigma-Aldrich 2018. Product specification: 2-Butanone.
4. Lee, H., Dellatore, S. M., Miller, W. M. & Messersmith, P. B. 2007. Mussel-inspired surface chemistry for multifunctional coatings. *Science (New York, N.Y.),* 318**,** 426-430.
5. Thompson, B. T. 2017. *Enhancing the conductivity of PEDOT:PSS on bulk substrates.* Doctor of Philosophy, University of Warwick.
6. Alemu, D., Wei, H.-y., Ho, K.-c. & Chu, C.-w. 2012. Highly conductive PEDOT:PSS electrode by simple film treatment with methanol for ITO-free polymer solar cells. *Energy Environ. Sci.,* 5**,** 9662-9671.
7. Li, X., Wang, R., Huang, S., Wang, Y. & Shi, H. 2018. A capillary rise method for studying the effective surface tension of monolayer nanoparticle-covered liquid marbles. *Soft Matter,* 14**,** 9877-9884.
8. Mathot, V., Pyda, M., Pijpers, T., Vanden Poel, G., de van, K., van Herwaarden, S., van Herwaarden, F. & Leenaers, A. 2011. The Flash DSC 1, a power compensation twin-type, chip- based fast scanning calorimeter (FSC): First findings on polymers. *Thermochimica Acta,* 522**,** 36-45.
9. Shimadzu Co. 2018. *Measurement Methods for Powder Samples* [Online]. Available: https://www.shimadzu.com/an/ftir/support/ftirtalk/talk8/intro.html [Accessed 12/03/18].
10. Cullity, B. D. 1956. *Elements of x-ray diffraction,* Reading, Mass. ; London, Addison-Wesley Publishing Company.
11. Murthy, N. S. 2016. X-ray Diffraction from Polymers. *In:* Guo, Q. (ed.) *Polymer Morphology: Principles, Characterization, and Processing.* Hoboken, NJ, USA: John Wiley & Sons, Inc.
12. Murthy, N. S. & Minor, H. 1995. Analysis of poorly crystallized polymers using resolution enhanced X-ray diffraction scans. *Polymer,* 36**,** 2499-2504.
13. Jin, X. & Kasal, B. 2016. Adhesion force mapping on wood by atomic force microscopy: influence of surface roughness and tip geometry. *Royal Society Open Science,* 3**,** 160248-160248.
14. Callister, W. D. 2000. Materials science and engineering: an introduction. 5th ed. New York; Chichester: Wiley.
15. Miccoli, I., Edler, F., Pfnur, H. & Tegenkamp, C. 2015. The 100th anniversary of the four-point probe technique: the role of probe geometries in isotropic and anisotropic systems. *Journal of Physics-Condensed Matter,* 27.
16. ASTM Standard D3359-17 2019. Standard Test Method for Rating Adhesion by Tape Test. West Conshohocken, PA: ASTM International. Available: www.astm.org
17. ASTM Standard D4541-17 2019. Standard Test Method for Pull-Off Strength of Coatings Using Portable Adhesion Testers. West Conshohocken, PA: ASTM International. Available: www.astm.org

Chapter 3: Results and Discussion – Thermal Analysis, Moisture Kinetics and Processing Optimisation of Pristine PEDOT:PSS

In this chapter, the thermal transitions and stability of pristine PEDOT:PSS, and the effect of temperature on conductivity will be investigated using a range of techniques. This will additionally indicate limits to the maximum annealing temperature during sample preparation. The moisture kinetics of pristine PEDOT:PSS films will also be evaluated. Finally, differing annealing parameters (e.g., temperature and time) will be explored to enable optimisation of processing conditions.

3.1 Thermal Analysis of Pristine PEDOT:PSS

3.1.1 Thermal Gravimetric Analysis (TGA)

The thermal stability of PEDOT:PSS is of significant importance since degradation has been shown to have a negative impact on conductivity,[1,2] meaning it is imperative to avoid it during processing. Pristine PEDOT:PSS degradation was initially analysed via TGA on samples that had been dried and allowed to equilibrate in atmospheric conditions. TGA was performed in both air (Figure 3-1), and inert argon (Figure 3-2). Two atmospheres were employed to determine difference in the onset of degradation when oxygen was present. When comparing both figures, no discernible difference in either percentage mass loss or rate of loss was observed between the differing atmospheres. Furthermore, the onset of degradation is the same for both atmospheres, at 250 – 300 °C. This suggests that the degradation of PEDOT:PSS up to 450 °C is not affected by the atmospheric conditions and that the degradation occurring is not oxidative.

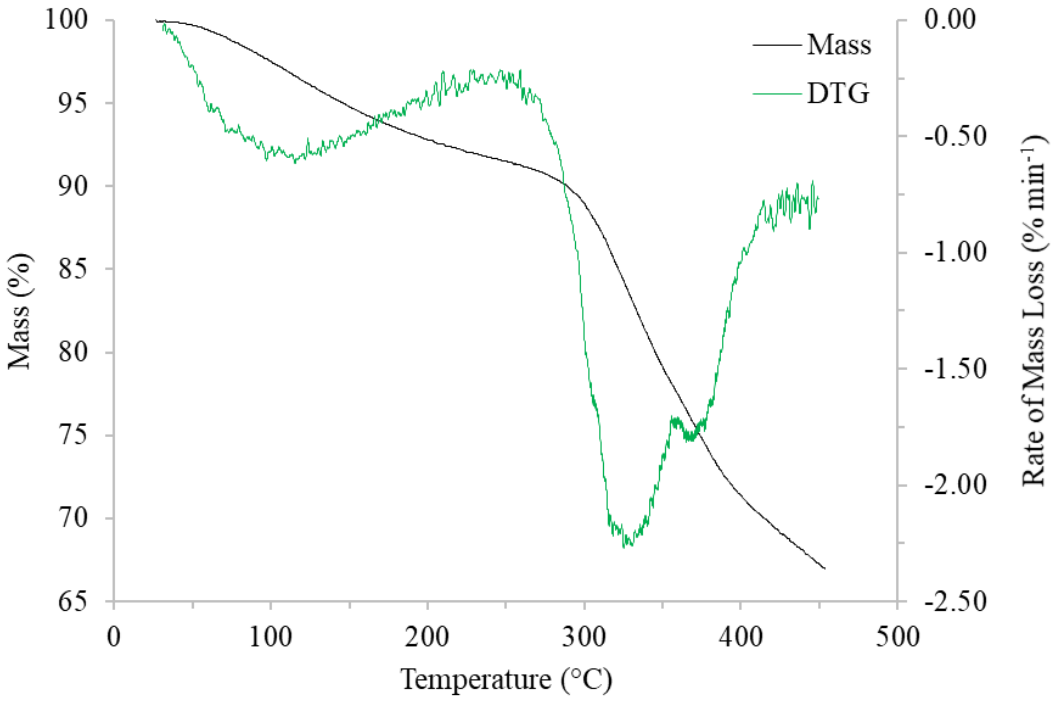

Figure 3-1: TGA of pristine PEDOT:PSS in air, showing percentage mass loss (black) and rate of mass loss, i.e., DTG (green), as a function of temperature

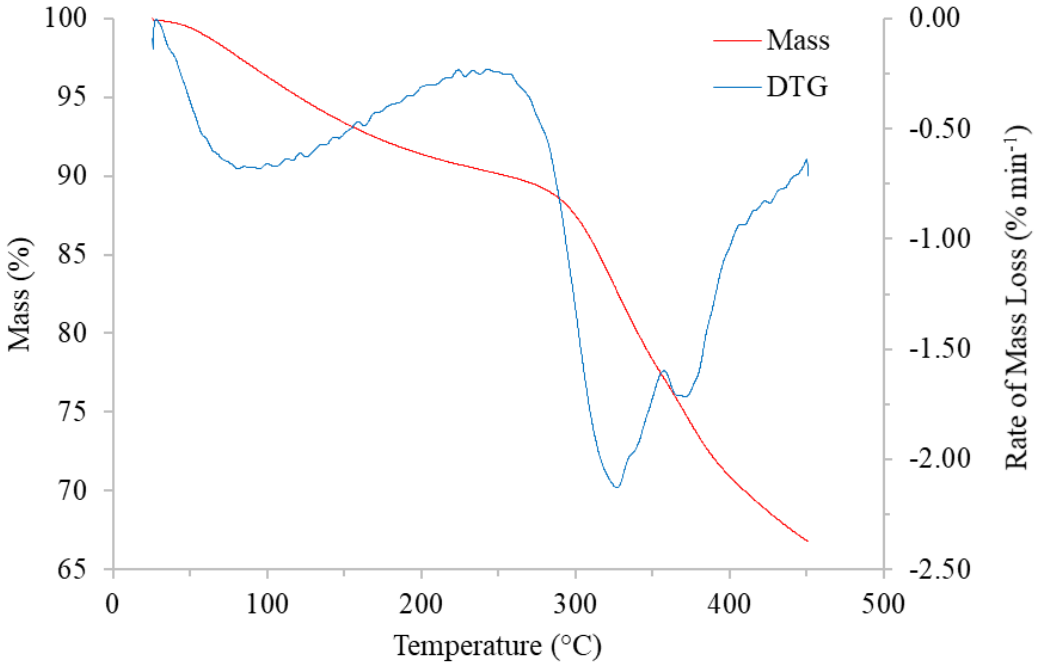

Figure 3-2: TGA of pristine PEDOT:PSS in argon, showing percentage mass loss (red) and rate of mass loss, i.e., DTG (blue), as a function of temperature

The initial mass loss seen up to 250 °C is attributed to the loss or removal of excess and bound water in the sample. While this is higher than literature values of 160 °C,[3-6] this is likely due to differences in sample geometry and heating rate. This is further evident by the maximum rate of loss for this first mass decrease being greatest at 100 °C, coinciding with the boiling point of water (Figure 3-1 & 3-2). In both atmospheres, up to 10 % sample mass is lost through this water removal (Figure 3-1 & 3-2), despite the samples being dried prior to testing. This is evidence of the affinity of water to PEDOT:PSS films since this moisture would have been reabsorbed during equilibration. These water loss measurements might be considered low, however, they are still within the literature suggested range for a mass loss of 10 – 25 % due to moisture removal.[1,3,5-9] This could partially be explained by the prolonged period of time the samples were exposed to a drier environment in the TGA after the gas purging phase. Some moisture would likely have diffused out of the sample during this phase due to the reduced humidity created inside the chamber. Other factors could also be having an effect. For example, in this work samples were subjected to a drying phase at elevated temperature in order to accelerate the film making process, something that was not employed in other studies.[3] This will have removed more moisture from the sample which might not fully replenish during the equilibration phase. There may also have been differences in the humidity of the equilibrium environment which could lead to less water being present in the samples.[10] Finally, there is evidence to suggest that PEDOT:PSS samples containing different concentrations of PSS will absorb varying amounts of water from the atmosphere. In general, when the PSS content is higher more moisture will be absorbed.[6,10-12]

The second noticeable mass loss initiates between 250 – 300 °C (Figure 3-1 & 3-2), which is reported as the start of degradation.[1,3,6,7] Up to 450 °C the sample shows a significant mass loss of 25 % with the rate of loss in air peaking at 2.30 $\%min^{-1}$ at approximately 350 °C (Figure 3-1).

This loss is attributed to the breakdown of the PSS phase, within the PEDOT:PSS structure, which begins at 250 °C.[1,5,13] It has also been shown that PEDOT on its own does not start degrading until 300 °C.[14,15]

This analysis has shown that processing of PEDOT:PSS must be kept below 250 °C in order to avoid degradation, and it has previously been suggested that PEDOT:PSS should not be heated above 200 °C to ensure no degradation occurs.[6] Furthermore, TGA analysis has also shown a significant amount of moisture present in PEDOT:PSS after drying and equilibration, showing the degree to which moisture will be absorbed.

3.1.1.1 Fourier Transform Infra-Red Spectroscopy (FTIR)

FTIR analysis was used to clarify the degradation mechanism of PEDOT:PSS (section 3.1.1). Firstly, the FTIR trace seen in Figure 3-3 shows the absorbance spectra for undegraded pristine PEDOT:PSS. All the main identifying peaks for the PEDOT and PSS components are present and align with what is seen in the literature.[1,16-19] The primary peaks identifying PEDOT are observed at 1530, 1230 and 1065 cm^{-1}, which is caused by the C-O-C stretching in the ethylenedioxy group.[1,16-19] The identifying PSS peaks occur at 1200 cm^{-1} and 1000 – 700 cm^{-1} which indicate the presence of S=O and S-phenyl bonds respectively.[1,16,17,19-21] The data also shows a sloped baseline, which has been seen in other studies, however, no reason for this phenomenon is given.[20] This could be caused by an absorption across the whole FTIR spectra or scattering and refraction from the PEDOT:PSS particles within the KBr disks.[22,23]

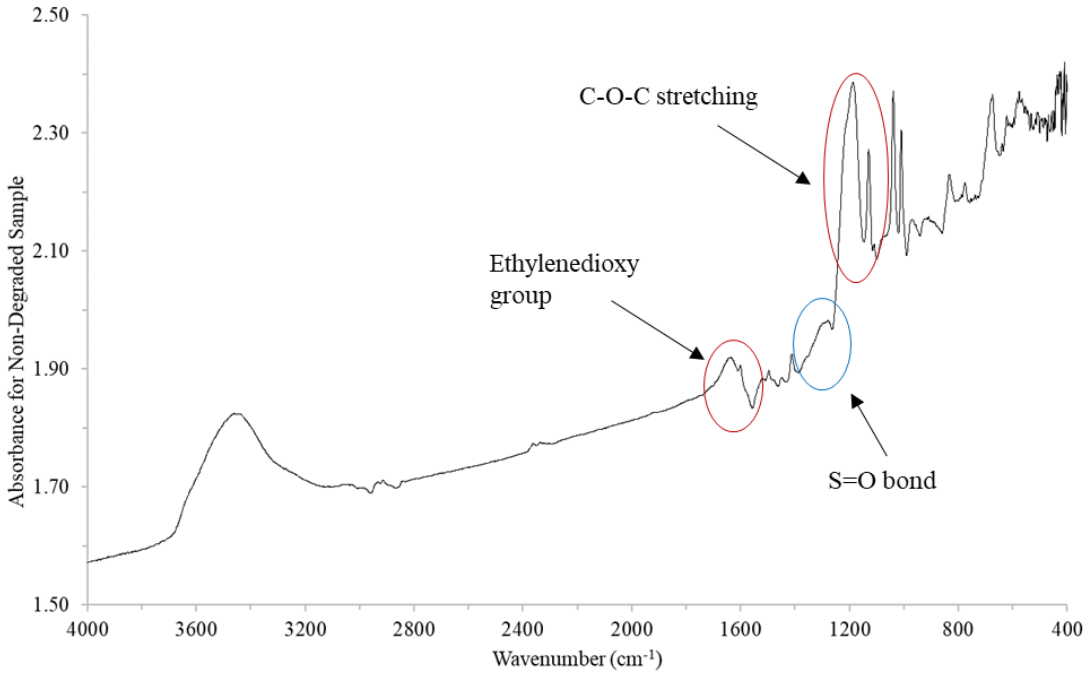

Figure 3-3: FTIR trace showing the absorbance peaks of pristine PEDOT:PSS. Main peaks identifying PEDOT (red circle), and PSS (blue circle) components are highlighted

Figure 3-4 shows the absorbance peaks for undegraded pristine PEDOT:PSS, and a sample degraded at 250 °C for 1 hour. It can be seen that the peaks identifying PEDOT, mainly the peaks at wavenumbers 1530 and 1230 cm^{-1}, are comparable in both traces suggesting that at 250 °C the PEDOT component is not degrading. This aligns with literature findings which suggest PEDOT will not degrade until 300 °C.[14,15] However, the peaks associated with PSS at 1200 cm^{-1} are no longer present. This indicates that these bonds have been broken due to the heat applied to the sample and is, therefore, the cause of the mass loss seen by TGA at 250 °C, as reported in the literature.[1,5,13]

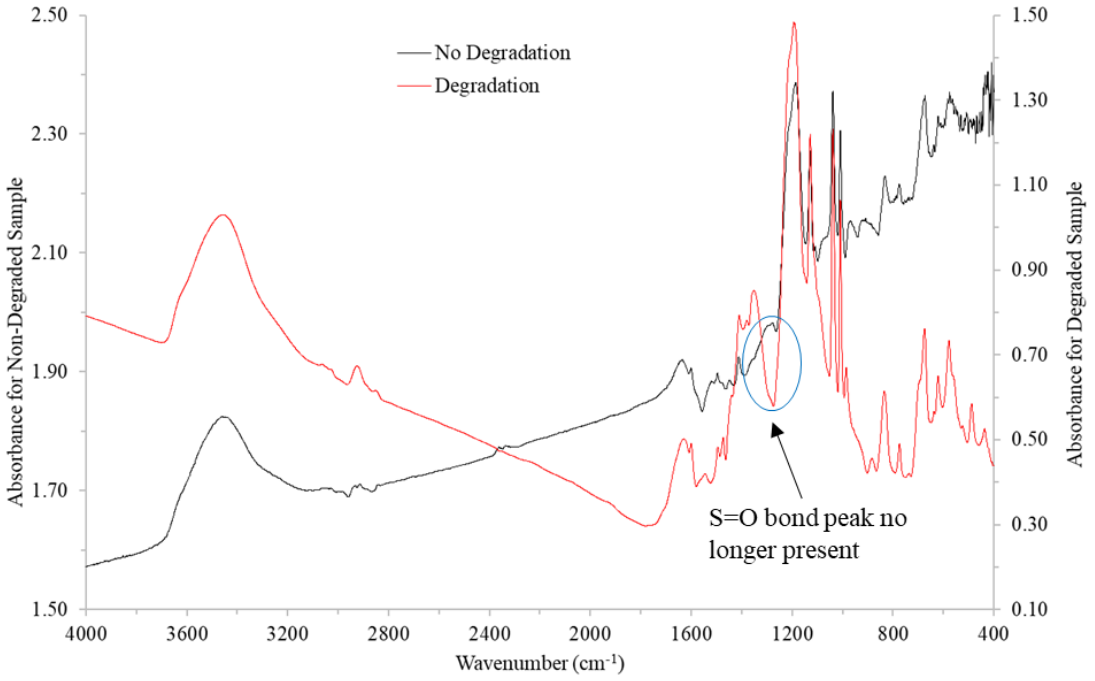

Figure 3-4: FTIR spectra showing the absorbance peaks for non-degraded (black) and degraded (red) PEDOT:PSS. Highlighted peak (blue circle) shows the PSS bond that is no longer present after degradation

3.1.2 Differential Scanning Calorimetry (DSC) and Flash DSC (FDSC)

DSC and FDSC analyses were performed on pristine PEDOT:PSS to ascertain whether any thermal transitions, such as T_m, T_c or T_g were present. The first heating trace obtained is dominated by the appearance of a large peak (Figure 3-5). This peak is caused by the removal of water with its maxima being at approximately 140 °C, as is commonly seen within the literature.[3-6] This is higher than expected since this is over the boiling point of water but is likely due the presence of bound water requiring higher temperatures to effectively remove it from the sample.[3] There is also another peak at 180 °C which is most likely an anomaly caused by movement of the sample within the pan, something that commonly occurs in DSC on the first run as the sample 'settles'.[24] Subsequent heating runs do not show any transitions related to

water removal or major thermal events This is evidence to suggest that all the moisture has been removed from the sample and the peak at 180 °C on the first run is insignificant.

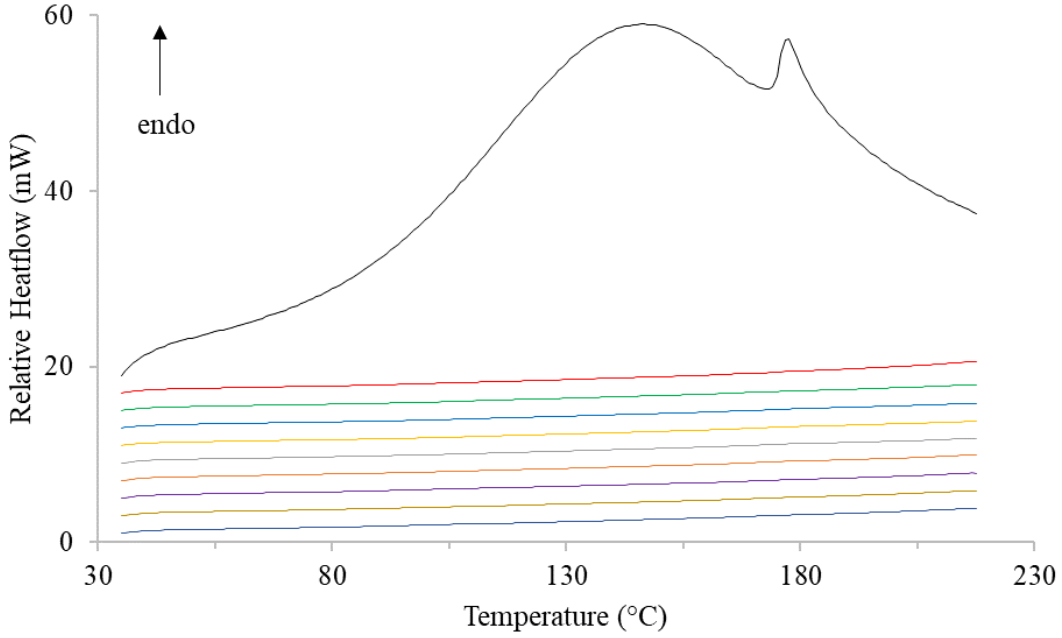

Figure 3-5: DSC trace of pristine PEDOT:PSS showing only the heating stages of the experiment (corresponding cooling traces seen in Figure 3-7). Runs are presented in order of completion with the first being on the top and the last being on the bottom. Heating was performed at 50 °Cmin^{-1} from 25 – 220 °C

Upon closer inspection of the heating runs (Figure 3-6), there is a small step transition similar to a T_g at approximately 170 °C. The cooling runs (Figure 3-7) show a comparable trend, with a possible T_g appearing at 140 °C but no major transitions being present. The small T_g seen on heating and cooling in this study could be a transition within the PSS that surrounds the PEDOT:PSS particles. This would comply with the literature since PSS on its own has a reported T_g of 152 °C.[25] This is also close to the T_g value of 120 – 140 °C suggested by Yu, *et al.* (2016)[26]. Whilst the transition temperature in this study is higher for heating and lower for cooling, this is likely to be evidence of thermal lag.[27] These observations are mostly in line with

what has already been seen in the literature with studies suggesting that the only observable peak is caused by water removal on the first heat and then subsequent heating and cooling cycles show no sign of further transitions for PEDOT:PSS.[1,3] This has been attributed to the strong ionic interactions between the PEDOT and PSS leading to restricted chain motion.[3,26,28] However, there has been no previous mention of a T_g appearing at 170 °C on heating but, as discussed, this likely to be the T_g of the PSS-rich phase.

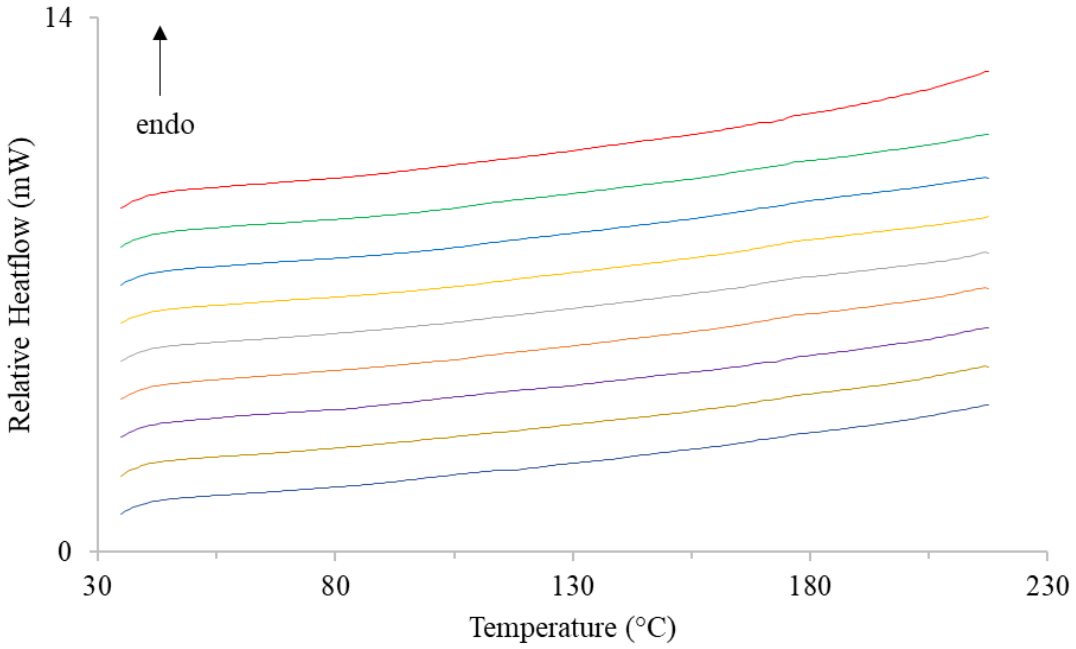

Figure 3-6: DSC trace of pristine PEDOT:PSS showing only the heating stages of the experiment (corresponding cooling traces seen in Figure 3-7). The traces shown are the same as those seen in Figure 3-5 except the first heating run has been removed. Heating was performed at 50 °Cmin^{-1} from 25 – 220 °C

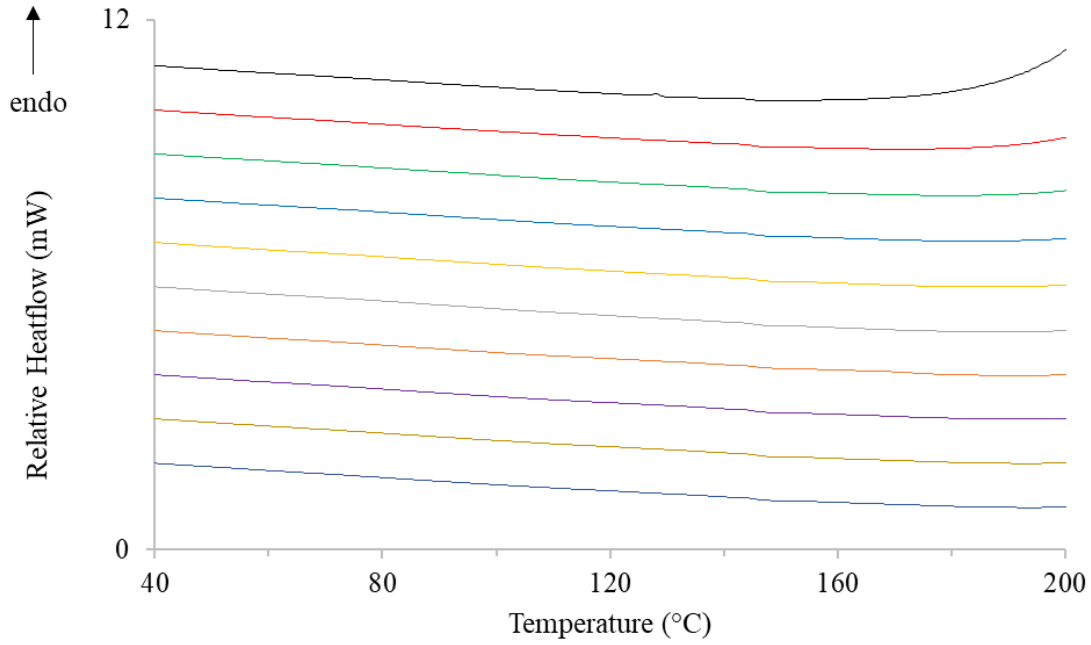

Figure 3-7: DSC trace of pristine PEDOT:PSS showing only the cooling stages of the experiment (corresponding heating traces seen in Figure 3-5). Runs are presented in order of completion with the first being on the top and the last being on the bottom. Cooling was performed at 20 °Cmin^{-1} from 25 – 220 °C

The FDSC was used in an attempt to exaggerate thermal transitions through the greater sensitivity of the FDSC chip and the higher heating rates compared to conventional DSC.[29] However, heating and cooling at 1000 °Cs^{-1} (Figure 3-8 & 3-9, respectively) does not show any further evidence of thermal transitions.

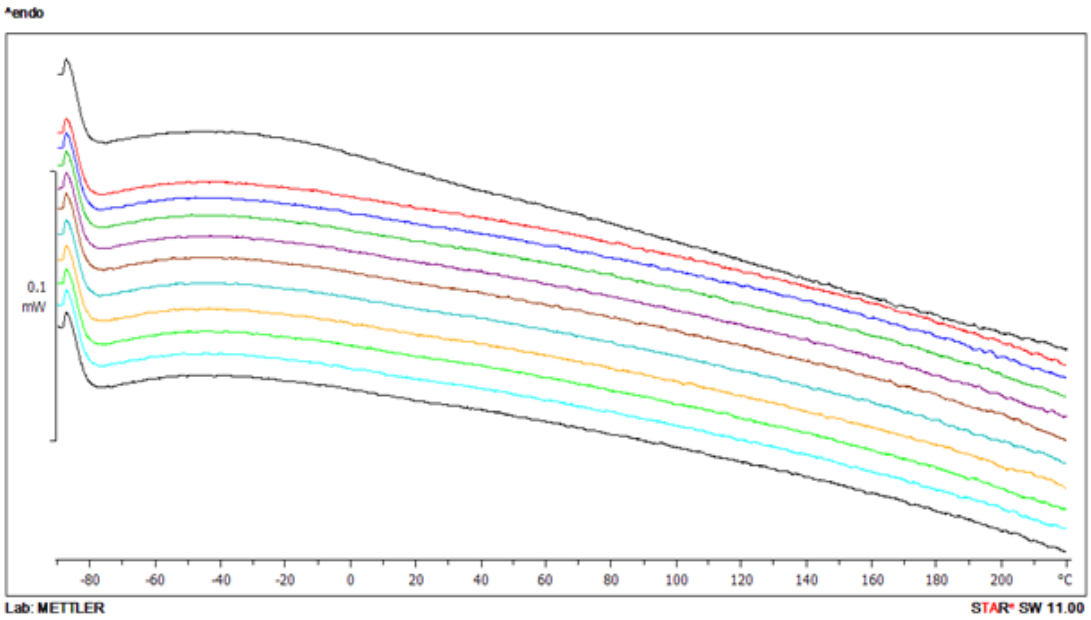

Figure 3-8: FDSC trace of pristine PEDOT:PSS showing only the heating stages of the experiment. Runs are presented in order of completion with the first being on the top and the last being on the bottom. Heating was performed at 1000 °Cs^{-1} from -90 – 220 °C

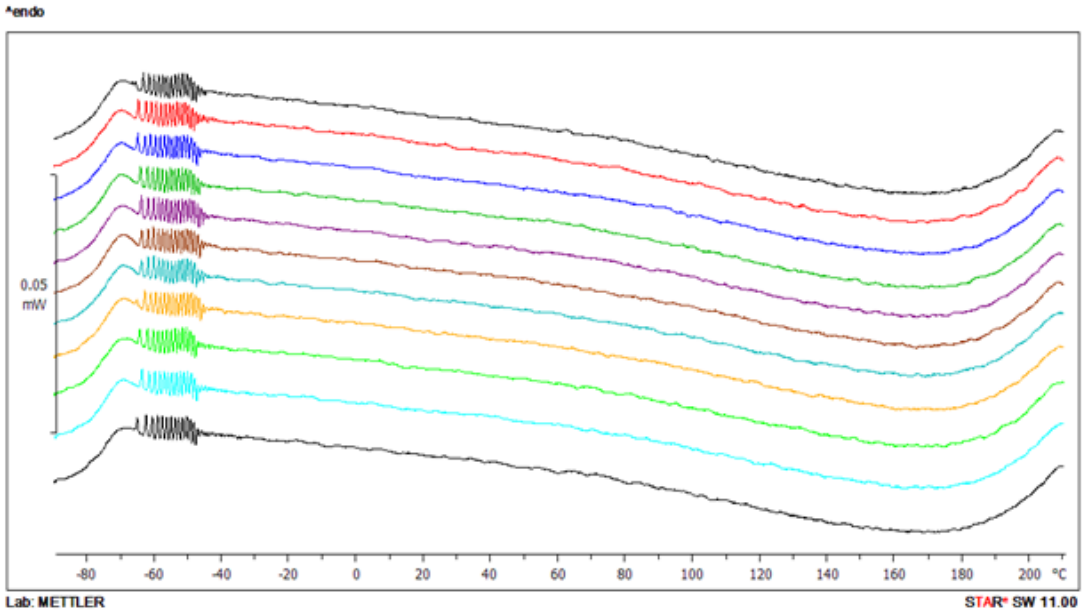

Figure 3-9: FDSC trace of pristine PEDOT:PSS showing only the cooling stages of the experiment. Runs are presented in order of completion with the first being on the top and the last being on the bottom. Cooling was performed at 1000 °Cs^{-1} from -90 – 220 °C

As with conventional DSC, the first heating run for the FDSC varies from the rest (Figure 3-8). This is likely due to the sample settling onto the FDSC chip. However, unlike with conventional DSC there is no evidence of water loss. Furthermore, additional heating and cooling showed no evidence of a T_g caused by the PSS-rich phase. These measurements could be erroneous since the FDSC requires a polymer to become liquid or melt onto the chip a to ensure good contact . However, since PEDOT:PSS does not appear to do either, there could be issues relating to the sample adherence to the chip, which could lead to inaccuracies.

3.1.3 Dielectric Thermal Analysis (DETA) of PEDOT:PSS Bulk Resistivity

DETA was used to measure the bulk resistivity[i] of pristine PEDOT:PSS throughout a temperature ramp from 20 to 140 °C (Figure 3-10). It can be seen that for the first run, as the temperature of the sample increases, the bulk resistivity of the sample drops from 330000 to 80000 Ωm, leading to a corresponding increase in the conductivity from $3x10^{-6}$ to $1.3x10^{-5}$ Sm^{-1}. A similar trend is seen in the second run except the values for bulk resistivity are lower due to the sample effectively being annealed by the heating process (this will be explained in more detail in section 3.3.1), A minimum bulk resistivity of 15000 Ωm was recorded, corresponding to a maximum conductivity of $6.8x10^{-5}$ Sm^{-1} (Figure 3-10). These conductivity values are much lower than expected for pristine PEDOT:PSS, with values commonly being quoted as 0.001 – 80 Scm^{-1}.[2,30-32] However, this difference has been caused by the varying measurement methods and corresponding differences between bulk and sheet resistivity.

[i] This is opposed to sheet resistivity which is measured by the 4-point probe. To allow for differentiation between conductivity that was calculated from bulk resistivity, the term 'bulk conductivity' is used. However, bulk conductivity has previously been defined by Kirchmeyer *et al.* (2007)[28] as the "charge transport properties along polymer chain, from one chain to another and across domain boundaries". While this may cause confusion between literature sources it was deemed necessary to define this differently here to provide distinction between conductivity calculated from bulk resistivity in this section, and sheet resistivity later in this study.

Normally the sheet resistivity, or alternative surface techniques, are used to calculate conductivity rather than the bulk resistivity.[6,33-38] It is expected that bulk resistivity values will be much higher due to the increase in insulating material electrons will have to flow through, as well as differences in surface and bulk morphologies.[39] This causes lower bulk conductivity measurements, which has been previously seen in the literature.[40]

It is also apparent from this data that PEDOT:PSS is a semi-conductor, which is well known in the literature,[6,41,42] with an increase in temperature resulting in a decrease in resistivity due to enhanced electron mobility.[42,43] The loss of water is also a likely factor (as discussed in 3.2.2) which would explain why the rate of decrease is faster at lower temperatures and appears to plateau above 100 °C. Therefore, up to this point two main mechanisms have been identified leading to the improvement of conductivity: sample annealing; and operating at elevated temperatures. However, the latter of these is less feasible to implement in regular operating conditions.

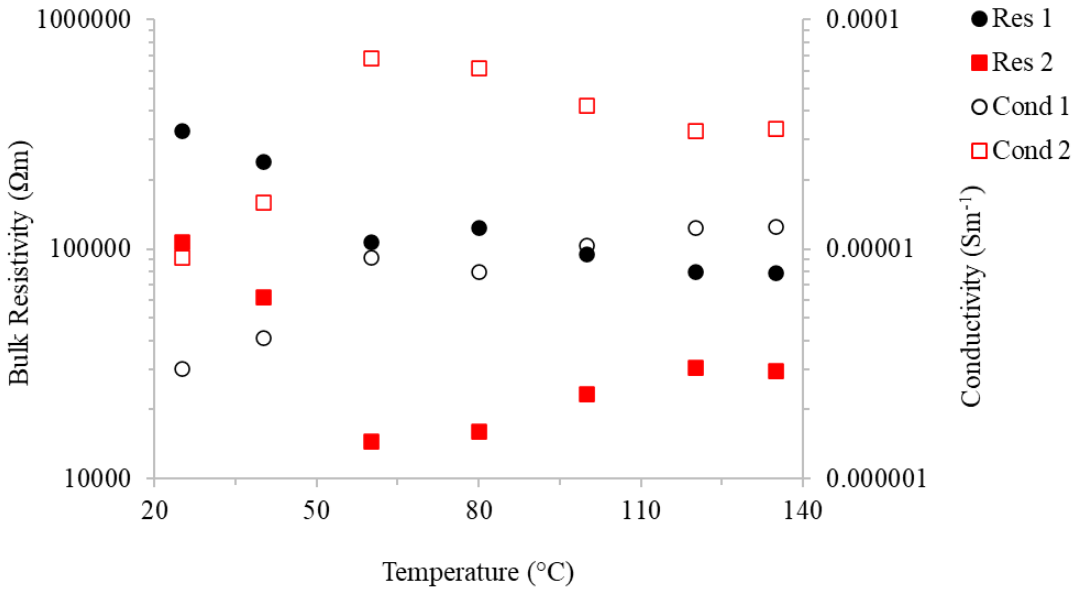

Figure 3-10: DETA analysis of pristine PEDOT:PSS film during temperature ramp from 20 – 140 °C at 1 °Cmin^{-1}. Two runs were performed on the sample measuring bulk resistivity (Ωm), labelled as 'Res 1' (solid black circle) & 'Res 2' (solid red square) referring to the first and second run on the sample, respectively. The corresponding "bulk" conductivity (Sm^{-1}) are labelled as 'Cond 1' (hollow black circle) and 'Cond 2' (hollow red square)

3.2 Water Kinetics

3.2.1 DSC Analysis of Moisture Uptake in PEDOT:PSS Samples

The effect of moisture uptake in pristine PEDOT:PSS was assessed using DSC. Samples were dried in the DSC by subjecting them to temperatures of 200 °C for 30 seconds. Once dried, the samples were exposed to atmospheric conditions for varying times. A pinhole was made in the top of the DSC pan to allow moisture to enter/escape. Figure 3-11 shows that as the time held in atmospheric conditions increases, the size of the peak on the first heating run, corresponding to the loss of water, also increases.

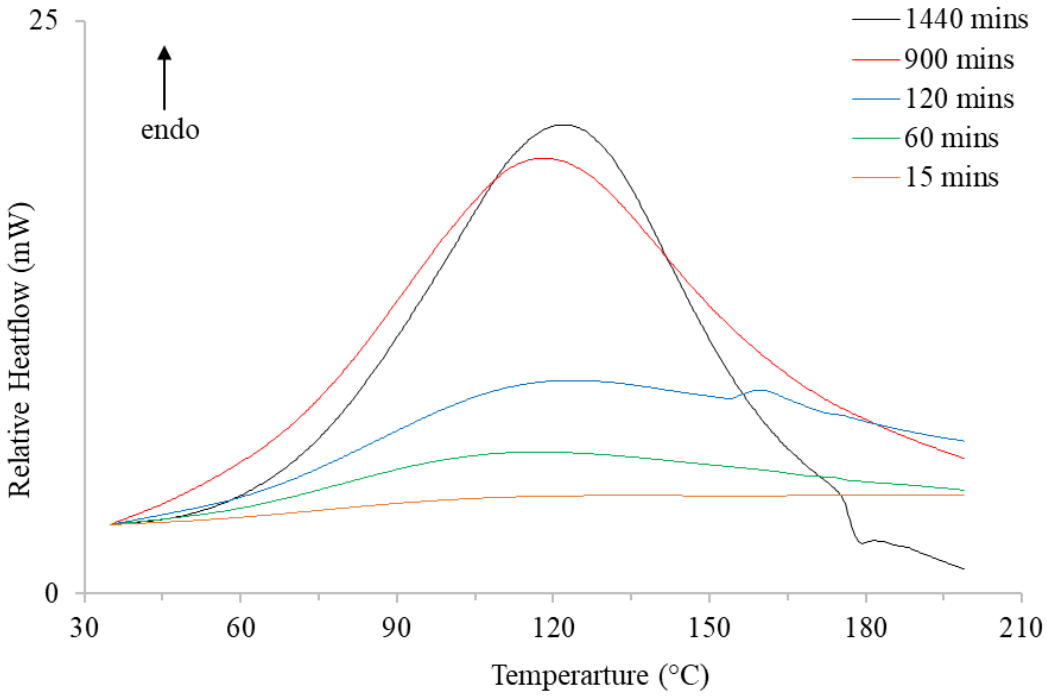

Figure 3-11: DSC traces of pristine PEDOT:PSS water loss peak after various atmospheric exposure times

To better understand this effect, the integrals of the peaks were measured to determine the energy required to remove the water after each atmospheric hold (Figure 3-12). Sample mass at the end of these atmospheric exposures was also measured (Figure 3-12). What is noticeable is that the integral and mass follow an almost identical trend. The rate of water uptake is initially fast with the majority occurring within the first 200 minutes. Moisture uptake then slows and tends toward a maximum with the largest mass gained after 1440 minutes being approximately 2.50 mg. It is worth noting that the sample mass was also measured after each DSC run to check all water had been removed. The dry sample mass remained constant at 9.905 mg (±0.005 mg) showing that the mass measurements represent only water uptake.

This increase is in line with literature findings and earlier TGA data, which suggest that approximately 20 % of PEDOT:PSS sample mass will be water.[1,3,5-9] This data shows that pristine PEDOT:PSS needs 12 hours to reach equilibrium in atmospheric conditions.

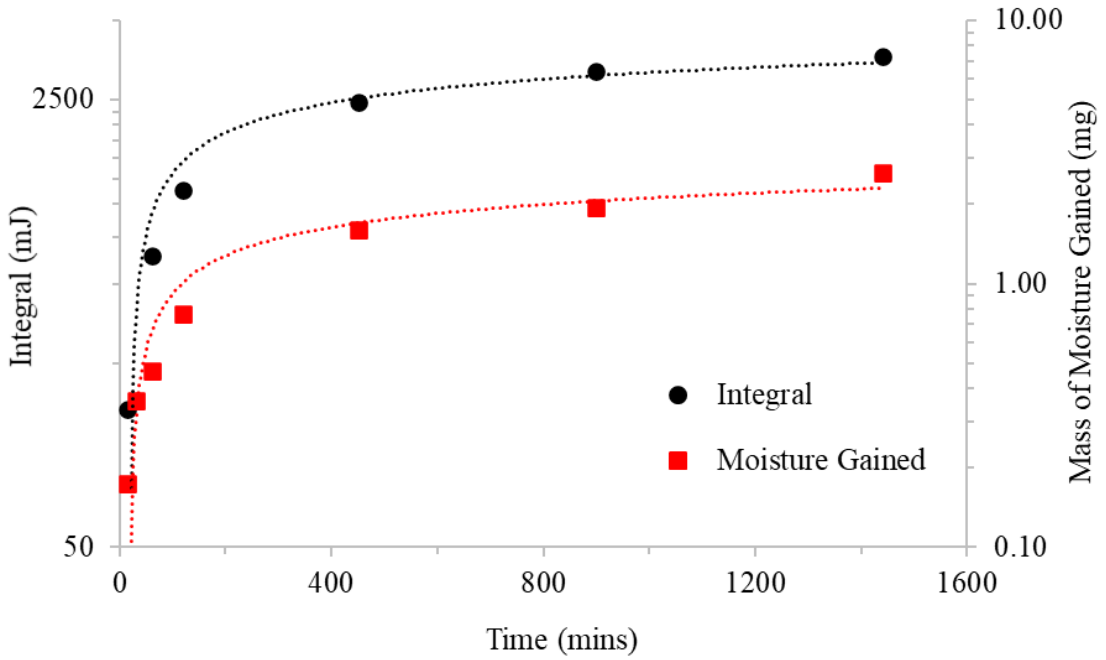

Figure 3-12: Graph showing the measured integrals of the water loss peaks seen in Figure 3-11 (black circle) and mass of moisture gained (red square) as a function of time held in atmospheric conditions

3.2.2 Moisture Uptake and Sheet Resistivity of PEDOT:PSS Film Samples

To further investigate the previous DSC data (section 3.2.1), pristine PEDOT:PSS films were created, dried, and held in atmospheric conditions to determine whether the same mass increase due to moisture uptake would be seen. This also allowed sheet resistivity to be measured to observe the effect of moisture on the film's electrical properties. Initially the uptake of water was quick and slowed down to a plateau after only 160 minutes (Figure 3-13 & 3-14). The slowing of the mass increase is due to the diffusion gradient between film and air moisture decreasing over time. This trend is similar to the previous DSC analysis (section 3.2.1), however, this equilibration is considerably faster than the DSC samples which were not fully

equilibrated after 1440 minutes. This is caused by the differences in sample geometry and the restriction of moisture to the sample caused by the DSC lid, despite the pinhole.[6,11]

However, the percentage of moisture uptake by the film samples cannot be calculated since an accurate measurement of mass for dry PEDOT:PSS could not be obtained for two reasons. Firstly, the sample was heated in an oven with no active cooling which meant in their dry state they were hot. Secondly, the high rate of moisture uptake caused the mass to continuously increase, so a stable reading could not be taken. Despite this, it can be suggested that as little as 3 hours would be needed to fully equilibrate film samples of pristine PEDOT:PSS.

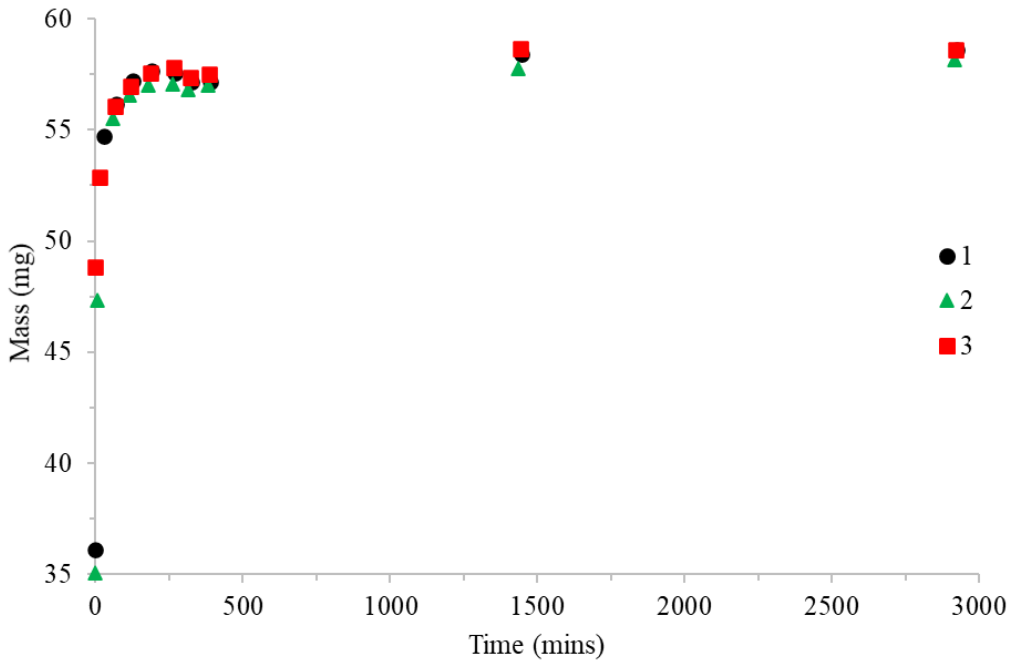

Figure 3-13: Pristine PEDOT:PSS film sample masses as a function of time held in atmospheric conditions. Each symbol represents a different sample

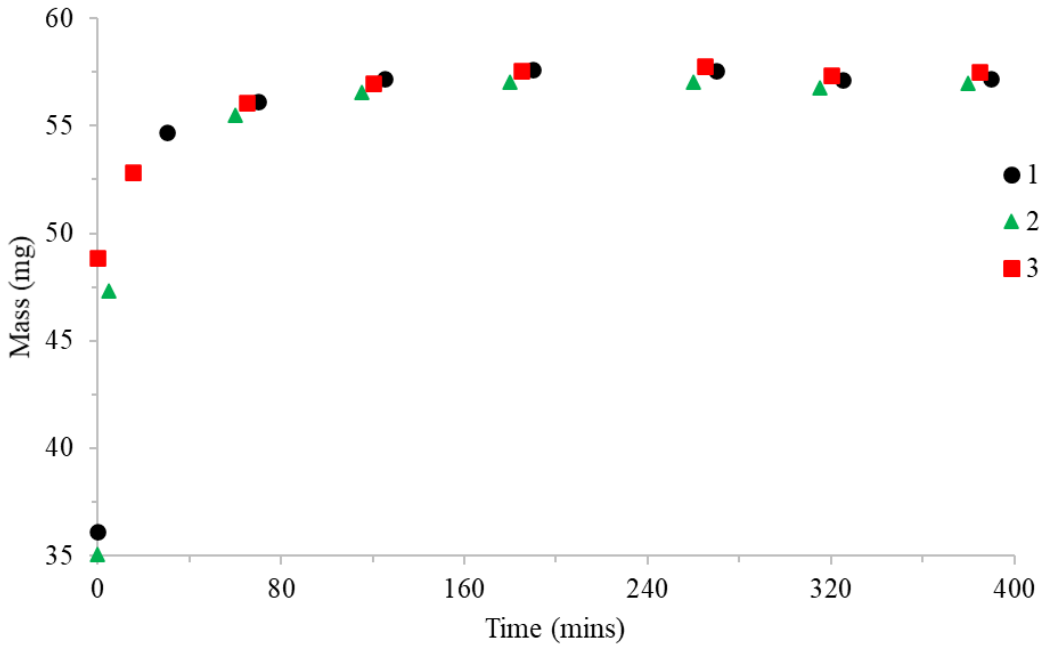

Figure 3-14: Highlighted section of the first 400 minutes of moisture gain taken from Figure 3-13

Analysis of these films (Figure 3-15) suggests an increase in sheet resistivity with moisture content. This increase does not appear to be of an exponential nature, like the mass increase, however, this may be due to the natural variation in the data seen when using this technique. Furthermore, the maximum variation across all the data is 35 $\Omega\square^{-1}$ which could be considered small when compared to other sample sets (E.g., section 3.3.1). Sheet resistivity would, however, be expected to increase with moisture content as water molecules will attach to the hydrophilic PSS region, causing them to expand and lead to an increased charge hopping distance.[1,3,44-46] Furthermore, water has a lower conductivity that PEDOT,[3,47] meaning that more water in PEDOT:PSS causes an increased sheet resistivity. It is, however, difficult to keep all moisture out of the sample, and can only be achieved via encapsulation.[6,28,48,49] Overall, even though the mass increase is significant due to moisture uptake, the effect of this on sheet resistivity is relatively small. This means that efforts to completely remove water from the

sample before testing are not necessary since small changes in atmospheric humidity are unlikely to induce large changes in sheet resistivity.

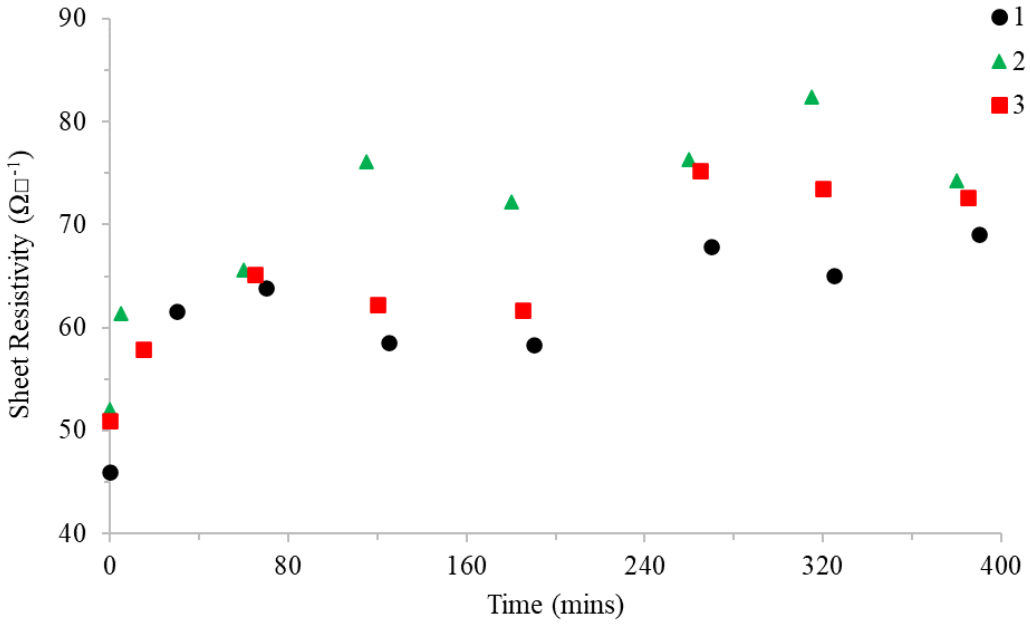

Figure 3-15: Sheet resistivity of pristine PEDOT:PSS films as a function of time held in atmospheric conditions. Each symbol represents a different film. The films are the same as those used in Figure 3-13 & 3-14

3.3 Processing Optimisation

3.3.1 Setting and Annealing Temperature Effect on PEDOT:PSS Sheet Resistivity

The effect of varying the setting and annealing conditions on the sheet resistivity of drop cast pristine PEDOT:PSS was assessed. Initially, samples created in a petri dish were annealed without employing a setting stage.[j] Even though in these conditions sheet resistivity dropped,

[j] In this study, 'setting' is defined as the stage whereby the material goes from solution to solid, primarily at lower temperatures 'Annealing' is then the process heating the sample at a higher temperature after setting.

temperatures of 80 °C and above caused bubbles to appear on the sample surface affecting the quality of the films. This was due to the water boiling and created the need for a 'setting' stage to make a solid film before the sample could be annealed. As seen in TGA and DSC experiments (sections 3.1.1 & 3.1.2), temperatures above 100 °C are needed to fully remove bound water from PEDOT:PSS. Therefore, annealing temperatures of 80 – 160 °C were focused on.

The effect of the differing setting temperatures on PEDOT:PSS can be seen in Figure 3-16. It was found that varying the setting temperature, without annealing, does not induce a significant change in the sheet resistivity. The samples set at 60 °C display a slightly reduced resistivity which could be caused by some moisture removal.[3-6] However, when annealing is then implemented, a variation with setting temperature can be seen. The samples set at 25 °C have little variation across all annealing temperatures with a maximum sheet resistivity of 742 $\Omega\square^{-1}$ and a minimum of 466 $\Omega\square^{-1}$ when annealed at 80 °C and 140 °C, respectively. However, setting at 40 °C leads to greater variation of 340 $\Omega\square^{-1}$ between maximum and minimum sheet resistivities, while setting at 60 °C causes resulted in a range of 654 $\Omega\square^{-1}$. Furthermore, the variation at 60 °C follows a linear trend with higher annealing temperature leading to a lower sheet resistivity. For example, the sample set at 60 °C then annealed at 80 °C resulted in a resistivity of 1115 $\Omega\square^{-1}$ compared to 461 $\Omega\square^{-1}$ when annealing at 160 °C (Figure 3-16). It was also noted that at annealing temperatures above 140 °C, the effect of setting temperature seems to be negated (Figure 3-17), with no significant difference for samples annealed at 140 °C and 160 °C for all setting temperatures. This suggests that, irrespective of the setting temperature, annealing over 140 °C is required to remove any possible differences in the samples.

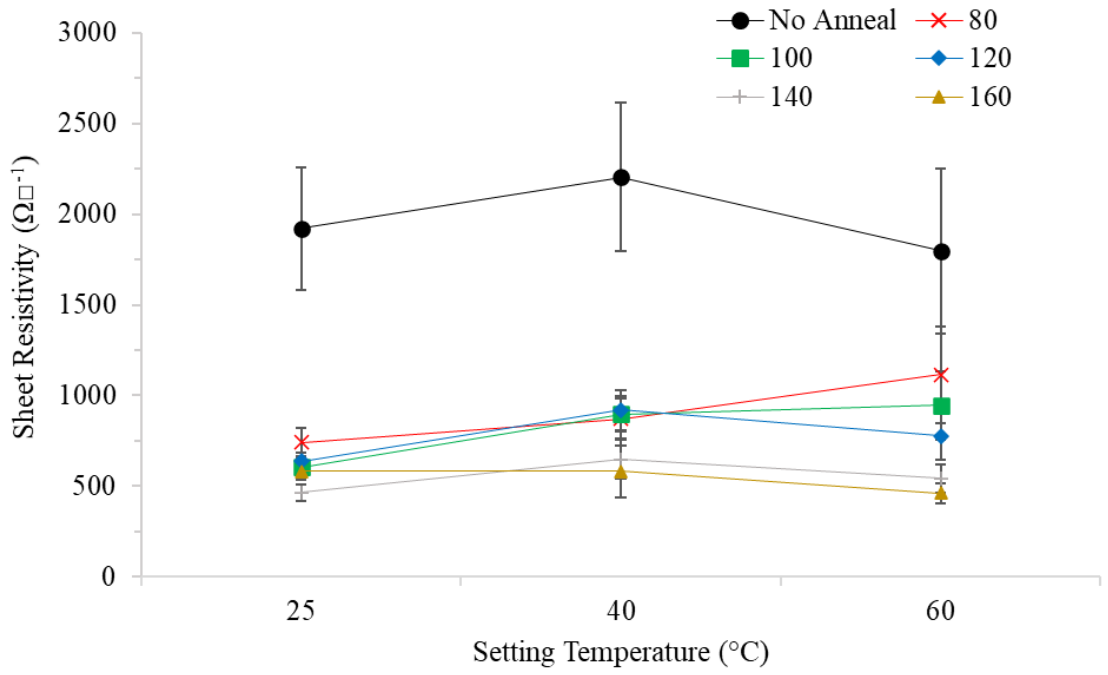

Figure 3-16: Effect of setting temperature (°C) on the sheet resistivity (Ω□$^{-1}$) for pristine PEDOT:PSS. Samples were set first then either not annealed (black circle) or annealed at 80 (red diagonal cross), 100 (green square), 120 (blue diamond), 140 (grey vertical cross) and 160 °C (gold triangle). Error bars show ± 1 SD

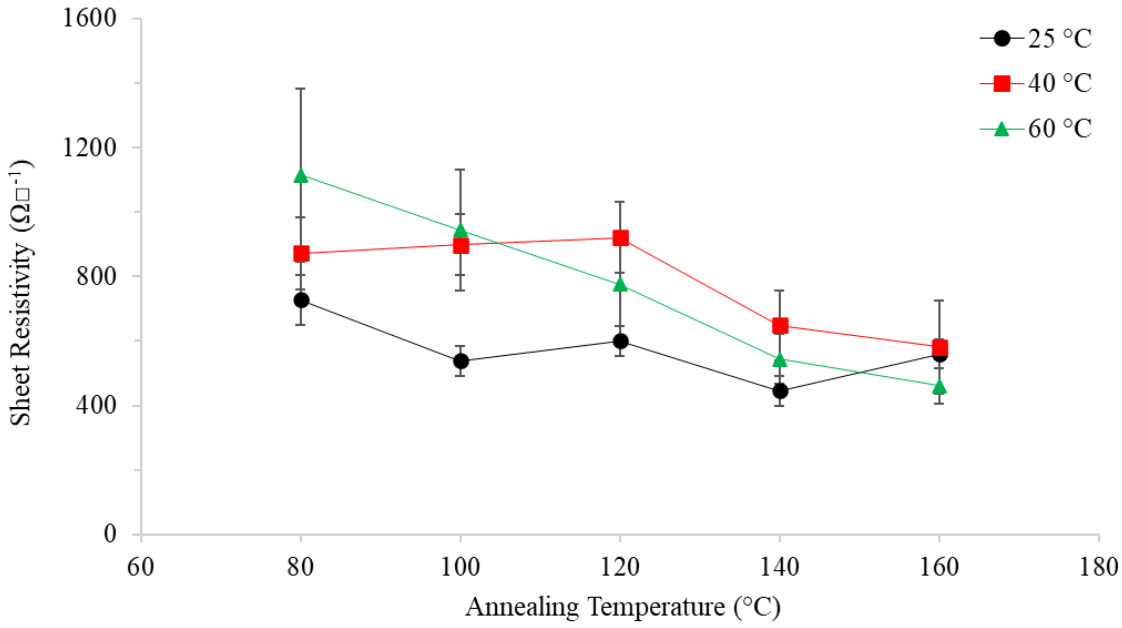

Figure 3-17: Graph representing the effect of annealing temperature (°C) on the sheet resistivity (Ω□$^{-1}$) of pristine PEDOT:PSS set at temperatures of 25 °C (black circle), 40 °C (red square) and 60 °C (green triangle). Error bars show ± 1 SD

Whilst not directly studied, it was hypothesised that the resistivity variations seen due to setting temperature were mainly caused by the increase rate of water removal at 60 °C. It is likely that at this temperature the PEDOT:PSS chains 'lock' in a more disordered state while lower setting temperatures allow for some chain reorganisation to occur before the sample is dry. It was also considered that at 60 °C, removal of bound water will begin to take place (sections 3.1.2 & 3.2.1), which would increase chain interaction, leading to reduced chain mobility.[3] This would also contribute to the chains 'locking' in a more disordered state. During annealing, the higher temperature could allow for chain movement but only above 140 °C.[1,50,51] This is in line with previous DSC data (section 3.1.2) in which a T_g of 140 °C was seen. At this temperature, the PSS chains have some mobility allowing for reorganisation, leading to decreased sheet resistivity.[1,50,51] This also explains why higher annealing temperatures do not further reduce resistivity. Based on these results, setting at 25 °C (i.e., room temperature) then annealing at 140 °C is the best route to process drop cast samples to avoid possible variation and achieve the lowest sheet resistivity. This annealing temperature is in line with previous literature findings.[45]

3.3.2 Vacuum Oven vs Regular Oven

To isolate the roles of water removal and high temperature in annealing, a set of samples were subject to 140 °C (high) and 40 °C (low) temperature in a vacuum oven. These were compared to annealing in a regular oven at 140 °C and a combination of low temperature in the vacuum oven followed by high temperature in the regular oven (Figure 3-18). It can be seen that prior to annealing, sheet resistivity is relatively comparable. However, after all annealing conditions, there is a significant decrease in sheet resistivity. For all samples subject to high temperature, a resistivity of approximately 375 $\Omega\square^{-1}$ was achieved. On the other hand, the low temperature vacuum oven sample did not show the same reduction, with resistivity measuring at 945 $\Omega\square^{-1}$.

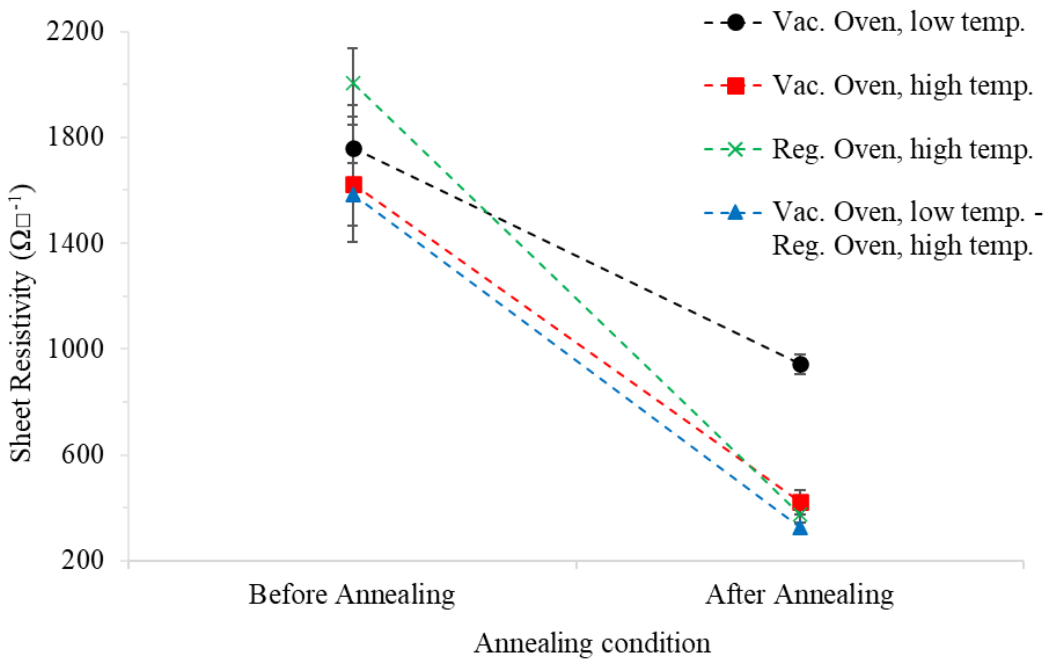

Figure 3-18: The effect on sheet resistivity ($\Omega\square^{-1}$) with differing annealing conditions using either a regular or vacuum oven. Conditions were as follows: Vacuum oven, low temperature (black circle); Vacuum oven, high temperature (red square); Regular oven, high temperature (green cross); Vacuum oven, low temperature then regular oven, high temperature (blue triangle). Low temperature was performed at 40 °C whilst high temperature was performed at 140 °C. Error bars show ± 1 SD

It was assumed that all moisture would be removed from PEDOT:PSS while in the vacuum oven. Therefore, the results show that a high temperature is required to produce significantly lower PEDOT:PSS sheet resistivity. This is further indicated by the sample subject to low temperature in the vacuum oven followed by high temperature in the regular oven having the same resistivity as the other high temperature samples. The reason for this is likely due to two factors. Firstly, while the assumption was made that all water was removed from the sample under vacuum at low temperature, DSC data has shown that temperatures up to 160 °C are needed to fully drive all water out of pristine PEDOT:PSS (section 3.2.1).[3-6] Furthermore, when the same process has previously been employed, samples have been under vacuum for several days.[10] Therefore, some water could remain in the sample leading to an elevated sheet

resistivity.[1-3,12,44,46,49] However, as previously discussed, the effect of water on sheet resistivity is relatively minimal (section 3.2.2). The second effect is that of chain reorganisation caused by the increase in temperature. The reorganisation effect has previously been linked to the softening of the PSS phase and improved alignment allowing for better conductivity pathways.[1,50,51] This shows that heat is needed in order to fully optimise PEDOT:PSS resistivity, with removal of water alone not being sufficient.

3.3.3 Annealing Time Effect on PEDOT:PSS Sheet Resistivity

Figure 3-19 shows the effect of annealing pristine PEDOT:PSS films at 140 °C for varying times. The data initially shows that 10 minutes is sufficient to induce a large drop in sheet resistivity, compared to no annealing, from 1500 to 430 $\Omega\square^{-1}$. Literature findings have suggested times as low as 20 seconds at this temperature could be utilised,[45] however, this was not compared to longer periods to assess whether the sample was fully annealed. While all annealing times in Figure 3-19 appear to produce comparable results, performing single factor ANOVA statistical analysis shows a significant decrease between 20 and 40 minutes annealing ($p<0.001$). The sample annealed for 40 minutes has the lowest measured sheet resistivity at 355 $\Omega\square^{-1}$ and is statistically different to all other annealing times except 60 minutes. Longer annealing time then cause the resistivity to slightly increase with 240 minutes having the highest resistivity after annealing at 466 $\Omega\square^{-1}$. The same effect was observed by Vitoratos, *et al.* (2009)[52] in which a noticeable decrease in conductivity was measured for samples annealed for longer than 3 hours at 120 °C, which continued to decrease for increasing annealing time. This data shows that the optimum annealing time is 40 minutes.

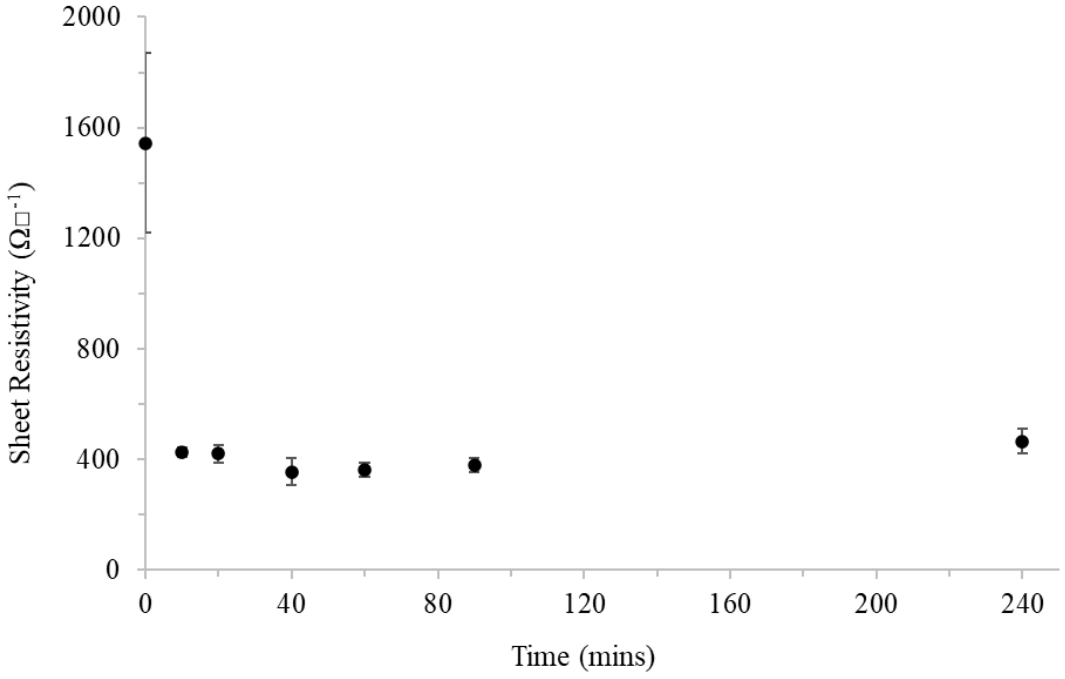

Figure 3-19: Effect of annealing time on the sheet resistivity (Ω□$^{-1}$) of pristine PEDOT:PSS. Error bars show ± 1 SD

3.4 Conclusion

Overall, it can be seen that the conditions under which pristine PEDOT:PSS is processed is an important consideration. Thermal analysis confirmed that PEDOT:PSS does not show any major thermal transitions after multiple heating runs. However, there was indication of a Tg at 140 °C which was linked to the softening of the PSS phase. It also showed that the uptake of water into PEDOT:PSS is significant and resulted in a rapid increase in sample mass, even in atmospheric conditions. However, encapsulation is not required since the effect on sheet resistivity of varying moisture contents that would arise from atmospheric humidity fluctuations is relatively small. This means that samples can be left to equilibrate in atmospheric conditions and small variations in humidity will not dramatically alter sheet resistivity measurements. The role of annealing PEDOT:PSS has been well established as the key driving factor that improves the conductivity properties, with water removal alone not being sufficient to optimise sample

processing. This has been linked to chain mobility at temperatures above 140 °C creating improved alignment and better conducting pathways. Additionally, it has been shown that the maximum annealing temperature is 220 °C, past which degradation becomes an issue. However, heating to 140 °C for 40 minutes is sufficient to fully anneal drop cast samples and remove any variation caused by differing setting conditions. This also means a slightly elevated setting temperature could be used to reduce the time taken to make samples.

3.5 References

1. Friedel, B., Keivanidis, P. E., Brenner, T. J. K., Abrusci, A., McNeill, C. R., Friend, R. H. & Greenham, N. C. 2009. Effects of layer thickness and annealing of PEDOT:PSS layers in organic photodetectors. *Macromolecules,* 42**,** 6741-6747.
2. Mengistie, D. A., Wang, P.-c. & Chu, C.-w. 2013. Effect of molecular weight of additives on the conductivity of PEDOT:PSS and efficiency for ITO-free organic solar cells. *Journal of Materials Chemistry A,* 1**,** 9907-9915.
3. Zhou, J., Anjum, D. H., Chen, L., Xu, X., Ventura, I. A., Jiang, L. & Lubineau, G. 2014. The temperature- dependent microstructure of PEDOT/ PSS films: insights from morphological, mechanical and electrical analyses. *J. Mater. Chem. C,* 2**,** 9903-9910.
4. Thompson, B. T. 2017. *Enhancing the conductivity of PEDOT:PSS on bulk substrates.* Doctor of Philosophy, University of Warwick.
5. Giuri, A., Masi, S., Colella, S., Listorti, A., Rizzo, A., Kovtun, A., Dell'Elce, S., Liscio, A. & Corcione, C. E. 2017. Rheological and physical characterization of PEDOT:PSS/Graphine Oxide nanocomposites for perovskite solar cells. *Polymer Engineering & Science,* 57**,** 546-552.
6. Elschner, A., Kirchmeyer, S., Lövenich, W., Merker, U. & Reuter, K. 2011. *PEDOT; principals and applications of an intrinsically conductive polymer*, CRC Press.
7. Romyen, N., Thongyai, S., Praserthdam, P. & Wacharawichanant, S. 2017. Effect of Surfactant Addition During Polymerization on Properties of PEDOT:PSS for Electronic Applications. *Journal of Electronic Materials,* 46**,** 6709-6716.
8. Nardes, A. M., Kemerink, M., de Kok, M. M., Vinken, E., Maturova, K. & Janssen, R. A. J. 2008. Conductivity, work function, and environmental stability of PEDOT:PSS thin films treated with sorbitol. *Organic Electronics,* 9**,** 727-734.
9. Kim, S.-M., Kim, C.-H., Kim, Y., Kim, N., Lee, W.-J., Lee, E.-H., Kim, D., Park, S., Lee, K., Rivnay, J. & Yoon, M.-H. 2018. Influence of PEDOT:PSS crystallinity and composition on electrochemical transistor performance and long-term stability. *Nature communications,* 9**,** 3858-3858.
10. Peters, K., Braun, J., Schmidt-Hansberg, B., Scharfer, P. & Schabel, W. 2011. Phase equilibrium of water in different types of PEDOT:PSS. *Chemical Engineering & Processing: Process Intensification,* 50**,** 555-557.
11. Huang, J., Miller, P. F., Wilson, J. S., De Mello, A. J., De Mello, J. C. & Bradley, D. D. C. 2005. Investigation of the Effects of Doping and Post-Deposition Treatments on the Conductivity, Morphology, and Work Function of Poly(3,4-ethylenedioxythiophene)/Poly(styrene sulfonate) Films. *Advanced Functional Materials,* 15**,** 290-296.
12. Kim, Y. H., Sachse, C., Machala, M. L., May, C., Müller-Meskamp, L. & Leo, K. 2011. Highly Conductive PEDOT:PSS Electrode with Optimized Solvent and Thermal Post-Treatment for ITO-Free Organic Solar Cells. *Advanced Functional Materials,* 21**,** 1076-1081.
13. Zhou, J., Ventura, I. & Lubineau, G. 2014. Probing the Role of Poly(3,4-ethylenedioxythiophene)/ Poly(styrenesulfonate)-Coated Multiwalled Carbon Nanotubes in the Thermal and Mechanical Properties of Polycarbonate Nanocomposites. *Industrial & Engineering Chemistry Research,* 53**,** 3539-3549.
14. Lakshmi, K. 2007. *Development of thermoplastic conducting polymer composites based on polyaniline and polythiophenes for microwave and electrical applications.* Doctor of Philosophy, Cochin University of Science and Technology.

15. Kiebooms, R., Aleshin, A., Hutchison, K., Wudl, F. & Heeger, A. 1999. Doped poly(3,4- ethylenedioxythiophene) films: Thermal, electromagnetical and morphological analysis. *Synthetic Metals,* 101**,** 436-437.
16. Kvarnström, C., Neugebauer, H., Blomquist, S., Ahonen, H. J., Kankare, J. & Ivaska, A. 1999. In situ spectroelectrochemical characterization of poly(3,4- ethylenedioxythiophene). *Electrochimica Acta,* 44**,** 2739-2750.
17. Han, M. G. & Foulger, S. H. 2004. Crystalline Colloidal Arrays Composed of Poly(3,4-ethylenedioxythiophene)-Coated Polystyrene Particles with a Stop Band in the Visible Regime. *Advanced Materials,* 16**,** 231-234.
18. Rutledge, S. A. & Helmy, A. S. 2015. Etch-free patterning of poly(3,4-ethylenedioxythiophene)-poly(styrenesulfonate) for optoelectronics. *ACS applied materials & interfaces,* 7**,** 3940-3948.
19. Glagovich, N. 2005. *IR Absorptions for Representative Functional Groups* [Online]. Available: http://www.instruction.greenriver.edu/kmarr/chem%20162/Chem162%20Labs/Interpreting%20IR%20Spectra/IR%20Absorptions%20for%20Functional%20Groups.htm [Accessed 08/03/2018].
20. Sriprachuabwong, C., Karuwan, C., Wisitsorrat, A., Phokharatkul, D., Lomas, T., Sritongkham, P. & Tuantranont, A. 2012. Inkjet- printed graphene- PEDOT:PSS modified screen printed carbon electrode for biochemical sensing. *Journal of Materials Chemistry,* 22**,** 5478-5485.
21. Alemu, D., Wei, H.-y., Ho, K.-c. & Chu, C.-w. 2012. Highly conductive PEDOT:PSS electrode by simple film treatment with methanol for ITO-free polymer solar cells. *Energy Environ. Sci.,* 5**,** 9662-9671.
22. Shimadzu Co. 2018. *Measurement Methods for Powder Samples* [Online]. Available: https://www.shimadzu.com/an/ftir/support/ftirtalk/talk8/intro.html [Accessed 12/03/18].
23. Shimadzu Co. 2018. *Q: Can you tell me why the spectrum baseline is curved?* [Online]. Available: https://www.shimadzu.com/an/ftir/support/faq/5.html [Accessed 23/02/18].
24. Neag, C. M. 1995. Coatings Characterization by Thermal Analysis. *In:* Koleske, J. V. (ed.) *Paint and coating testing manual : fourteenth edition of the Gardner-Sward handbook.* 14th ed. Philadelphia, PA: ASTM.
25. polymersource.com 2010. Poly(4-styrene sulfonic acid) or poly(styrene sulfonic acid) in dialysed form or undialysed form. Sample #: P4998-USSO3H-Undialysed form.
26. Yu, Z., Xia, Y., Du, D. & Ouyang, J. 2016. PEDOT:PSS Films with Metallic Conductivity through a Treatment with Common Organic Solutions of Organic Salts and Their Application as a Transparent Electrode of Polymer Solar Cells. *ACS Appl. Mater. Interfaces,* 8**,** 11629-11638.
27. Svoboda, R., Maqueda, L. P., Podzemná, V., Perejon, A. & Svoboda, O. 2020. Influence of DSC thermal lag on evaluation of crystallization kinetics. *Journal of Non-Crystalline Solids,* 528**,** 119738.
28. Kirchmeyer, S., Reuter, K. & Simpson, J. 2007. Poly(3,4-ethylene dioxythiophene) scientific importance, remarkable properties, and applications. *In:* Skotheim, T. & Reynolds, J. (eds.) *Handbook of conducting polymers.* 3rd ed. Boca Raton, London and New York: CRC press.
29. Schawe, J. 2012. Practical aspects of the Flash DSC 1: Sample preparation for the measurements of polymers. *Mettler Toledo UserCom 36***,** 17-24.

30. Kim, N., Kee, S., Lee, S. H., Lee, B. H., Kahng, Y. H., Jo, Y. R., Kim, B. J. & Lee, K. 2014. Highly Conductive PEDOT:PSS Nanofibrils Induced by Solution- Processed Crystallization. *Advanced Materials,* 26**,** 2268-2272.
31. Zotti, G., Zecchin, S., Schiavon, G., Louwet, F., Groenendaal, L., Crispin, X., Osikowicz, W., Salaneck, W. & Fahlman, M. 2003. Electrochemical and XPS studies toward the role of monomeric and polymeric sulfonate counterions in the synthesis, composition, and properties of poly(3,4- ethylenedioxythiophene). *Macromolecules,* 36**,** 3337-3344.
32. Stöcker, T., Moos, R. & Köhler, A. 2012. Why does the electrical conductivity in PEDOT:PSS decrease with PSS content? A study combining thermoelectric measurements with impedance spectroscopy. *Journal of Polymer Science, Part B: Polymer Physics,* 50**,** 976-983.
33. Ouyang, J. 2013. "Secondary doping" methods to significantly enhance the conductivity of PEDOT:PSS for its application as transparent electrode of optoelectronic devices. *Displays,* 34**,** 423-436.
34. Po, R., Carbonera, C., Bernardi, A., Tinti, F. & Camaioni, N. 2012. Polymer- and carbon-based electrodes for polymer solar cells: Toward low-cost, continuous fabrication over large area. *Solar Energy Materials and Solar Cells,* 100**,** 97-114.
35. Shi, H., Liu, C., Jiang, Q. & Xu, J. 2015. Effective Approaches to Improve the Electrical Conductivity of PEDOT:PSS: A Review. *Advanced Electronic Materials,* 1**,** 1-16.
36. Sun, K., Zhang, S., Li, P., Xia, Y., Zhang, X., Du, D., Isikgor, F. & Ouyang, J. 2015. Review on application of PEDOTs and PEDOT:PSS in energy conversion and storage devices. *Journal of Materials Science: Materials in Electronics,* 26**,** 4438-4462.
37. Wen, Y. & Xu, J. 2017. Scientific Importance of Water-Processable PEDOT–PSS and Preparation, Challenge and New Application in Sensors of Its Film Electrode: A Review. 55**,** 1121-1150.
38. Kroon, R., Mengistie, D. A., Kiefer, D., Hynynen, J., Ryan, J. D., Yu, L. & Mller, C. 2016. Thermoelectric plastics: from design to synthesis, processing and structureproperty relationships. *Chemical Society Reviews,* 45**,** 6147-6164.
39. Kemerink, M., Timpanaro, S., De Kok, M. M., Meulenkamp, E. A., Touwslager, F. J. & Timpanaro, F. J. 2004. Three-dimensional inhomogeneities in PEDOT:PSS films. *Journal of Physical Chemistry B,* 108**,** 18820-18825.
40. Friedel, B., Brenner, T. J. K., McNeill, C. R., Steiner, U. & Greenham, N. C. 2011. Influence of solution heating on the properties of PEDOT:PSS colloidal solutions and impact on the device performance of polymer solar cells. *Organic Electronics,* 12**,** 1736-1745.
41. Groenendaal, L., Jonas, F., Freitag, D., Pielartzik, H. & Reynolds, J. R. 2000. Poly(3,4-ethylenedioxythiophene) and Its Derivatives: Past, Present, and Future. *Advanced Materials,* 12**,** 481-494.
42. Callister, W. D. 2000. Materials science and engineering: an introduction. 5th ed. New York; Chichester: Wiley.
43. Bubnova, O., Khan, Z. U., Wang, H., Braun, S., Evans, D. R., Fabretto, M., Hojati-Talemi, P., Dagnelund, D., Arlin, J.-B., Geerts, Y. H., Desbief, S., Breiby, D. W., Andreasen, J. W., Lazzaroni, R., Chen, W. M., Zozoulenko, I., Fahlman, M., Murphy, P. J., Berggren, M. & Crispin, X. 2013. Semi-metallic polymers. *Nature Materials,* 13**,** 190.
44. Yoon, S. S. & Khang, D. 2016. Roles of Nonionic Surfactant Additives in PEDOT:PSS Thin Films. *J. Phys. Chem. C,* 120**,** 29525-29532.
45. Koidis, C., Logothetidis, S., Kapnopoulos, C., Karagiannidis, P. G., Laskarakis, A. & Hastas, N. A. 2011. Substrate treatment and drying conditions effect on the properties of roll-to-roll gravure printed PEDOT:PSS thin films. *Materials Science & Engineering B,* 176**,** 1556-1561.

46. Lombardo, V., Apos, Urso, L., Mannino, G., Scalese, S., Spucches, D., La Magna, A., Terrasi, A. & Puglisi, R. A. 2018. Transparent conductive polymer obtained by in-solution doping of PEDOT:PSS. *Polymer*, 155**,** 199-207.
47. Lenntech. 2018. *Water Conductivity* [Online]. Available: https://www.lenntech.com/applications/ultrapure/conductivity/water-conductivity.htm [Accessed 24/05/18].
48. Azzopardi, B., Emmott, C. J. M., Urbina, A., Krebs, F. C., Mutale, J. & Nelson, J. 2011. Economic assessment of solar electricity production from organic-based photovoltaic modules in a domestic environment. *Energy Environmental Science*, 4**,** 3741-3753.
49. Kawano, K., Pacios, R., Poplavskyy, D., Nelson, J., Bradley, D. D. C. & Durrant, J. R. 2006. Degradation of organic solar cells due to air exposure. *Solar Energy Materials & Solar Cells*, 90**,** 3520-3531.
50. Huang, J., Miller, P. F., de Mello, J. C., de Mello, A. J. & Bradley, D. D. C. 2003. Influence of thermal treatment on the conductivity and morphology of PEDOT/PSS films. *Synthetic Metals,* 139**,** 569-572.
51. Aasmundtveit, K. E., Samuelsen, E. J., Pettersson, L. A. A., Inganäs, O., Johansson, T. & Feidenhans, R. 1999. Structure of thin films of poly(3,4-ethylenedioxythiophene). *Synthetic Metals,* 101**,** 561-564.
52. Vitoratos, E., Sakkopoulos, S., Dalas, E., Paliatsas, N., Karageorgopoulos, D., Petraki, F., Kennou, S. & Choulis, S. A. 2009. Thermal degradation mechanisms of PEDOT:PSS. *Organic Electronics: physics, materials, applications,* 10**,** 61-66.

Chapter 4: Results and Discussion – Effect of Tween 80 on the Properties of PEDOT:PSS

In this chapter, the effects of adding the non-ionic surfactant Tween 80 to aqueous PEDOT:PSS (titled PEDOT:PSS/Tween 80) in differing quantities will be explored. This will cover variations in the thermal and physical properties of the combined materials and how this impacts processing. Additionally, the conductivity of PEDOT:PSS/Tween 80 films will be studied both in sheet and bulk resistivity testing. Techniques such as AFM, XRD and Raman spectroscopy will be used to identify structural changes between PEDOT:PSS and the PEDOT:PSS/Tween 80 mixture in order to provide explanations for any variations in conductivity. Finally, the solution properties of PEDOT:PSS/Tween 80 will be examined to determine how surfactant variation alters viscosity and wettability.

4.1 Tween 80 Concentration

The concentrations of Tween 80 are expressed as a wt% of the surfactant in the initial PEDOT:PSS/Tween 80 mixture and not the films. It is important to emphasise that the PEDOT:PSS solid content is 1.2 wt%,[1] meaning the ratio between PEDOT:PSS and Tween 80 is much higher. Furthermore, when the water is removed, the wt% of surfactant in the film will also be greater. For example, when 1.2 wt% of surfactant is added to this solution, the weight ratio of PEDOT:PSS to Tween 80 would be 1:1 (further examples can be seen in Table 4-1).[2] This shows that when the films are dry it is possible for excess quantities of surfactant to be present which cause issues as discussed throughout the following chapters.

Table 4-1: Examples of how Tween 80 weight percentage (wt%) in solution relates to the approximate wt% Tween 80 in a dried PEDOT:PSS/Tween 80 film assuming all water has been removed

Tween 80 Concentration in PEDOT:PSS solution (wt%)	PEDOT:PSS solid content in PEDOT:PSS/Tween 80 solution (wt%)	PEDOT:PSS to Tween 80 ratio	Tween 80 percentage in film (wt%)
0.00	1.20	n/a	0
0.50	1.19	2.38:1	29.5
1.00	1.19	1.19:1	45.7
1.50	1.18	0.79:1	55.9
2.00	1.18	0.59:1	63.0
2.50	1.17	0.47:1	68.1
3.00	1.16	0.39:1	72.0

4.2 Thermal Analysis of PEDOT:PSS/Tween 80

4.2.1 Thermal Gravimetric Analysis (TGA)

Initial work on PEDOT:PSS/Tween 80 mixtures focused on the effect of Tween 80 on the thermal stability and therefore suitability of the previously identified processing conditions. As discussed (section 3.1.1), the TGA of PEDOT:PSS in air shows an initial mass loss of about 10 % due to water and then degradation onsets around 250 °C Figure 4-1.[2-5] However, in air, the TGA trace significantly changes with the addition of Tween 80. Whilst there is a comparable mass loss that can be attributed to moisture, the surfactant addition causes the onset of degradation to appear at approximately 160 °C, much lower than pristine PEDOT:PSS. This becomes more pronounced in samples with a higher Tween 80 content. Between 160 – 260 °C the sample containing 0.37 wt% surfactant loses around 10 % mass whereas samples containing 0.93 and 1.32 wt% Tween 80 decrease by approximately 30 %. Samples of 0.37 and 0.93 wt% also shows a second mass reduction which coincides with the degradation of pristine

PEDOT:PSS at 250 °C. However, this drop reduces with increasing Tween 80 concentration and eventually disappears for the highest surfactant concentration. This may partially be explained by the relative concetration of surfactant in the dry sample contributing to a much greater proportion of the sample (Table 4-1).

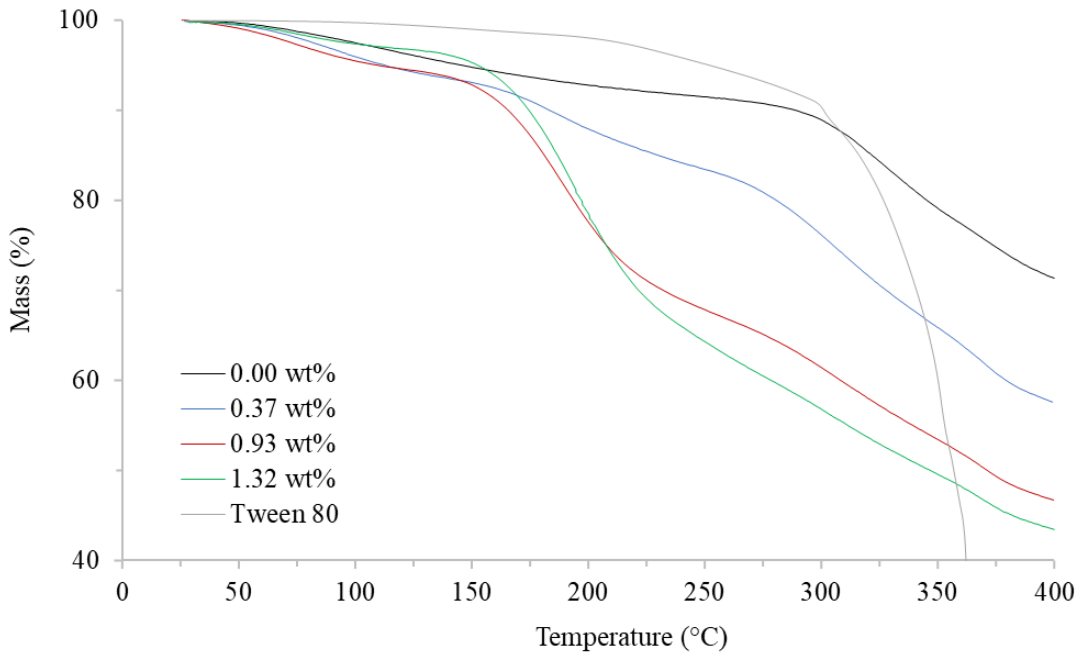

Figure 4-1: TGA trace showing the degradation properties of pristine PEDOT:PSS (black), Tween 80 (grey), and PEDOT:PSS/Tween 80 with surfactant percentages of 0.37 (blue), 0.93 (red) and 1.32 (green) wt%. Samples run from 25 °C to 400 °C at 10 °Cmin^{-1} in air

It is clear that the earlier degradation, seen in the PEDOT:PSS/Tween 80 samples, is caused by the addition of surfactant. However, Tween 80 on its own does not display significant degradation until 220 °C (Figure 4-1).[6] Even though mass loss is more significant at this point, there is still only a 10 % mass decrease up to 300 °C at which point major degradation occurs.[6] Therefore, this does not explain why, when added to PEDOT:PSS, the mass loss is substantially greater at lower temperatures.

One explanation is that the addition of the surfactant to PEDOT:PSS alters the properties of the system is such a way that degradation will occur earlier. A similar case was seen with the use of PF_6^- as a counterion to PEDOT, instead of PSS, in which the samples degraded at 150 °C.[7] However, despite this demonstrating the potential for decreased thermal stability, an alternative counterion is not being used in this study. The addition of surfactants DDAPS and SDBA have been reported to reduce the onset of degradation by 10 – 15 °C.[8] However, these reported changes are significantly smaller than the change in degradation onset caused by Tween 80 addition (Figure 4-1).

To provide further insight, Tween 80 was heated in air to assess signs of degradation at lower temperatures which may not incur significant mass loss. Visual inspection of the surfactant showed a colour change as the temperature increased above 160 °C (Figure 4-2). Tween 80 can undergo auto-oxidation at elevated temperatures, explaining the yellowish colour seen.[9,10] This could provide an alternate explanation as to why the PEDOT:PSS/Tween 80 system starts to show signs of degradation at 150 °C. Furthermore, as Tween 80 degrades there is chain scission of the C–O and C–C bonds leading to the creation of acids, such as formic and acetic acid.[6,9-12] It is, therefore, possible that the presence of these acids within the sample causes degradation of PEDOT:PSS.

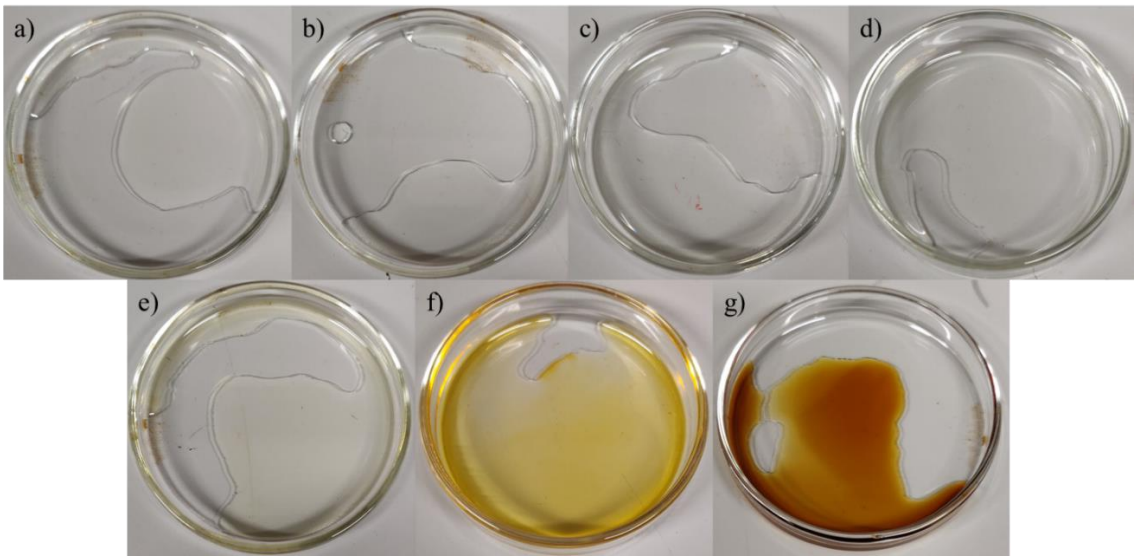

Figure 4-2: Tween 80 degradation images showing the change in colour caused by higher temperature. Samples held for 1 hour at a) 60, b) 100, c) 120, d) 160, e) 180, f) 200 and g) 220 °C

The TGA data shows that the addition of Tween 80 into PEDOT:PSS reduces the degradation temperature, therefore, impacting the maximum annealing temperature that can be used. Whereas pristine PEDOT:PSS could feasibly be annealed up to 200 °C, the PEDOT:PSS/Tween 80 samples are limited to 140 °C to ensure no degradation occurs which could negatively impact the conductivity of the films.[13,14]

4.2.2 Fourier Transform Infra-Red Spectroscopy (FTIR)

Figure 4-3 shows the FTIR spectra of undegraded Tween 80 which is similar to that seen in the literature.[15] The CH_2 and CH_3 groups in the surfactant show up as peaks at 840, 945 and two large peaks between 2850 – 2900 cm^{-1}. There is also a large amount of OH units within the Tween 80 chemical structure which appear as a broad peak between 3100 – 3700 cm^{-1}.[16] Finally, there are two peaks at 1100 and 1730 cm^{-1} which are associated with the C-O and C=O bonds of the ester group, respectively.[15-17]

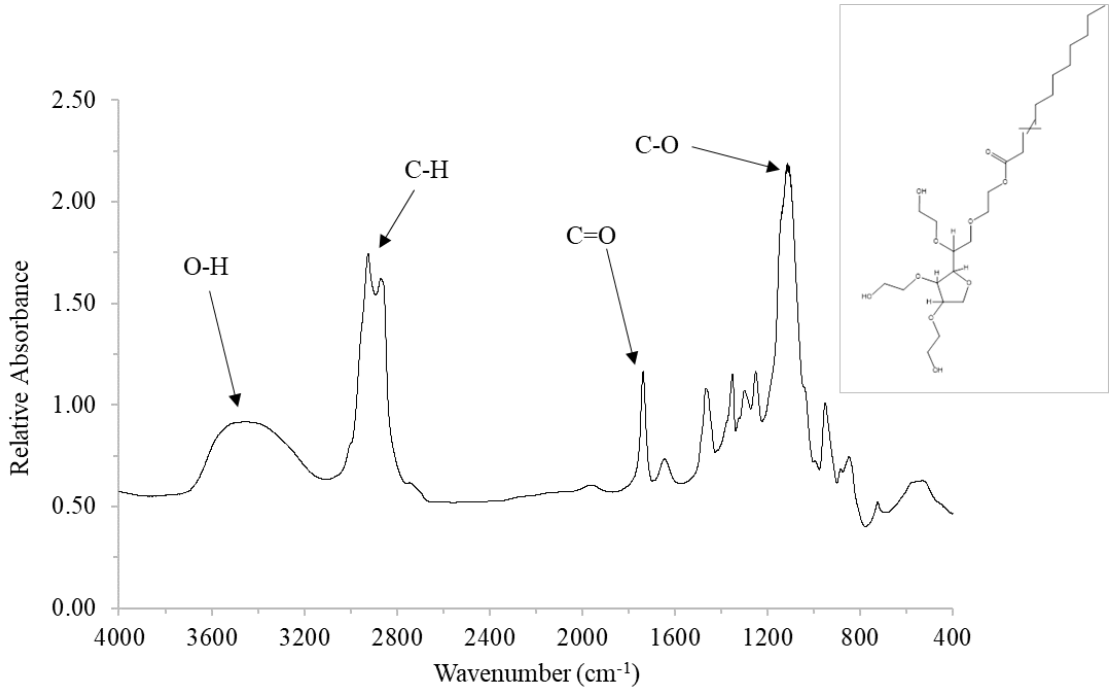

Figure 4-3: FTIR spectra of undegraded Tween 80 with key peaks highlighted. Insert shows Tween 80 chemical structure replicated from Pubchem (2018)[18]

The effect of heating and degrading Tween 80 can be seen in Figure 4-4. There is no discernible difference between the undegraded sample and Tween 80 heated to 140 °C suggesting no degradation occurs at this temperature. However, the sample heated to 250 °C shows a significant reduction in the ratio of key absorbance peaks. This is particularly prominent for the C-O peak at 1100 cm^{-1} which is to be expected since Tween 80 degrades via chain scission of the C-O and C-C bonds, leading to the creation of acids.[6,9-11]

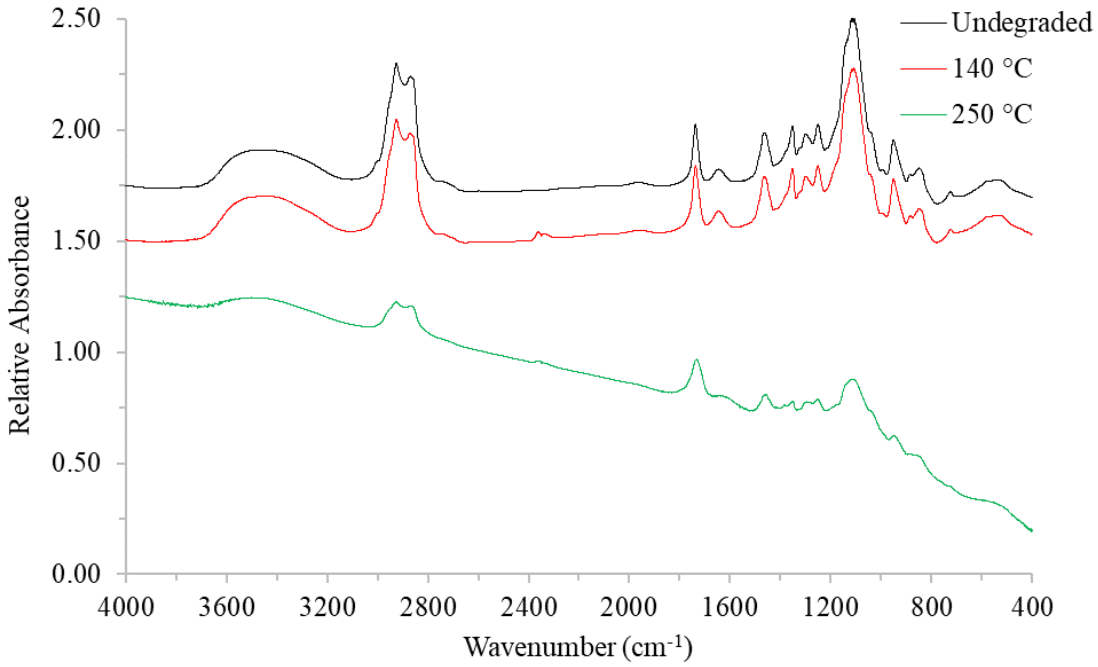

Figure 4-4: FTIR traces of Tween 80 after exposure to varying temperatures. Temperatures given in °C in legend

The FTIR data in Figure 4-5 shows the effect of adding increasing quantities of Tween 80 to PEDOT:PSS. As expected, with more surfactant there is a corresponding increase in the peaks primarily associated with Tween 80 (Figure 4-4). However, the majority of these bonds can also be found within the structure of PEDOT:PSS so using them as identifying peaks for the presence of Tween 80 is not sufficient. On the other hand, the peak seen at 1730 cm^{-1} only appears once the surfactant has been added and continues to increase in size with further surfactant addition. This is because it represents the C=O unit of the ester in Tween 80, which is not present in PEDOT:PSS.[15-17] It has also been suggested that this peak might be an indicator for the level of doping in PEDOT.[19] However, given the significant change it is more likely related to the increase in C=O concentration.

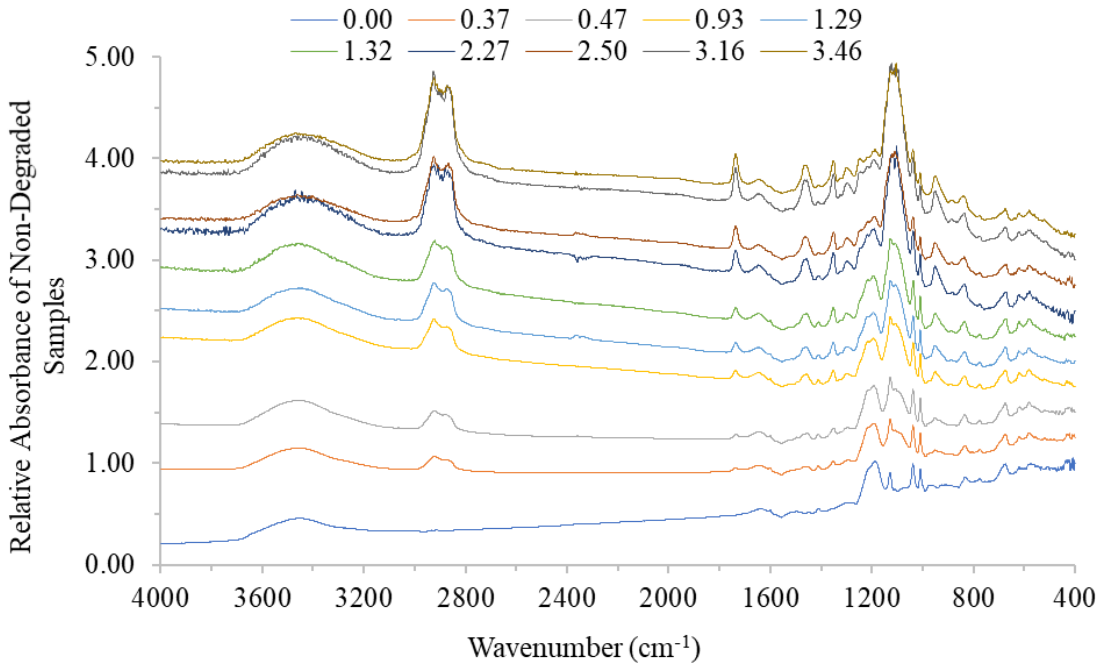

Figure 4-5: FTIR traces of undegraded PEDOT:PSS containing varying concentrations of Tween 80 measured in transmission. Samples dried at 140 °C The trace with the lowest Tween 80 concentration is at the bottom with progressively greater concentrations further up. All concentrations used are shown as a weight percentage in the legend

The samples from Figure 4-5 were degraded at 250 °C for 1 hour and the resultant IR spectra for Tween 80 concentrations of 0.00, 0.93, 2.27 and 2.46 wt% are shown in Figure 4-6. As before (section 3.1.1.1), the peak at a 1200 cm^{-1} disappears after degradation due to the loss of the sulfonate group within PSS.[2,13,20] Whilst there are still larger peaks at 2850 – 2900 cm^{-1} for increasing Tween 80 concentration, the size of these peaks is reduced compared to the undegraded samples. There is also a reduction in peak size at wavenumber 1100 cm^{-1}, associated with the chain scission of C-O bonds in Tween 80.[6,9-11] However, the peak at 1730 cm^{-1}, representing C=O,[15-17] was unaffected by degradation, due to the double bond between carbon and oxygen requiring more energy to break. This shows that the degradation mechanisms of PEDOT:PSS and Tween 80 are unaffected when used in combination.

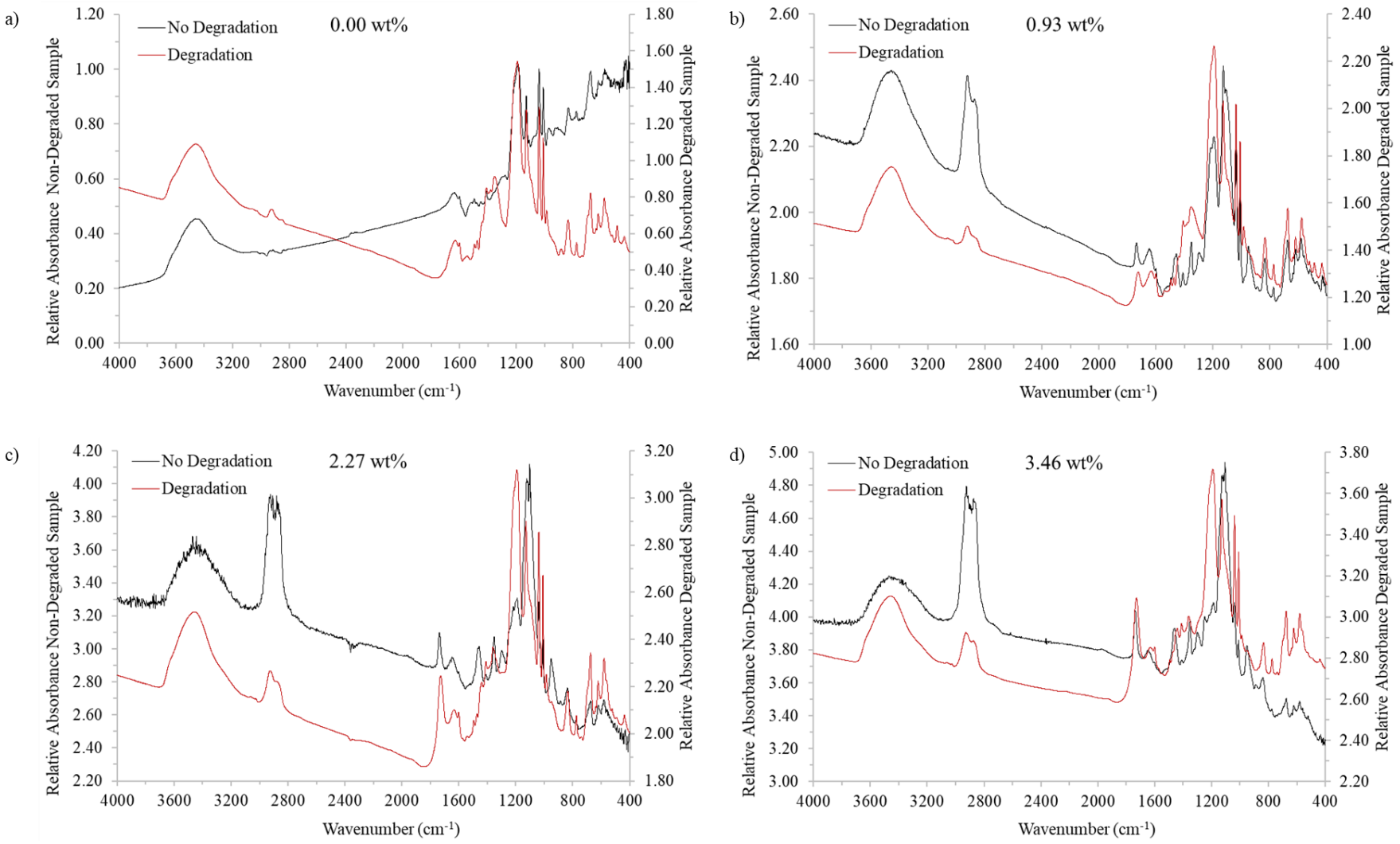

Figure 4-6: FTIR traces of non-degraded (black) and degraded (red) samples of PEDOT:PSS/Tween 80 containing surfactant concentrations of a) 0.00, b) 0.93, c) 2.27 & d) 3.46 wt%. Samples dried at 140 °C then degraded at 250 °C. Measurement performed in transmission

4.3 Processing Optimisation for PEDOT:PSS/Tween 80 Films

A series of experiments were run to assess the optimum processing conditions for PEDOT:PSS/Tween 80 films, while keeping surfactant concentration constant (approximately 0.52 wt% following work done by Thompson (2017)[21]) and compare these to pristine PEDOT:PSS. It has already been shown that the maximum annealing temperature was limited due to an earlier onset of degradation caused by the addition of Tween 80 (section 4.2.1) which brought into question whether other processing parameters would change. Optimisation was done in regard to the resistivity of the films and was considered optimal when the resistivity reached the lowest value.

4.3.1 Annealing Temperature Effect on PEDOT:PSS/Tween 80 Sheet Resistivity

Sheet resistivity was measured, after atmospheric equilibration for 12 hours, to analyse the effect of annealing temperature on samples of pristine PEDOT:PSS compared to PEDOT:PSS/Tween 80 containing approximately 0.52 wt% surfactant (calculated from volume addition) (Figure 4-7). What is initially noticeable is that as the annealing temperature increased, the sheet resistivity decreased for samples with and without surfactant. The data shows that the lowest resistivity achieved with the surfactant present was 210 $\Omega\square^{-1}$ after annealing at 140 °C which was significantly lower than samples annealed at 100 and 120 °C ($p<0.001$). This is also the first indication that the addition of Tween 80 is positively impacting the conductivity since for each annealing condition, the sample containing the surfactant has a lower resistivity and reduced variation.

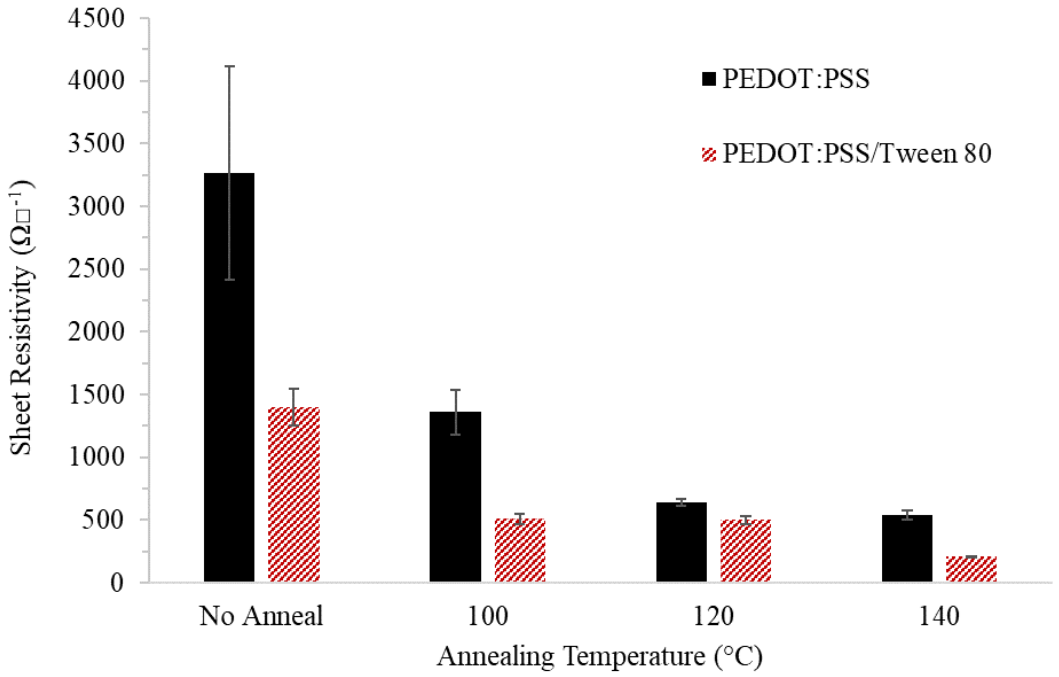

Figure 4-7: Mean sheet resistivity (Ω□$^{-1}$) of pristine PEDOT:PSS (blocked out black) and PEDOT:PSS/Tween 80 (striped, red) for different annealing temperatures. Error bars show ± 1 SD

Similar to pristine PEDOT:PSS (section 3.3.1), the samples containing Tween 80 show a lower resistivity at elevated temperatures due to removal of water from the film.[3,13,21-23] It is well known that removal of excess water from the PSS-rich phase causes a reduction in swelling and therefore a shortening of the hopping distance between PEDOT-rich sites distance.[3,13,21-23] It is also thought that the increased temperature causes the PSS to soften, and structural rearrangement can occur leading to a decrease in sheet resistivity (section 3.3.1).[13,24,25] This may be more significant here given it is suspected that the surfactant will be disrupting the PEDOT and PSS interaction, allowing for increased chain mobility.[14,26,27] The mechanisms causing the sheet resistivity decrease in samples containing Tween 80 will be discussed further in section 4.4.5.

These results show that 140 °C is the optimum annealing temperature to obtain the lowest resistivity from PEDOT:PSS/Tween 80 films, without causing degradation.

4.3.2 Annealing Time Effect on PEDOT:PSS/Tween 80 Sheet Resistivity

Figure 4-8 shows the effect of annealing time on PEDOT:PSS/Tween 80 film resistivity for a surfactant concentration of approximately 0.52 wt% (calculated from volume addition). Samples were annealed at 140 °C for various times and resistivity was measured after equilibration in atmospheric conditions for 12 hours. The data shows a large drop in sheet resistivity, even at the short annealing time of 20 minutes. Furthermore, ANOVA showed a statistically significant decrease in the mean sheet resistivity between samples annealed for 20 and 40 minutes, and samples for above 60 minutes ($p<0.05$). However, the results are not significantly different from 60 to 120 minutes.

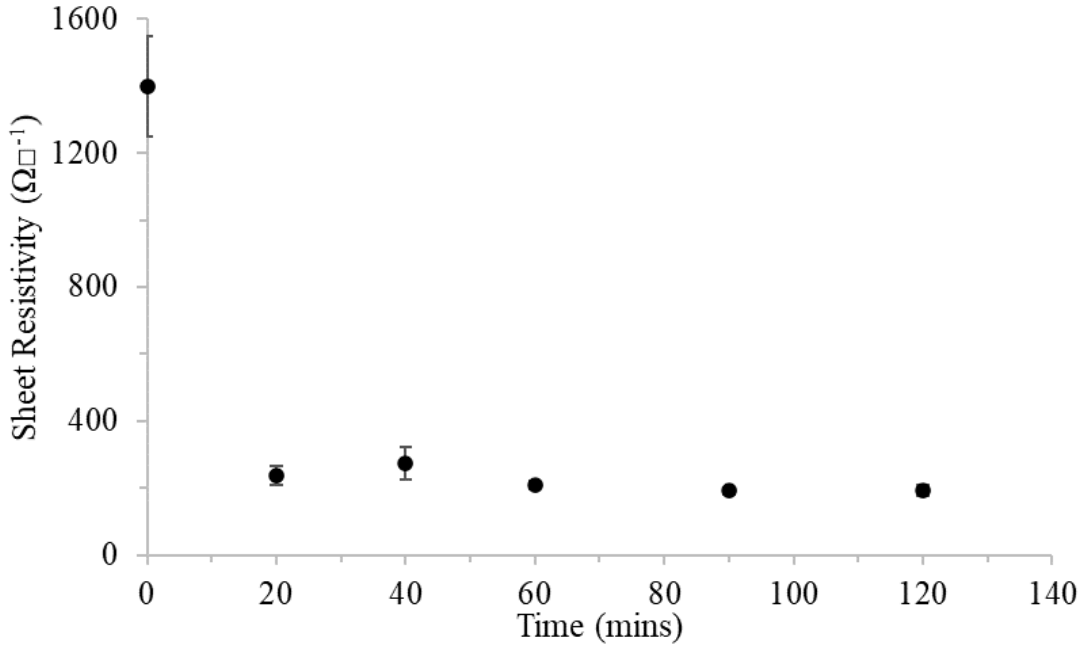

Figure 4-8: Mean sheet resistivity (Ω□$^{-1}$) of PEDOT:PSS/Tween 80 films for varying annealing times. Error bars show ± 1 SD

As previously mentioned, (section 4.3.1), it is likely that water removal and chain reorganisation are the main causes of the decrease in resistivity with increasing annealing time.[3,13,21-25] It was seen in the previous chapter that at least 40 minutes was needed to anneal pristine PEDOT:PSS (section 3.3.3), however, it is clear from this data that a minimum of 60 minutes is required for PEDOT:PSS/Tween 80. It is likely that the water removal from the sample will be quicker, due to less moisture being absorbed when the surfactant is present.[28] However, whilst not discussed in the literature, the extended annealing time required could be attributed to an increase in the time needed for chain reorganisation when Tween 80 is added. It is already well established that the ionic interaction between the PEDOT and PSS hinders chain mobility,[3,27,29] with motion being limited to excess PSS.[24] Therefore, despite the surfactant being a plasticiser,[21] the presence of this large molecule attached to the PSS could provide a barrier to chain movement.[30]

4.4 PEDOT:PSS/Tween 80 Film Properties

The processing optimisation experiments discussed above show that PEDOT:PSS/Tween 80 films require annealing at 140 °C for 60 minutes to achieve the lowest sheet resistivity. However, a significant reduction in sheet resistivity, caused by the addition of Tween 80, regardless of processing conditions, is also clear (Figure 4-9). To explore this effect in more detail, surfactant concentration within the PEDOT:PSS solution was varied, and the resulting films analysed. The addition of Tween 80 to PEDOT:PSS in this section was established by mass measurement as opposed to previous wt% being calculated from volumes. This helped to reduce error in quoted surfactant concentration, particularly for smaller quantities. Processing parameters were kept constant as follows (unless otherwise specified): films set at room temperature for 12 hours prior to annealing at 140 °C for 60 minutes; annealed films allowed 12 hours to equilibrate in atmospheric conditions. At this stage, two different casting methods

were also implemented (dip and drop casting) in an attempt to replicate R2R and IJP manufacturing methods. Details of each method are expanded on in the relevant sections.

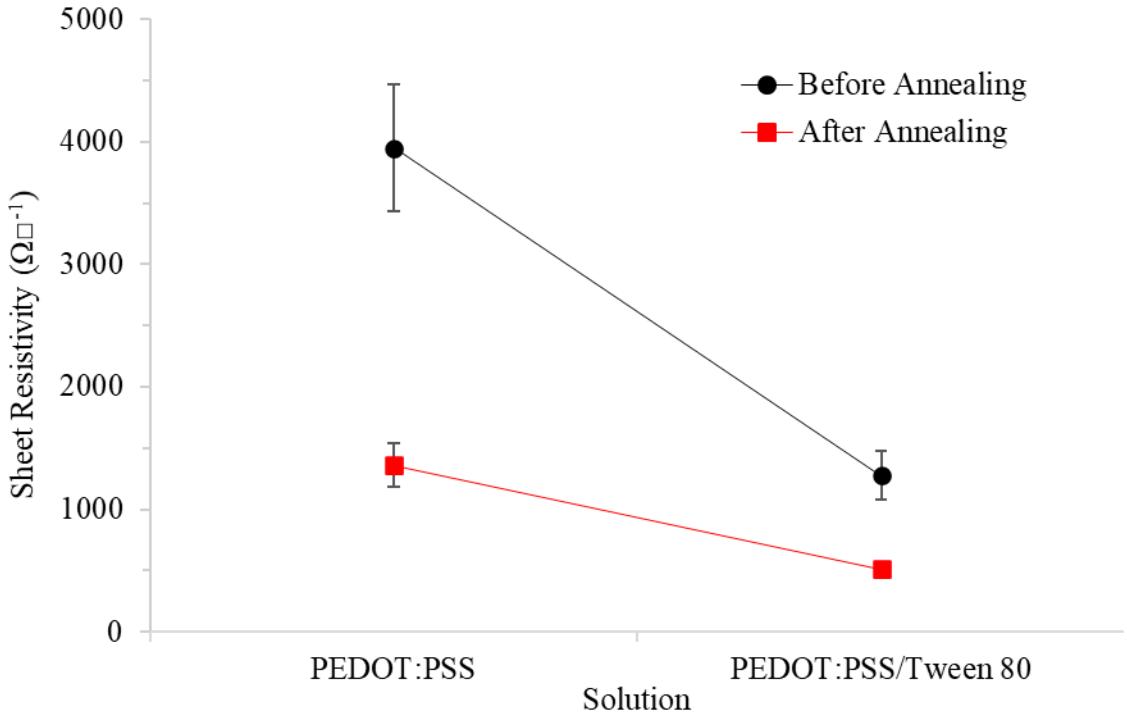

Figure 4-9: Mean sheet resistivity (Ω□$^{-1}$) of films made from solutions of pristine PEDOT:PSS and PEDOT:PSS/Tween 80 containing approximately 0.52 wt% surfactant before and after annealing. Error bars show ± 1 SD

4.4.1 Dip Cast PEDOT:PSS/Tween 80 Film Sheet Resistivity and Conductivity

PEDOT:PSS/Tween 80 solutions, with varying surfactant concentrations, were dip cast onto glass substrates. This was done by submerging half of the substrate in solution then allowing the film to set in atmospheric conditions in a horizontal orientation. Various dip times were tested, with 30 seconds selected as the shortest time needed to produce a coherent film. Analysis of the films showed a reduction in sheet resistivity with increasing Tween 80 concentration (Figure 4-10). A large initial reduction in sheet resistivity from over 1000 to 130 Ω□$^{-1}$ occurs

once a concentration of 0.90 wt% has been reached followed by a continued, but less substantial, decrease with further surfactant addition. The lowest resistivity recorded was 61 $\Omega\square^{-1}$ at a Tween 80 concentration of 3.46 wt%. A large difference in the variability of results is also present with samples containing no or low surfactant concentrations displaying a substantial scattering of results. This is likely due to non-uniform distribution of PEDOT and PSS caused by the core/shell structure leading to areas of higher and lower resistivity. However, scattering is reduced above 0.90 wt% Tween 80 addition suggesting the surfactant is disrupting the core/shell structure and a more uniform distribution of the two components is present. This is particularly important since this figure shows data collected from three different batches of PEDOT:PSS/Tween 80 solutions, all of which were made with different bottles but the same grade of aqueous PEDOT:PSS. This shows that, while there may be variation initially caused by the different PEDOT:PSS batches, the surfactant appears to appreciatively reduce this issue.

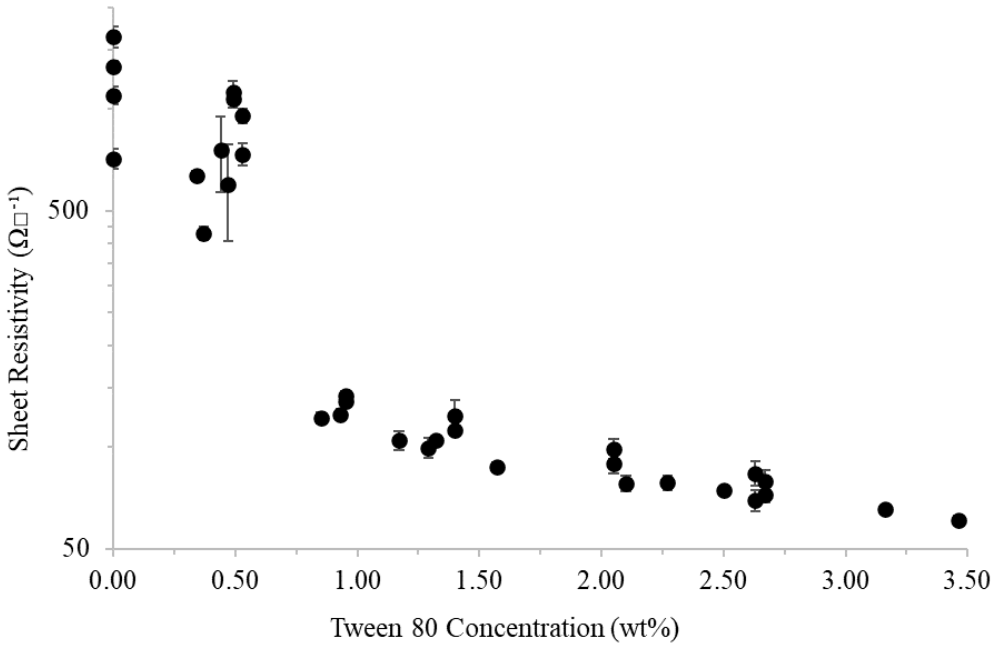

Figure 4-10: Effect of varying weight percentage (wt%) of Tween 80 in PEDOT:PSS on the sheet resistivity ($\Omega\square^{-1}$) of dip cast films. Results collected from three separate batches of PEDOT:PSS/Tween 80. Error bars show ± 1 SD

Figure 4-11 shows the corresponding conductivity, obtained from the sheet resistivity measurements, calculated after measuring average film thickness (section 2.6). As expected, the opposite trend to resistivity is seen, with increasing surfactant concentration causing an improvement in conductivity. There is an increase from around 3 Scm^{-1}, for pristine PEDOT:PSS, to 20 Scm^{-1} when the concentration is above 0.90 wt%. However, unlike with resistivity, the conductivity does not continue to steadily increase with further surfactant. The highest conductivity recorded was 26.8 Scm^{-1} at 1.40 wt% surfactant. Above this concentration, results decrease slightly to 14 – 18 Scm^{-1}. The reduction in variation also appears to be less pronounced once conductivity is calculated.

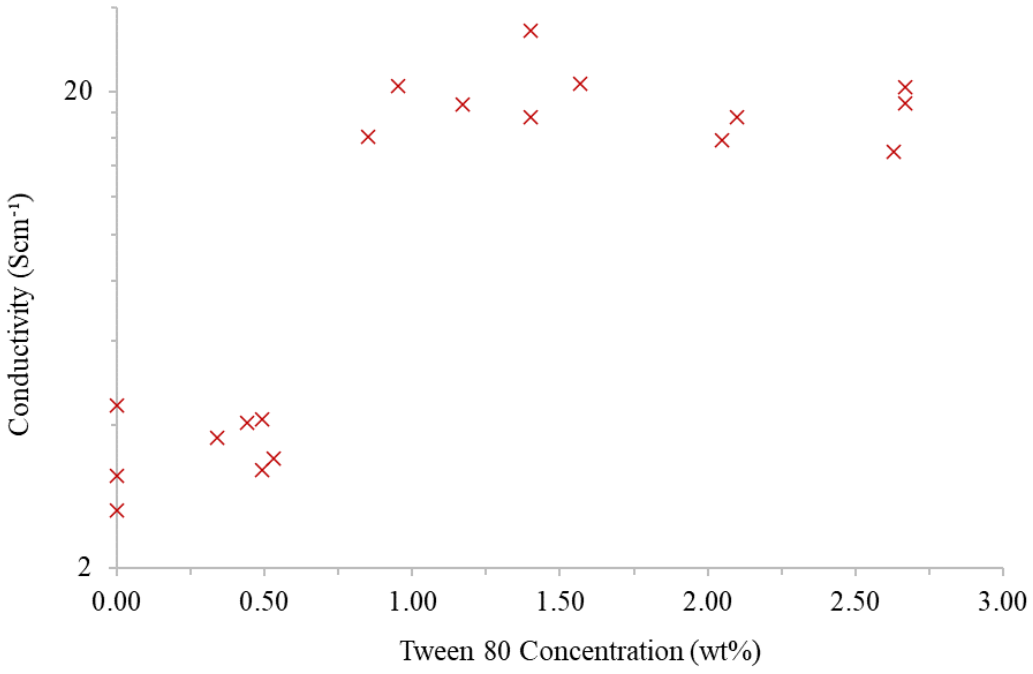

Figure 4-11: Effect of varying weight percentage (wt%) of Tween 80 in PEDOT:PSS on the conductivity (Scm^{-1}) of dip cast films. Results collected from three separate batches of PEDOT:PSS/Tween 80

It has been suggested in the literature that any addition will initially interact with the excess PSS in solution before disrupting the ionic bond between PEDOT and PSS.[31] Given Tween 80 is also an insulator, at low concentrations the surfactant is adding to the insulating material and a threshold of 0.90 wt% is required before any improvement is seen. Above this concentration, the Tween 80 will interfere with the bound PEDOT:PSS, allowing for separation of the two components and chain alignment, as is commonly seen in the literature for other surfactants and solvents.[2,14,26,27,32-44] Critically, this is the same reasoning given by Kim, *et al.* (2017)[31] and Oh, *et al.* (2014)[45] as to why Triton X-405 and Triton X-100 surfactants show improved conductivity when added to PEDOT:PSS. This will be explored in more detail with evidence to strengthen this argument in section 4.4.5.

Similarly, a plateau in electrical performance is seen in the literature, however, the concentration at which this occurs depends on the additive.[31,45] As discussed at the start of this chapter (section 4.1), the Tween 80 concentrations are quoted as the wt% in solution but once the water is removed, the surfactant concentration in the dry film will contribute to a much larger proportion. The start of the plateau is likely the point at which saturation of the PEDOT:PSS – Tween 80 interaction occurs.[8,14] While the sheet resistivity data suggests continued addition will cause a further resistivity decrease, this saturation effect is more obvious in the conductivity data. Here, the conductivity does not continue to increase and instead falls above approximately 1.25 wt%.

The reason for the discrepancy between the sheet resistivity and conductivity trends for surfactant concentrations above 0.90 wt% is likely linked to sample thickness (Figure 4-12). The data shows a clear increase in the thickness of dip cast PEDOT:PSS/Tween 80 films with increasing surfactant concentration. It has been established in the literature that an increase in thickness shows a non-linear decrease in sheet resistivity, with values plateauing at greater

thicknesses,[42,46-49] however, this does not translate to conductivity. For example, Martin, *et al.* (2004)[42] found a sheet resistivity of 4300 $\Omega\square^{-1}$ at 0.17 µm and 1800 $\Omega\square^{-1}$ at 0.53 µm, which would equate to conductivity values of 13.7 Scm^{-1} and 10.5 Scm^{-1}, respectively. In this case, there is a decrease in conductivity despite the large decrease in sheet resistivity.

Furthermore, PEDOT:PSS is made up of conductive (PEDOT-rich) and non-conductive (PSS-rich) areas. The non-conductive regions can be thought of as resistors in a circuit which follow Thevenin's theorem. When current flows through resistors in series (i.e., in line along the same path), then the contribution of each resistor is added together to provide the overall resistance. However, in parallel (i.e., stacked on top of each other running along different paths) the resistance is calculated as the sum of the inverse of each resistor. Therefore, in a thinner PEDOT:PSS sample, the PSS-rich regions can be thought of as resistors in series since the current will be forced to flow through these areas. However, thicker samples provide more opportunity for these regions to stack on top of each other and may allow for more conductive PEDOT-rich areas to reside more closely together. This would, in effect, mimic the circuit with resistors in parallel meaning the overall resistivity to current is lower. This may then be contributing to the discrepancy between resistivity and conductivity. This highlights the need for thickness to be factored in when assessing the electrical properties of a material.

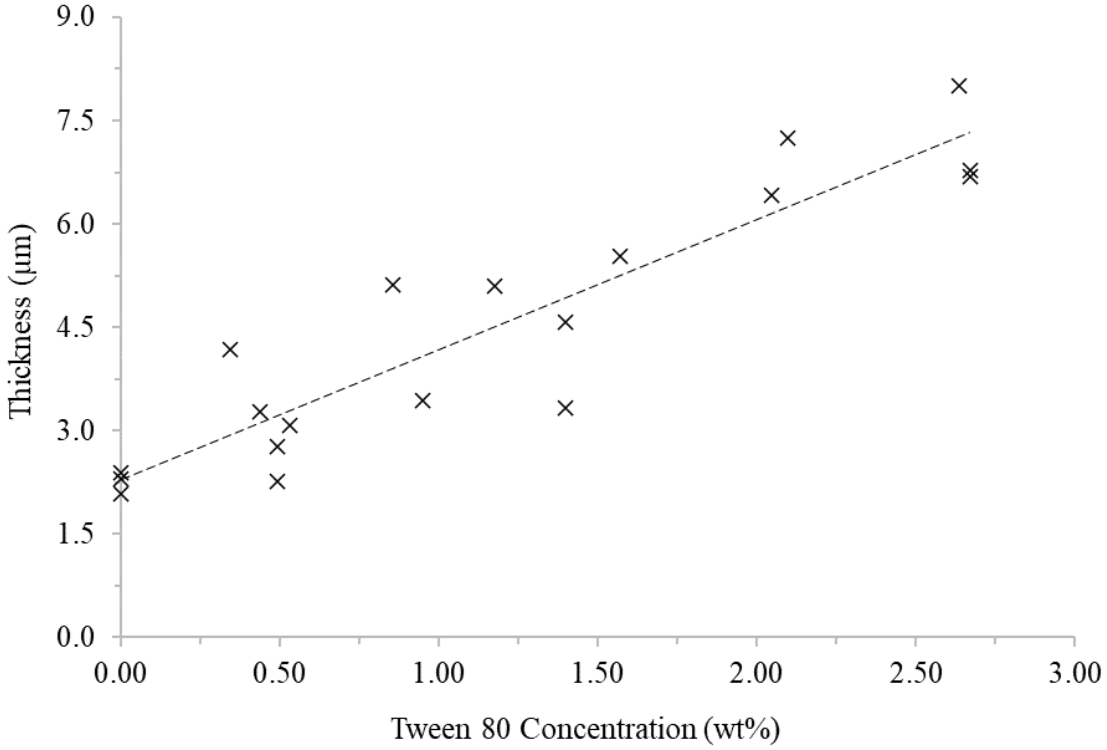

Figure 4-12: Average thickness (µm) of dip cast PEDOT:PSS/Tween 80 films for various surfactant concentrations (wt%). Dotted line is present to show data trend

While the data shows a substantial increase in the conductivity when Tween 80 is added, the maximum conductivity reached was approximately 26 Scm^{-1}. When compared to other literature values, this increase is relatively low. For example, improvements of 0.16 to 70 Scm^{-1}, 0.21 to 206 Scm^{-1} and 0.16 to 224 Scm^{-1} have been seen with SDS, Triton X-405 and SDBS, respectively.[31,40] The reason for this lower conductivity is most likely linked to the larger Mw of the Tween 80 molecule. The Mw of Tween 80 is 1310 $gmol^{-1}$, which is more than double that of Triton X-100.[50,51] The effect of Mw on conductivity enhancement was shown by Kim, *et al.* (2017)[31] in which a range of Triton X surfactants were assessed. It was found that the greatest conductivity improvement was achieved with the lowest Mw additive, which in this case was Triton X-405.[31] A similar result has also been seen with PEG, in which higher Mw

resulted in smaller conductivity improvements.[14] It has previously been suggested that a greater Mw will negatively impact chain mobility leading to a lower conductivity improvement.[14] It is also possible that there is an increase in the hopping distance created by larger molecules between conductive PEDOT-rich sites, hindering conductivity. Despite this, Tween 80 has been shown to positively impact conductivity strengthening the evidence that non-ionic surfactants can be used as effective enhancing agents.

4.4.2 Drop Cast PEDOT:PSS/Tween 80 Film Sheet Resistivity and Conductivity

PEDOT:PSS/Tween 80 solutions, with varying surfactant concentrations, were drop cast onto glass substrates. This was done by pipetting 0.4 ml of each solution onto the substrate, ensuring full coverage. The effect of surfactant concentration on sheet resistivity is comparable to dip cast films (Figure 4-13) with increasing surfactant concentrations decreasing sheet resistivity. As before, this only occurs above 0.50 wt% Tween 80 and the results also show a plateau at 1.21 wt% producing a resistivity of 276 $\Omega\square^{-1}$. However, unlike dip cast samples, resistivity does not continue to decrease with increasing surfactant concentration, with the greatest concentration of 2.63 wt% yielding 260 $\Omega\square^{-1}$. There is a degree of fluctuation in the sheet resistivity between these points, and the lowest recorded resistivity obtained for drop cast films was 255 $\Omega\square^{-1}$ at a concentration of 2.13 wt%.

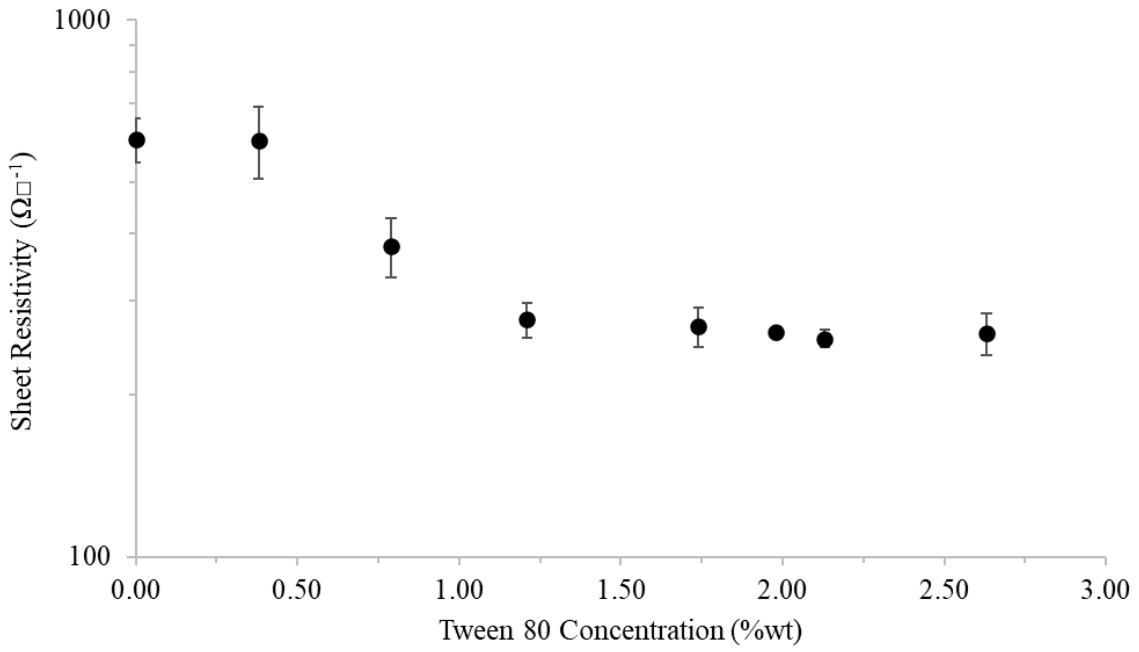

Figure 4-13: Effect of varying weight percentage (wt%) of Tween 80 in PEDOT:PSS solution on the sheet resistivity ($\Omega\square^{-1}$) of drop cast films. Error bars show ± 1 SD

As discussed in more detail for the dip cast films (section 4.4.1), a decrease in resistivity will only occur once a suitable quantity of surfactant has been added to interact with the excess PSS, followed by further addition disrupting the ionic interaction.[31] Improvement then plateaus once the concentration of Tween 80 is similar to that of the solid content of PEDOT:PSS in solution (i.e., 1.2 wt%). There are, however, some discrepancies in the resistivity between the coating methods. Firstly, the sheet resistivity of pristine PEDOT:PSS is lower for drop cast samples (599 $\Omega\square^{-1}$) that dip cast (715 $\Omega\square^{-1}$). This was due to the drop cast films being consistently thicker than dip cast films (Figure 4-14), causing to sheet resistivity to be lower.[42,46-49] However, it is also clear that the reduction in resistivity obtained when adding Tween 80 is not as great with drop casting. The lowest measurement for dip casting was 61 $\Omega\square^{-1}$ at 3.46 wt%, compared to 260 $\Omega\square^{-1}$ at 2.63 wt% for drop cast films.

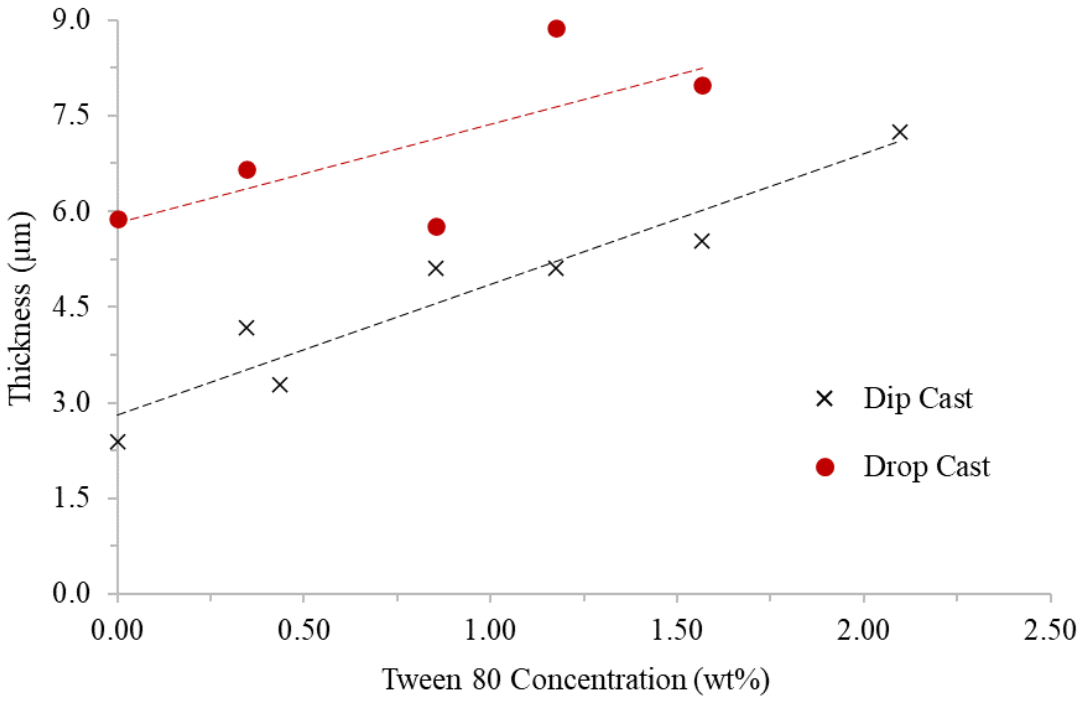

Figure 4-14: Average thickness (µm) of PEDOT:PSS/Tween 80 films with varying surfactant concentration (wt%) for dip cast (cross) and drop cast (red circle) films. Dotted guidelines show data trends

When conductivity is calculated for dip cast samples (Figure 4-15), a value of 2.9 Scm^{-1} is obtained for pristine PEDOT:PSS. This is similar to dip cast pristine PEDOT:PSS films which gave an approximate conductivity of 3 Scm^{-1} (Figure 4-11). However, conductivity on a drop cast film at 1.21 wt% Tween 80 gave a result of 6.6 Scm^{-1}, which is considerably lower than 20 Scm^{-1} for a dip cast film at the same concentration. This indicates there is a significant effect on PEDOT:PSS/Tween 80 conductive properties caused by the casting method.

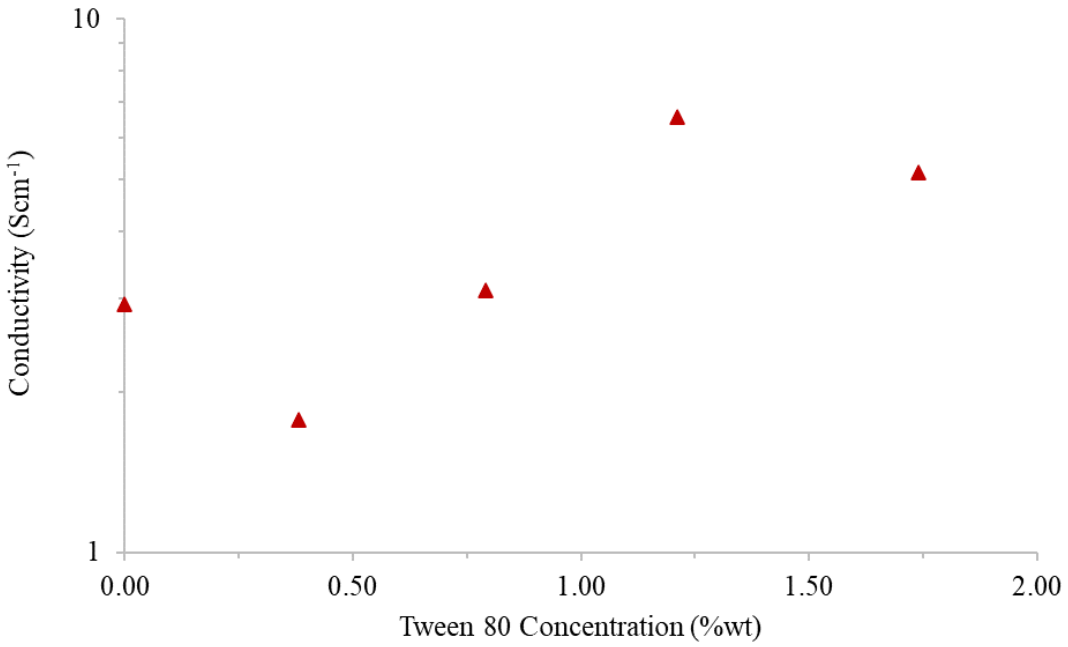

Figure 4-15: Effect of varying weight percentage (wt%) of Tween 80 in PEDOT:PSS on the conductivity (Scm^{-1}) of drop cast films

The reason for this discrepancy between casing methods in resistivity/conductivity, when Tween 80 is present, is due to two factors. The first variable is that during dip casting, the samples are held in a vertical position while depositing material. This may induce a small degree of orientation in the polymer chains due to gravity, similar to that caused by spin casting.[52,53] However, this would only account for a small difference since dip cast samples were allowed to set whilst horizontal, reducing the effect of gravity. Furthermore, there is no difference in conductivity between the two casting methods for pristine PEDOT:PSS samples, suggesting this orientation effect is unlikely to be significantly influencing results. The second, and most likely factor, is the difference in the deposited material when using each casting method. During dip casting, excess Tween 80 is less likely to be picked up by the substrate. However, with drop casting, all excess surfactant is deposited which will add a substantial amount of insulating

material to the film. These issues with drop casting suggest that the dip casting film manufacturing method is superior.

Based on this data and previous dip casting results (section 4.4.1), an optimum Tween 80 concentration can be established. While the dip cast resistivity data shows a decrease to 61 $\Omega\square^{-1}$ at 3.46 wt%, there is a clear decrease in the calculated conductivity above 1.25 wt%. Resistivity of drop cast films also plateaus at the same percentage indicating that between 1.00 – 1.25 wt% Tween 80 is needed for optimal enhancement. However, there are other considerations, such as film quality (section 4.4.4) and solution properties (section 4.5), that will further inform the optimal concentration.

4.4.3 DETA of PEDOT:PSS/Tween 80 Bulk Resistivity

PEDOT:PSS is a p-type semiconductor meaning that a rise is temperature will lead to a decrease in measured resistance due to increased electron mobility.[2,30,54,55] The following experiments were performed using a DETA set up to establish how the Tween 80 concentration in PEDOT:PSS affects this property. Due to the geometry of the bottom plate (section 2.4.4), it was not possible to dip cast films for bulk resistivity analysis, therefore, all samples were drop cast. Furthermore, samples were allowed to set as normal in atmospheric conditions, but the annealing stage was not performed prior to the first heating ramp. This means that the first heating run also acted as an annealing stage. A second ramp was then performed on the same samples following cooling and re-equilibration for 12 hours in atmospheric conditions. The data seen in Figure 4-16 shows that samples containing Tween 80 are still of a semi-conductive nature for all surfactant concentrations. This is highlighted by the general decrease in resistivity, and corresponding increase in conductivity, with temperature for both heating runs. Finally, there is also a decrease in bulk resistivity associated with increasing surfactant concentration (Figure 4-17).

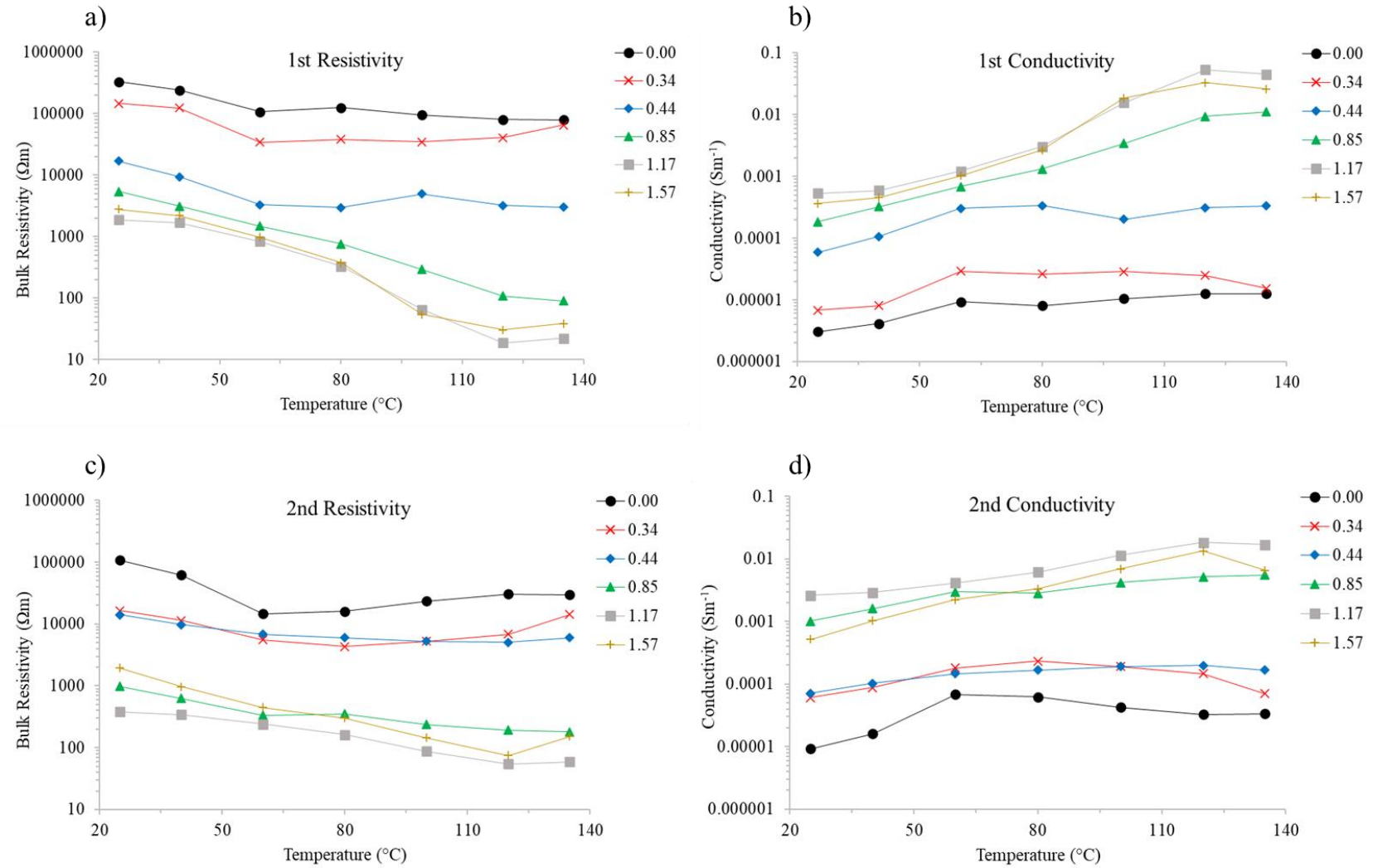

Figure 4-16: Effect of temperature (°C) on the bulk resistivity (Ωm) on the (a) first (c) & second heating runs, with corresponding calculated conductivity (Sm^{-1}) (b & d), for PEDOT:PSS/Tween 80 samples containing varying surfactant concentrations (wt%) as seen in the legend

The data shows that the increase in Tween 80 concentration causes bulk resistivity to decrease at all temperatures on both the first and second runs (Figure 4-17). In every case, the lowest bulk resistivity obtained was at 1.17 wt% Tween 80, with resistivity marginally increasing at 1.57 wt%. This increase is not seen in the previous sheet resistivity data, with results either continuing to decrease or plateau with higher surfactant concentrations (section 4.4.1 & 4.4.2). Furthermore, at temperatures of 80 °C and below, there is an improvement in the second run across all Tween 80 concentrations. The surfactant addition not only reduces bulk resistivity, but also decreases the difference between the first and second runs. For example, at 25 °C with pristine PEDOT:PSS improved from 330000 to 110000 Ωm after annealing (i.e., after the first heating run) compared to 1900 to 400 Ωm at 1.17 wt% Tween 80 addition. However, the same trends do not apply at 120 °C. Whilst at lower Tween 80 concentrations there is still an improvement with the second run, above 0.85 wt% surfactant addition the bulk resistivity of the second run becomes greater than that of the first.

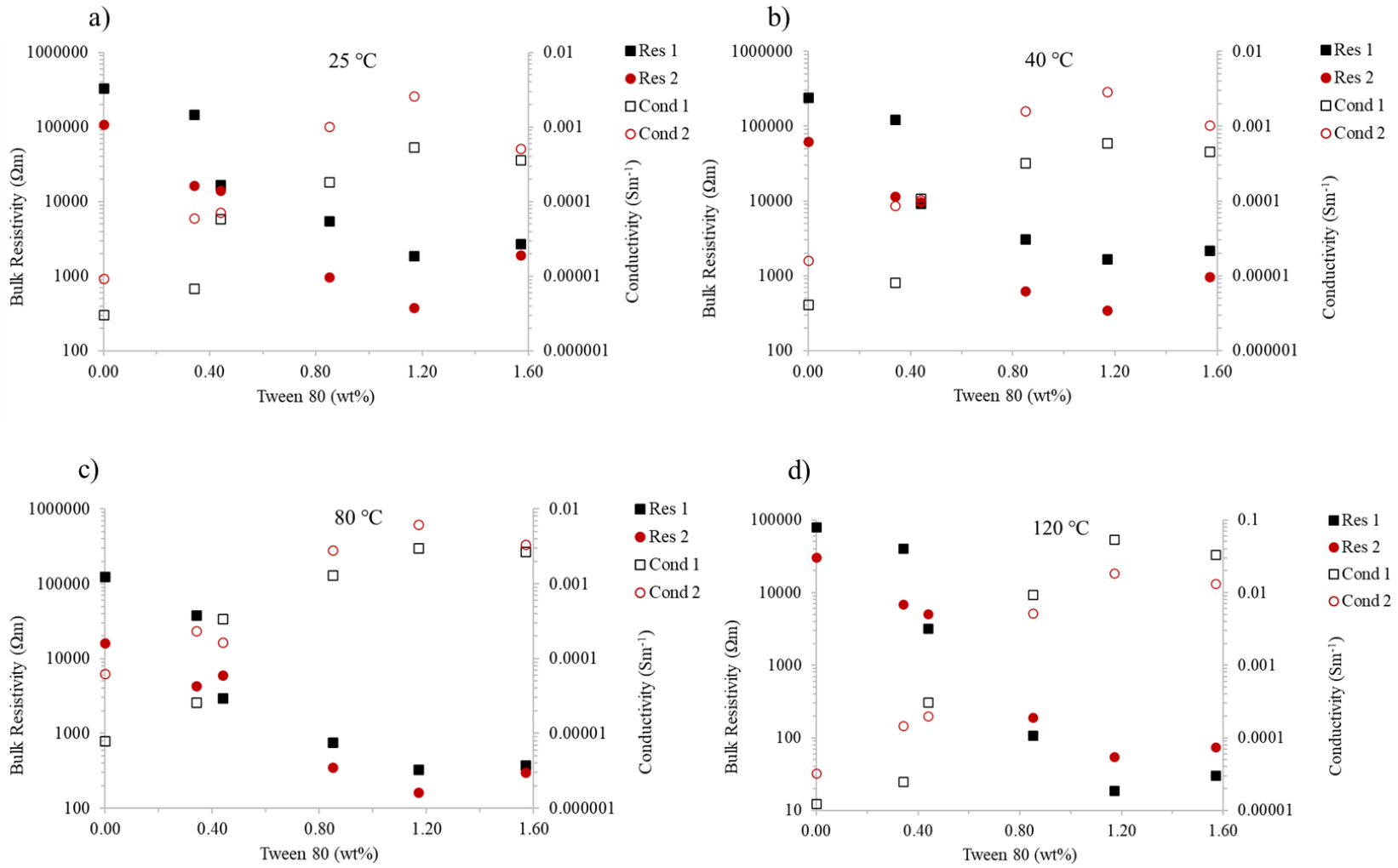

Figure 4-17: Bulk resistivity (Ωm) (left axis, filled shapes) and corresponding calculated conductivity (Sm^{-1}) (right axis, hollow shapes) of PEDOT:PSS/Tween 80 samples for varying surfactant concentrations (wt%), measured at different temperatures as follows: a) 25, b) 40, c) 80 & d) 120 °C. 'Res 1' & 'Cond 1' (black squares) correspond to the first run performed and 'Res 2' & 'Cond 2' (red circles) correspond to the second run

As mentioned, the bulk resistivity is at a minimum for a Tween 80 concentration of 1.17 wt% and does not follow previous sheet resistivity data. Due to the bulk resistivity samples being made using the drop casting method, excess Tween 80 is deposited. This increases the amount of insulating material and is likely further exacerbated when measuring the bulk resistivity since the resistance through the whole sample is considered rather than just the sample surface. Due to the high Mw of both Tween 80 and excess PSS, these components will move away from the surface during film setting.[14,56-58] This leads to a more conductive surface, which is the primary region being measured with the 4-point probe. This also explains why calculated conductivity values from bulk resistivity (Figure 4-16 & 4-17) are much lower than from sheet resistivity (section 4.4.1) and literature values.[2,34-38] The best conductivity calculated from bulk resistivity at 25 °C was 0.00053 Sm^{-1} at 1.17 wt% surfactant, compared to 26.8 Scm^{-1} at 1.40 wt% Tween 80 when calculated using sheet resistivity of dip cast films. In the literature, 100 Scm^{-1} was obtained when adding Triton X-100[45] and 224 Scm^{-1} for SDBS addition.[41] However, this difference is likely caused by the calculation of conductivity from bulk resistivity in this study, as opposed to sheet resistivity which is more often used in the literature.[2,35-39] There will also be differences associated with in-plane versus through plane measurements. Although PEDOT:PSS is considered amorphous,[22,43,59-63] there is evidence of short range $\pi - \pi$ stacking,[61-66] which will favour in-plane measurements, causing 4-point probe conductivity to be greater.

Despite these differences, the bulk resistivity data shows that the addition of Tween 80 is improving conductivity throughout the whole sample and not just at the surface. The data also highlights the positive impact of annealing, particularly at lower temperatures. This is of greater importance since PEDOT:PSS films will most likely be used in ambient temperature conditions. Furthermore, measurements could only be taken up to a surfactant concentration of 1.57 wt%,

after which the excess surfactant on the film surface interfered with the test. This provides some further indication of the maximum quantity of Tween 80 that can be added to PEDOT:PSS before the polymer available for interaction with the surfactant becomes saturated.

4.4.4 Effect on Film Quality with Varying Tween 80 Concentration

Whilst an increase in Tween 80 concentration has been shown to be beneficial for both bulk and sheet resistivity, there were indications that greater amounts of surfactant cause issues regarding film quality. At the start of this chapter, the issue of Tween 80 concentration in solution and subsequently in the film was highlighted. Visual analysis of drop cast films (Figure 4-18) showed no obvious indication of excess Tween 80 at lower concentrations (0.79 wt%), however, at 2.13 wt% a waxy white layer appeared on the surface. Furthermore, the highest concentration (2.63 wt%) produced an uneven 'bubbly' film finish. At high concentrations, Tween 80 accounts for approximately 65 wt% of the dry film suggesting that the surfactant – PEDOT:PSS interaction may be saturated. It also emphasises the issues seen in sheet resistivity and bulk resistivity measurements caused by the accumulation of excess surfactant. Similar issues could also be identified for dip cast samples.

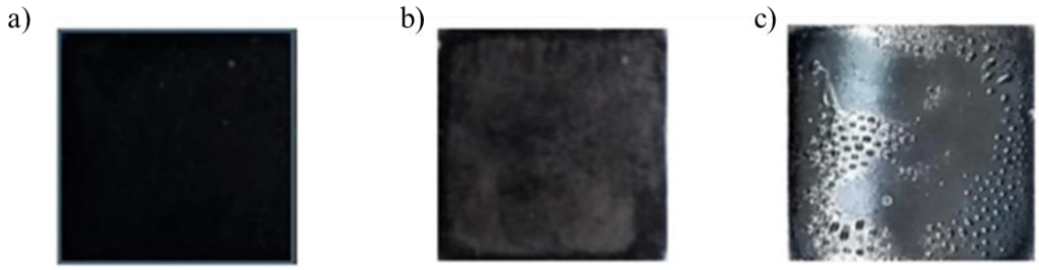

Figure 4-18: Images of films produced using PEDOT:PSS/Tween 80 solutions with surfactant concentrations of a) 0.79, b) 2.13, and c) 2.63 wt%

These findings emphasise the previously alluded to suggestion that there is a saturation point of PEDOT:PSS solution, past which further additions of Tween 80 are unable to interact with the polymer. This leads to detrimental effects on film quality. To further assess film quality, the roughness average (Ra) of PEDOT:PSS/Tween 80 films was calculated. Table 4-2 shows a comparison of Ra for dip cast and drop cast films with differing surfactant concentrations. The data shows there is a greater degree of variability in the drop cast technique, with Ra values reaching 1.115 µm for a Tween 80 concentration of 1.57 wt% but as low as 0.042 µm at 0.34 wt%. The equivalent Ra values for the dip cast films are 0.049 and 0.079 µm, respectively. Furthermore, other than at 0.34 wt%, Ra values for drop cast films are greater than dip cast samples. This suggests that dip casting is a superior method with regards to repeatability and film quality.

Table 4-2: Ra (µm) for dip cast and drop cast PEDOT:PSS/Tween 80 films with varying surfactant concentration (wt%)

Tween 80 Concentration (wt%)	**Dip Cast Ra (µm)**	**Drop Cast Ra (µm)**
0.00	0.047	0.444
0.34	0.079	0.042
0.85	0.056	0.059
1.57	0.049	1.115

From Table 4-2, the effect of altering surfactant concentration on film quality is unclear. It has already been shown that the addition of Tween 80 to PEDOT:PSS causes the dry film thickness to increase with concentration for both coating methods (Figure 4-14). Whilst not directly measured in this study, this increase in thickness may lead to a reduced film transparency, causing them to be unsuitable for use in optoelectronic devices.[42,70,71] Figure 4-19 shows the Ra

for dip cast films across a greater range of Tween 80 concentrations. Initially, the addition of Tween 80 was found to improve the quality, with pristine PEDOT:PSS Ra value being 0.047 µm compared to the lowest Ra of 0.016 µm at 1.40 wt%. However, above this concentration the Ra significantly increases to 0.062 at 2.63 wt%. As seen from the visual analysis (Figure 4-18), at this concentration there is a considerable amount of surfactant residing on the surface of the film which is likely to increase roughness. This also shows that 1.50 wt% is the optimal concentration for film quality.

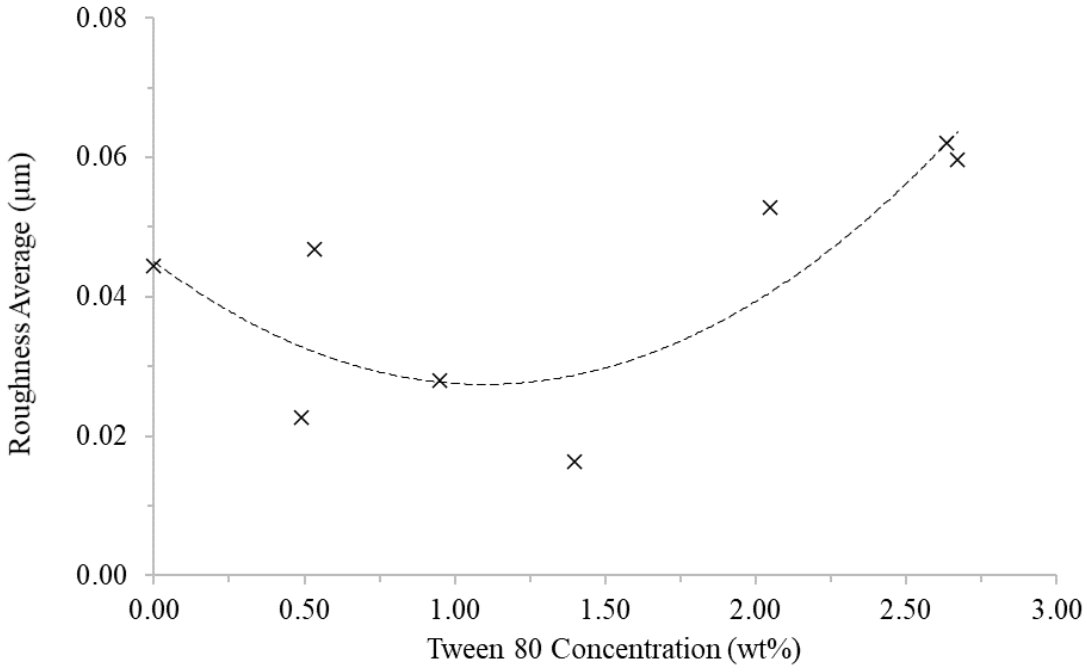

Figure 4-19: Ra (µm) of PEDOT:PSS/Tween 80 dip cast films with varying surfactant concentration (wt%). Dotted guideline shows data trend

4.4.5 Structural Analysis of PEDOT:PSS/Tween 80 Films

The microstructure of PEDOT:PSS/Tween 80 films was analysed using three techniques: AFM, XRD and Raman spectroscopy. It was hypothesised that the addition of the surfactant would

cause similar structural changes to other surfactants and chemicals seen in the literature.[14,31,43,44,56] Tween 80 is suspected to disrupt the ionic bond between PEDOT and PSS much in the same way as other surfactants such as the Triton X series.[21,31,45] This would initially cause the PEDOT and PSS to segregate, creating larger conducting regions and reducing the number of barriers to electron flow through the material.[14,26,27] There would also be an 'uncoiling' of the PEDOT chains as they adopt a more linear structure through a benzoid to quinoid resonance structure transformation.[14,44] This has the effect of allowing for greater chain alignment and increased π-π stacking, providing better conduction pathways for electron flow.[2,14,32-39] In this section, the evidence for these mechanisms is explored.

4.4.5.1 Atomic Force Microscopy (AFM)

The AFM images in Figure 4-20 show the comparison between pristine PEDOT:PSS (Figure 4-20a-c) and PEDOT:PSS/Tween 80 with 1.40 wt% surfactant concentration (Figure 4-20d-f). Pristine PEDOT:PSS was observed to have no structural alignment or separation, commonly seen in the literature,[14,26,56] however, the PEDOT:PSS/Tween 80 film clearly shows evidence of phase separation. This is most clearly seen in 'c' and 'f', representing pristine PEDOT:PSS and PEDOT:PSS/Tween 80 respectively, where the adhesion measurements (a & d) are normalised to the surface profiling data (b & e). As explained in section 2.5.3, the light phases represent PEDOT-rich regions while the darker phases PSS-rich regions.[64,72,73]

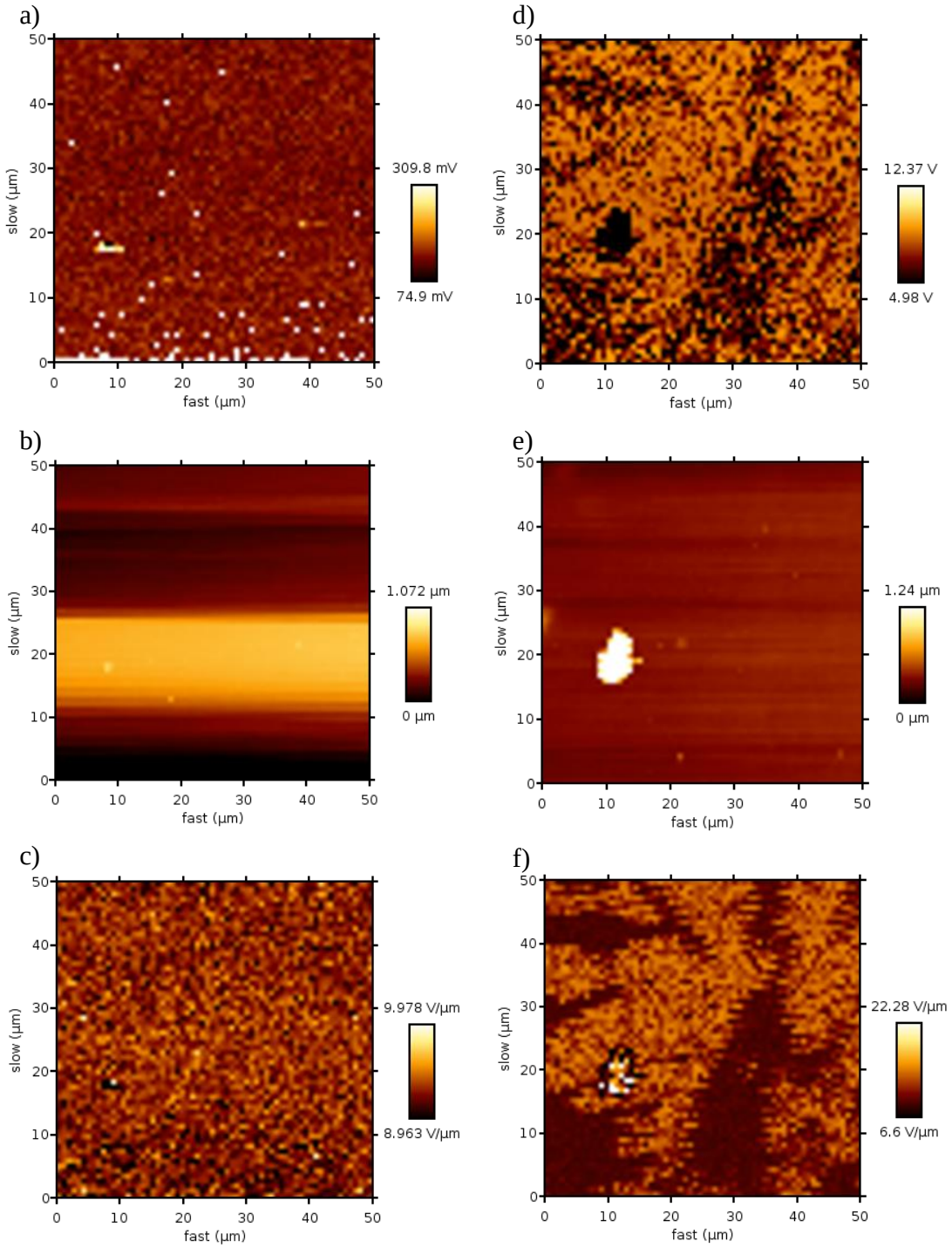

Figure 4-20: AFM imagine of pristine PEDOT:PSS (a, b, c) and PEDOT:PSS films containing 1.40 wt% Tween 80 (d, e, f). Showing a) and d) adhesion scan, b) and e) surface roughness, c) and f) surface roughness normalised to surface profiling. Note: bright spot on image 'e' is contamination

This separation is likely a factor in the overall conductivity improvement of PEDOT:PSS with the addition of Tween 80. It shows evidence that the surfactant is interfering with the ionic bond between the two components, causing PEDOT and PSS to segregate into more and less conductive regions.[14,26,27,45,46] This leads to a reduction in the energy barrier between PEDOT-rich regions, improving conductivity.[43] However, it is also possible the AFM images are showing the immiscibility of Tween 80 and PEDOT:PSS at this concentration given this amount of surfactant equates to over 50 wt% in the dry film. Similar issues were seen by Kim, *et al.* (2017)[31] with the addition of some Triton X surfactants. It has previously been observed, with a scan area of 1 x 1 µm, that some additives, including Triton X-100, result in a 'nanofibril' structure appearing.[21,31,45] The AFM analysis in this study was limited in the resolution and magnification to 50 x 50 µm therefore, it is unknown whether Tween 80 addition would cause the same microstructure.

4.4.5.2 X-Ray Diffraction (XRD)

The XRD traces seen in Figure 4-21 show the relative intensity of diffraction peaks for films of pristine PEDOT:PSS and PEDOT:PSS/Tween 80 with surfactant concentrations of 0.47 & 1.32 wt%. Firstly, the data shows that pristine PEDOT:PSS is amorphous since broad peaks appear around 26 ° and 18 °, with no other sharp peaks being present.[21,42,59-63] This compliments the AFM data (section 4.4.5.1) and literature showing no organisation or alignment of the polymer.[32,61,63,74,75] Additionally, the film containing 0.47 wt% surfactant can also be considered amorphous with a very similar trace to that of pristine PEDOT:PSS. However, the PEDOT:PSS/Tween 80 sample containing 1.32 wt% surfactant shows the appearance of two sharper, more defined peaks at 2.3 and 6.8 ° with two smaller peaks at 4.6 and 11.3 ° indicative of alignment within the polymer.

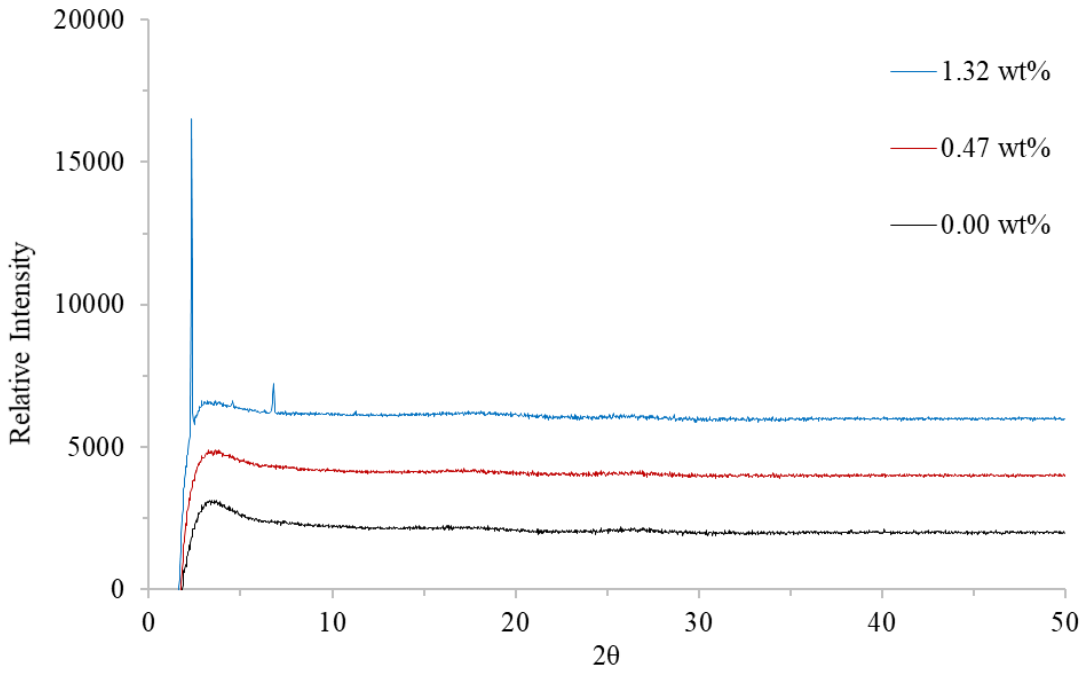

Figure 4-21: XRD traces showing relative intensity of diffraction peaks for differing film samples. From bottom to top traces are as follows: pristine PEDOT:PSS (black), PEDOT:PSS/Tween 80 with 0.47 wt% surfactant (red), PEDOT:PSS/Tween 80 with 1.32 wt% surfactant (blue). Baseline of glass substrate was removed

The XRD trace for the sample containing 1.32 wt% Tween 80 provides further evidence of the surfactant interfering with the PEDOT – PSS ionic interaction. This allows the PEDOT to adopt the 'uncoiled' quinoid form[21,31,46,61] and leads to long range order of the PSS chains, represented by the larger peaks.[30,76,77] As already mentioned, the alignment of the structure will create better conducting pathways which reduces the barriers to electron flow and improves conductivity.[2,14,32-39,45] Yoon, *et al.* (2016)[21] reported that Triton X-100 addition caused similar changes in peak intensity caused by closer chain packing. In this work, the peaks are sharper and more well defined, indicating that Tween 80 has a more substantial effect on the chain alignment of PEDOT:PSS. This also compliments the AFM data (section 4.4.5.1) strengthening the hypothesis that Tween 80 refines the PEDOT:PSS structure.

The data also highlights the need for a minimum amount of surfactant before conductivity is affected. The sheet resistivity measurements for dip cast samples (section 4.4.1) showed that less than 0.50 wt% Tween 80 caused no significant resistivity decrease. These XRD results demonstrate that smaller quantities of surfactant do not induce the structural change needed to improve conductivity.

4.4.5.3 Raman

Raman analysis was performed on the PEDOT:PSS/Tween 80 films to probe possible changes in the PEDOT double bond structure from benzoid to quinoid. Pristine PEDOT:PSS displays three peaks in the Raman spectra (Figure 4-22). The two main peaks at 1600 and 1460 cm^{-1} represent the C=C bonds in the aromatic rings of PEDOT and PSS.[78] The shoulder at 1360 cm^{-1} is associated with the SO_2 group in the PSS.[78] When Tween 80 is added there is little obvious change except the shoulder at 1360 cm^{-1} becomes less pronounced, especially at 1.32 wt%.

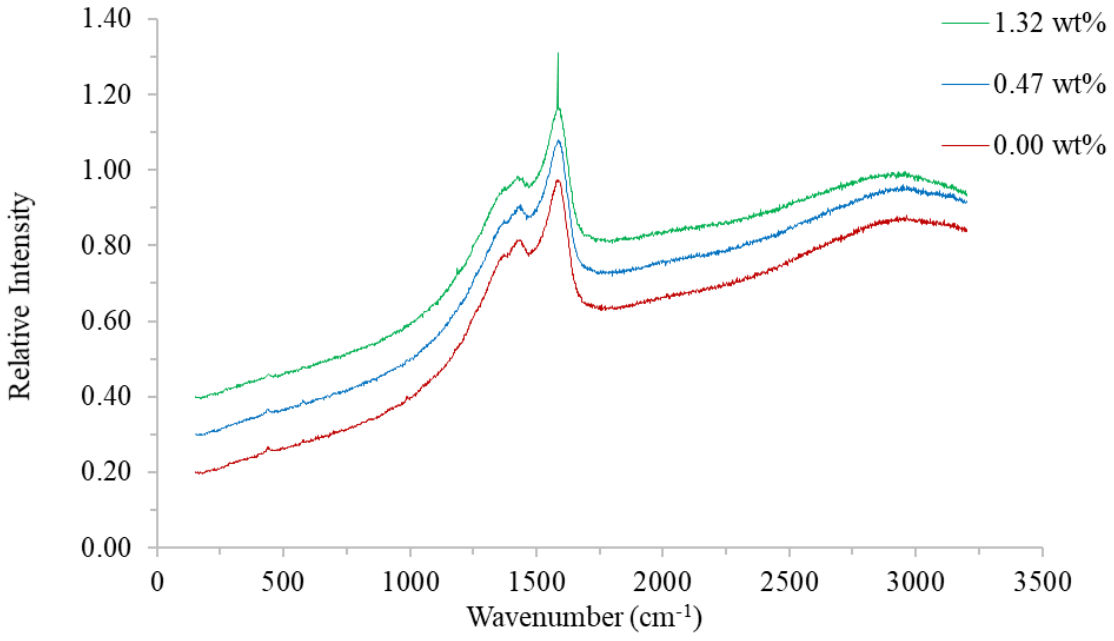

Figure 4-22: Raman spectra of PEDOT:PSS/Tween 80 films containing 0.00, 0.47 & 1.32 wt% surfactant (from bottom to top)

Within the literature, it has been reported that this resonance structural change can be seen through a red-shift and narrowing of the 1400 – 1500 cm^{-1} band, representing the $C_\alpha=C_\beta$ bond in the thiophene ring of PEDOT.[19,21,44] As this was seen by Yoon, *et al.* (2016)[21] with the addition of Triton X-100, a similar shift in the peak at 1460 cm^{-1} would be expected with Tween 80. However, whilst the decrease in the prominence of the shoulder at 1360 cm^{-1} could be a sign of a red-shift of the 1460 cm^{-1} peak, it is not possible to determine with certainty. The addition of Tween 80 also increases the concentration of OH and CH groups, both of which show peaks within this region.[78] There is also limitation in the resolution of the measurement and analysis method. Without deconvolution of the peaks, it is difficult to discern whether a shift caused by a benzoid/quinoid change has occurred. However, this conclusion has been reported by others, with the implication being that the addition of surfactant does change the resonance structure but not substantially enough to be detected by Raman.[40] Therefore, it is likely that the addition of Tween 80 is allowing the PEDOT to shift to a more quinoidal structure even if this cannot be accurately deduced from the analysis in this study. This notion is further strengthened by the XRD data (section 4.4.5.2) in which the diffraction peaks observed with 1.32 wt% Tween 80 are linked to this resonance structure change.[21,31,46,61]

4.5 PEDOT:PSS/Tween 80 Solution Properties

4.5.1 Rheology of PEDOT:PSS/Tween 80 Solutions

The rheology of pristine PEDOT:PSS solution shows a decrease in viscosity with increasing shear rate (Figure 4-23) similar to shear thinning.[59,79,80] However, there is a degree of uncertainty in this considering PEDOT:PSS is primarily water, which has a high surface tension, and may skew results at low shear rates.[81] Results show that at 1 s^{-1} the viscosity of pristine PEDOT:PSS solution is approximately 0.20 Pa.s which correlates closely to the literature values.[59,79] There have been reports that this value could be higher,[80] but these

discrepancies are likely caused by different concentrations of PEDOT:PSS in solution.[80] The viscosity of Tween 80 is greater than PEDOT:PSS (0.43 Pa.s) and stays relatively constant regardless of the shear rate (Figure 4-23).

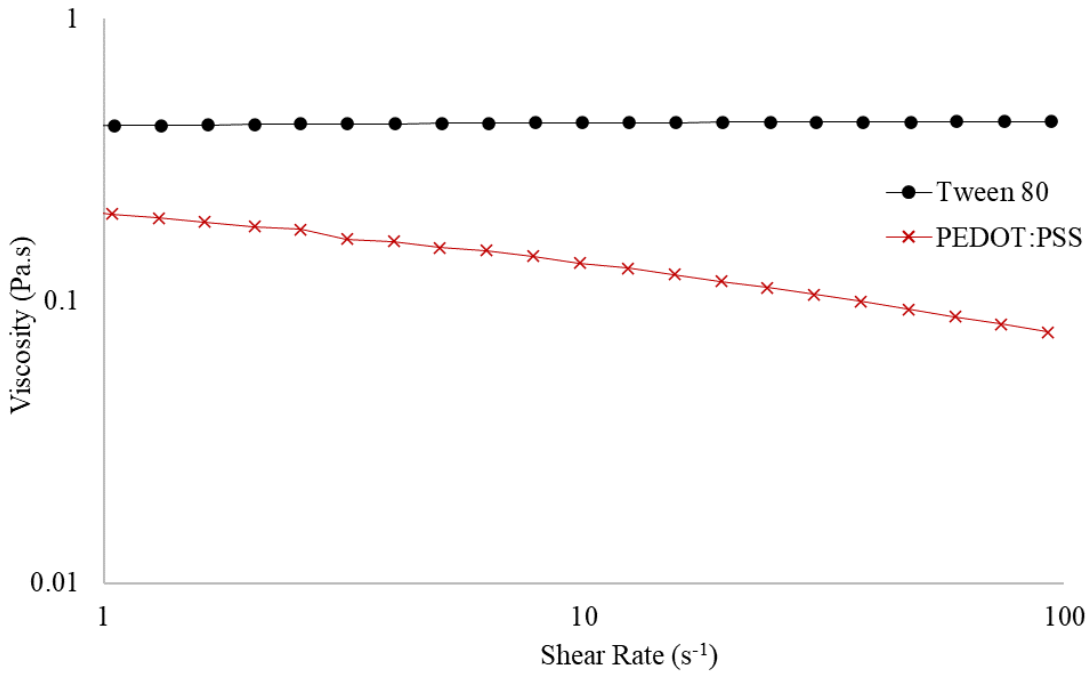

Figure 4-23: Shear viscosity (Pa.s) of pristine PEDOT:PSS solution (red cross) and Tween 80 surfactant (black circle) for varying shear rates (s^{-1}) from 0.1 – 100 s^{-1}

The effect of Tween 80 on the viscosity of PEDOT:PSS can be seen in Figure 4-24. The data shows that, initially, there is an increase in the viscosity with surfactant concentration. This increase continues until a percentage of 0.93 wt% is reached at which point the viscosity then begins to decrease. Whilst there is a spread in the viscosity for differing shear rates, the trends across all rates are the same.

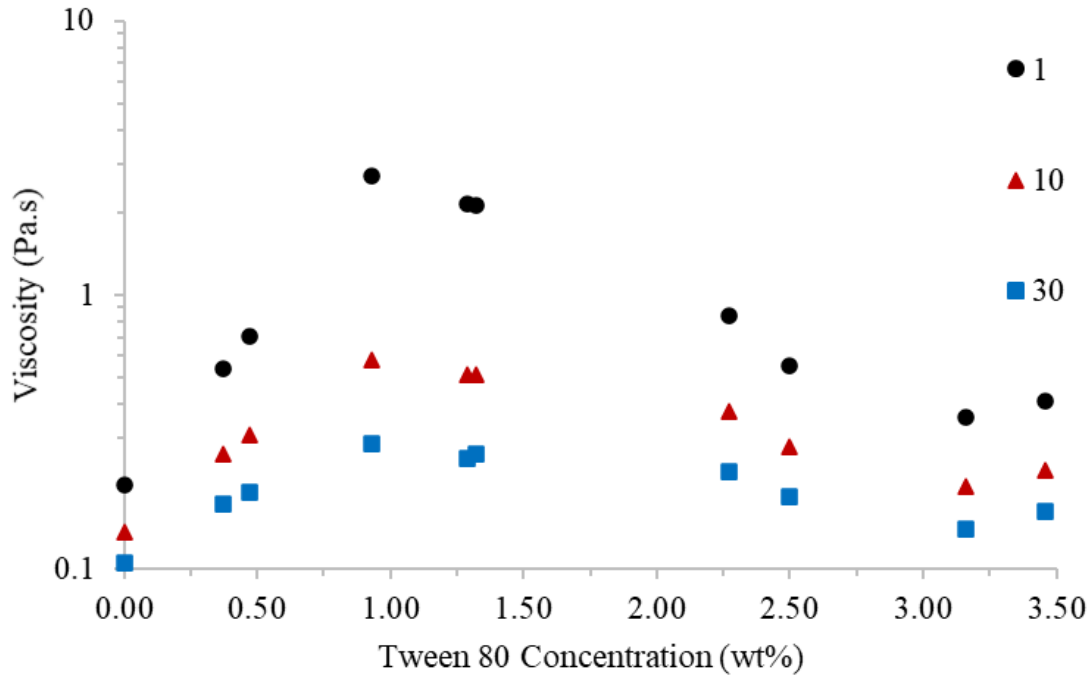

Figure 4-24: Viscosity (Pa.s) of PEDOT:PSS/Tween 80 solutions with varying Tween 80 concentration (wt%) for different shear rates (s^{-1}). Shear rates are 1 (black circle), 10 (red triangle) and 30 s^{-1} (blue square)

Furthermore, the higher the shear rate, the lower the viscosity at any given Tween 80 concentration which shows the solution has retained a shear thinning like behaviour (Figure 4-25). This effect becomes more exaggerated as surfactant wt% increases until 0.93 wt% where it reduces. The greatest viscosity obtained at a surfactant concentration of 0.93 wt% for a shear rate of 1 s^{-1} was 2.71 Pa.s which is 2.51 Pa.s greater than that of pristine PEDOT:PSS at the same shear rate (Figure 4-24). The lowest viscosity obtained at 1 s^{-1} for a PEDOT:PSS/Tween 80 solution was for a surfactant addition of 3.16 wt% giving a viscosity of 0.36 Pa.s. Whilst significantly lower than the viscosity at 0.93 wt%, this is still greater than pristine PEDOT:PSS.

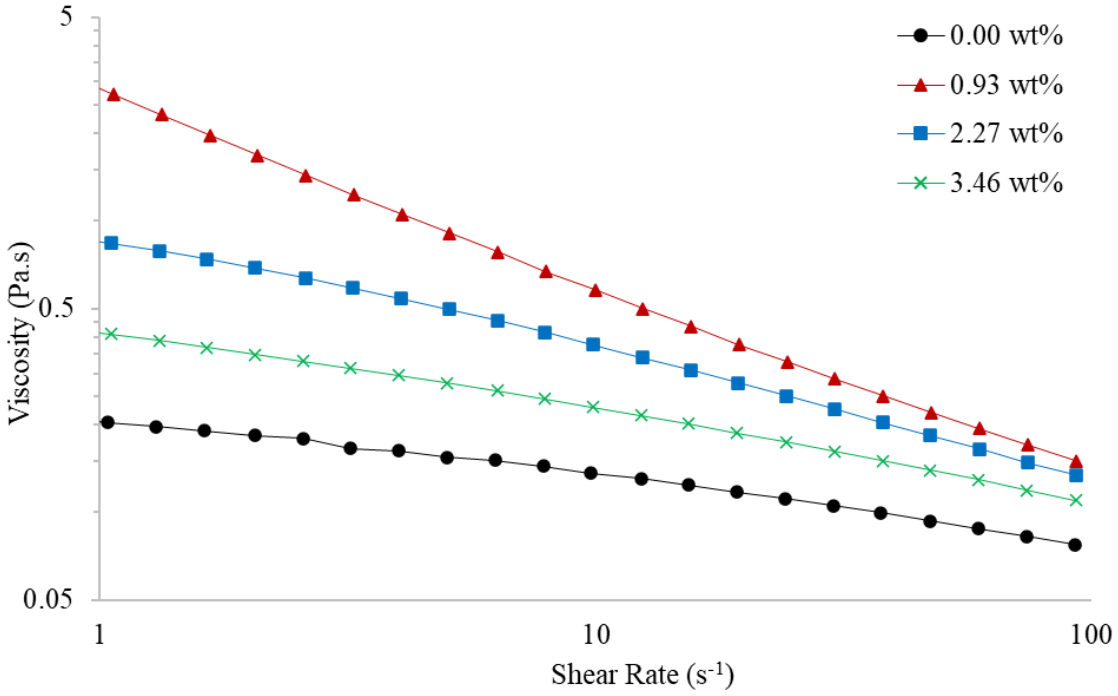

Figure 4-25: Shear viscosity (Pa.s) of pristine PEDOT:PSS/Tween 80 solutions with surfactant concentration 0.00 (black circle), 0.93 (red triangle), 2.27 (blue square) and 3.46 wt% (green cross) for varying shear rates (s^{-1}) from 0.1 – 100 s^{-1}

The initial increase in viscosity caused by Tween 80 follows the reported literature findings,[79,80,82,83] which can partially be accounted for by the greater viscosity of Tween 80 (0.43 Pa.s) (Figure 4-23). However, results for PEDOT:PSS/Tween 80 at 0.93 wt% are significantly higher, suggesting alternative mechanisms are influencing viscosity. The influence of Tween 80 on water is shown in Figure 4-26. While the data at low shear rate (1 s^{-1}) is varied, this is likely due to the surface tension of water creating an elevated viscosity reading which is overcome as shear rate increases.[81] At higher shear rates the viscosity is more consistent and shows the addition of Tween 80 to have no significant effect on the viscosity of the solution. This shows that the effect seen with aqueous PEDOT:PSS must be due to the interaction of the surfactant with the polymer.

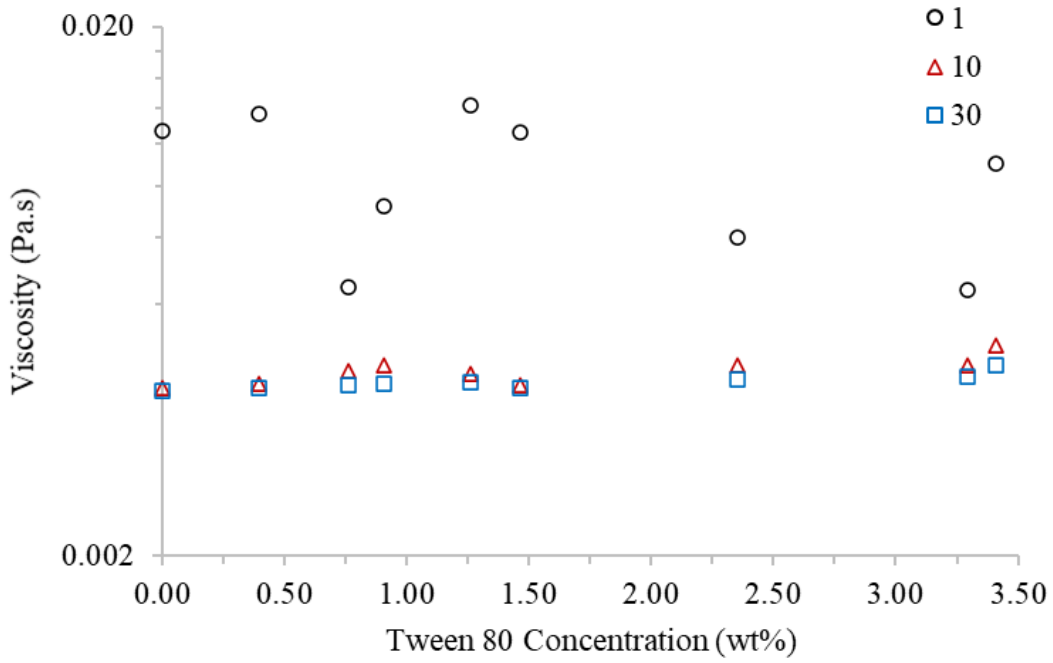

Figure 4-26: Viscosity (Pa.s) of water/Tween 80 solutions with varying Tween 80 concentration (wt%) for different shear rates (s^{-1}). Shear rates are 1 (black circle), 10 (red triangle) and 30 (blue square) s^{-1}

The cause for this trend relates to the notion that there is a saturation of the interaction between Tween 80 and the solid content of PEDOT:PSS in solution, which has been alluded to throughout this chapter. It has previously been suggested that the surfactant will create PEDOT – surfactant and PSS – surfactant complexes.[21] Therefore, the Tween 80 will be contributing to the polymer content in solution up to 0.93 wt%, without adding to the surrounding solution. However, the decrease seen above 0.93 wt% Tween 80 (Figure 4-24) is not reported in the literature for other surfactants. Above this concentration, it is hypothesised that there will be no further interaction between Tween 80 and PEDOT:PSS meaning any further addition will dilute the solution. This explains the decrease in viscosity seen for concentrations above 0.93 wt%.

These results inform the suitability of PEDOT:PSS/Tween 80 solutions for bulk manufacturing. Tween 80 addition has previously been shown to produce an effective PEDOT:PSS ink for IJP[84,85] and R2R methods when used in conjunction with other additive.[83] IJP and R2R generally favour lower viscosity inks.[86] While limitations to attainable shear rates make it difficult to determine solution suitability for IJP,[79] pristine PEDOT:PSS is thought to be appropriate.[79,80] At 3.16 wt%, the PEDOT:PSS/Tween 80 viscosity is comparable to that of pristine PEDOT:PSS (0.36 and 0.20 Pa.s at 1 s^{-1}, respectively). Viscosity also substantially decreases with increasing shear rate, most noticeable demonstrated at 0.93 wt% (2.71 & 0.29 Pa.s at 1 & 30 s^{-1}, respectively). This suggests a PEDOT:PSS/Tween 80 system could be suitable for bulk manufacturing, however, further investigation would be needed.

4.5.2 Surface Tension of PEDOT:PSS/Tween 80 Solutions

The wettability and surface tension of PEDOT:PSS/Tween 80 solutions, with varying surfactant concentrations, were assessed. The contact angle of pristine PEDOT:PSS on glass was 21.8 °, significantly lower than the contact angle of water (~55 °),[87] suggesting that PEDOT:PSS alters the surface tension of the solution. The contact angle appears to increase up to 0.47 wt% surfactant followed by a decrease for greater Tween 80 concentrations (Table 4-3). To assess this effect in greater detail a capillary climb method was employed (section 2.3.2.2), from which surface tension was calculated (Table 4-3).

Table 4-3: Contact angle (°), capillary climb height (mm) and calculated surface tension (mNm^{-1}) of PEDOT:PSS/Tween 80 solutions for varying surfactant concentration.

Tween 80 Concentration (wt%)	Contact Angle (°)	Capillary Height (mm)	Surface Tension (mNm^{-1})
0.00	21.8	15	30.6
0.37	28.5	14	30.1
0.47	31.6	16	36.8
0.93	27.1	8	16.5
1.29	27.6	12	26.6
1.32	27.6	9	18.8
2.27	25.3	13	28.2
2.50	23.8	15	32.7
3.16	28.4	17	36.8
3.46	25.4	17	35.9

The surface tension data calculated in Table 4-3 is represented in Figure 4-27. The surface tension of pristine PEDOT:PSS solution was calculated to be 30.6 mNm^{-1}. The data then closely resembled the contact angle results with a significant decrease in surface tension up to 0.93 wt% Tween 80. At this concentration surface tension was lowest measuring 16.5 mNm^{-1}, followed by an increase with further surfactant to 36.8 mNm^{-1} at 3.16 wt% Tween 80, surpassing the surface tension of pristine PEDOT:PSS.

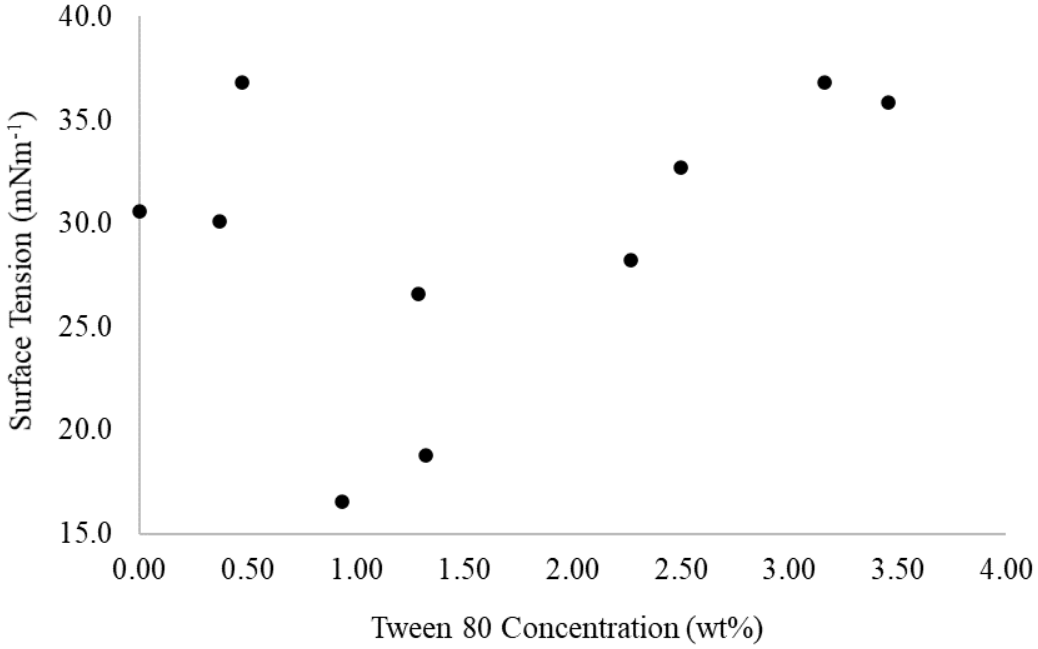

Figure 4-27: Surface tension (mNm^{-1}) of PEDOT:PSS/Tween 80 solutions for difference Tween 80 concentrations (wt%)

In accordance with the contact angle data, the surface tension of pristine PEDOT:PSS is significantly lower than that of water, 72 mNm^{-1}.[22,79,88,89] While literature sources often quote PEDOT:PSS solution as having a similar surface tension to water,[45,79,80,83,90] it has previously been measured as low as 44 mNm^{-1},[82] substantially closer to the values found in this study. It is likely that these differences have come from the measurement method used. In this case, there is likely a greater interaction of PEDOT:PSS with the capillary walls. Therefore, while the dominant force for other testing methods is water, using this method will allow more polymer to interact with the substrate material, potentially hindering the movement of solution up the capillary.

With the addition of Tween 80, surface tension (Figure 4-27) shows an inverse trend to viscosity (Figure 4-24) with 0.93 wt% Tween 80 causing both the lowest surface tension and greatest viscosity. A similar occurrence has been reported in the literature with the addition of Tween 80

in small quantities.[82] This drop in surface tension has been seen with alternative surfactants and other additives.[45,79,90] Notably, the addition of Triton X-100 decreased surface tension from 72 to 30 mNm^{-1}.[45] However, consideration of surface tension and contact angle together complicate the effect of Tween 80. Below 0.93 wt%, it is thought that the surfactant contributes to the amount of polymer in solution by interacting with the solid PEDOT:PSS component. This means the surfactant will have little to no effect on the water component. Furthermore, the surfactant will saturate the polar bond of the hydrophilic PSS, freeing polar groups within the water. This creates a system whereby the polymer is less dissolved, and the water has a higher surface energy. The contact angle (Table 4-3) and surface tension (Figure 4-27) results marginally increase at low concentrations, reflecting these changes.

Above 0.93 wt% it is suspected the PEDOT:PSS – surfactant interaction is saturated, therefore, allowing the Tween 80 to influence the surface tension of the water component. Again, this is demonstrated in the contact angle data with a gradual decrease appearing at higher concentrations. The effect of Tween 80 on water is well established, and has been shown to decrease surface tension with increasing concentration.[91] However, despite the drop in surface tension aligning with contact angle results at 0.93 wt%, higher values do not follow the same trend. Above this concentration, surface tension begins to increase, which is contrary to contact angle and literature findings for other surfactants.[48] As mentioned, the use of a capillary method is likely distorting surface tension results through interaction of the polymer with the capillary wall. Nevertheless, it is still unclear why surface tension and contact angle data do not correlate. A hypothesis is that at higher surfactant concentrations, the PEDOT:PSS in solution becomes more dilute. This would then cause less polymer to interact with the capillary and surface tension would tend towards a Tween 80 – water mix. The surface tension of water with 1 wt%

Tween 80 has been quoted as 38.1 mNm^{-1}.[91] This is comparable to the surface tension of PEDOT:PSS/Tween 80 solution with 3.16 wt% surfactant at 36.8 mNm^{-1}.

Therefore, this difference in results shows that the properties of a PEDOT:PSS solution droplet on a substrate will primarily be dominated by the water component with the polymer acting to reduce surface tension. However, the behaviour of the liquid in a capillary has been shown to be different and is likely due to increased chain interaction with the capillary wall. This has potential connotations for bulk manufacture, especially IJP in which the solution will likely pass through a small nozzle. However, lowering the surface tension is advantageous when considering R2R manufacture as a lower surface tension will improve the wettability of the solution and allows for a more even coating.[40,49,90,92,93] This is particularly important when considering PP, PET or other polymeric substrates used in R2R manufacture since pristine PEDOT:PSS solution coverage and adhesion on these substrates is usually poor.[40] By lowering the surface energy and more closely matching this between solution and substrate, higher quality films can be produced.[45]

4.6 Conclusion

This chapter has explored the effect of Tween 80 on the thermal, film and solution properties of PEDOT:PSS. TGA analysis initially showed that the thermal stability of the polymer was altered by the presence of the surfactant causing earlier onset of degradation. Whilst the cause of this is somewhat unclear, it is likely that the formation of acids during Tween 80 degradation could be a contributing factor. It was also shown that the primary degradation mechanism in PEDOT:PSS/Tween 80 samples was cleavage of the PSS sulfonate group, consistent with pristine PEDOT:PSS. This data concludes that PEDOT:PSS/Tween 80 films cannot be annealed above 140 °C. Furthermore, the time needed to fully anneal a PEDOT:PSS/Tween 80 sample was found to be 60 minutes.

The addition of Tween 80 also significantly improved the conductivity of PEDOT:PSS films. This improvement was greatest up to a concentration of approximately 1 wt% surfactant for both drop and dip cast samples. It was also shown that both sheet and bulk resistivity decreased with the addition of Tween 80, indicating an effect throughout the bulk of the material and not just at the surface. Structural analysis through AFM and XRD showed that the surfactant causes separation of the PEDOT and PSS components whilst also allowing the polymer chains to align. The latter was attributed to the change from a benzoid to quinoid structure in the PEDOT, despite Raman not being able to substantiate this claim. These changes produced superior conducting pathways and limited the barriers to electron flow. However, these results showed that adding too much surfactant caused a plateau in the resistivity for the drop cast samples. Even though this was not seen for dip cast samples, conductivity data showed a similar plateau, alluding to PEDOT:PSS – Tween 80 interaction saturation. Furthermore, excess Tween 80 was seen on the surface of the film, negatively impacting film quality.

Finally, Tween 80 was shown to alter the solution properties of PEDOT:PSS, with an increase in surfactant concentration leading to a higher viscosity. The greatest viscosity occurred at approximately 1 wt% surfactant, further strengthening the saturation hypothesis. Above this, viscosity decreased and was attributed to higher concentrations of Tween 80 diluting the solid polymer content in solution. The surface tension showed the opposite trend, with an initial decrease followed by an increase above 1 wt%. Whilst it was not possible to discern for sure if this system would be suitable for IJP or R2R manufacturing, the reduction in surface tension would be beneficial. This would improve the wettability of the solution on flexible polymer substrates used in bulk manufacturing leading to enhanced film quality.

4.7 References

1. Sigma-Aldrich 2015. Certificate of Analysis: Poly(3,4 ethylene dioxythiophene)-poly(styrene sulfonate).
2. Elschner, A., Kirchmeyer, S., Lövenich, W., Merker, U. & Reuter, K. 2011. *PEDOT; principals and applications of an intrinsically conductive polymer*, CRC Press.
3. Zhou, J., Anjum, D. H., Chen, L., Xu, X., Ventura, I. A., Jiang, L. & Lubineau, G. 2014. The temperature- dependent microstructure of PEDOT/ PSS films: insights from morphological, mechanical and electrical analyses. *J. Mater. Chem. C,* 2**,** 9903-9910.
4. Greczynski, G., Kugler, T. & Salaneck, W. R. 1999. Characterization of the PEDOT-PSS system by means of X-ray and ultraviolet photoelectron spectroscopy. *Thin Solid Films,* 354**,** 129-135.
5. Peters, K., Braun, J., Schmidt-Hansberg, B., Scharfer, P. & Schabel, W. 2011. Phase equilibrium of water in different types of PEDOT:PSS. *Chemical Engineering & Processing: Process Intensification,* 50**,** 555-557.
6. Kishore, R. S. K., Pappenberger, A., Dauphin, I. B., Ross, A., Buergi, B., Staempfli, A. & Mahler, H.-C. 2011. Degradation of Polysorbates 20 and 80: Studies on Thermal Autoxidation and Hydrolysis. *Journal of Pharmaceutical Sciences,* 100**,** 721-731.
7. Kiebooms, R., Aleshin, A., Hutchison, K., Wudl, F. & Heeger, A. 1999. Doped poly(3,4- ethylenedioxythiophene) films: Thermal, electromagnetical and morphological analysis. *Synthetic Metals,* 101**,** 436-437.
8. Romyen, N., Thongyai, S., Praserthdam, P. & Wacharawichanant, S. 2017. Effect of Surfactant Addition During Polymerization on Properties of PEDOT:PSS for Electronic Applications. *Journal of Electronic Materials,* 46**,** 6709-6716.
9. Kerwin, B. A. 2008. Polysorbates 20 and 80 Used in the Formulation of Protein Biotherapeutics: Structure and Degradation Pathways. *Journal of Pharmaceutical Sciences,* 97**,** 2924-2935.
10. Dahotre, S., Tomlinson, A., Lin, B. & Yadav, S. 2018. Novel markers to track oxidative polysorbate degradation in pharmaceutical formulations. *Journal of Pharmaceutical and Biomedical Analysis,* 157**,** 201-207.
11. Kishore, R. S. K., Kiese, S., Fischer, S., Pappenberger, A., Grauschopf, U. & Mahler, H.-C. 2011. The Degradation of Polysorbates 20 and 80 and its Potential Impact on the Stability of Biotherapeutics. *Pharmaceutical Research,* 28**,** 1194-1210.
12. Larson, N. R., Wei, Y., Prajapati, I., Chakraborty, A., Peters, B., Kalonia, C., Hudak, S., Choudhary, S., Esfandiary, R., Dhar, P., Schöneich, C. & Middaugh, C. R. 2020. Comparison of Polysorbate 80 Hydrolysis and Oxidation on the Aggregation of a Monoclonal Antibody. *Journal of Pharmaceutical Sciences,* 109**,** 633-639.
13. Friedel, B., Keivanidis, P. E., Brenner, T. J. K., Abrusci, A., McNeill, C. R., Friend, R. H. & Greenham, N. C. 2009. Effects of layer thickness and annealing of PEDOT:PSS layers in organic photodetectors. *Macromolecules,* 42**,** 6741-6747.
14. Mengistie, D. A., Wang, P.-c. & Chu, C.-w. 2013. Effect of molecular weight of additives on the conductivity of PEDOT:PSS and efficiency for ITO-free organic solar cells. *Journal of Materials Chemistry A,* 1**,** 9907-9915.
15. Fu, X., Kong, W., Zhang, Y., Jiang, L., Wang, J. & Lei, J. 2015. Novel solid–solid phase change materials with biodegradable trihydroxy surfactants for thermal energy storage. *RSC advances,* 5**,** 68881-68889.
16. Glagovich, N. 2005. *IR Absorptions for Representative Functional Groups* [Online]. Available:

http://www.instruction.greenriver.edu/kmarr/chem%20162/Chem162%20Labs/Interpreting%20IR%20Spectra/IR%20Absorptions%20for%20Functional%20Groups.htm [Accessed 08/03/2018].
17. Liu, Y., Gu, J., Zhang, J., Yu, F., Wang, J., Nie, N. & Li, W. 2015. LiFePO4 nanoparticles growth with preferential (010) face modulated by Tween-80. *RSC advances,* 5**,** 9745-9751.
18. Pubchem. 2018. *Compound summary for CID 443315, Tween 80* [Online]. National Center for Biotechnology Information. Available: https://pubchem.ncbi.nlm.nih.gov/compound/443315 [Accessed 21/06/2018].
19. Rutledge, S. A. & Helmy, A. S. 2015. Etch-free patterning of poly(3,4-ethylenedioxythiophene)-poly(styrenesulfonate) for optoelectronics. *ACS applied materials & interfaces,* 7**,** 3940-3948.
20. Zhou, J., Ventura, I. & Lubineau, G. 2014. Probing the Role of Poly(3,4-ethylenedioxythiophene)/ Poly(styrenesulfonate)-Coated Multiwalled Carbon Nanotubes in the Thermal and Mechanical Properties of Polycarbonate Nanocomposites. *Industrial & Engineering Chemistry Research,* 53**,** 3539-3549.
21. Yoon, S. S. & Khang, D. 2016. Roles of Nonionic Surfactant Additives in PEDOT:PSS Thin Films. *J. Phys. Chem. C,* 120**,** 29525-29532.
22. Koidis, C., Logothetidis, S., Kapnopoulos, C., Karagiannidis, P. G., Laskarakis, A. & Hastas, N. A. 2011. Substrate treatment and drying conditions effect on the properties of roll-to-roll gravure printed PEDOT:PSS thin films. *Materials Science & Engineering B,* 176**,** 1556-1561.
23. Lombardo, V., Apos, Urso, L., Mannino, G., Scalese, S., Spucches, D., La Magna, A., Terrasi, A. & Puglisi, R. A. 2018. Transparent conductive polymer obtained by in-solution doping of PEDOT:PSS. *Polymer,* 155**,** 199-207.
24. Huang, J., Miller, P. F., de Mello, J. C., de Mello, A. J. & Bradley, D. D. C. 2003. Influence of thermal treatment on the conductivity and morphology of PEDOT/PSS films. *Synthetic Metals,* 139**,** 569-572.
25. Aasmundtveit, K. E., Samuelsen, E. J., Pettersson, L. A. A., Inganäs, O., Johansson, T. & Feidenhans, R. 1999. Structure of thin films of poly(3,4-ethylenedioxythiophene). *Synthetic Metals,* 101**,** 561-564.
26. Timpanaro, S., Kemerink, M., Touwslager, F. J., De Kok, M. M. & Schrader, S. 2004. Morphology and conductivity of PEDOT/PSS films studied by scanning–tunneling microscopy. *Chemical Physics Letters,* 394**,** 339-343.
27. Yu, Z., Xia, Y., Du, D. & Ouyang, J. 2016. PEDOT:PSS Films with Metallic Conductivity through a Treatment with Common Organic Solutions of Organic Salts and Their Application as a Transparent Electrode of Polymer Solar Cells. *ACS Appl. Mater. Interfaces,* 8**,** 11629-11638.
28. Nardes, A. M., Kemerink, M., de Kok, M. M., Vinken, E., Maturova, K. & Janssen, R. A. J. 2008. Conductivity, work function, and environmental stability of PEDOT:PSS thin films treated with sorbitol. *Organic Electronics,* 9**,** 727-734.
29. Kirchmeyer, S., Reuter, K. & Simpson, J. 2007. Poly(3,4-ethylene dioxythiophene) scientific importance, remarkable properties, and applications. *In:* Skotheim, T. & Reynolds, J. (eds.) *Handbook of conducting polymers.* 3rd ed. Boca Raton, London and New York: CRC press.
30. Callister, W. D. 2000. Materials science and engineering: an introduction. 5th ed. New York; Chichester: Wiley.

31. Kim, S., Cho, S., Lee, S. J., Lee, G., Kong, M., Moon, S., Myoung, J.-M. & Jeong, U. 2017. Boosting up the electrical performance of low-grade PEDOT:PSS by optimizing non-ionic surfactants. *Nanoscale,* 9**,** 16079-16085.
32. Aleshin, A. N., Williams, S. R. & Heeger, A. J. 1998. Transport properties of poly(3,4-ethylenedioxythiophene)/ poly(styrenesulfonate). *Synthetic Metals,* 94**,** 173-177.
33. Dimitriev, O. P., Piryatinski, Y. P. & Pud, A. A. 2011. Evidence of the controlled interaction between PEDOT and PSS in the PEDOT:PSS complex via concentration changes of the complex solution. *The Journal of Physical Chemistry. B,* 115**,** 1357.
34. Ouyang, J. 2013. "Secondary doping" methods to significantly enhance the conductivity of PEDOT:PSS for its application as transparent electrode of optoelectronic devices. *Displays,* 34**,** 423-436.
35. Po, R., Carbonera, C., Bernardi, A., Tinti, F. & Camaioni, N. 2012. Polymer- and carbon-based electrodes for polymer solar cells: Toward low-cost, continuous fabrication over large area. *Solar Energy Materials and Solar Cells,* 100**,** 97-114.
36. Shi, H., Liu, C., Jiang, Q. & Xu, J. 2015. Effective Approaches to Improve the Electrical Conductivity of PEDOT:PSS: A Review. *Advanced Electronic Materials,* 1**,** 1-16.
37. Sun, K., Zhang, S., Li, P., Xia, Y., Zhang, X., Du, D., Isikgor, F. & Ouyang, J. 2015. Review on application of PEDOTs and PEDOT:PSS in energy conversion and storage devices. *Journal of Materials Science: Materials in Electronics,* 26**,** 4438-4462.
38. Wen, Y. & Xu, J. 2017. Scientific Importance of Water-Processable PEDOT–PSS and Preparation, Challenge and New Application in Sensors of Its Film Electrode: A Review. 55**,** 1121-1150.
39. Kroon, R., Mengistie, D. A., Kiefer, D., Hynynen, J., Ryan, J. D., Yu, L. & Mller, C. 2016. Thermoelectric plastics: from design to synthesis, processing and structureproperty relationships. *Chemical Society Reviews,* 45**,** 6147-6164.
40. Kishi, N., Kondo, Y., Kunieda, H., Hibi, S. & Sawada, Y. 2018. Enhancement of thermoelectric properties of PEDOT:PSS thin films by addition of anionic surfactants. *Journal of Materials Science: Materials in Electronics,* 29**,** 4030-4034.
41. Zhang, S., Kumar, P., Nouas, A., Fontaine, L., Tang, H. & Cicoira, F. 2015. Solvent-induced changes in PEDOT: PSS films for organic electrochemical transistors. *APL Mater.,* 3.
42. Martin, B. D., Nikolov, N., Pollack, S. K., Saprigin, A., Shashidhar, R., Zhang, F. & Heiney, P. A. 2004. Hydroxylated secondary dopants for surface resistance enhancement in transparent poly(3,4- ethylenedioxythiophene)– poly(styrenesulfonate) thin films. *Synthetic Metals,* 142**,** 187-193.
43. Lubianez, R. P., Kirchmeyer, S. & Gaiser, D. 2008. Advances in PEDOT: PSS conductive polymer dispersions.
44. Ouyang, J., Xu, Q., Chu, C.-W., Yang, Y., Li, G. & Shinar, J. 2004. On the mechanism of conductivity enhancement in poly(3,4- ethylenedioxythiophene): poly(styrene sulfonate) film through solvent treatment. *Polymer,* 45**,** 8443-8450.
45. Oh, J. Y., Shin, M., Lee, J. B., Ahn, J. H., Baik, H. K. & Jeong, U. 2014. Effect of PEDOT nanofibril networks on the conductivity, flexibility, and coatability of PEDOT:PSS films. *ACS Applied Materials and Interfaces,* 6**,** 6954-6961.
46. Alemu, D., Wei, H.-y., Ho, K.-c. & Chu, C.-w. 2012. Highly conductive PEDOT:PSS electrode by simple film treatment with methanol for ITO-free polymer solar cells. *Energy Environ. Sci.,* 5**,** 9662-9671.
47. Kim, Y. H., Sachse, C., Machala, M. L., May, C., Müller-Meskamp, L. & Leo, K. 2011. Highly Conductive PEDOT:PSS Electrode with Optimized Solvent and Thermal Post-Treatment for ITO-Free Organic Solar Cells. *Advanced Functional Materials,* 21**,** 1076-1081.

48. Mengistie, D. A., Ibrahem, M. A., Wang, P.-C. & Chu, C.-W. 2014. Highly conductive PEDOT:PSS treated with formic acid for ITO-free polymer solar cells. *ACS applied materials & interfaces,* 6**,** 2292-2299.
49. Yoshioka, Y. & Jabbour, G. 2006. Desktop inkjet printer as a tool to print conducting polymers. *Synth. Met.,* 156**,** 779-783.
50. Sigma-Aldrich. 2021. *Triton X-100 Laboratory Grade* [Online]. Available: https://www.sigmaaldrich.com/catalog/product/sial/x100?lang=en&region=GB&cm_sp=Insite-_-caSrpResults_srpRecs_srpModel_9002-93-1-_-srpRecs3-1 [Accessed 03/02/2021].
51. Sigma-Aldrich. 2021. *Tween 80 Viscous Liquid* [Online]. Available: https://www.sigmaaldrich.com/catalog/product/sial/p1754?lang=en&region=GB&cm_sp=Insite-_-caSrpResults_srpRecs_srpModel_9005-65-6-_-srpRecs3-1#productDetailSafetyRelatedDocs [Accessed 03/02/2021].
52. Nardes, A. M., Kemerink, M., Janssen, R. A. J., Bastiaansen, J. A. M., Kiggen, N. M. M., Langeveld, B. M. W., van Breemen, A. J. J. M. & de Kok, M. M. 2007. Microscopic Understanding of the Anisotropic Conductivity of PEDOT:PSS Thin Films. *Advanced Materials,* 19**,** 1196-1200.
53. Thompson, B. T. 2017. *Enhancing the conductivity of PEDOT:PSS on bulk substrates.* Doctor of Philosophy, University of Warwick.
54. Bubnova, O., Khan, Z. U., Wang, H., Braun, S., Evans, D. R., Fabretto, M., Hojati-Talemi, P., Dagnelund, D., Arlin, J.-B., Geerts, Y. H., Desbief, S., Breiby, D. W., Andreasen, J. W., Lazzaroni, R., Chen, W. M., Zozoulenko, I., Fahlman, M., Murphy, P. J., Berggren, M. & Crispin, X. 2013. Semi-metallic polymers. *Nature Materials,* 13**,** 190.
55. Groenendaal, L., Jonas, F., Freitag, D., Pielartzik, H. & Reynolds, J. R. 2000. Poly(3,4-ethylenedioxythiophene) and Its Derivatives: Past, Present, and Future. *Advanced Materials,* 12**,** 481-494.
56. Zotti, G., Zecchin, S., Schiavon, G., Louwet, F., Groenendaal, L., Crispin, X., Osikowicz, W., Salaneck, W. & Fahlman, M. 2003. Electrochemical and XPS studies toward the role of monomeric and polymeric sulfonate counterions in the synthesis, composition, and properties of poly(3,4- ethylenedioxythiophene). *Macromolecules,* 36**,** 3337-3344.
57. Jönsson, S. K. M., Birgerson, J., Crispin, X., Greczynski, G., Osikowicz, W., Denier van Der Gon, A. W., Salaneck, W. R. & Fahlman, M. 2003. The effects of solvents on the morphology and sheet resistance in poly(3,4-ethylenedioxythiophene)–polystyrenesulfonic acid (PEDOT–PSS) films. *Synthetic Metals,* 139**,** 1-10.
58. Sigma-Aldrich 2018. Product Specifaction: Tween 80.
59. Giuri, A., Masi, S., Colella, S., Listorti, A., Rizzo, A., Kovtun, A., Dell'Elce, S., Liscio, A. & Corcione, C. E. 2017. Rheological and physical characterization of PEDOT:PSS/Graphine Oxide nanocomposites for perovskite solar cells. *Polymer Engineering & Science,* 57**,** 546-552.
60. Horikawa, M., Fujiki, T., Shirosaki, T., Ryu, N., Sakurai, H., Nagaoka, S. & Ihara, H. 2015. The development of a highly conductive PEDOT system by doping with partially crystalline sulfated cellulose and its electric conductivity. *J. Mater. Chem. C,* 3**,** 8881-8887.
61. Kim, N., Kee, S., Lee, S. H., Lee, B. H., Kahng, Y. H., Jo, Y. R., Kim, B. J. & Lee, K. 2014. Highly Conductive PEDOT:PSS Nanofibrils Induced by Solution- Processed Crystallization. *Advanced Materials,* 26**,** 2268-2272.
62. Kim, N., Lee, B. H., Choi, D., Kim, G., Kim, H., Kim, J.-R., Lee, J., Kahng, Y. H. & Lee, K. 2012. Role of interchain coupling in the metallic state of conducting polymers. *Physics Review Letters,* 109**,** 106405-106405.

63. Wang, X., Kyaw, A. K. K., Yin, C., Wang, F., Zhu, Q., Tang, T., Yee, P. I. & Xu, J. 2018. Enhancement of thermoelectric performance of PEDOT:PSS films by post-treatment with a superacid. *RSC Adv.,* 8**,** 18334-18340.
64. Crispin, X., Jakobsson, F. L. E., Crispin, A., Grim, P. C. M., Andersson, P., Volodin, A., Van Haesendonck, C., Van Der Auweraer, M., Salaneck, W. R. & Berggren, M. 2006. The origin of the high conductivity of poly(3,4-ethylenedioxythiophene)- poly(styrenesulfonate) (PEDOT-PSS) plastic electrodes. *Chemistry of Materials,* 18**,** 4354-4360.
65. Geskin, V. M. & Brédas, J. L. 2003. Polaron Pair versus Bipolaron on Oligothiophene Chains: A Theoretical Study of the Singlet and Triplet States. *Chemphyschem,* 4**,** 498-505.
66. Martinez, C., R. & Iverson, B., L. 2012. Rethinking the term "pi-stacking". *Chemical Science,* 3**,** 2191-2201.
67. Kim, S.-M., Kim, C.-H., Kim, Y., Kim, N., Lee, W.-J., Lee, E.-H., Kim, D., Park, S., Lee, K., Rivnay, J. & Yoon, M.-H. 2018. Influence of PEDOT:PSS crystallinity and composition on electrochemical transistor performance and long-term stability. *Nature communications,* 9**,** 3858-3858.
68. Lefebvre, M., Qi, Z., Rana, D. & Pickup, P. G. 1999. Chemical synthesis, characterization, and electrochemical studies of poly(3,4- ethylenedioxythiophene)/ Poly(styrene- 4- sulfonate) composites. *Chemistry of Materials,* 11**,** 262-268.
69. Lingstedt, L. V., Ghittorelli, M., Lu, H., Koutsouras, D. A., Marszalek, T., Torricelli, F., Crăciun, N. I., Gkoupidenis, P. & Blom, P. W. M. 2019. Effect of DMSO Solvent Treatments on the Performance of PEDOT:PSS Based Organic Electrochemical Transistors. *Advanced Electronic Materials,* 5**,** 1800804.
70. Crawford, G. P. 2005. *Flexible flat panel displays,* Chichester, John Wiley & Sons, Ltd.
71. Lee, J.-H., Liu, D. N. & Wu, S.-T. 2008. *Introduction to flat panel displays,* Chichester, Wiley.
72. Xia, Y. & Ouyang, J. 2011. PEDOT:PSS films with significantly enhanced conductivities induced by preferential solvation with cosolvents and their application in polymer photovoltaic cells. *Journal of materials chemistry,* 21**,** 4927.
73. Volkov, A. V., Wijeratne, K., Mitraka, E., Ail, U., Zhao, D., Tybrandt, K., Andreasen, J. W., Berggren, M., Crispin, X. & Zozoulenko, I. V. 2017. Understanding the Capacitance of PEDOT:PSS. *Advanced Functional Materials,* 27**,** 1700329.
74. Cho, C.-K., Hwang, W.-J., Eun, K., Choa, S.-H., Na, S.-I. & Kim, H.-K. 2011. Mechanical flexibility of transparent PEDOT:PSS electrodes prepared by gravure printing for flexible organic solar cells. *Solar Energy Materials & Solar Cells,* 95**,** 3269-3276.
75. Ouyang, J., Chu, C. W., Chen, F. C., Xu, Q. & Yang, Y. 2005. High-Conductivity Poly(3,4-ethylenedioxythiophene):Poly(styrene sulfonate) Film and Its Application in Polymer Optoelectronic Devices. *Advanced Functional Materials,* 15**,** 203-208.
76. Murthy, N. S. 2016. X-ray Diffraction from Polymers. *In:* Guo, Q. (ed.) *Polymer Morphology: Principles, Characterization, and Processing.* Hoboken, NJ, USA: John Wiley & Sons, Inc.
77. Murthy, N. S. & Minor, H. 1995. Analysis of poorly crystallized polymers using resolution enhanced X-ray diffraction scans. *Polymer,* 36**,** 2499-2504.
78. Lambert, J. B. 1987. *Introduction to Organic Spectroscopy,* New York, USA, Macmillan.
79. Hoath, S. D., Hsiao, W.-K., Martin, G. D., Jung, S., Butler, S. A., Morrison, N. F., Harlen, O. G., Yang, L. S., Bain, C. D. & Hutchings, I. M. 2015. Oscillations of aqueous PEDOT:PSS fluid droplets and the properties of complex fluids in drop-on-demand inkjet printing. *Journal of Non-Newtonian Fluid Mechanics,* 223**,** 28-36.

80. Hoath, S. D., Jung, S., Hsiao, W.-K. & Hutchings, I. M. 2012. How PEDOT:PSS solutions produce satellite- free inkjets. *Organic Electronics,* 13**,** 3259-3262.
81. Johnston, M. T. & Ewoldt, R. H. 2013. Precision rheometry: Surface tension effects on low-torque measurements in rotational rheometers. *Journal of Rheology,* 57**,** 1515-1532.
82. Kopola, P., Tuomikoski, M., Suhonen, R. & Maaninen, A. 2009. Gravure printed organic light emitting diodes for lighting applications. *Thin Solid Films,* 517**,** 5757-5762.
83. Kopola, P. 2010. High efficient plastic solar cells fabricated with a high-throughput gravure printing method. *Solar Energy Materials & Solar Cells,* 94**,** 1673-1681.
84. Setti, L., Fraleoni-Morgera, A., Ballarin, B., Filippini, A., Frascaro, D. & Piana, C. 2005. An amperometric glucose biosensor prototype fabricated by thermal inkjet printing. *Biosensors and Bioelectronics,* 20**,** 2019-2026.
85. Hrehorova, E., Pekarovicova, A. & Fleming, P. D. 2006. Gravure Printability of Conducting Polymer Inks. *Proceedings of IS&T Digital Fabrication, Denver*.
86. Søndergaard, R., Hösel, M., Angmo, D., Larsen-Olsen, T. T. & Krebs, F. C. 2012. Roll-to-roll fabrication of polymer solar cells. *Materials Today,* 15**,** 36-49.
87. Mohsin, H., Sultan, U., Joya, Y. F., Ahmed, S., Awan, M. S. & Arshad, S. N. 2016. Development and characterization of cobalt based nanostructured super hydrophobic coating. *IOP Conference Series: Materials Science and Engineering,* 146**,** 12038.
88. Claussen, W. F. 1967. Surface Tension and Surface Structure of Water. *Science,* 156**,** 1226-1227.
89. Khattab, I. S., Bandarkar, F., Fakhree, M. A. A. & Jouyban, A. 2012. Density, viscosity, and surface tension of water+ethanol mixtures from 293 to 323K. *The Korean Journal of Chemical Engineering,* 29**,** 812-817.
90. Kommeren, S., Coenen, M. J. J., Eggenhuisen, T. M., Slaats, T. W. L., Gorter, H. & Groen, P. 2018. Combining solvents and surfactants for inkjet printing PEDOT:PSS on P3HT/PCBM in organic solar cells. *Organic Electronics,* 61**,** 282-288.
91. Kothekar, S. C., Ware, A. M., Waghmare, J. T. & Momin, S. A. 2007. Comparative Analysis of the Properties of Tween-20, Tween-60, Tween-80, Arlacel-60, and Arlacel-80. *Journal of Dispersion Science and Technology,* 28**,** 477-484.
92. Eom, S. H., Senthilarasu, S., Uthirakumar, P., Yoon, S. C., Lim, J., Lee, C., Lim, H. S., Lee, J. & Lee, S.-H. 2009. Polymer solar cells based on inkjet-printed PEDOT:PSS layer. *Organic Electronics,* 10**,** 536-542.
93. Sirringhaus, H., Kawase, T., Friend, R. H., Shimoda, T., Inbasekaran, M., Wu, W. & Woo, E. P. 2000. High-resolution inkjet printing of all-polymer transistor circuits. *Science (New York, N.Y.),* 290**,** 2123-2126.

Chapter 5: Results and Discussion – Alternative Conductivity Enhancement Methods of PEDOT:PSS

In this chapter, various conductivity enhancement methods will be explored including multiple dip castings, the addition of the solvent MEK to PEDOT:PSS/Tween 80 solutions, and solvent washing using MEK, ethanol and methanol. In most cases, these were performed alongside pre-treatment with Tween 80 expanding on the previous chapter. The effects of each treatment on the sheet resistivity were measured along with XRD and Raman analysis of the microstructure and visual assessment of film quality.

5.1 Multiple Dip Cast PEDOT:PSS/Tween 80 Films

Multiple dip cast samples were prepared using the method described previously (section 2.2.2.2). Glass substrates were dipped for 30 seconds in solution and annealed at 140 °C for 1 hour with a range of surfactant concentrations being used. The process was then repeated up to five times for each PEDOT:PSS/Tween 80 solution. This, in effect, placed multiple layers of the corresponding solution onto the already existing layer. The annealing process was repeated for every dip performed and 12 hours of equilibration was allowed after the last dip layer, prior to any measurements. The rational for this was to determine whether the film thickness, and subsequent effect on the conducting properties of PEDOT:PSS/Tween 80, could be controlled in this manner, similar to previous literature findings for pristine PEDOT:PSS.[1,2]

5.1.1 Sheet Resistivity of Multiple Dip PEDOT:PSS/Tween 80 Films

The sheet resistivity of PEDOT:PSS/Tween 80 multiple layered films was found to decrease with the number of dips across all surfactant concentrations (Figure 5-1). The number of dips also alters the trend in the data with Tween 80 concentration. The '1 Dip' samples (reported in section 4.4.1) show that as the concentration of Tween 80 increases, the sheet resistivity decreases. The scatter at concentrations between 0.35 and 0.55 wt% are caused by the Tween 80 initially interacting with the excess PSS before disrupting the PEDOT – PSS interaction (section 4.4.1).[3] The data then shows the same pronounced decrease in sheet resistivity up to 1 wt% surfactant with greater concentrations resulting in a much subtler improvements in results (section 4.4.1). However, once a second layer is added the sheet resistivity for pristine PEDOT:PSS is significantly lowered. Furthermore, low concentrations of surfactant increase resistivity until 1 wt% after which the trend is similar to the '1 Dip' samples.

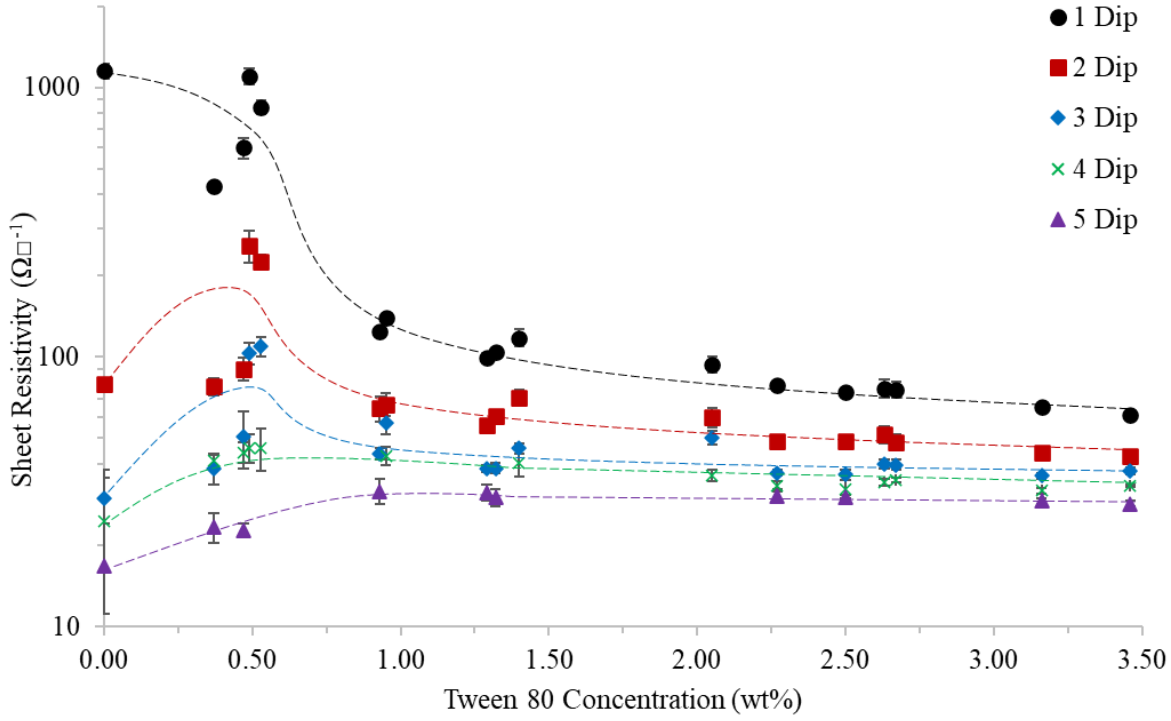

Figure 5-1: Sheet resistivity ($\Omega\square^{-1}$) of PEDOT:PSS/Tween 80 films with increasing concentrations of surfactant (wt%) for varying layer numbers. Legend indicates the layer (or 'Dip') number for each set of data. Dotted guidelines hand drawn to highlight overall trend of each data set. Error bars show ±1 SD

For higher dip numbers, the pristine PEDOT:PSS resistivity continues to drop, however, the addition of Tween 80 causes resistivity to decrease less with each layer applied. For 3 to 5 dips, the lowest resistivities were for pristine PEDOT:PSS with results for films containing the surfactant plateauing at 1 wt%. This effect is more clearly seen in Figure 5-2 in which the sheet resistivity has been plotted against dip number for selected Tween 80 concentrations. This figure also highlights that the difference in resistivity between pristine PEDOT:PSS and samples containing Tween 80 gets smaller with increasing dip number. The lowest sheet resistivity (16.75 $\Omega\square^{-1}$) recorded across all samples was obtained for the '5 Dip' pristine PEDOT:PSS sample. This is significantly smaller than the lowest sheet resistivity obtained for '1 Dip' which contained 3.46 wt% surfactant (60.86 $\Omega\square^{-1}$).

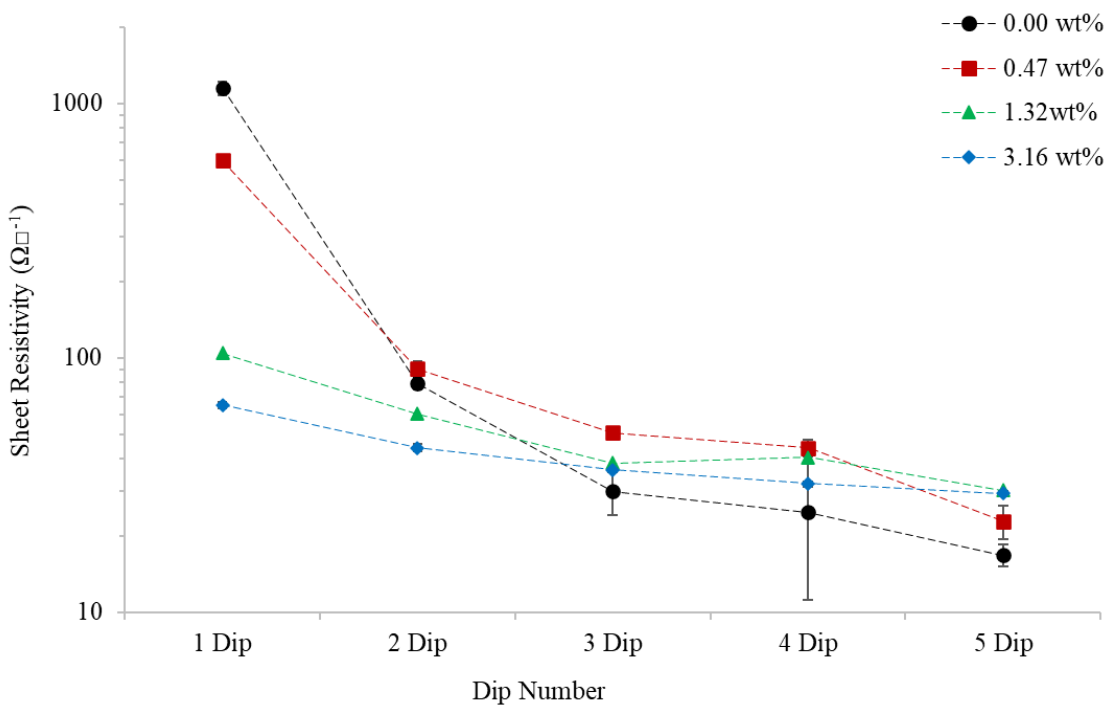

Figure 5-2: Sheet resistivity ($\Omega\square^{-1}$) of PEDOT:PSS/Tween 80 films for increasing layer (or 'Dip') number. Data plotted for films containing surfactant concentrations of 0.00 (black circle), 0.93 (red square), 1.32 (green triangle) and 3.16 (blue diamond) wt%. Error bars show ±1 SD. Dotted guidelines present to show trend of the data

The effect on film thickness for increasing dip application is seen in Figure 5-3. As expected, the increase in dip number leads to an increase in film thickness for all surfactant concentrations. As previously seen (section 4.4.1), the '1 Dip' sample shows an increase in thickness with greater Tween 80 addition, which is not observed with 2 – 4 layers. In these situations, the greatest thickness is obtained when no Tween 80 is present. The increase in thickness is smallest for samples containing 0.49 wt%, with films containing 1.40 wt% showing a slightly larger increase with each layer applied.

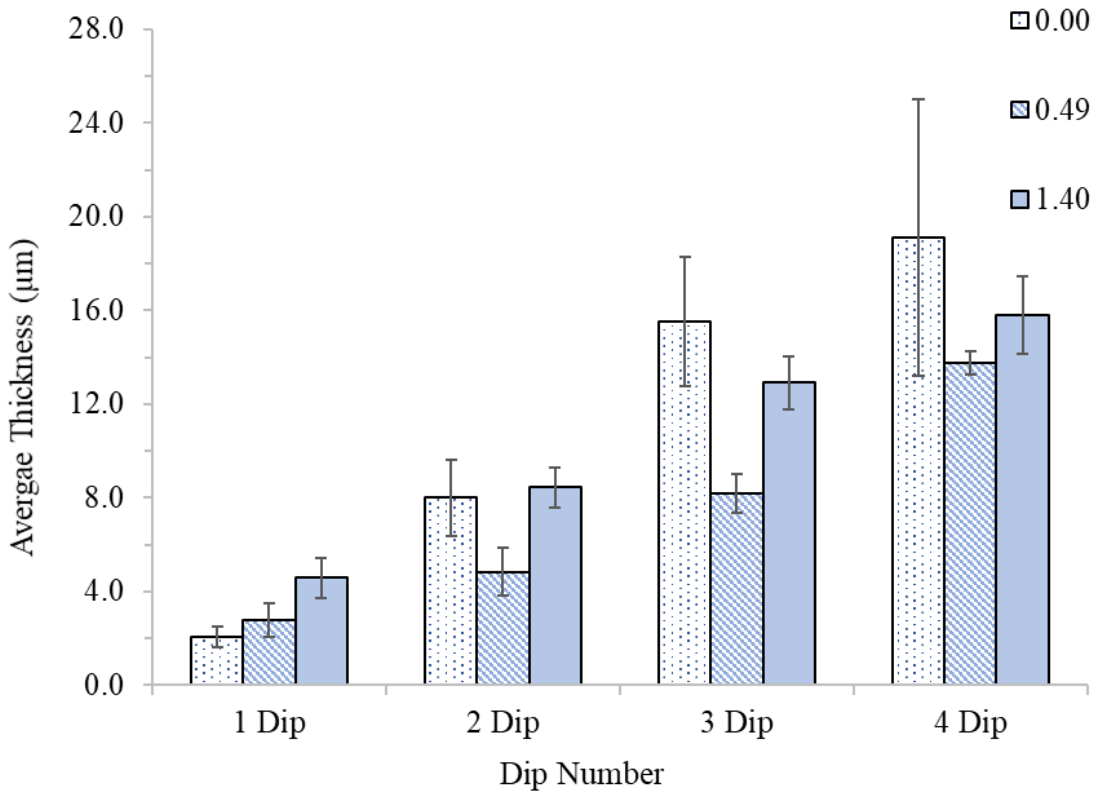

Figure 5-3: Average thickness (µm) of PEDOT:PSS/Tween 80 films containing 0.00 (dotted), 0.49 (striped) and 1.40 (block colour) wt% surfactant for differing dip numbers. Error bars show ±1 SD. Average was taken from a 4 µm x 5 µm area as specified in the Experimental Chapter, section 2.5.5

When sheet resistivity is considered with regard to thickness, there is a large decrease in resistivity as the samples get thicker (Figure 5-4). This is true for all concentrations of Tween 80, with the decrease being more prominent for samples containing 0 or 0.49 wt%. For these samples, an increase in thickness initially causes a large decrease in resistivity, which becomes less prominent at greater thicknesses. While the decrease in resistivity for the sample containing 1.40 wt% surfactant is still substantial, this shows a more linear trend and an initially lower resistivity for thinner samples. The latter shows a 63 % decrease in the sheet resistivity across a 12 µm increase, compared to a 97 % decrease for pristine PEDOT:PSS samples for the same thickness increase.

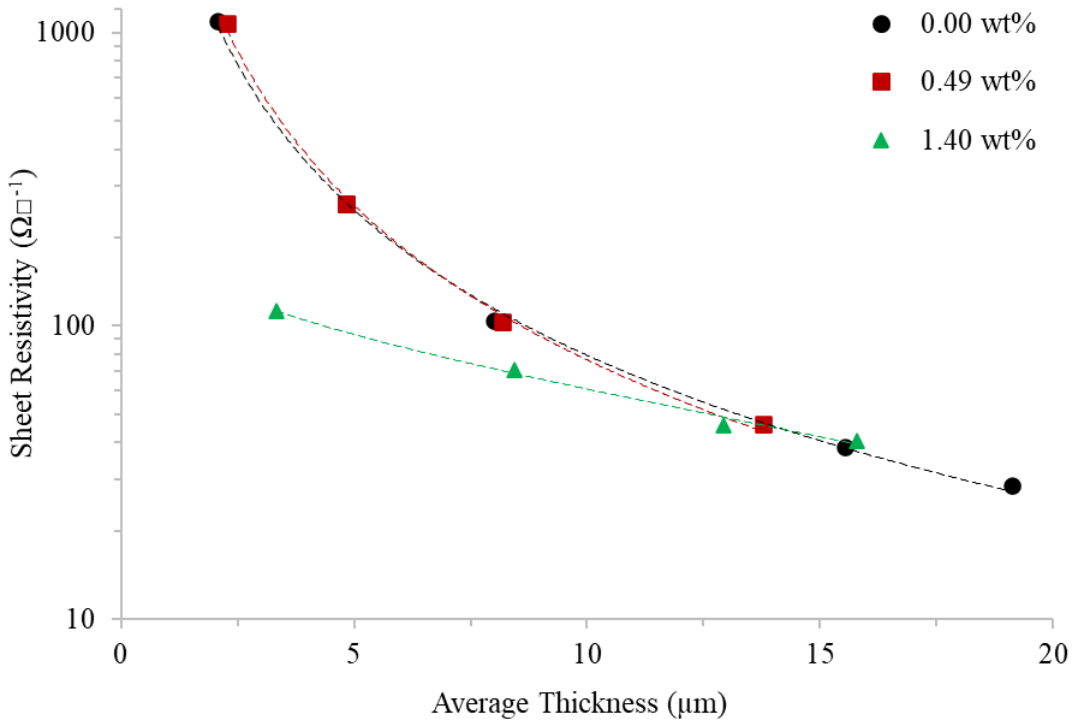

Figure 5-4: Sheet resistivity (Ω□$^{-1}$) as a function of average PEDOT:PSS/Tween 80 film thickness (µm) for surfactant concentrations (wt%) of 0.00 (black circle), 0.49 (red square) and 1.40 wt% (green triangle). Thickness was increased by increasing the dip number, effectively adding another layer to the film. The layer number increased from 1 to 4 with '1 Dip' being the left most data point. Dotted guidelines present to show the trend of the data

Similar trends of a decrease in sheet resistivity with thickness has been seen previously within the literature.[1,2,4-6] However, whist the trend is similar, the resistivity values differ between this study and other reports. For example, in the case of Martin, *et al.* (2004)[5], pristine PEDOT:PSS sheet resistivity decreased from 4300 to 1800 Ω□$^{-1}$ with an increase from 0.17 to 0.53 µm. This equated to a 58 % drop in resistivity which, despite the large drop in absolute values, is a much smaller percentage decrease. However, this was with much thinner films, meaning the thickness range is considerably smaller, and films were manufactured via spin coating making direct comparison difficult. Alternatively, Alemu, *et al.* (2012)[1] saw a decrease from 140 to 25 Ω□$^{-1}$ for a thickness increase from 50 (1 layer) to 300 nm (6 layers). These results were closely

matched by Mengistie, *et al.* (2014)[2] and, in both cases, the percentage decrease was approximately 83 %. This is closer to results seen in this study and is more comparable since the method of thickness increase was through multiple layer application. There is still, however, limitations to this comparison since these two studies implemented a solvent wash too. As discussed previously (section 1.5.1.3), it is likely that the thickness effect may be limited to sheet resistivity measurements, caused by the thickness correction factors implement when using the 4-point probe.[7] Furthermore, as previously discussed (section 1.5.1.3) conductivity calculations factor in thickness (section 2.6) and often show trends that do not follow resistivity data. However, due to the multiple layer approach used to increase thickness, it was deemed that converting to conductivity for comparison would not be suitable since the 4-point probe only measured the surface resistivity. Therefore, a true representation of conductivity through the whole sample cannot be established.

Despite this, there are other aspects that can be considered as to why sheet resistivity is lower for pristine PEDOT:PSS when more layers are applied. As discussed in section 4.4.1, the PSS-rich regions can be thought of as resistors in a circuit which follow Thevenin's theorem. Therefore, thicker films provide more opportunity for resistance to be lower since the PSS-rich regions are more likely to stack and replicate a circuit with resistors in parallel. There is also greater opportunity for conductivity PEDOT-rich regions to reside closer together, further reducing resistance to electron flow.

There are other suggestions which may contribute, as follows. Firstly, the multiple dip method involves submerging an existing film into the PEDOT:PSS solution, which could then be acting as a solvent wash. Washes are a common method used with solvents, such as methanol, removing excess PSS from the film to improve conductivity (sections 1.5.2.3 & 5.3).[1,8-10] Whilst water is not a common wash solvent, it has been previously used as a post-treatment

method to improve conductivity from 3 to 10 Scm^{-1}.[11,12] This could also partially explain why sheet resistivity decreases less when Tween 80 is present since the surfactant may be acting as a barrier to PSS removal. However, the 4-point probe predominantly measures the film surface meaning the outer PEDOT:PSS layer would not have the reduced PSS content caused by washing, therefore, this theory is inconclusive. However, thicker films allow some electron flow under the surface of the sample.[7] Since PSS is likely removed from layers under the surface, more conductive subsurface layers may cause a reduction in resistivity.

Another factor is repeat processing results in previous layers being annealed multiple times. While logically this may reduce sheet resistivity, it has already been shown that 1 hour of annealing is sufficient to achieve the maximum reduction (section 4.3.2). Furthermore, the top layer would only have been annealed once and measurement with the 4-point probe is primarily on the surface. Therefore, regardless of any affect further annealing might have on layers underneath, it is unlikely this would have a direct effect on the sheet resistivity. This would also be unaffected by the presence of Tween 80.

The final theory is that when a new layer is added to an already present PEDOT:PSS film, the PEDOT:PSS solution interacts differently than with the glass substrate. Due to the surface energy of the PEDOT:PSS film, PEDOT-rich regions may deposit as a new layer more readily, or excess PSS may not be deposited as easily. Alternatively, the PEDOT:PSS film under the newly deposited solution might cause the PEDOT and PSS to segregate leading to more of the conductive PEDOT residing at the film surface. The possible removal of PSS through washing may also affect the deposition of a new PEDOT:PSS layer. This may also explain why the addition of Tween 80 results in a less pronounced sheet resistivity decrease. The surfactant will be interacting with the free polar group of the PEDOT and PSS which may hinder their

interaction to already deposited film. However, these suggestions are more hypothetical and evidence of this would require further research.

The overall likelihood is that a combination of effects occurs with progressively higher dip numbers. Despite not knowing the exact mechanism behind the resistivity reduction for higher dip numbers, this does provide an alternative method of conductivity enhancement without the need for additives. However, from a processing perspective this is a less convenient method, due to increases in cost and time, therefore, is unlikely to replace current conductivity enhancement methods.

5.1.2 Structural Analysis of Multiple Dip Samples

5.1.2.1 X-Ray Diffraction (XRD)

The XRD traces in Figure 5-5 show the effect of increasing dip number for pristine PEDOT:PSS films on chain alignment. As has been discussed previously (section 4.4.5.2), the '1 Dip' sample shows weak, broad peaks around 26 and 18 °. These peaks become more prominent as the number of dips increase. Whilst the increased intensity of these peaks might be assumed to be evidence of chain alignment, their broadness still suggests no long range order.[5,13-18] Furthermore, significant changes in alignment would either cause peaks to shift or new sharper peaks to appear.[19-21] A comparable trace was seen by Kim, *et al.* (2014)[15] in which similar peaks were reported and it was concluded that pristine PEDOT:PSS did not show long range order or alignment. The growth of the peaks, especially for the sample consisting of 5 dips, is most likely due to concentration effects as the films become significantly thicker with each dip. This data is also evidence that alignment does not contribute to the decrease in sheet resistivity seen for the multiple dip sample (section 5.1.1).

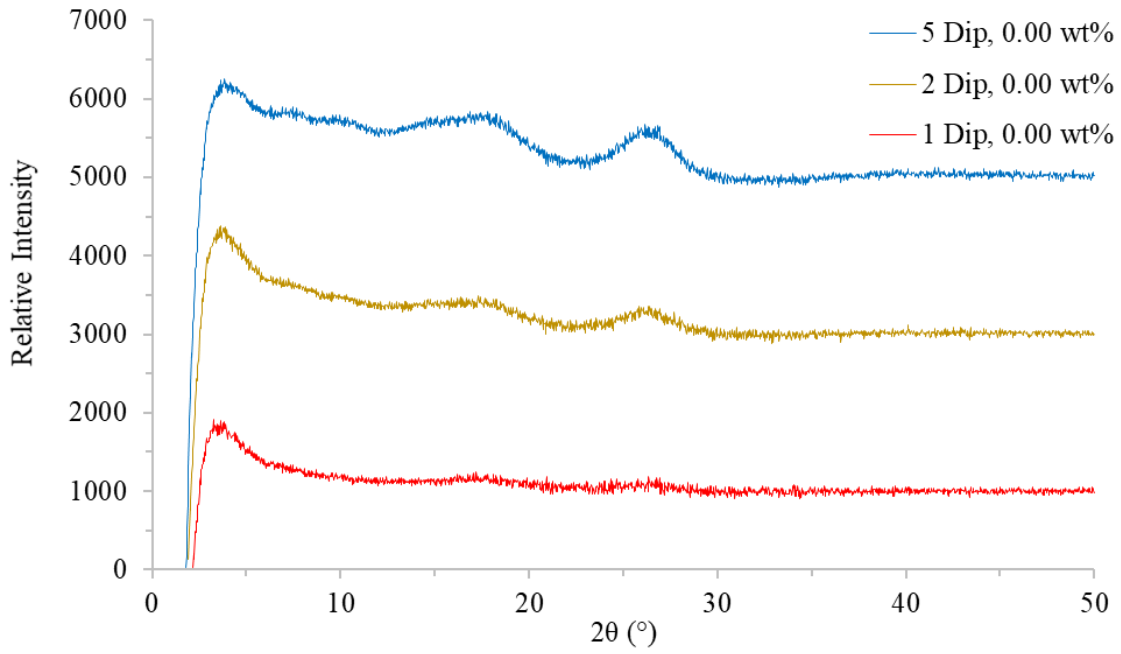

Figure 5-5: XRD traces showing the effect of increasing dip number (from bottom to top) on the diffraction pattern for pristine PEDOT:PSS (0.00 wt% Tween 80). Baseline of glass substrate was removed

The effect of multiple dip casting for PEDOT:PSS/Tween 80 films with a surfactant concentration of 1.32 wt% can be seen in Figure 5-6. As previously discussed (section 4.4.5.2), the '1 Dip' sample (Figure 5-6a) displays sharp, defined peaks at 2.3 and 6.8 ° and two smaller peaks at 4.6 and 11.3 ° due to the addition of Tween 80 disrupting the PEDOT and PSS interaction and allowing for chain alignment.[3,15,18] The broad peaks seen for pristine PEDOT:PSS are also visible for 1 and 2 layer samples (Figure 5-6a & b, respectively). This can clearly be seen in Figure 5-6d when compared to the '2 Dip' sample containing no Tween 80. However, these broader peaks are not clear once 5 dips have been applied as the intensity of the sharp peaks are much greater (Figure 5-6c).

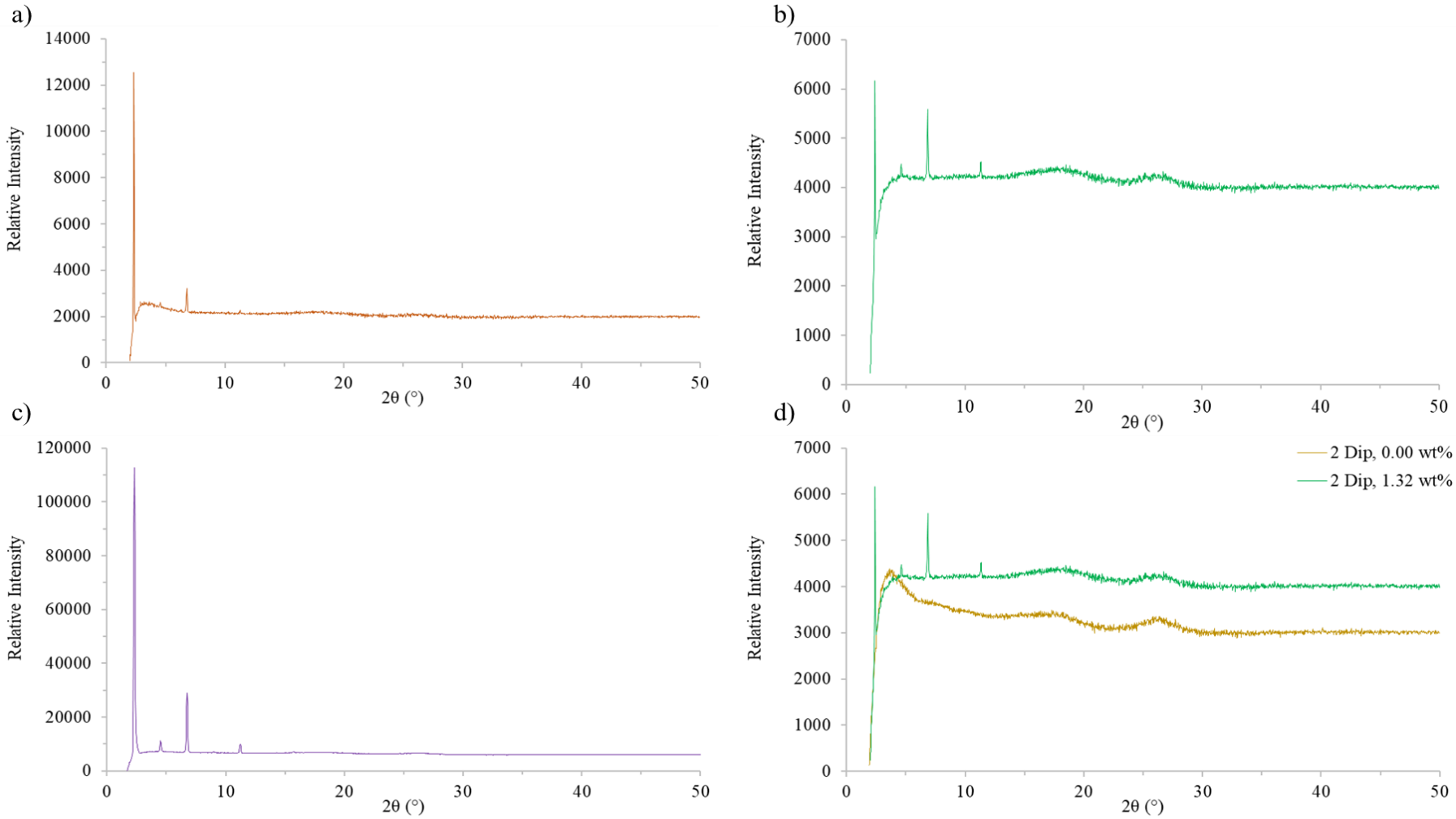

Figure 5-6: XRD traces of PEDOT:PSS/Tween 80 films with 1.32 wt% surfactant showing a) 1 dip, b) 2 dip & c) 5 dip samples. d) shows comparison of pristine PEDOT:PSS (0.00 wt%) and 1.32 wt% surfactant 2 dip samples. Baseline of glass substrate was removed

As already discussed, the broad peaks seen in the pristine samples are evidence of no long range order[5,13-18] with the intensity of the peaks increasing due to the higher quantity of PEDOT:PSS present for the '5 Dip' sample. This is also the reason why the sharp peaks are much more prominent in the '5 Dip' sample when the Tween 80 is present. It is well understood that the addition of the surfactant causes alignment of the polymer chains,[3,15,18] however, it appears that for the '5 Dip' sample the ratios of the peak intensities change. When considering only the biggest peaks at 2.3 and 6.8 °, the ratio between them changes from 1.60 to 3.98 from 1 to 5 dips, respectively. This shows that the peak at 2.3 ° is increasing more rapidly per dip. This does not appear to be the case for the '2 Dip' sample, however, a baseline is harder to determine for the peak at 2.3 ° due to the distortion of the trace at these angles. In a previous study by Kim, *et al.* (2014)[15], two similar sharp peaks were seen at 4.4 and 6.3 ° after washing with concentrated H_2SO_4 which were attributed to stacking of the PEDOT:PSS following excess PSS removal.[15] Therefore, the XRD results seen in this study could be providing evidence that PSS is being removed during the application of multiple layers. Alternatively, the data might be showing that excess PSS is not deposited as readily on an already present layer of PEDOT:PSS. This would then support the hypothesis that there may be preferential interaction of PEDOT-rich components within solution to a pre-existing PEDOT:PSS layer. However, it is difficult to distinguish between these two mechanisms. Whilst this data does not provide evidence that multiple dips improve the chain alignment further, it does show evidence of variation in the surface composition when additional layers are cast.

5.1.2.2 Raman Spectroscopy

Figure 5-7 shows the Raman spectra for pristine PEDOT:PSS films with increasing dip number. It can be seen that for '1 Dip' there are two main peaks at 1600 and 1460 cm^{-1} with a shoulder appearing at 1360 cm^{-1}. As before (section 4.4.5.3), these correspond to the C=C aromatic

structure and SO_3 group in PEDOT and PSS, respectively.[22] It can be seen that there is no significant change or shift in these peaks following further dips which suggests that the multiple dipping process does not significantly change the chemical structure of the material.

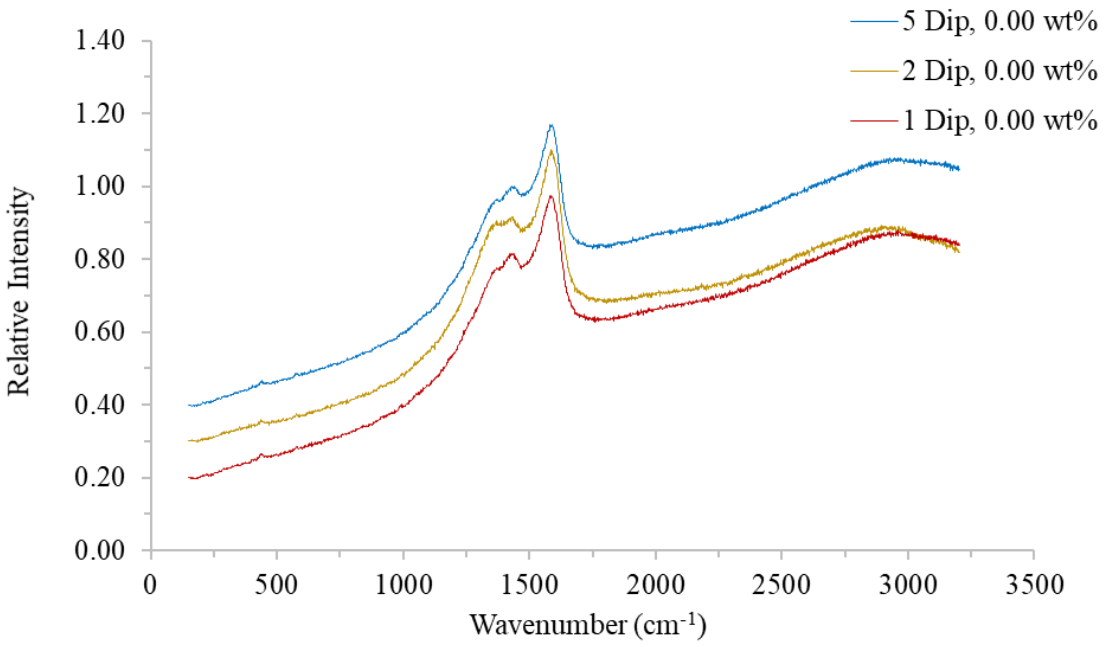

Figure 5-7: Raman spectra of pristine PEDOT:PSS (0.00 wt% Tween 80) films for 1, 2 and 5 dip samples (from bottom to top)

Figure 5-8 shows the Raman spectra for multiple dipped samples of PEDOT:PSS/Tween 80 with 1.32 wt% surfactant. As the dip number increases, the shoulder at 1360 cm^{-1} becomes more pronounced while the small peak at 1460 cm^{-1} reduces. By 5 dips, these two features become nearly indistinguishable from one another, however, the main peak at 1600 cm^{-1} remains unchanged regardless of dip number.

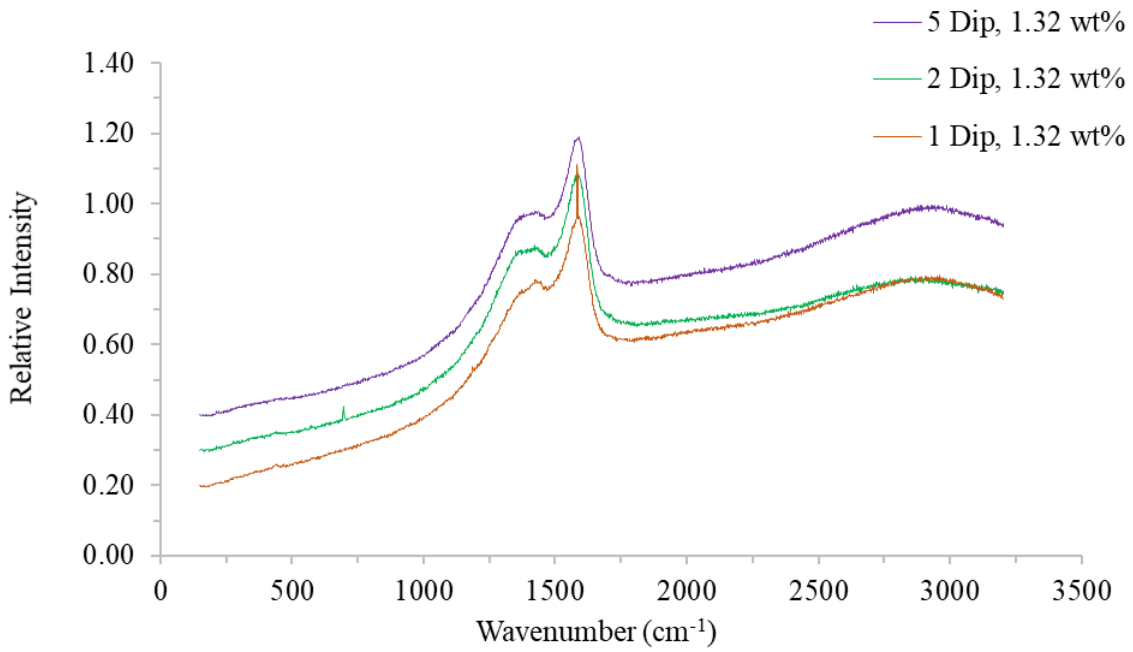

Figure 5-8: Raman spectra of PEDOT:PSS/Tween 80 films containing 1.32 wt% surfactant for 1, 2 and 5 dip samples (from bottom to top)

The likelihood of a benzoid/quinoid change was discussed previously (section 4.4.5.3) and it was established that, while this may be occurring with the addition of Tween 80, it was unlikely to induce a large enough change to be detected by Raman. The shoulder at 1360 cm^{-1} is associated with the SO_3 group in PSS, meaning this could be evidence of greater quantities of PSS being present in the films with further dips. This would indicate that PSS is preferentially being deposited onto the film with each subsequent casting. This would provide evidence against the hypothesis that PEDOT is preferentially deposited, as suggested in the previous section. Furthermore, it is known that CH and OH groups show peaks in this range[22] meaning these results could be showing a build-up of Tween 80 causing the peaks for PEDOT:PSS to appear less prominent. While all these suggestions are hypothetical, without higher resolution or deconvolution of the peaks the cause of the change cannot be established with certainty.

5.1.3 Surface Roughness of Multiple Dip PEDOT:PSS/Tween 80 Films

Despite the use of multiple dips reducing the sheet resistivity of pristine PEDOT:PSS films there are issues with using this as a method of resistivity improvement. One issue is the film roughness substantially increases with each layer (Figure 5-9).

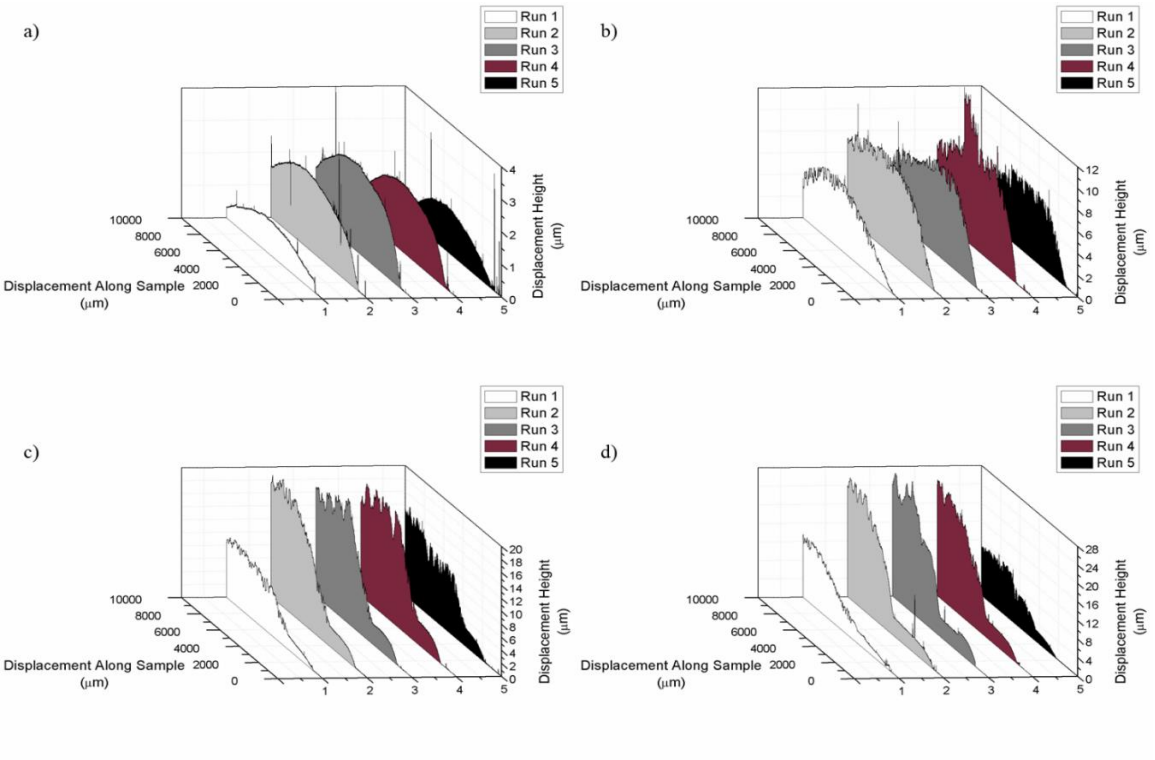

Figure 5-9: Surface profiling of pristine PEDOT:PSS for a) 1, b) 2, c) 3 and d) 4 dips. Profile shows the displacement height (μm) along the sample with 5 profiling runs being performed spaced 2 mm apart

This was also indicated by an increase in the error bar size for thickness measurements of pristine PEDOT:PSS (Figure 5-3). After calculating the Ra of these films, an increase from 0.04 to 0.41 μm can be seen between the 1 and 2 layered pristine PEDOT:PSS films (Figure 5-10).

The Ra continues to increase, but to a lesser extent after 3 and 4 dips, with a maximum Ra value of 0.71 µm being obtained for the '4 Dip' sample (Figure 5-10).

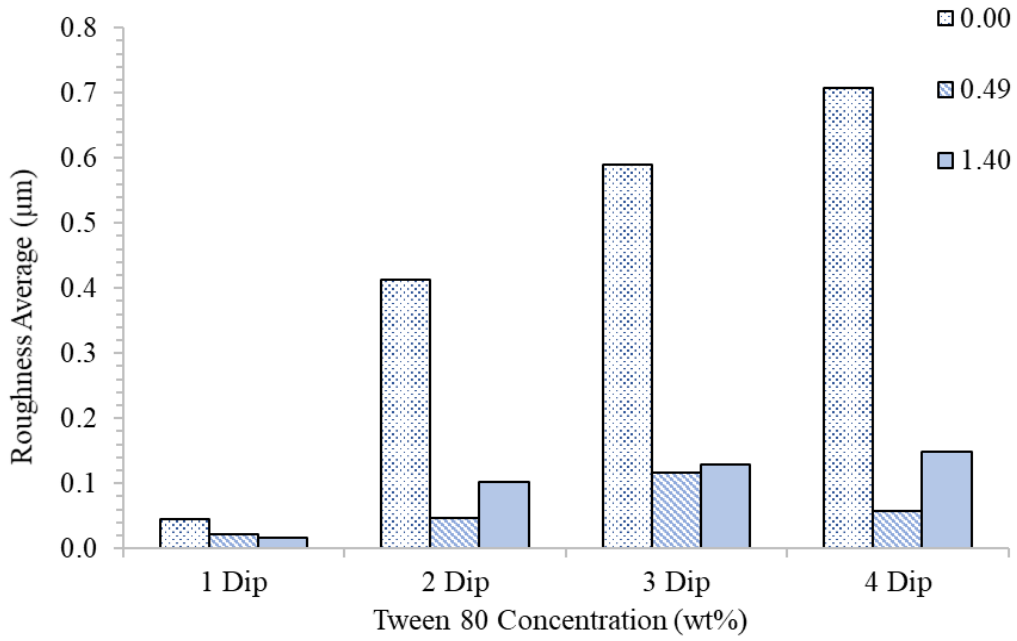

Figure 5-10: Ra (µm) of PEDOT:PSS/Tween 80 films containing 0.00 (spotted), 0.49 (striped) and 1.40 wt% (block colour) surfactant for different dip numbers

The multiple dip method has a noticeable negative impact on the surface quality of the films which could have an adverse effect on an overall application. However, the addition of Tween 80 can significantly mitigate this issue (Figure 5-10), as well as marginally reducing the Ra of the '1 Dip' sample. In the case of 2 layers and above, the lower quantity of surfactant appears to produce the best results giving the lowest Ra regardless of dip number. A similar result was previously seen (section 4.4.4) in which the Ra initially dropped with Tween 80 before increasing at higher concentrations. The surface profiling plots seen in Figure 5-11 for samples containing 1.40 wt% Tween 80 also verify the improved Ra with the presence of the surfactant.

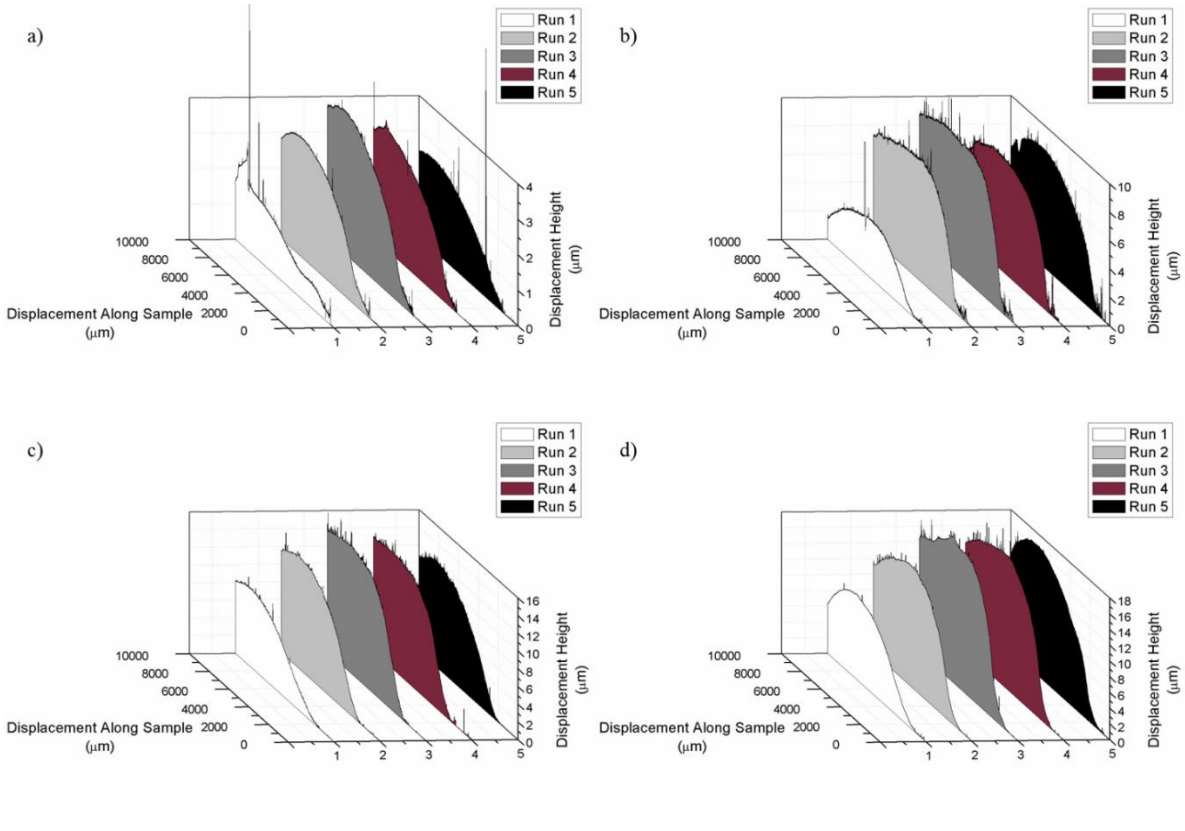

Figure 5-11: Surface profiling of PEDOT:PSS/Tween 80 films containing 1.40 wt% surfactant for a) 1, b) 2, c) 3 and d) 4 dips. Profile shows the displacement height (μm) along the sample with 5 profiling runs being performed on each sample spaced 2 mm apart

The improvement in surface roughness with surfactant can be attributed to an alteration of the surface energy and wettability of the solution. As was discussed in section 4.4.4, Tween 80 reduces the surface tension of PEDOT:PSS solution which leads to better coating during the casting stage.[9,23,24] However, even though this solves the issue of surface quality, the resistivity was shown to improve more significantly with pristine PEDOT:PSS, and after 3 layers the pristine samples were showing better results than those with Tween 80 (section 5.1.1).

Overall, the use of multiple dipping as a method for conductivity enhancement may not be as effective as the sheet resistivity data initially suggests. While more dips cause the resistivity to drop substantially, this not necessarily the case when conductivity is considered. However, this

could not be accurately calculated here due to the multiple layer application and 4-point probe only measuring surface resistivity, which does not allow for accurate conductivity representation. Additionally, this multiple layer method becomes more problematic once film quality is considered as without the presence of surfactant, the roughness increases with each layer. Furthermore, the complexity and increase in time and materials needed to implement this is not ideal for bulk manufacture. Finally, even though it has not been analysed in this study, the increased thickness will reduce the transmission of light through the film.[1,2,5] This is problematic in optoelectronic devices since they require high light transmission in order to function optimally.[1,2,5]

5.2 Methyl Ethyl Ketone (MEK) Solvent Addition to PEDOT:PSS/Tween 80 Solution

The addition of MEK to the PEDOT:PSS/Tween 80 mixture was initially reported by Thompson (2017)[25] as a method to improve the wettability and adherence to polymer substrates. The resistivity of the PEDOT:PSS/Tween 80/MEK system was also analysed showing a decrease in resistivity above a 2 v/v% total addition of surfactant and solvent.[25] However, the effect of solely adding MEK to PEDOT:PSS was not assessed. Furthermore, as a Tween 80/MEK solution was mixed prior to adding to PEDOT:PSS,[25] it was suspected that a large degree of solvent would be lost during this process due to a high evaporation potential.[26] This would bring a degree of uncertainly into the quantities of each addition to PEDOT:PSS. Therefore, this study aims to improve upon the existing findings by adding known quantities of either additive directly to PEDOT:PSS solution. It should be noted that during the stirring stage, solutions containing MEK significantly reduced in volume due to evaporation of the solvent. This brought into question the accuracy to which the concentrations could be quoted. To counteract this, all solutions were mixed in a sealed vial and lid removal time was kept short to

minimise evaporation. Furthermore, the boiling point of MEK is 80 °C,[26,27] meaning it would be completely removed from the film during annealing phases. However, studies have shown that alternative low boiling point additives can still impart changes in the PEDOT:PSS structure despite not remaining in the final film.[4] Throughout this section, all additives were measured by volume and the ratio of MEK to Tween 80 kept at 3:1.[25] To enable comparison with previous results (section 4.4.2), the volume percentages have been converted to weight percentages (wt%) (section 2.2.1). With limitations in mind, the sheet resistivity, and thermal properties of PEDOT:PSS/Tween 80/MEK and PEDOT:PSS/MEK were assessed.

5.2.1 Sheet Resistivity of PEDOT:PSS/Tween 80/MEK

Sheet resistivity was performed to establish whether MEK improved the resistivity of PEDOT:PSS and PEDOT:PSS/Tween 80 (Figure 5-12). The Tween 80 and MEK concentrations was initially kept constant at approximately 0.52 wt% and 1.19 wt%, respectively, and films were drop cast. MEK was found to increase the resistivity of PEDOT:PSS from 1360 to 2030 $\Omega\square^{-1}$ at 1.19 wt%. The same was also seen when MEK was added to PEDOT:PSS/Tween 80 solution with an increase in resistivity from 510 to 910 $\Omega\square^{-1}$.

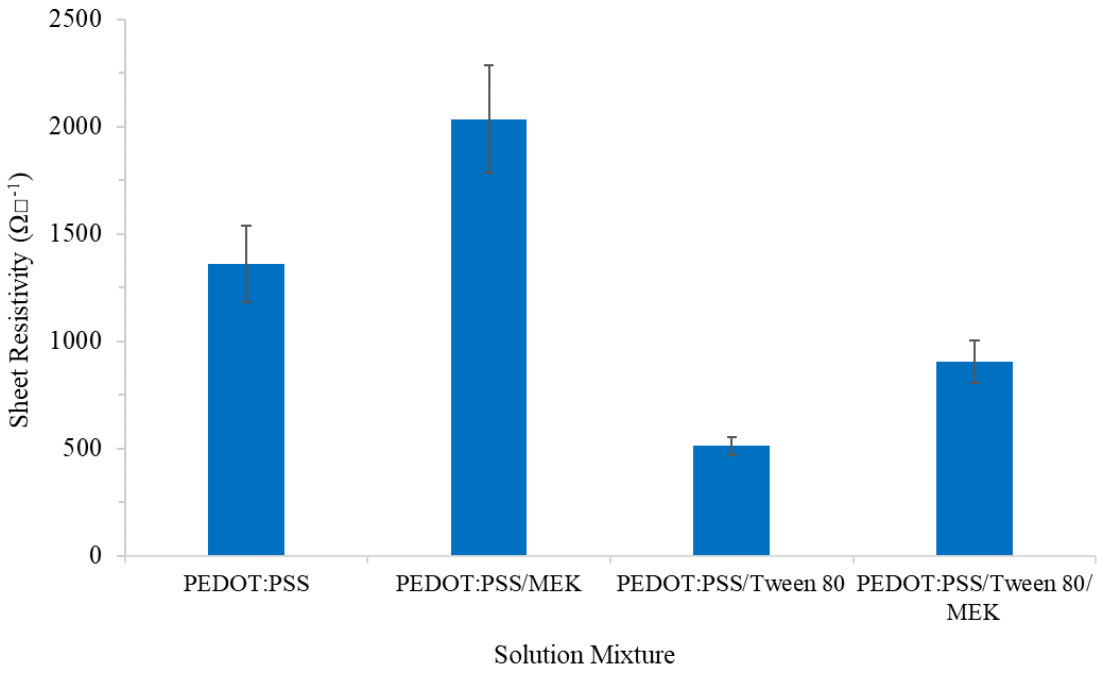

Figure 5-12: Mean sheet resistivity ($\Omega\square^{-1}$) of differing PEDOT:PSS solution mixtures either containing Tween 80, MEK or both. Concentrations of Tween 80 and MEK were approximately 0.52 wt% and 1.19 wt%, respectively. Samples were annealed at 100 °C for 4 hours and left to equilibrate before measurements were taken. Error bars show ± 1 SD

The effect of altering the concentration of Tween 80/MEK to PEDOT:PSS solution (maintaining the 1:3 ratio between surfactant and solvent) was assessed in comparison to the addition of the surfactant alone (Figure 5-13) for drop cast films. The concentration of additives is quoted as the Tween 80 concentration in the total solution. The trends between samples with and without MEK do not vary significantly, with a large resistivity reduction observed until approximately 1 wt% at which point results plateau. These results are similar to data seen previously in this study (section 4.4.2), and in the work conducted by Thompson (2017)[25].

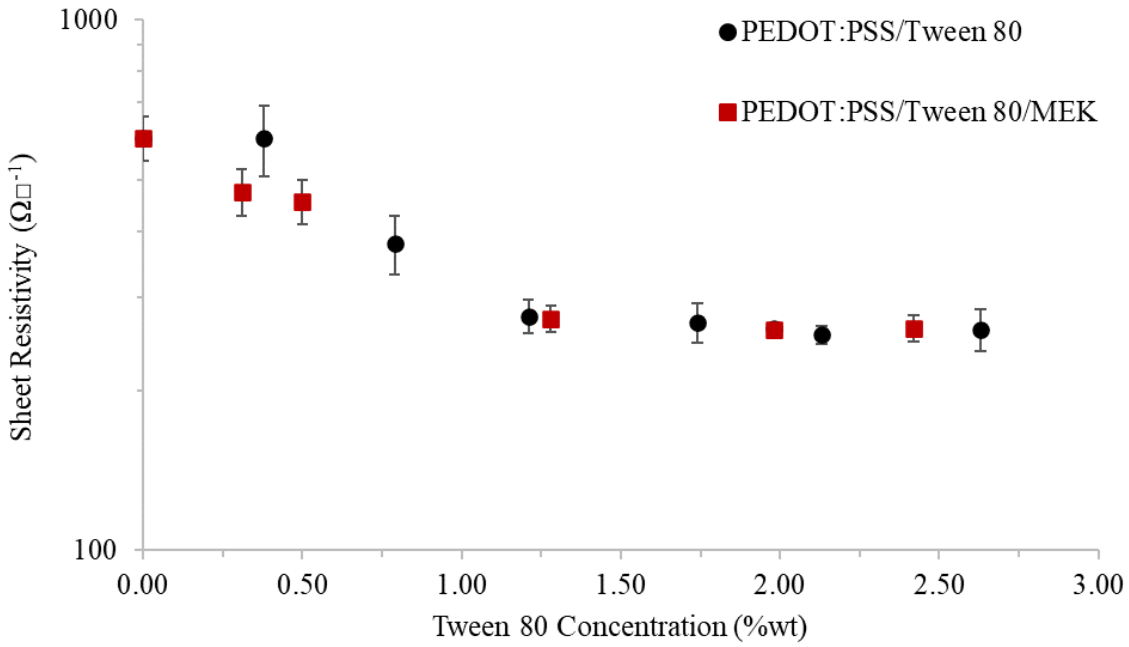

Figure 5-13: Sheet resistivity (Ω□$^{-1}$) of PEDOT:PSS/Tween 80 (black circle) and PEDOT:PSS/Tween 80/MEK (red square) films for varying surfactant concentration (wt%). MEK to Tween 80 ratio was 3:1. Error bars show ± 1 SD

The data presented leads to the conclusion that the addition of MEK to PEDOT:PSS is not beneficial to the conductive properties, regardless of the presence of Tween 80. Furthermore, MEK causes the resistivity to deteriorate when the solvent was added to the PEDOT:PSS with and without the surfactant (Figure 5-12). The addition of Tween 80 causes the interaction between the PEDOT and PSS to be disrupted which leads to the improvement in conductivity (section 4.4.2).[10,11,28-37] It has previously been reported that any addition to PEDOT:PSS requires two or more polar groups to disrupt this bond and increase conductivity.[38] Given that MEK contains only one polar group, the PEDOT – PSS interaction is unlikely to be affected explaining why resistivity does not decrease.[38] Similar accounts to this have been reported with more polar solvents that only contain one polar group, such as methanol.[39,40] However, this does not address why resistivity increases when only MEK is added to PEDOT:PSS. It is possible that the MEK addition dilutes the PEDOT:PSS solution, meaning less conductive material is

deposited and a thinner film is produced. Additionally, MEK has a pH similar to water[41] which, when added to PEDOT:PSS solution, will decrease acidity. In doing so, this could lead to fewer H^+ ion being available, increasing the interaction between the PEDOT and PSS and reducing possibility for chain alignment (section 1.5.2.1 & 1.5.3).[28,42] Even though Tween 80 is likely to be causing a similar effect with regards to pH,[43,44] the overwhelming enhancement effects caused by the disruption of the bonding between the two components nullifies any pH effect.

5.2.2 Thermal and FTIR Analysis

Thermal analysis of PEDOT:PSS/Tween 80/MEK was limited to TGA and samples of PEDOT:PSS/MEK were not tested due to the detrimental effect of the solvent addition to conductivity (section 5.2.1).

TGA of PEDOT:PSS/Tween 80 and PEDOT:PSS/Tween 80/MEK shows the presence of the solvent does not significantly alter the trace (Figure 5-14). The onset of degradation appears at approximately 150 °C for both samples, which is significantly earlier than pristine PEDOT:PSS at 260 °C. There is no noticeable mass loss due to the removal of MEK during TGA since samples were heated to 90 °C during preparation (section 2.4.1.1) which is above the boiling point of MEK.[26,27] The traces of PEDOT:PSS/Tween 80 and PEDOT:PSS/Tween 80/MEK show varying degradation rates around 200 °C. However, this is due to the varying quantities of surfactant in the two samples which has previously been shown to affect TGA measurements (section 4.2.1).

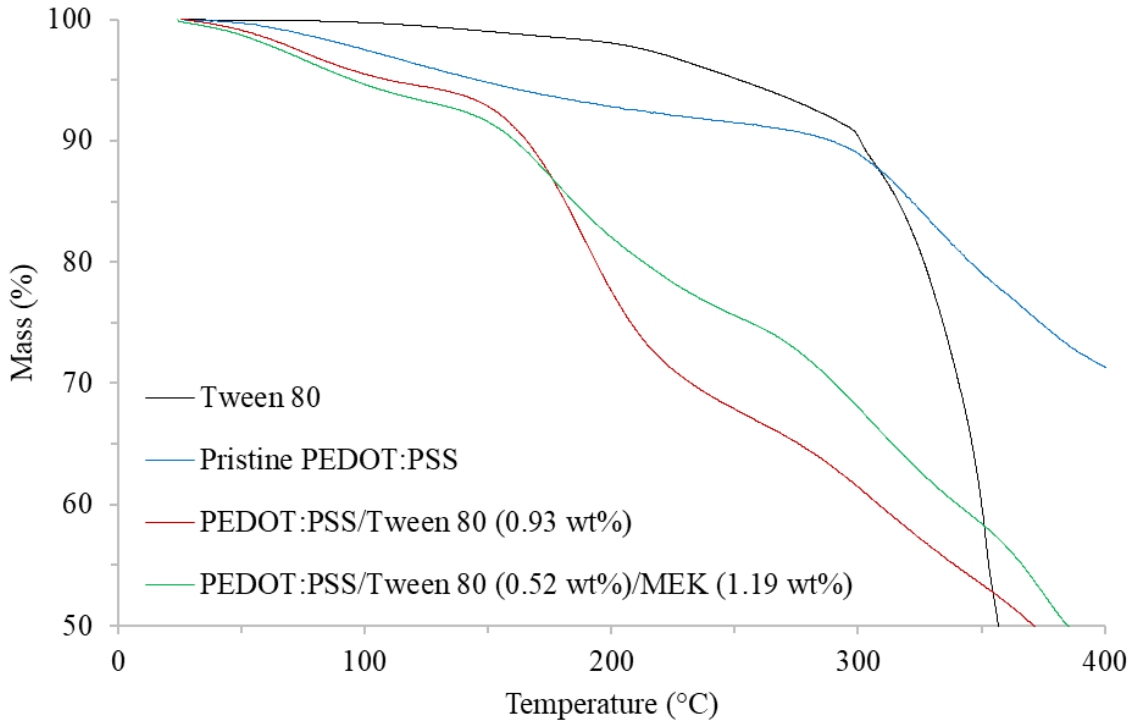

Figure 5-14: TGA trace of Tween 80 (black), pristine PEDOT:PSS (blue), PEDOT:PSS/Tween 80 containing 0.93 wt% surfactant (red) and PEDOT:PSS/Tween 80/MEK containing approximately 0.52 wt% surfactant and 1.19 wt% solvent (green). Samples run from 25 °C to 400 °C at 10 °Cmin^{-1} in air

The FTIR spectra seen in Figure 5-15 shows the comparison of pristine PEDOT:PSS and a PEDOT:PSS/Tween 80/MEK sample containing approximately 0.52 wt% surfactant and 1.19 wt% solvent. There are some slight differences between the two traces, mainly the increase in size of the C-H peaks at 2850 – 2900 cm^{-1} and the broad OH peak at 3100 – 3700 cm^{-1}.[45] The main bonds in MEK are C-H, C-C and C=O, however, C-H and C-C can all be found in both PEDOT:PSS and Tween 80. As previously seen (section 4.2.2), the addition of Tween 80 causes both of these peaks to become more prominent. However, the C=O in MEK is a ketone, unlike the C=O bond in Tween 80 which is an ester. Therefore, a ketone peak would be expected to appear at approximately 1715 cm^{-1} if MEK was present.[45] Since this peak does not appear in the PEDOT:PSS/Tween 80/MEK trace, this shows MEK is not present in the sample. This is likely due to the samples being dried at 110 °C causing the solvent to evaporate.

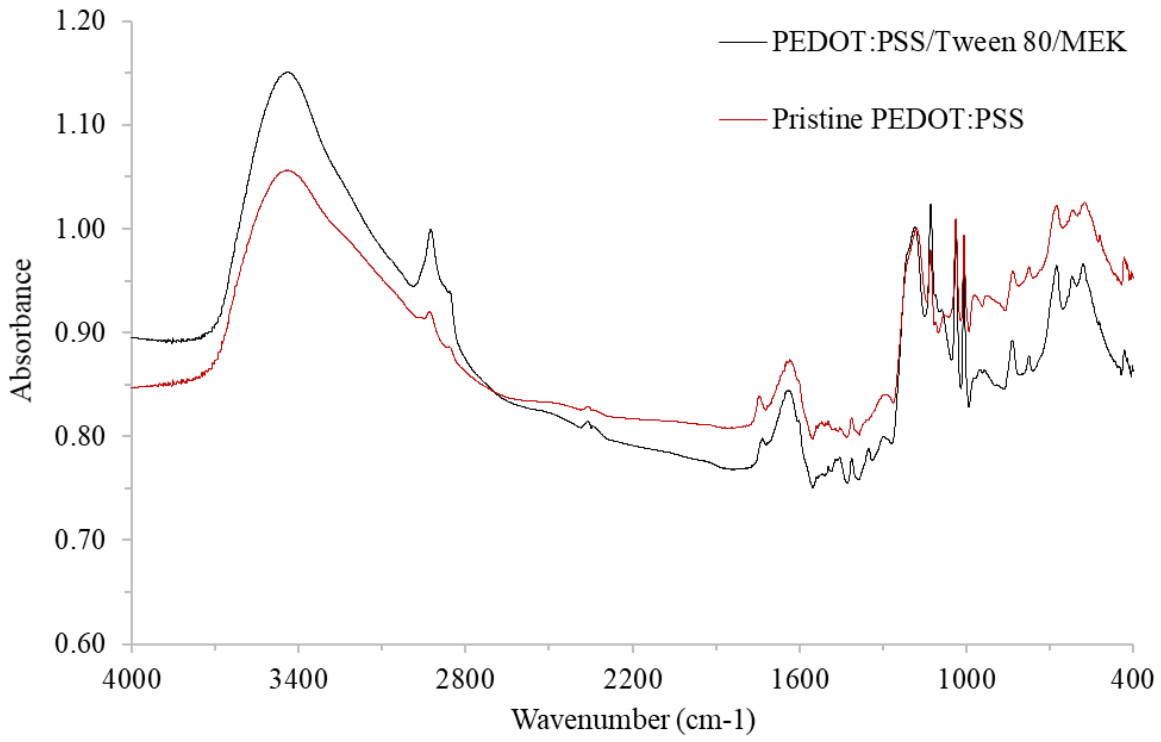

Figure 5-15: FTIR spectra of PEDOT:PSS/Tween 80/MEK (top, black trace) and pristine PEDOT:PSS (bottom, red trace) as comparison to show the effect of MEK within the solution mix. Samples were analysed in transmission by combining with KBr and pressing into discs. A blank KBr disc was used to obtain a background scan

Overall, while the use of MEK has been reported in the literature to improve the wettability of PEDOT:PSS,[25] it is not a good additive to improve conductivity. The low vapor pressure of MEK also caused issues in the accuracy of the measurements due to it evaporating from solution.[26,27] The discussion in this section assumed that the ratio of MEK to Tween 80 was unaltered in PEDOT:PSS solution. However, regardless of careful handling, it is impossible to ensure that no solvent was lost prior to film forming. This alters the ratio of Tween 80 to MEK and, as a result, the true masses of each component added to PEDOT:PSS are uncertain. This volatility and error make MEK unsuitable for use in bulk manufacturing processes.

5.3 Solvent Washing of PEDOT:PSS/Tween 80 Films

The use of solvent washes is a well-established method to improve the conductivity of PEDOT:PSS films,[1,3,9,15,17,38] with the highest conductivity being achieved after washing with concentrated H_2SO_4.[15] Whilst just using a solvent wash has proven beneficial, there have also been studies to show that the combination of chemical addition to PEDOT:PSS solution followed by a solvent wash can further enhance the conductivity of PEDOT:PSS films.[9,18,36,38] This has been shown to be the case when using Triton X-100 surfactant as a pre-treatment.[9,18] Oh, *et al.* (2014)[9] found that the addition of Triton X-100 initially improved conductivity to 100 Scm^{-1}, with further improvement to 350, 650 and 900 Scm^{-1} achieved by washing with butanol, ethanol, or methanol, respectively.[9] In this study, the effect of washing pristine PEDOT:PSS and PEDOT:PSS/Tween 80 films with MEK, ethanol and methanol were assessed. While methanol is a well-established wash solvent, it has not been used alongside the addition of Tween 80. Ethanol and MEK were also tested as less volatile/toxic, more environmentally friendly alternatives to methanol. The sheet resistivity, conductivity, and micro-structure of washed samples were analysed.

5.3.1 Sheet Resistivity

Each of the solvent washes produced an improvement in the film resistivity of pristine PEDOT:PSS but to differing degrees (Figure 5-16). The use of MEK caused a decrease in resistivity from 935 to 400 $\Omega\square^{-1}$ with ethanol and methanol washes lead to significantly larger decreases to 50 and 36 $\Omega\square^{-1}$, respectively.

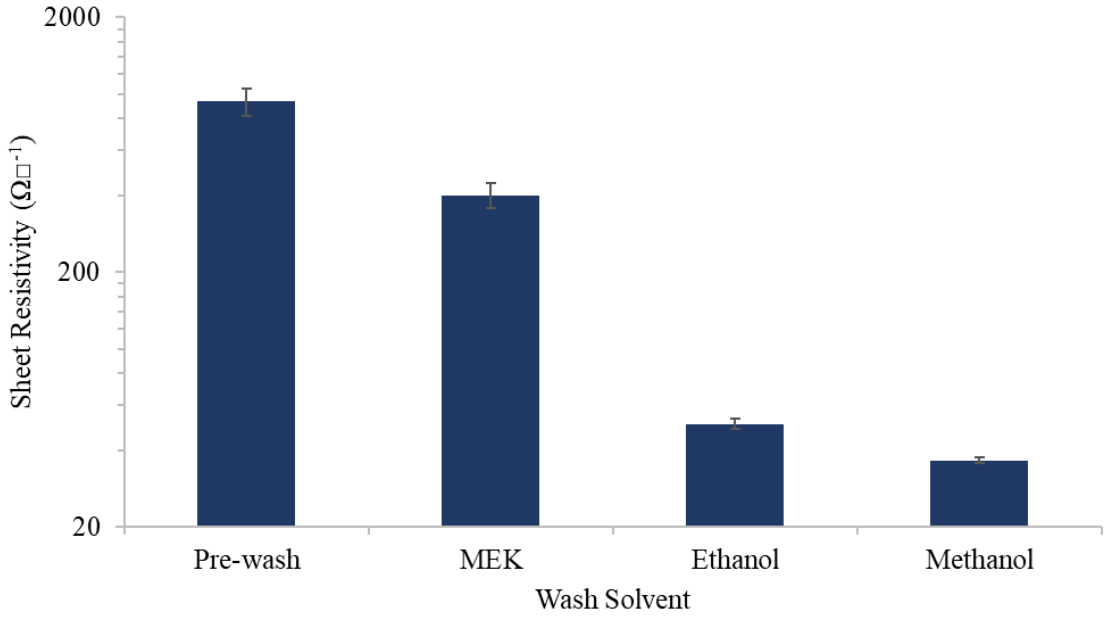

Figure 5-16: Sheet resistivity (Ω□$^{-1}$) of pristine PEDOT:PSS films with pre-wash and after washing with MEK, ethanol and methanol. Error bars show ±1 SD

The decrease in sheet resistivity of pristine PEDOT:PSS films that have been washed with different solvents follows an expected trend. It has previously been seen in the literature that washing with methanol improves the conductivity more than ethanol.[9,12] It was also expected that MEK would not improve the conductivity as much as ethanol or methanol due to it having a lower polarity.[39,40] The reason for conductivity enhancement after a solvent wash is mainly linked to the removal of insulating excess PSS from the PEDOT:PSS film, reducing electron hopping distance between PEDOT-rich areas (section 1.5.3).[1,8,15,28,36,46-48] Furthermore, it has been suggested that if bound PSS is removed from PEDOT, then the PEDOT will more freely align upon the second annealing (after the wash has been performed) at a nano scale, providing better conducting pathways.[15] However, this is less likely to be the case with the washes used in this study since interference with the ionic bond between PEDOT and PSS is unlikely, due to the solvents only containing one polar group.[38]

Using a similar technique to Alemu, *et al.* (2012)[1], the solvents used to wash the PEDOT:PSS/Tween 80 films were analysed by FTIR to detect PSS removal (Figure 5-17). In each case, a small peak or shoulder appears in the region of 1600 to 1700 cm^{-1} consistent with the C=C in the phenyl structure of PSS found at 1624 cm^{-1}.[45,49-51] Although MEK contains a peak at approximately 1725 cm^{-1} representing the carbonyl group,[27,45] neither ethanol or methanol show peaks in this region.[45,52,53] However, these solutions were used to wash all PEDOT:PSS/Tween 80 samples, therefore, it is possible that the surfactant could also have been washed out of the film. This was seen within the literature whereby Triton X-100 surfactant was removed by methanol wash as well as excess PSS.[3,18] However, while the C=O group in Tween 80 would show at 1732 cm^{-1},[45] the peak that appears in the solvent washes is closer to 1624 cm^{-1} suggesting only PSS is being removed.

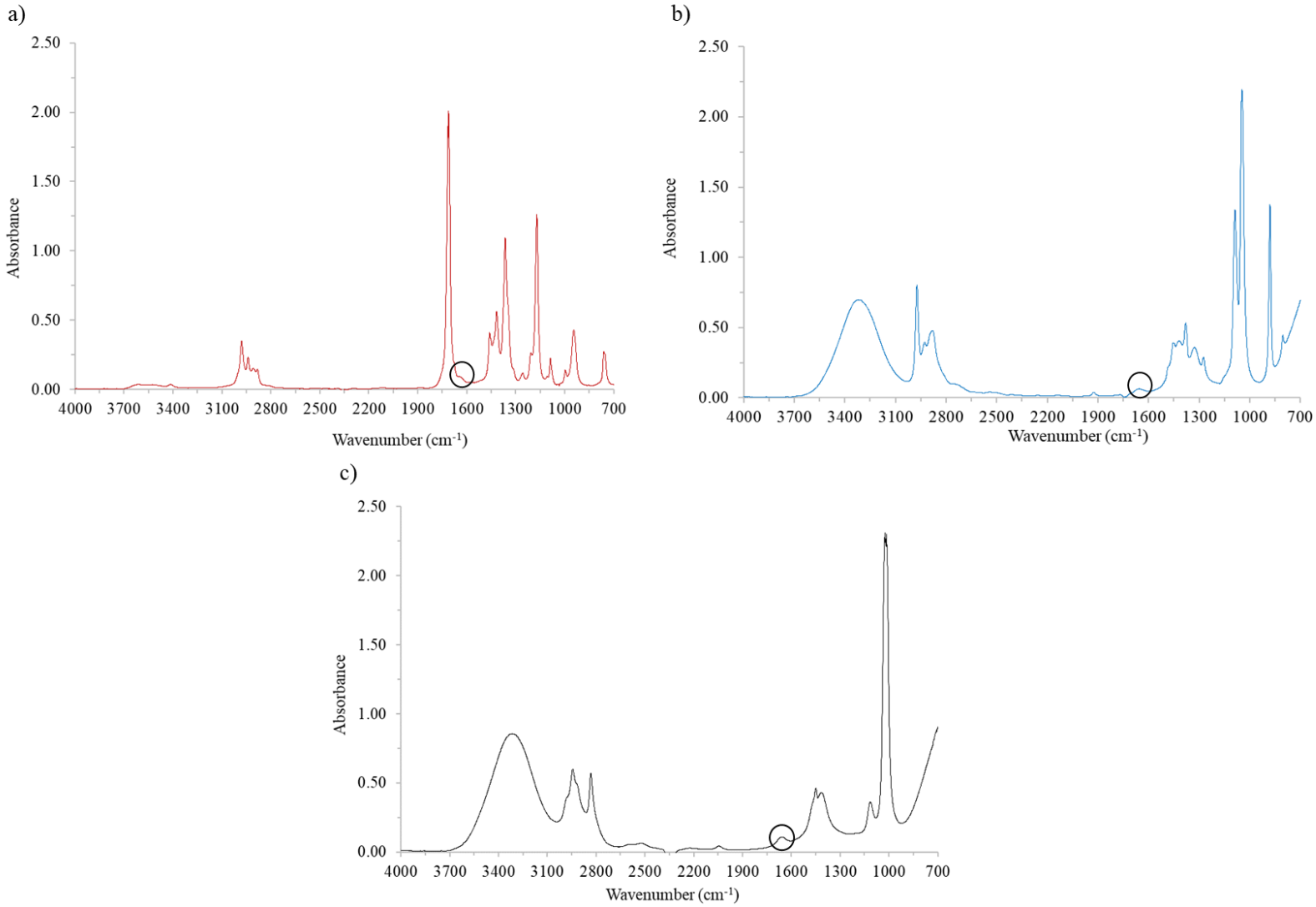

Figure 5-17: FTIR spectra of a) MEK, b) ethanol & c) methanol solvents used to wash PEDOT:PSS/Tween 80 films. Black rings highlight contamination from washing

The effect of solvent washing on the resistivity of PEDOT:PSS/Tween 80 films with differing surfactant concentrations can be seen in Figure 5-18 & 5-19. The use of MEK shows a noticeable difference to the pre-wash samples at surfactant concentrations between 0.00 – 0.50 wt% with no effect at higher concentrations of Tween 80. In the case of ethanol and methanol, both solvent washes give the lowest results when no Tween 80 is present (Figure 5-19). The addition of the surfactant causes the sheet resistivity to decrease less for methanol and ethanol washes with results plateau above approximately 0.50 wt%. At 3.46 wt% surfactant the sheet resistivity measured after washing with methanol was 49 $\Omega\square^{-1}$ which is 13 $\Omega\square^{-1}$ greater than the pristine PEDOT:PSS methanol washed films. There is a trend across the different solvents with methanol producing the lowest sheet resistivity across all Tween 80 concentrations, followed by ethanol. However, the difference in sheet resistivity becomes much smaller at higher surfactant concentrations, with a difference of only 14 $\Omega\square^{-1}$ between methanol and MEK at 3.46 wt% Tween 80.

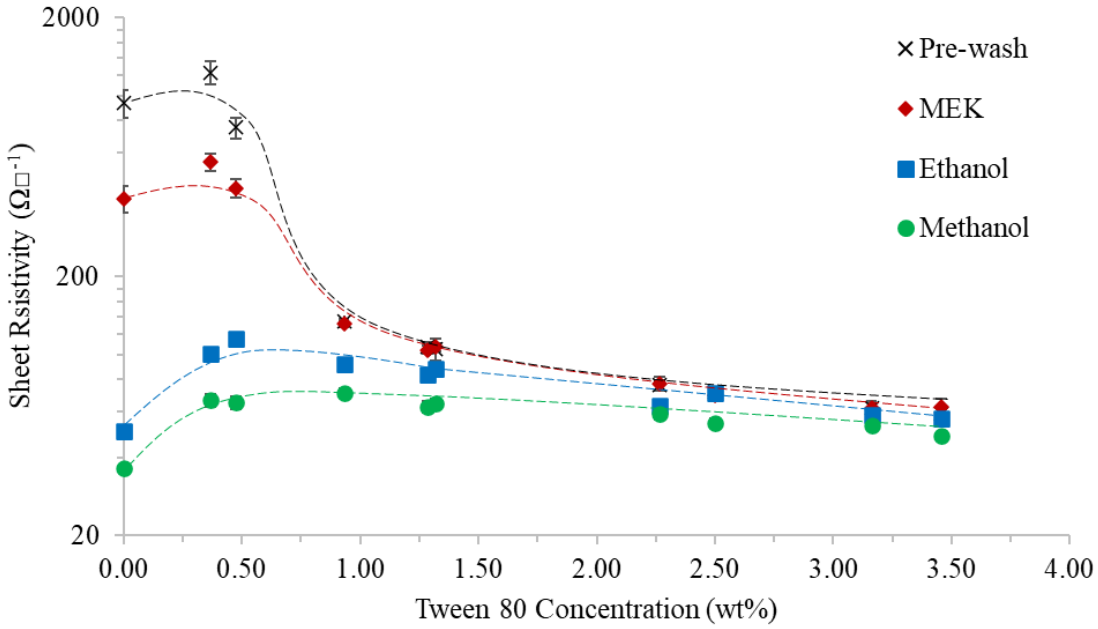

Figure 5-18: Sheet resistivity (Ω□$^{-1}$) of PEDOT:PSS/Tween 80 films for varying surfactant concentration (wt%) pre-wash (black cross) and after washing with MEK (red diamond), ethanol (blue square) and methanol (green circle). Error bars show ±1 SD. Dotted guidelines present to show trend of the data

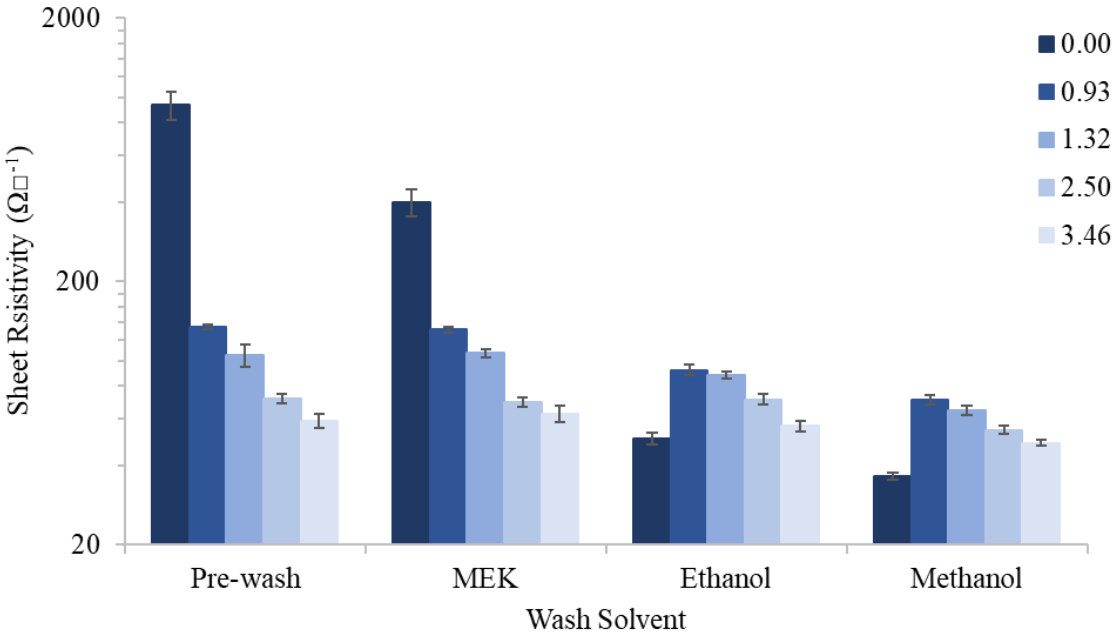

Figure 5-19: Sheet resistivity (Ω□$^{-1}$) of PEDOT:PSS/Tween 80 films after washing with different solvents for different surfactant concentrations (wt%). Concentrations increase from left to right and quantities are indicated in the legend. Error bars show ±1 SD

A similar reverse trend can be seen in the conductivity data (Figure 5-20). For pristine PEDOT:PSS, MEK gives the lowest conductivity of 8.06 Scm^{-1} with methanol showing the highest of 64.38 Scm^{-1}. When Tween 80 is added, the MEK wash shows a drop in conductivity at lower concentrations, followed by an increase that plateaus after 0.93 wt%. Ethanol and methanol both show higher conductivities when no surfactant, with conductivity improvement being smaller as the Tween 80 concentration increases. The methanol wash for a sample containing 0.93 wt% surfactant providing the highest calculated conductivity of 74.42 Scm^{-1}. However, this result does not appear to follow the expected trend, so it is likely to be an anomalous result. This could have been caused by a difference or error in thickness measurements which would be reflected when conductivity is calculated. It should also be noted that the use of solvent washes did not show any significant difference in the thickness or roughness of the films and the trend of increasing thickness with increasing surfactant concentration was also unaffected (section 4.4.1).

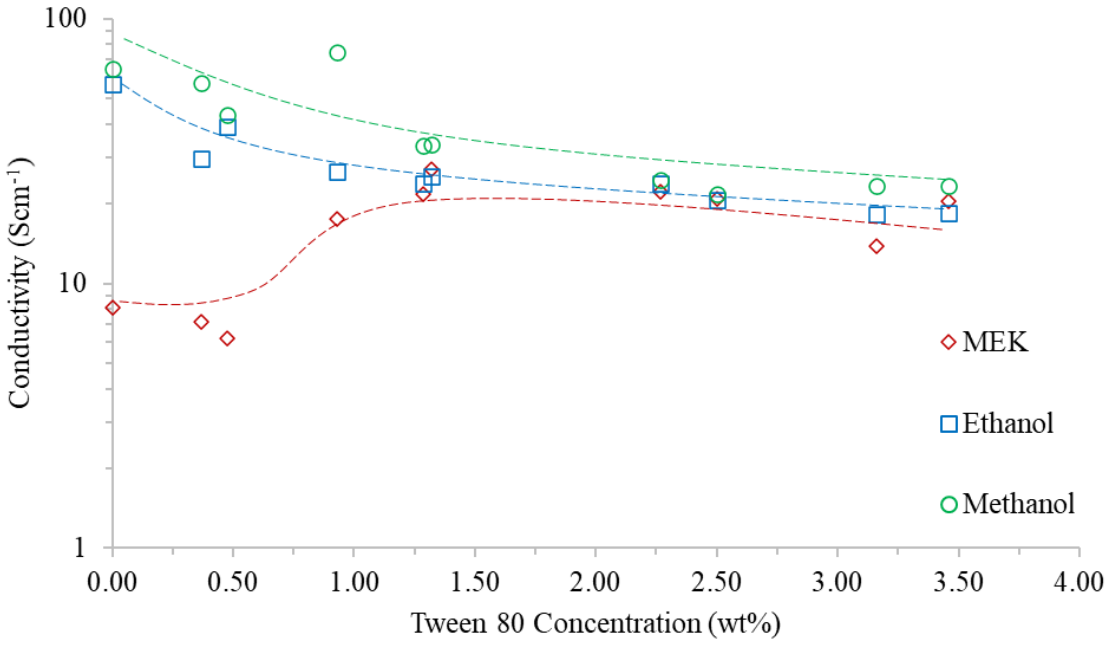

Figure 5-20: Conductivity (Scm^{-1}) of PEDOT:PSS/Tween 80 films for varying surfactant concentration (wt%) after washing with MEK (red diamond), Ethanol (blue square) and methanol (green circle). Dotted guidelines present to show trend of the data

It has previously been seen that the use of the surfactant Triton X-100 followed by a solvent wash improves the conductivity by a greater extent than washing pristine PEDOT:PSS.[3,18] This was attributed to the surfactant causing PEDOT – surfactant and PSS – surfactant complexes. During washing, the excess PSS, excess surfactant, and PSS – surfactant are thought to all be removed from the film, with the presence of the surfactant aiding in PSS removal.[18] The film then largely comprises of PEDOT – surfactant complex which are structurally dominated by the PEDOT chains.[18] However, the same trend does not occur with Tween 80 (Figure 5-18 & 5-19) and instead it reduces the effect of solvent washing with methanol and ethanol. This could be due to Tween 80 having a higher Mw (1310 $gmol^{-1}$) and larger repeat unit compared to Triton X-100 (625 $gmol^{-1}$),[54] reducing the solubility in the solvents used.[55] This is confirmed by the FTIR data in which no Tween 80 is present in the solvents used for washing (Figure 5-17). When bonded to the PSS, Tween 80 could therefore act as a barrier to the

polymer being removed from the film during washing. The Mw of Tween 80 could also affect the mobility of the PEDOT chains to which it is bonded.[56] Therefore, once the excess PSS has been removed, the remaining PEDOT – surfactant complex might not be able to re-align as freely during the post-wash annealing stage. This would potentially explain why at higher Tween 80 concentrations, the measured resistivity for different solvent washes is very similar since the present of the surfactant will dominate the PEDOT chain alignment.

5.3.2 Structural Analysis

5.3.2.1 X-Ray Diffraction (XRD)

The XRD data in Figure 5-21 shows the effect of differing solvent washes on pristine PEDOT:PSS films. It can be seen that all three washes give identical traces with broad peaks at 18 and 26 ° typical of PEDOT:PSS.[5,13-18] Unlike with the addition of Tween 80 (section 4.4.5.2), no sharp peaks appear after solvent washing. This is indicative that a wash alone does not cause chain alignment suggesting that the primary improvement in the conductivity is due to the removal of PSS.[5,13-18]

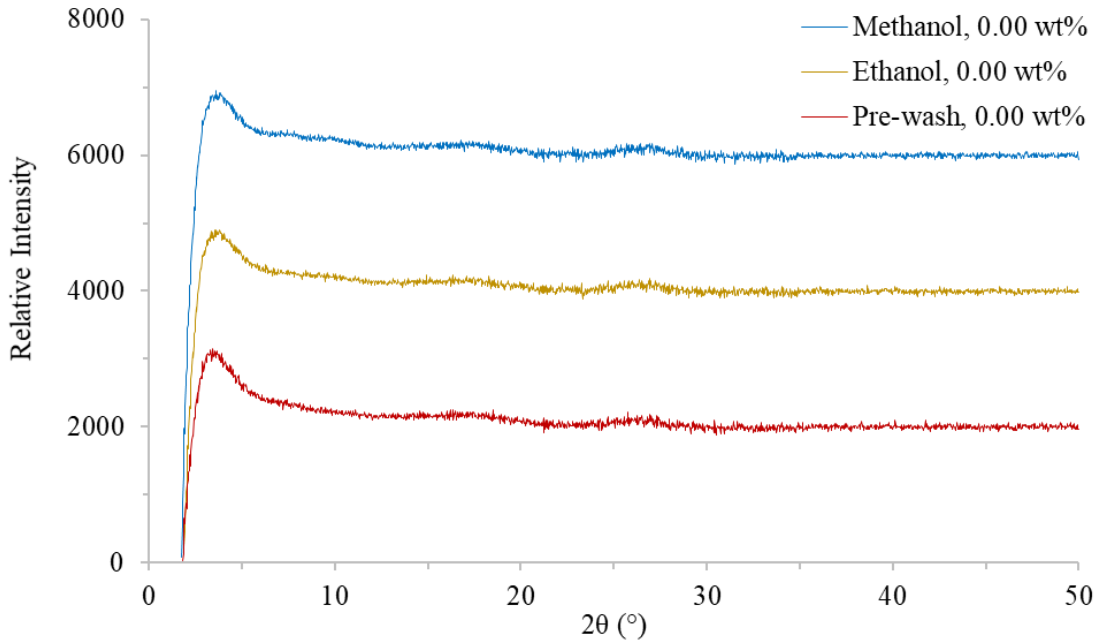

Figure 5-21: XRD traces showing the effect of different solvent washes (pre-wash at the bottom, methanol at the top) on the diffraction pattern of pristine PEDOT:PSS films. Baseline of glass substrate was removed

As has been highlighted before (section 4.4.5.2), the addition of Tween 80 causes the appearance of peaks with the main two at 2.3 and 6.8 °. Both of these peaks can be clearly seen in the pre-wash sample when 1.32 wt% surfactant is present (Figure 5-22). However, when the sample was subsequently washed with methanol, they disappear with only the peaks at 18 and 26 °, associated with the disordered nature of PEDOT:PSS, remaining.

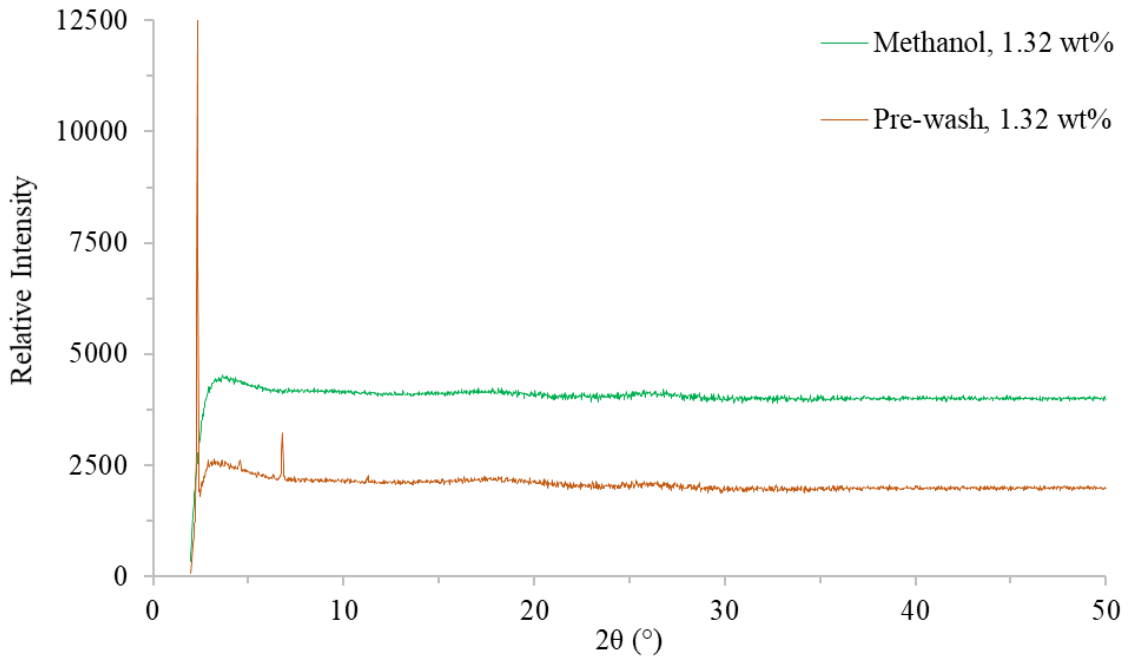

Figure 5-22: XRD traces showing the effect of a methanol wash (pre-wash at the bottom, methanol at the top) on the diffraction pattern of PEDOT:PSS/Tween 80 films with a surfactant concentration of 1.32 wt%. Baseline of glass substrate was removed

It is known that the use of methanol as a solvent wash treatment will primarily remove PSS from a PEDOT:PSS film, as shown in the FTIR analysis (Figure 5-17).[1,3,17] Therefore, the disappearance of the sharp peaks after methanol washing suggests that the primary orientation caused by Tween 80 must be within the excess PSS regions. This could come from induced segregation triggered by surfactant addition[11,36,37] allowing larger areas of PSS to align without being disrupted by PEDOT. This also shows that the polymer bonded to the surfactant is not in an ordered state, indicating the reduction in chain mobility caused by the presence of the Tween 80.

5.3.2.2 Raman

The Raman spectra of pristine PEDOT:PSS remains unchanged after solvent washing (Figure 5-23) with similar peaks appearing at 1600 and 1460 cm^{-1} and a shoulder at 1360 cm^{-1} (section 4.4.5.3). This shows that washing does not induce any noticeable benzoid/quinoid change, nor is there a noticeable reduction in the 1360 cm^{-1} shoulder, associated with the SO_2 group in PSS.[22]

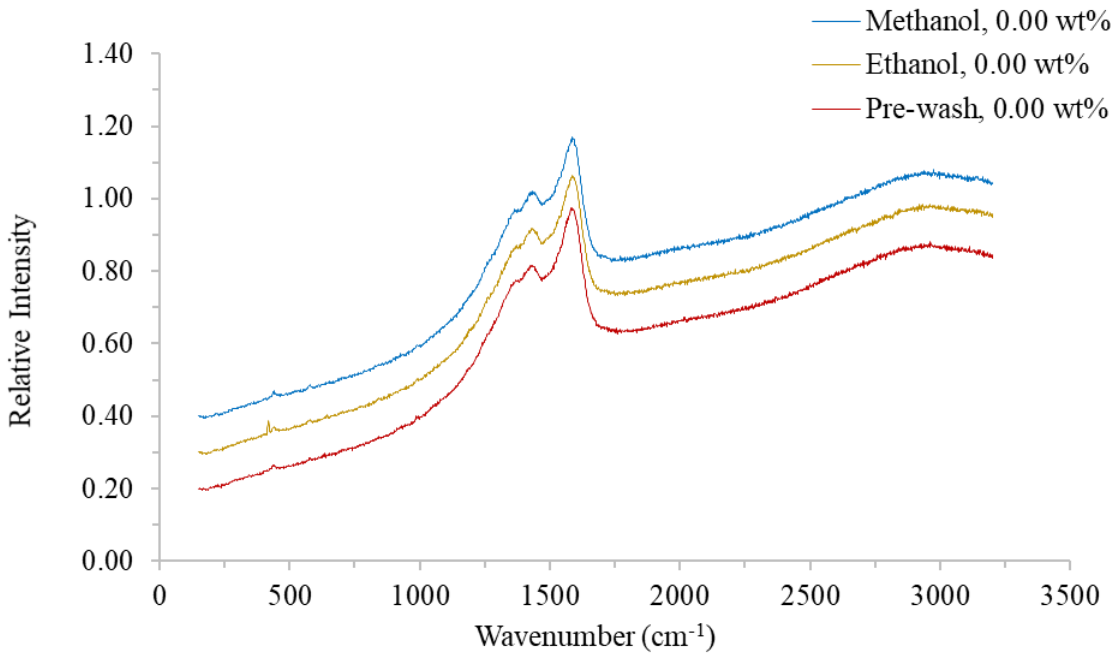

Figure 5-23: Raman spectra of pristine PEDOT:PSS (bottom trace,) and PEDOT:PSS films after methanol and ethanol solvent washes

Similarly, the same is true for PEDOT:PSS/Tween 80 films (Figure 5-24) consistent with the literature that PSS removal is undetected by Raman.[15,17,18]

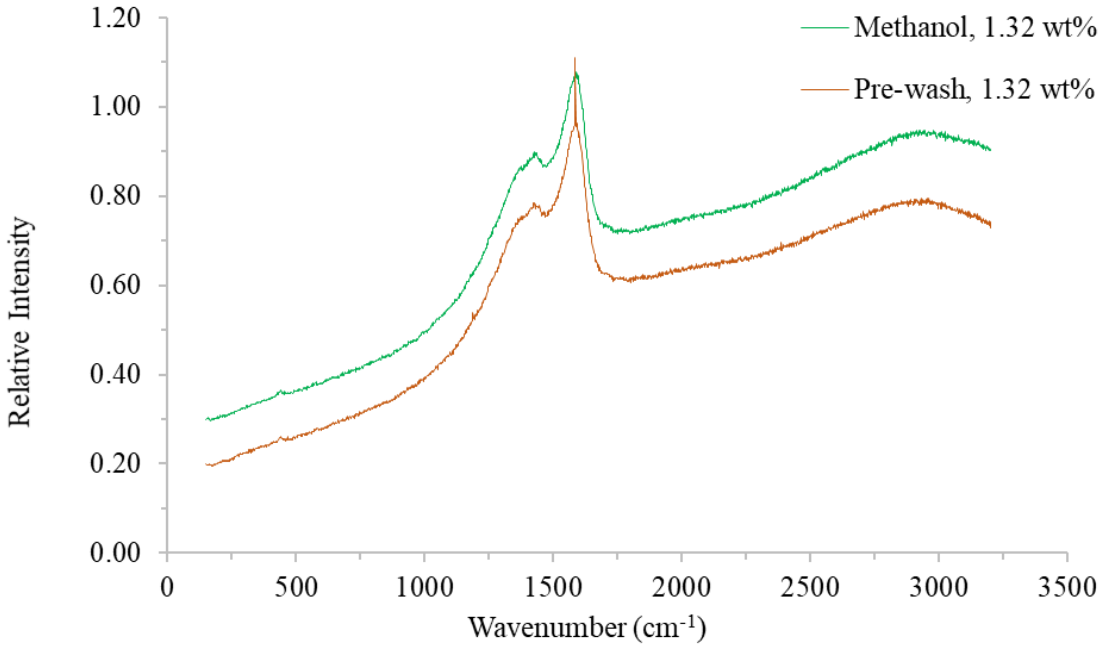

Figure 5-24: Raman spectra of glass (bottom trace) and PEDOT:PSS/Tween 80 films, containing 1.32 wt% surfactant, with and without a methanol wash (methanol wash being the top trace)

5.4 Conclusion

This chapter analyses the use of additional conductivity enhancement methods for PEDOT:PSS, with and without Tween 80. This included the use of multiple dip casting, the addition of MEK to PEDOT:PSS solution, and solvent washes with MEK, ethanol and methanol.

It was shown that sheet resistivity for multiple dip cast pristine PEDOT:PSS films decreased with increasing dip number. This initially appeared to provide a better method to reduce resistivity compared to the addition of Tween 80. It was also found that the addition of the surfactant caused the sheet resistivity to be worse when more than 3 layers were applied. Structural analysis showed no signs of further improvement in either chain alignment or any evidence of a benzoid/quinoid change of the resonance structure. Despite this, three theories were suggested to explain the decrease in sheet resistivity as follows: reduced PSS in subsurface

layers due to removal by water in PEDOT:PSS solution; multiple annealing stages; increase in PEDOT or decrease in PSS deposition when interacting with an existing PEDOT:PSS layer. Of these, the latter was considered the most likely to cause a major effect in sheet resistivity, although a combination of effects may have occurred. However, it was deemed that conductivity could not be accurately calculated due to the layering effect and the 4-point probe only measuring the film surface. It was also shown that surface roughness increased (indicating reducing film quality) with each layer of pristine PEDOT:PSS applied. This issue was counteracted with the presence of Tween 80, however, resistivity was negatively impacted. Finally, the practically of this method on a bulk manufacturing scale was questioned since applying multiple layers would increase time and processing costs.

The addition of MEK solvent to PEDOT:PSS in conjunction with Tween 80 showed no further improvement to the sheet resistivity of PEDOT:PSS. Furthermore, when added to PEDOT:PSS without the surfactant present, MEK increased sheet resistivity. It was identified that the evaporation potential of the solvent meant it would unlikely remain in the film, especially after the annealing stage. Because of this, the accuracy of the Tween 80 concentrations quoted for any sample containing MEK becomes limited. Whilst the use of MEK has previously been shown to improve the wettability of PEDOT:PSS solution,[25] it is not suitable as an additive for conductivity enhancement or for use on a bulk manufacturing scale.

Finally, the effect of differing solvent washes on PEDOT:PSS/Tween 80 films was assessed. The results showed that pristine PEDOT:PSS films washed with methanol gave the lowest sheet resistivity compared to ethanol and MEK washes. When the concentration of Tween 80 was varied, it was seen that only MEK showed a similar trend to the pre-wash samples. For ethanol and methanol, the presence of the surfactant reduced the improvement attained by the washes. Conductivity showed a similar trend with a methanol wash of pristine PEDOT:PSS giving the

highest conductivity recorded in this study at 64.38 Scm^{-1}. This is significantly higher than the best conductivity of an un-washed PEDOT:PSS/Tween 80 film containing 1.40 wt% surfactant which gave 26.80 Scm^{-1}. This improvement was linked to the removal of PSS from the film through FTIR analysis, where the addition of Tween 80 presented a barrier to PSS removal. It was clear from the XRD data that there was no chain alignment occurring in the pristine PEDOT:PSS samples after washing, and the Raman data showed no evidence of a benzoid to quinoid shift. However, the sharp peaks in the XRD data, caused by the addition of Tween 80, disappeared after washing with methanol. This suggests the alignment being detected is the long range orientation of PSS chains. Whilst this may imply that there is no alignment of the PEDOT chains, it could be that due to a shorter chain length this alignment is not detected by XRD. The main reason for reduced improvement in the wash samples containing Tween 80 was attributed to a higher Mw than other surfactants seen in the literature (e.g., Triton X-100). This reduces the solubility of Tween 80 in the solvents, meaning less is removed from the film during washing. This was also confirmed by FTIR analysis in which no evidence of the surfactant was seen in the wash solvents.

Overall, the use of multiple dip casting or MEK addition are less effective conductivity enhancement methods than adding Tween 80. However, rather than having a cumulative effect, the presence of the surfactant becomes a hindrance when washing with methanol is implemented compared to with pristine PEDOT:PSS. This chapter has shown that even though PEDOT:PSS conductivity is improved with the addition of Tween 80, it can be increased more by solely washing with methanol. However, this method is less desirable when considering the volatility, extra time and cost in processing, and the negative environmental impacts of using methanol on a bulk manufacturing scale.

5.5 References

1. Alemu, D., Wei, H.-y., Ho, K.-c. & Chu, C.-w. 2012. Highly conductive PEDOT:PSS electrode by simple film treatment with methanol for ITO-free polymer solar cells. *Energy Environ. Sci.,* 5**,** 9662-9671.
2. Mengistie, D. A., Ibrahem, M. A., Wang, P.-C. & Chu, C.-W. 2014. Highly conductive PEDOT:PSS treated with formic acid for ITO-free polymer solar cells. *ACS applied materials & interfaces,* 6**,** 2292-2299.
3. Kim, S., Cho, S., Lee, S. J., Lee, G., Kong, M., Moon, S., Myoung, J.-M. & Jeong, U. 2017. Boosting up the electrical performance of low-grade PEDOT:PSS by optimizing non-ionic surfactants. *Nanoscale,* 9**,** 16079-16085.
4. Kim, Y. H., Sachse, C., Machala, M. L., May, C., Müller-Meskamp, L. & Leo, K. 2011. Highly Conductive PEDOT:PSS Electrode with Optimized Solvent and Thermal Post-Treatment for ITO-Free Organic Solar Cells. *Advanced Functional Materials,* 21**,** 1076-1081.
5. Martin, B. D., Nikolov, N., Pollack, S. K., Saprigin, A., Shashidhar, R., Zhang, F. & Heiney, P. A. 2004. Hydroxylated secondary dopants for surface resistance enhancement in transparent poly(3,4- ethylenedioxythiophene)– poly(styrenesulfonate) thin films. *Synthetic Metals,* 142**,** 187-193.
6. Yoshioka, Y. & Jabbour, G. 2006. Desktop inkjet printer as a tool to print conducting polymers. *Synth. Met.,* 156**,** 779-783.
7. Miccoli, I., Edler, F., Pfnur, H. & Tegenkamp, C. 2015. The 100th anniversary of the four-point probe technique: the role of probe geometries in isotropic and anisotropic systems. *Journal of Physics-Condensed Matter,* 27.
8. Kirchmeyer, S., Reuter, K. & Simpson, J. 2007. Poly(3,4-ethylene dioxythiophene) scientific importance, remarkable properties, and applications. *In:* Skotheim, T. & Reynolds, J. (eds.) *Handbook of conducting polymers.* 3rd ed. Boca Raton, London and New York: CRC press.
9. Oh, J. Y., Shin, M., Lee, J. B., Ahn, J. H., Baik, H. K. & Jeong, U. 2014. Effect of PEDOT nanofibril networks on the conductivity, flexibility, and coatability of PEDOT:PSS films. *ACS Applied Materials and Interfaces,* 6**,** 6954-6961.
10. Shi, H., Liu, C., Jiang, Q. & Xu, J. 2015. Effective Approaches to Improve the Electrical Conductivity of PEDOT:PSS: A Review. *Advanced Electronic Materials,* 1**,** 1-16.
11. Yu, Z., Xia, Y., Du, D. & Ouyang, J. 2016. PEDOT:PSS Films with Metallic Conductivity through a Treatment with Common Organic Solutions of Organic Salts and Their Application as a Transparent Electrode of Polymer Solar Cells. *ACS Appl. Mater. Interfaces,* 8**,** 11629-11638.
12. Takano, T., Masunaga, H., Fujiwara, A., Okuzaki, H. & Sasaki, T. 2012. PEDOT nanocrystal in highly conductive PEDOT:PSS polymer films. *Macromolecules,* 45**,** 3859-3865.
13. Giuri, A., Masi, S., Colella, S., Listorti, A., Rizzo, A., Kovtun, A., Dell'Elce, S., Liscio, A. & Corcione, C. E. 2017. Rheological and physical characterization of PEDOT:PSS/Graphine Oxide nanocomposites for perovskite solar cells. *Polymer Engineering & Science,* 57**,** 546-552.
14. Horikawa, M., Fujiki, T., Shirosaki, T., Ryu, N., Sakurai, H., Nagaoka, S. & Ihara, H. 2015. The development of a highly conductive PEDOT system by doping with partially crystalline sulfated cellulose and its electric conductivity. *J. Mater. Chem. C,* 3**,** 8881-8887.
15. Kim, N., Kee, S., Lee, S. H., Lee, B. H., Kahng, Y. H., Jo, Y. R., Kim, B. J. & Lee, K. 2014. Highly Conductive PEDOT:PSS Nanofibrils Induced by Solution- Processed Crystallization. *Advanced Materials,* 26**,** 2268-2272.

16. Kim, N., Lee, B. H., Choi, D., Kim, G., Kim, H., Kim, J.-R., Lee, J., Kahng, Y. H. & Lee, K. 2012. Role of interchain coupling in the metallic state of conducting polymers. *Physics Review Letters,* 109**,** 106405-106405.
17. Wang, X., Kyaw, A. K. K., Yin, C., Wang, F., Zhu, Q., Tang, T., Yee, P. I. & Xu, J. 2018. Enhancement of thermoelectric performance of PEDOT:PSS films by post-treatment with a superacid. *RSC Adv.,* 8**,** 18334-18340.
18. Yoon, S. S. & Khang, D. 2016. Roles of Nonionic Surfactant Additives in PEDOT:PSS Thin Films. *J. Phys. Chem. C,* 120**,** 29525-29532.
19. Cullity, B. D. 1956. *Elements of x-ray diffraction,* Reading, Mass. ; London, Addison-Wesley Publishing Company.
20. Murthy, N. S. 2016. X-ray Diffraction from Polymers. *In:* Guo, Q. (ed.) *Polymer Morphology: Principles, Characterization, and Processing.* Hoboken, NJ, USA: John Wiley & Sons, Inc.
21. Murthy, N. S. & Minor, H. 1995. Analysis of poorly crystallized polymers using resolution enhanced X-ray diffraction scans. *Polymer,* 36**,** 2499-2504.
22. Lambert, J. B. 1987. *Introduction to Organic Spectroscopy,* New York, USA, Macmillan.
23. Kommeren, S., Coenen, M. J. J., Eggenhuisen, T. M., Slaats, T. W. L., Gorter, H. & Groen, P. 2018. Combining solvents and surfactants for inkjet printing PEDOT:PSS on P3HT/PCBM in organic solar cells. *Organic Electronics,* 61**,** 282-288.
24. Hoath, S. D., Hsiao, W.-K., Martin, G. D., Jung, S., Butler, S. A., Morrison, N. F., Harlen, O. G., Yang, L. S., Bain, C. D. & Hutchings, I. M. 2015. Oscillations of aqueous PEDOT:PSS fluid droplets and the properties of complex fluids in drop-on-demand inkjet printing. *Journal of Non-Newtonian Fluid Mechanics,* 223**,** 28-36.
25. Thompson, B. T. 2017. *Enhancing the conductivity of PEDOT:PSS on bulk substrates.* Doctor of Philosophy, University of Warwick.
26. Sigma-Aldrich 2018. Product specification: 2-Butanone.
27. Chu, P. M., Guenther, F. R., Rhoderick, G. C. & Lafferty, W. J. 1998. *National Institute of Standards and Technology Chemistry WebBook: 2-Butanone* [Online]. Available: https://webbook.nist.gov/cgi/cbook.cgi?ID=78-93-3&Type=IR-SPEC&Index=QUANT-IR,0 [Accessed 07/10/21].
28. Aleshin, A. N., Williams, S. R. & Heeger, A. J. 1998. Transport properties of poly(3,4-ethylenedioxythiophene)/ poly(styrenesulfonate). *Synthetic Metals,* 94**,** 173-177.
29. Dimitriev, O. P., Piryatinski, Y. P. & Pud, A. A. 2011. Evidence of the controlled interaction between PEDOT and PSS in the PEDOT:PSS complex via concentration changes of the complex solution. *The Journal of Physical Chemistry. B,* 115**,** 1357.
30. Elschner, A., Kirchmeyer, S., Lövenich, W., Merker, U. & Reuter, K. 2011. *PEDOT; principals and applications of an intrinsically conductive polymer,* CRC Press.
31. Ouyang, J. 2013. "Secondary doping" methods to significantly enhance the conductivity of PEDOT:PSS for its application as transparent electrode of optoelectronic devices. *Displays,* 34**,** 423-436.
32. Po, R., Carbonera, C., Bernardi, A., Tinti, F. & Camaioni, N. 2012. Polymer- and carbon-based electrodes for polymer solar cells: Toward low-cost, continuous fabrication over large area. *Solar Energy Materials and Solar Cells,* 100**,** 97-114.
33. Sun, K., Zhang, S., Li, P., Xia, Y., Zhang, X., Du, D., Isikgor, F. & Ouyang, J. 2015. Review on application of PEDOTs and PEDOT:PSS in energy conversion and storage devices. *Journal of Materials Science: Materials in Electronics,* 26**,** 4438-4462.

34. Wen, Y. & Xu, J. 2017. Scientific Importance of Water-Processable PEDOT–PSS and Preparation, Challenge and New Application in Sensors of Its Film Electrode: A Review. 55**,** 1121-1150.
35. Kroon, R., Mengistie, D. A., Kiefer, D., Hynynen, J., Ryan, J. D., Yu, L. & Mller, C. 2016. Thermoelectric plastics: from design to synthesis, processing and structureproperty relationships. *Chemical Society Reviews,* 45**,** 6147-6164.
36. Mengistie, D. A., Wang, P.-c. & Chu, C.-w. 2013. Effect of molecular weight of additives on the conductivity of PEDOT:PSS and efficiency for ITO-free organic solar cells. *Journal of Materials Chemistry A,* 1**,** 9907-9915.
37. Timpanaro, S., Kemerink, M., Touwslager, F. J., De Kok, M. M. & Schrader, S. 2004. Morphology and conductivity of PEDOT/PSS films studied by scanning–tunneling microscopy. *Chemical Physics Letters,* 394**,** 339-343.
38. Ouyang, J., Xu, Q., Chu, C.-W., Yang, Y., Li, G. & Shinar, J. 2004. On the mechanism of conductivity enhancement in poly(3,4- ethylenedioxythiophene): poly(styrene sulfonate) film through solvent treatment. *Polymer,* 45**,** 8443-8450.
39. Reichardt, C. & Welton, T. 2011. *Solvents and Solvent Effects in Organic Chemistry,* Weinheim, Wiley-VCH Verlad & Co.
40. Murov, S. 2010. *Solvent Polarity Table - Miller's Home* [Online]. Available: https://sites.google.com/site/miller00828/in/solvent-polarity-table [Accessed 11/01/2021].
41. National Center for Biotechnology Information. 2018. *PubChem Compound Database: Methyl Ethyl Ketone* [Online]. Available: https://pubchem.ncbi.nlm.nih.gov/compound/6569 [Accessed 22/10/2018].
42. Zotti, G., Zecchin, S., Schiavon, G., Louwet, F., Groenendaal, L., Crispin, X., Osikowicz, W., Salaneck, W. & Fahlman, M. 2003. Electrochemical and XPS studies toward the role of monomeric and polymeric sulfonate counterions in the synthesis, composition, and properties of poly(3,4- ethylenedioxythiophene). *Macromolecules,* 36**,** 3337-3344.
43. Sigma-Aldrich 2018. Product Specifaction: Tween 80.
44. Sigma-Aldrich 2015. Certificate of Analysis: Poly(3,4 ethylene dioxythiophene)-poly(styrene sulfonate).
45. Glagovich, N. 2005. *IR Absorptions for Representative Functional Groups* [Online]. Available: http://www.instruction.greenriver.edu/kmarr/chem%20162/Chem162%20Labs/Interpreting%20IR%20Spectra/IR%20Absorptions%20for%20Functional%20Groups.htm [Accessed 08/03/2018].
46. Kirchmeyer, S. & Reuter, K. 2005. Scientific importance, properties and growing applications of poly(3,4-ethylenedioxythiophene). *Journal of Materials Chemistry,* 15**,** 2077-2088.
47. Crispin, X., Marciniak, S., Osikowicz, W., Zotti, G., van der Gon, A. W. D., Louwet, F., Fahlman, M., Groenendaal, L., De Schryver, F. & Salaneck, W. R. 2003. Conductivity, morphology, interfacial chemistry, and stability of poly(3,4-ethylene dioxythiophene)–poly(styrene sulfonate): A photoelectron spectroscopy study. *Journal of polymer science. Part B, Polymer physics,* 41**,** 2561-2583.
48. Greczynski, G., Kugler, T. & Salaneck, W. R. 1999. Characterization of the PEDOT-PSS system by means of X-ray and ultraviolet photoelectron spectroscopy. *Thin Solid Films,* 354**,** 129-135.
49. Friedel, B., Keivanidis, P. E., Brenner, T. J. K., Abrusci, A., McNeill, C. R., Friend, R. H. & Greenham, N. C. 2009. Effects of layer thickness and annealing of PEDOT:PSS layers in organic photodetectors. *Macromolecules,* 42**,** 6741-6747.

50. Han, M. G. & Foulger, S. H. 2004. Crystalline Colloidal Arrays Composed of Poly(3,4-ethylenedioxythiophene)-Coated Polystyrene Particles with a Stop Band in the Visible Regime. *Advanced Materials,* 16**,** 231-234.
51. Rutledge, S. A. & Helmy, A. S. 2015. Etch-free patterning of poly(3,4-ethylenedioxythiophene)-poly(styrenesulfonate) for optoelectronics. *ACS applied materials & interfaces,* 7**,** 3940-3948.
52. Coblentz Society Inc. 2018. *National Institute of Standards and Technology Chemistry WebBook: Methyl Alcohol* [Online]. Available: https://webbook.nist.gov/cgi/cbook.cgi?ID=C67561&Type=IR-SPEC&Index=2 [Accessed 07/10/21].
53. Coblentz Society Inc. 2018. *National Institute of Standards and Technology Chemistry WebBook: Ethanol* [Online]. Available: https://webbook.nist.gov/cgi/cbook.cgi?ID=C64175&Type=IR-SPEC&Index=2 [Accessed 07/10/21].
54. Sigma-Aldrich. 2021. *Tween 80 Viscous Liquid* [Online]. Available: https://www.sigmaaldrich.com/catalog/product/sial/p1754?lang=en&region=GB&cm_sp=Insite-_-caSrpResults_srpRecs_srpModel_9005-65-6-_-srpRecs3-1#productDetailSafetyRelatedDocs [Accessed 03/02/2021].
55. Sigma-Aldrich. 2021. *Triton X-100 Laboratory Grade* [Online]. Available: https://www.sigmaaldrich.com/catalog/product/sial/x100?lang=en&region=GB&cm_sp=Insite-_-caSrpResults_srpRecs_srpModel_9002-93-1-_-srpRecs3-1 [Accessed 03/02/2021].
56. Callister, W. D. 2000. Materials science and engineering: an introduction. 5th ed. New York; Chichester: Wiley.

Chapter 6: Results and Discussion – Improvement of PEDOT:PSS Adhesion on Polymeric Substrates

The use of PEDOT:PSS in applications suitable for bending (e.g., flexible flat panel displays) or in some bulk manufacturing process (e.g., gravure printing) has already been shown within the literature (section 1.3.4).[1-6] These processes require substrate materials that are flexible, meaning polymers such as PP and PET are often used.[1-6] This is particularly problematic since the affinity of PEDOT:PSS to such substrates is known to be weak[7-9] due to their poor adhesive and hydrophobic properties.[7,10] Surface modification of the substrate, such as corona treatment of PET, has been shown to improve PEDOT:PSS adhesion, however, such processes can be time consuming and expensive.[11,12] Investigation into PEDOT:PSS adhesion on polymer substates is limited and therefore further study is needed.

This chapter explores the use of PDA, a semi-conductive biopolymer (section 1.6.1),[13,14] as a primer applied to PET, PP, and glass substrates prior to PEDOT:PSS film casting. The adhesive nature of this material means it has already been widely used as a surface modifier in many applications, such as noble metals, metal oxides, ceramics, and polymers (including PET, PE, and PTFE).[13-16] Furthermore, the semi-conductive nature suggests an even greater suitability since it is less likely to interfere with the conductive properties of PEDOT:PSS. The following chapter provides an initial assessment of the suitability of PDA through contact angle analysis, film quality assessment, scratch tape test and force pull-off tests. These systems will also be tested in conjunction with the use of varying Tween 80 concentrations since it was suspected that the surfactant may also improve PEDOT:PSS solution wettability on polymer substrates. Finally, sheet resistivity was measured to analyse any effect on the conductive properties of the PEDOT:PSS/Tween 80 films.

6.1 Pristine PEDOT:PSS on PDA Coated Substrates

Initially, the effectiveness of PDA as a primer was investigated with pristine PEDOT:PSS (i.e., without the addition of Tween 80). Wetting properties, film quality and adhesion were assessed on PP, PET, and glass substrates with and without PDA.

6.1.1 Wettability of Pristine PEDOT:PSS Solution on Substrates with and without PDA Primer

The wettability of pristine PEDOT:PSS solution was assessed through contact angle measurements on each substrate, with and without a PDA coating. Results show that when no PDA was present, glass has the greatest wettability (22 °), with polymeric substrates displaying poor wetting (72.5 ° and 52 ° for PP and PET, respectively) (Figure 6-1). The use of a PDA primer appears to alter the contact angle differently for each of the substrates. In the case of glass and PET there is an increase in the contact angles of 4 and 18.5 °, respectively, however, there is a 12 ° decrease for PP.

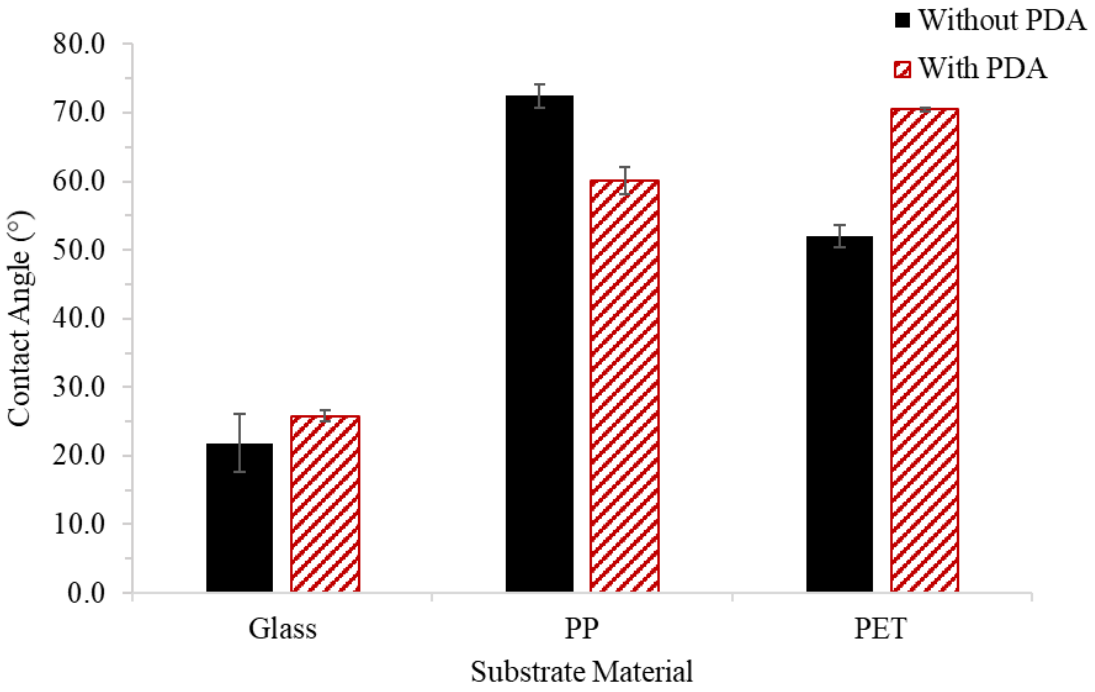

Figure 6-1: Contact angle (°) of pristine PEDOT:PSS solution droplet on substrates of glass, PET, and PP without (block black) and with (red stripes) a PDA primer coating. Error bars show data range

There are three main factors that can alter the contact angle of a solution on a substrate, namely, the surface energy of the substrate, the surface tension of the solution, and the substrate roughness.[10,17-19] Of these, it can be assumed that the substrate surface roughness is the least important. It has been shown that an increase in roughness for a hydrophilic substrate will decrease contact angle, but then increase contact angle on a hydrophobic substrate.[17] However, this is difficult to control between substrates and is closely linked to differences in surface tension and surface energy of the solution and substrate, respectively.[17] Furthermore, when comparing between substrates with and without a PDA coating, the change in roughness is likely to be minimal due to the PDA layer only being 50 nm thick.[13,20,21] Therefore, variations in roughness were omitted as a source of contact angle change in this study.

Given aqueous PEDOT:PSS is primarily water it will likely behave as such when considering contact angle.[22-24] It was also previously highlighted that the presence of PEDOT:PSS in solution can affect wetting and surface tension properties (section 4.5). However, surface tension will remain consistent given the same PEDOT:PSS solution was used throughout. On the other hand, the surface energy of the substrates will differ greatly making it the main cause of variation in the contact angles. In the case of glass, the surface energy is around 83 mNm^{-1},[25] with PET and PP having surface energies of 33 and 45 mNm^{-1}, respectively.[26] The surface tension of water is approximately 72 mNm^{-1}, with PEDOT:PSS solution often being quoted as similar.[7,11,27-31] This is more closely matched to glass meaning PEDOT:PSS solution will show better wettability on this substrate compared to PP and PET.[7,29]

As highlighted, the results do not follow the same trends when PDA is present. One reason for this could be that the surface energy of PDA has been quoted as approximately 55 mNm^{-1}.[32] This would explain why wettability gets worse on glass but better on PP, since the difference between surface tension and surface energies will increase and decrease, respectively.[7,25,26,29] However, this does not explain why there is a substantial increase for PET. Given the surface energy of PDA is closer to the surface tension of PEDOT:PSS than PET, a slight decrease in contact angle should have been evident. This could be linked to the orientation of the PDA molecules when they polymerise onto the surface of the substrate. It has been seen that PDA can either orientate with the more polar carbonyl attaching to or facing away from the substrate.[20,33-35] It is possible that on PET, polar groups will attach to the carbonyl groups in PDA causing the less polar benzene ring, containing the NH group, to be at the surface. This means the surface energy will be lower than if the carbonyl groups were facing outwards,[35] likely causing the surface energy to decrease when PDA is coated onto PET. Therefore, the difference in surface energy between PET/PDA and PEDOT:PSS solution surface tension will

be greater than PET without PDA, resulting in an increased contact angle.[7,29] Regardless of the points discussed, it can be said that the PDA coating is thin enough to allow some interaction to still occur with the substrate material. If the PDA coating was thick, then each substrate would show similar contact angle results, varying only with the PDA bonding orientation.

6.1.2 Film Quality of PEDOT:PSS on PDA Coated Polymeric Substrates

As explained in the experimental chapter (section 2.7), drop and dip casting methods were used to create films for force pull of and scratch tape testing, respectively. However, the film quality for each casting method had to be assessed prior to testing, with cracked or insufficiently coherent films being removed from the test batch. In all cases, the quality of the films on the glass substrate, were adequate for testing regardless of PDA application. The quality of the dip cast pristine PEDOT:PSS films on polymeric substrates with and without a PDA coating can be seen in Figure 6-2. On substrates without PDA, there was a noticeable lack of films formed on both PP (Figure 6-2a) and PET (Figure 6-2c). This is problematic for scratch tape testing since a full film is required to perform the test. However, a significant improvement in film formation was observed when PDA was used as a primer on both substrates (PP/PDA – Figure 6-2b, PET/PDA – Figure 6-2d).

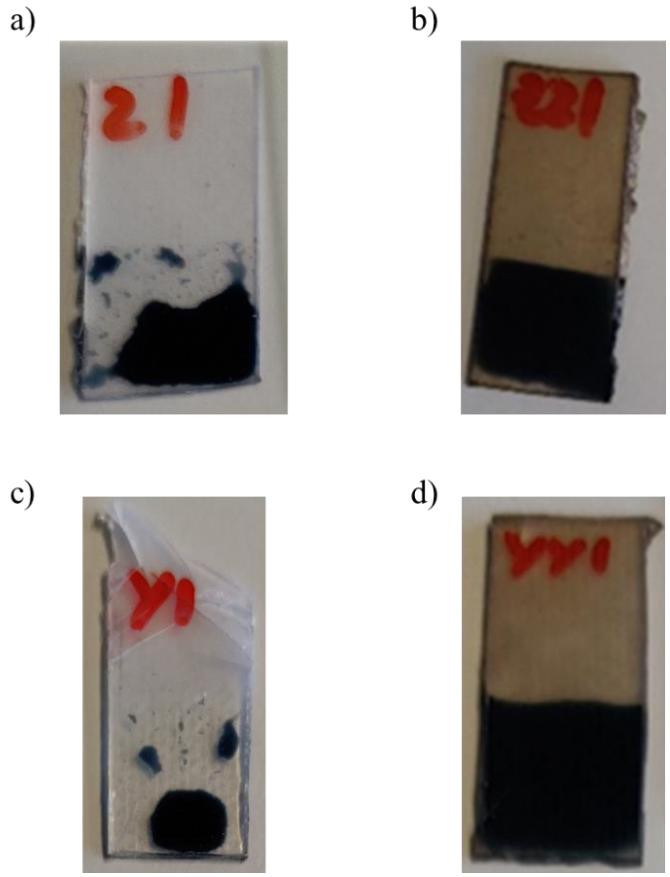

Figure 6-2: Dip cast PEDOT:PSS films on substates of a) PP, b) PP/PDA, c) PET, & d) PET/PDA

The ability for these substrates to pick up solution via dip casting is mainly liked to the wettability and availability of polar groups on the surface of these materials. The glass substrate used was untreated soda lime glass which contains Si-O bonds and also O^- groups due to the presence of sodium and calcium oxides (Na_2O and CaO).[19] These groups have a high polarity which means glass has a high surface energy and will readily interact with water and PEDOT:PSS.[7,25,29,36] However, whilst PET does have polar groups in the form of C=O, these groups are less polar and in the case of PP there are no polar groups.[26,36] This means that in both cases the PEDOT:PSS solution is less likely to be picked up via dip casting and, therefore, no film was formed.

PDA has previously been used as a surface modifier, even on polymeric materials that are known for having poor adhesion properties.[13-16] Due to the highly polar functional groups contained within the material, strong interactions with other molecules can form[13,14,20] and wettability is improved on these substrates,[33] as previously shown with PP (Figure 6-1). This would, in part, explain the improved film formation seen for PP/PDA substrates, however, the wettability of PET was worsened when primed with PDA (Figure 6-1). This suggests an alternative mechanism is allowing for the PEDOT:PSS to be deposited on PET when PDA is present. It was postulated that even though wettability decreases, the functional groups present in PDA can interact more readily with PEDOT:PSS, effectively removing the polymer from solution when the substrate is submerged. This is also likely to be happening with the PP/PDA, with the added improvement of better wettability. However, this is hypothetical and would require further investigation.

As with dip casting, there were no issues relating to film quality for drop cast PEDOT:PSS films on glass, regardless of the PDA primer. The outcome of drop casting on PET and PP substrates with and without PDA is shown in Figure 6-3. On all substrates, unsuitable films were produced either due to cracking or non-uniformity. This was the case even with the PDA primer, showing its ability to improve film quality for drop cast films is not as significant as dip casting. However, it could be argued that the films on substrates primed with PDA (Figure 6-3b & d) show marginally better qualities. This is apparent due to the extensiveness of the cracks on PP (Figure 6-3a) and the lack of film formation on PET (Figure 6-3c) when no PDA is present.

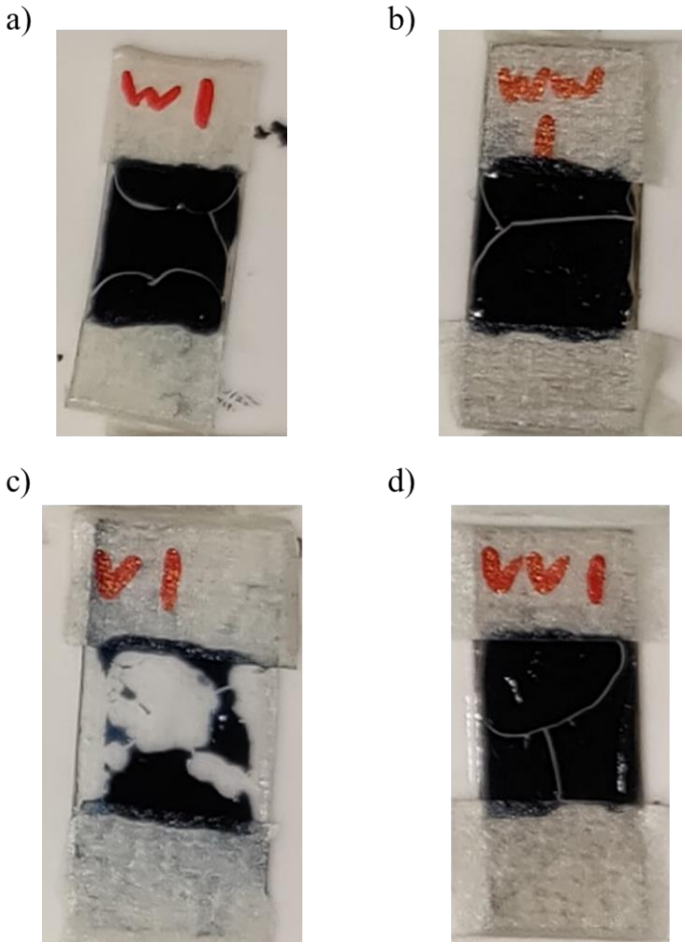

Figure 6-3: Drop cast PEDOT:PSS films on substates of a) PP, b) PP/PDA, c) PET, & d) PET/PDA

As before, the film quality is linked to wettability, however, with drop casting there is no reliance on the substrate needing to pick up PEDOT:PSS since it is deposited directly onto the surface. This may explain why a better film is formed on PP for drop casting than dip casting. However, it appears that film cracking is more of an issue with this casting method. While there is uncertainty as to why this is the case, cracking can occur when a thicker film dries too quickly and causes strain through material shrinkage. A thicker PEDOT:PSS film is known to be produced via drop casting (section 4.4.2), so this is likely the main factor leading to cracking. These cracks are problematic for force pull off testing since the adhesive could penetrate the cracks and adhere to the substrate below.

The film quality for both dip and drop cast films acted as an initial assessment of the effectiveness of PDA as a primer for PEDOT:PSS application on polymer substrates. While there is improvement on both substrates when PDA is present, there are clear issues when films were drop cast. However, the improvement seen for dip cast films was more significant, with no cracking occurring on substrates coated in PDA.

6.1.3 Adhesion of PEDOT:PSS Films on Uncoated and PDA Coated Substrates

The adhesion of pristine PEDOT:PSS films on various substrates was analysed using two methods: scratch tape testing for dip cast films; and pull-off strength for drop cast films. From the film quality analysis (section 6.1.2), films that were cracked or incoherent were not tested. This is because they were deemed unsuitable for analysis and low adhesive properties can be inferred from the poor film formation.

Table 6-1 shows the scratch tape test data for pristine PEDOT:PSS on glass, PP and PET substrates with and without a PDA primer. The data shows PDA improves the adhesion of the PEDOT:PSS films to all substrates. On glass, an improvement from >65% to <5% of the film being removed was observed with the addition of PDA. Whilst both polymer substrates show >65% being removed with a PDA layer, this is still evidence of improved adhesion since these samples had coherent films, unlike substrates with no PDA (section 6.1.2). However, compared to glass, it is clear that the adhesion to polymeric substrates is still poor even with the application of PDA.

Table 6-1: Scratch tape test classification and relevant percentage removed of pristine PEDOT:PSS films on various substrates. Not applicable (N/A) given where incoherent films were formed after casting

Substrate	Classification	Percentage Removed
Glass	0B	>65 %
Glass/PDA	4B	<5 %
PP	N/A	N/A
PP/PDA	0B	>65 %
PET	N/A	N/A
PET/PDA	0B	>65%

Due to poor film quality (section 6.1.2), no pull-off strength data for PEDOT:PSS on polymeric substrates with or without PDA could be obtained. However, there was an improvement on glass from 0.137 to 0.275 MPa with the addition of PDA. It should also be noted that with PDA present the glue/PEDOT:PSS adhesion failed before the film to substrate bond meaning the result of 0.275 MPa is not a true maximum. This is unusual since the bond strength of the adhesive is quoted as 15 MPa[37] and the point of failure is much lower than this value. Regardless, the increase in force pull-off is still evidence for the improvement in adhesion caused by the addition of PDA.

The reasoning for the improvement in adhesion is likely similar to those already discussed regarding the wettability and film quality (sections 6.1.1 & 6.1.2, respectively). Glass has a higher surface energy, compared to the polymer substrates, due to more polar functional groups which promotes better adhesion.[10,13,14,18-20] When glass is then coated in PDA, this adds to the availability of functional groups, further strengthening the interaction to PEDOT:PSS.

6.2 PEDOT:PSS/Tween 80 on Various Substrates

Following the analysis on pristine PEDOT:PSS, the effect of Tween 80 addition on wettability, film quality and adhesion were investigated on glass, PP and PET. This was initially done without priming these substrates with PDA to more accurately identify the effects caused by the surfactant.

6.2.1 PEDOT:PSS/Tween 80 Solution Wettability on Various Substrates

Figure 6-4 shows the contact angle of PEDOT:PSS/Tween 80 solutions for varying surfactant concentration on three substrate materials. The wettability of these solutions on glass has previously been discussed (section 4.5.2) but is included here for comparison to the polymer substrates. It was shown that the addition of Tween 80 caused surface contact angle on glass to initially increase from 21.8 ° for pristine PEDOT:PSS, up to 31.6 ° at 0.47 wt% surfactant. Above this concentration results, decreased to approximately 27 ° at 0.93 wt%, followed by a plateau with greater surfactant addition. Unlike on glass, the addition of Tween 80 causes a significant decrease in the contact angle of PEDOT:PSS on the polymer substrates, even at low concentrations. Results decrease from 72 to 56 ° for PP and from 52 to 45 ° for PET at 0.00 and 0.37 wt%, respectively. This downward trend continues for increasing surfactant concentration, with results plateauing above 2.27 wt% Tween 80 at approximately 40 and 36 ° for PP and PET, respectively. Greater variation in the results is seen for PP, mainly be due to the anomalous result at 0.47 wt% Tween 80 skewing the data. Despite the large reduction in contact angle achieved on both substrates, solution wettability on glass is still superior, with a lower contact angle observed throughout.

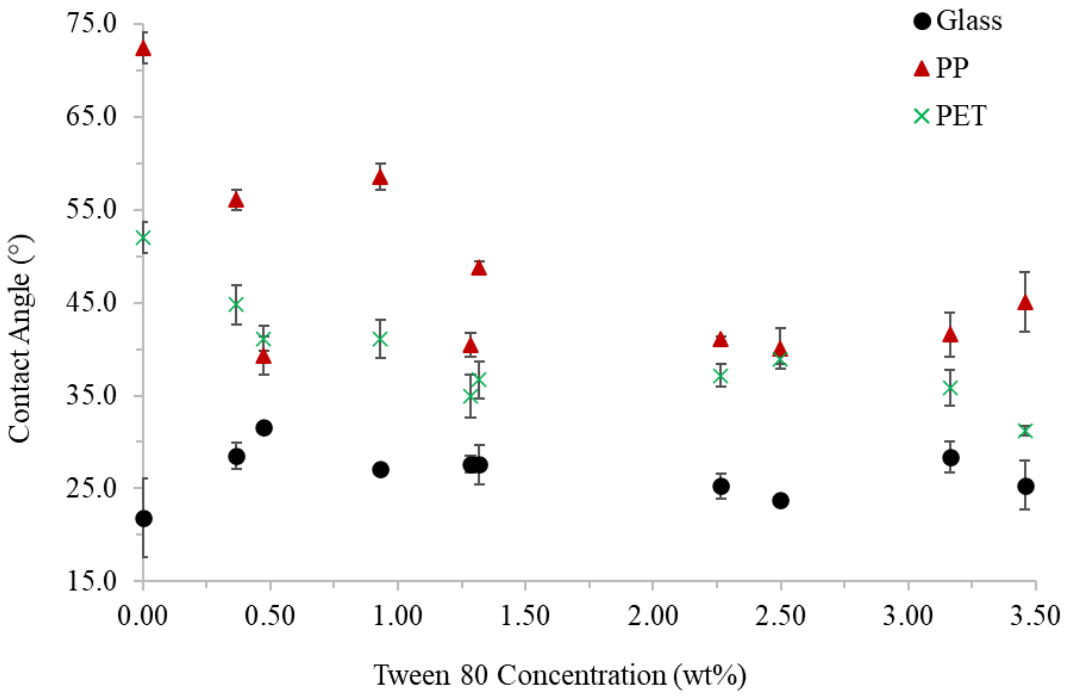

Figure 6-4: Contact angle (°) of droplets of PEDOT:PSS/Tween 80 solutions for differing surfactant concentration (wt%) on substrates of glass (black circle), PP (red triangle) and PET (green cross). Error bars show data range

The decrease in contact angle seen on polymeric substrates is due to a reduction in the surface tension of the solution leading to more closely matched surface energies between solution and substrate.[29] Therefore, it can be deduced that Tween 80 is causing a reduction in PEDOT:PSS solution surface tension, which is commonly seen throughout the literature with other surfactants reportedly improving wettability of PEDOT:PSS on Teflon, PDMS and PET.[7,27,29,38-40] The discrepancies seen between polymeric substrates and glass can be linked to the differences in the already discussed polar functional groups of the varying materials (sections 6.1.1 & 6.1.2).

6.2.2 PEDOT:PSS/Tween 80 Film Quality on Various Substrates

As was the case for pristine PEDOT:PSS, films on glass were coherent with no cracks, regardless of the addition of Tween 80. The improvement in wettability on polymer substrates subsequently led to an enhancement of film quality for both dip cast (Figure 6-5 & 6-6) and drop cast (Figure 6-7 & 6-8) samples. For dip cast samples on PP (Figure 6-5), coherent films were formed at concentrations of 0.47 wt% and above (samples labelled Z3 – Z10). This was not the case for PET in which only samples containing 1.29 to 2.50 wt% Tween 80 produced good quality films. Solutions with Tween 80 concentrations outside these limits produced incoherent films (Figure 6-6).

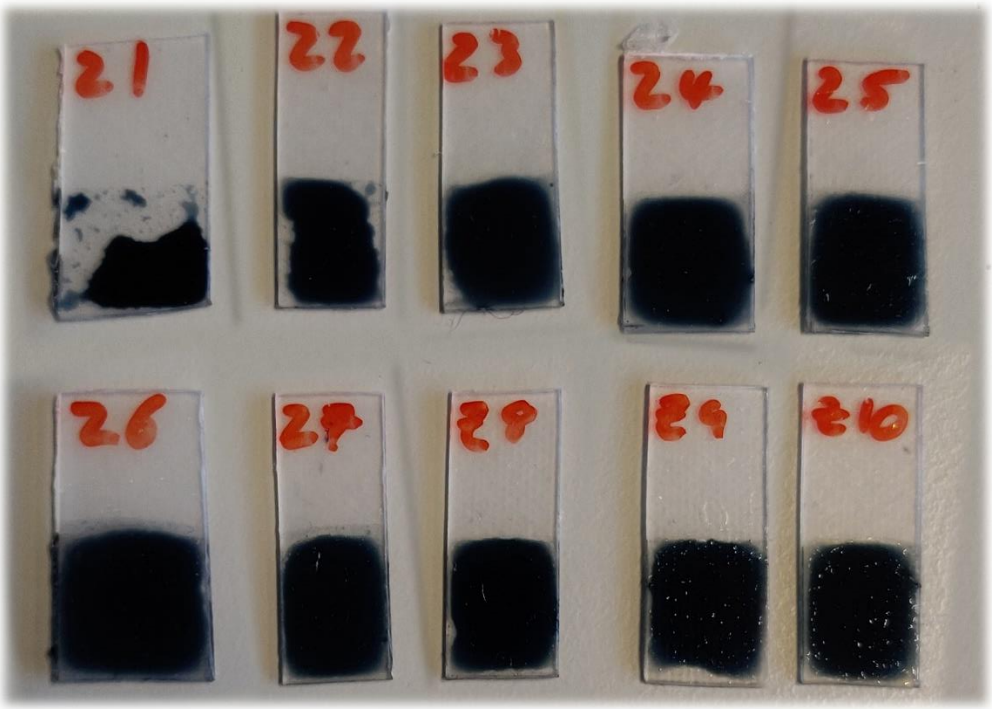

Figure 6-5: PEDOT:PSS/Tween 80 dip cast film samples on PP substrates used for adhesion scratch testing. Surfactant concentration increases with increasing number

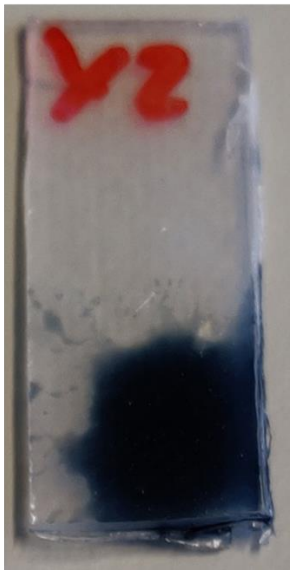

Figure 6-6: Dip cast PEDOT:PSS/Tween 80 film with 0.37 wt% surfactant on PET

In the case of drop cast samples, cracking is apparent in films up to and including 0.47 wt% surfactant (those labelled 1 – 3) on both PP (Figure 6-7) and PET (Figure 6-8). However, for concentrations of 0.93 wt% and above these issues are mitigated. As mentioned previously (section 6.1.2), this cracking is most likely linked to shrinkage of the films on drying. However, the presence of the surfactant is thought to plasticise the PEDOT:PSS, improving its tolerance to such mechanical stresses.[41] It is likely that at concentrations lower than 0.93 wt%, the interaction with PEDOT:PSS is not saturated (section 4.5.2)[42,43] meaning films will be comparatively more brittle and susceptible to cracking. However, as previously seen on glass (section 4.4.4), the increase in Tween 80 concentration above 2 wt% reduced film quality on PP and PET due to excess surfactant appearing on the surface of the film, giving it a waxy texture.

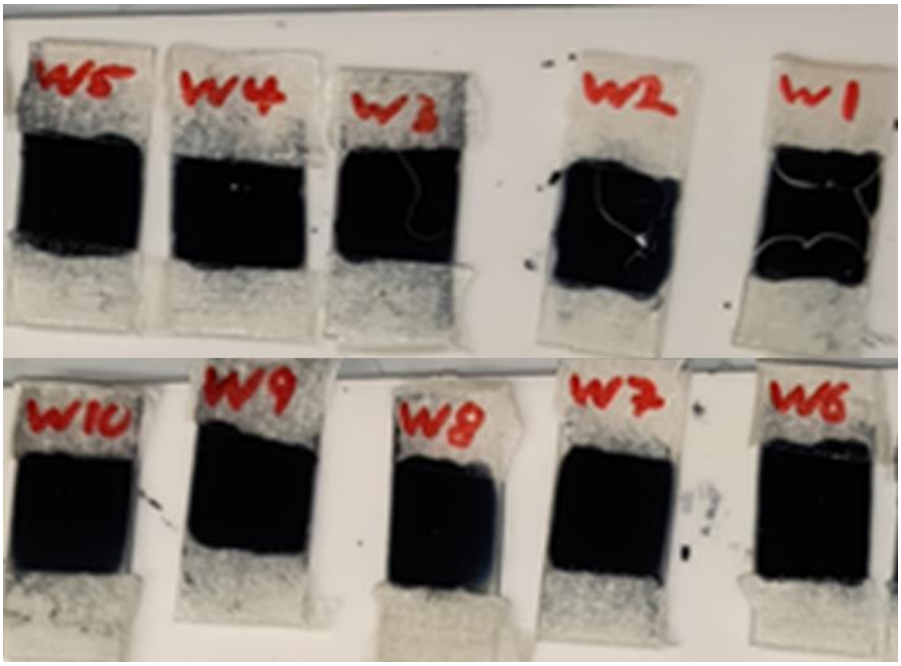

Figure 6-7: PEDOT:PSS/Tween 80 drop cast film samples on PP substrates used for adhesion scratch testing. Surfactant concentration increases with increasing number

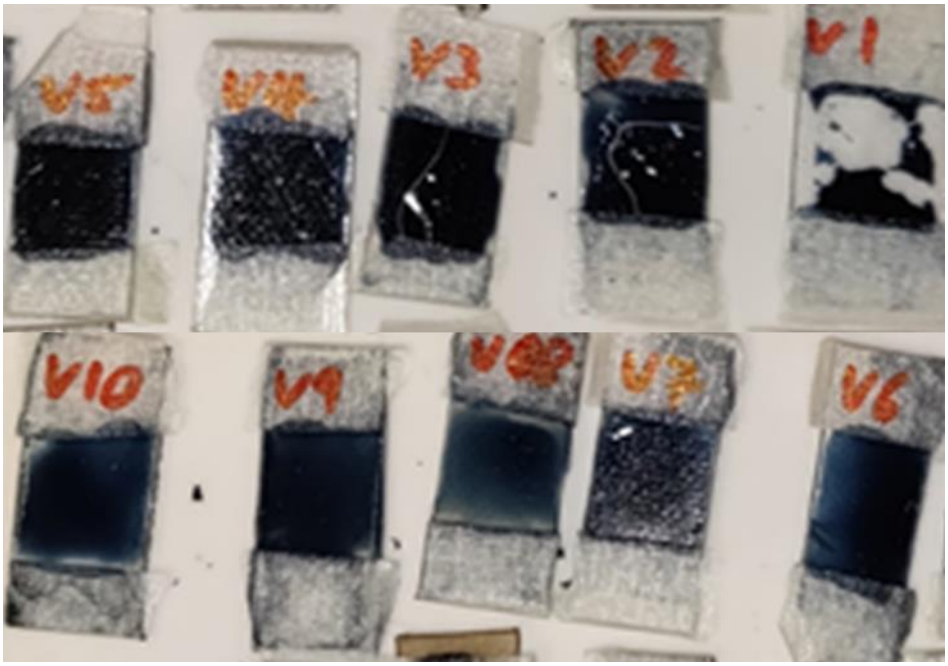

Figure 6-8: PEDOT:PSS/Tween 80 drop cast film samples on PET substrates used for adhesion scratch testing. Surfactant concentration increases with increasing number

6.2.3 PEDOT:PSS/Tween 80 Film Adhesion to Various Substrates

As with pristine PEDOT:PSS (section 6.1.2), films that were either cracked or incoherent were removed from the sample set. Scratch tape and force pull off tests, for dip and drop cast films respectively, were performed on PEDOT:PSS/Tween 80 films with varying surfactant concentrations.

6.2.3.1 Scratch Tape Testing

Table 6-2 shows the awarded classification for films of varying Tween 80 concentrations on differing substrates. The data for the glass substrate shows that with up to 0.93 wt% Tween 80, over 65 % of the films were removed by the tape. At 1.29 and 1.32 wt%, less film was removed, with concentrations of 2.27 and 2.50 wt% showing no film removal (given the classification 5B), suggesting adhesion was improving. However, it is likely the excess surfactant on the sample surface (section 6.1.2) was acting as a barrier to adequate tape adhesion. Furthermore, the films at Tween 80 concentrations of 3.16 and 3.46 wt% were damaged during the cross-hatching preparation, with large amounts of the film being removed before the tape could be applied. This showed that the adhesion of the films was affected by the high surfactant concentration.

Films of up to 1.32 wt% Tween 80 on PP were given a 0B classification. Above this concentration there is some improvement in film adhesion, especially at 3.46 wt% where 15 – 35 % of the film remained intact. In the case of PET, all of the tested films showed >65% film removal from the substrate, even with the highest surfactant concentrations. There were also a large number of samples that could not be tested due to incoherent film formation, particularly on PET. Furthermore, poor tape adhesion due to excess surfactant and film damage during cross hatching for higher surfactant concentrations were also issues for samples on these polymer substrates.

Table 6-2: Scratch tape test classification PEDOT:PSS/Tween 80 films on varying substrates. Not applicable (N/A) results given where films were not coherently formed after casting. Each classification represents percentage removed as follows: 5B, 0%; 4B, <5%; 3B, 5 – 15%; 2B, 15 – 35%; 1B, 35 – 65%; 0B, >65%

Tween 80 Concentration (wt%)	**Substrate**		
	Glass	PP	PET
0.00	0B	N/A	N/A
0.37	0B	N/A	N/A
0.47	0B	0B	N/A
0.93	0B	0B	N/A
1.29	4B	0B	0B
1.32	2B	0B	0B
2.27	5B	1B	0B
2.50	5B	0B	0B
3.16	1B	1B	N/A
3.46	0B	2B	N/A

It is clear from this data that limited observations can be made. The addition of Tween 80 can be considered to improve adhesion to polymeric substrates, but this conclusion can only be drawn from the fact coherent films are formed when the surfactant is present. This is mainly due to limitations in this testing method, some of which, such as the interference of excess surfactant and the samples being damaged during cross hatching, have already been discussed. Furthermore, there is clear limitation in the classification method, especially at the lower classification bands. For example, the 0B band indicates 0 – 35 % of the film is left on the substrate. This is a large percentage range and causes many of the results to fall within the same classification, suggesting they all adhere in equal amounts which is unlikely to be true. Additionally, there is exposure to large amounts of human error due to the subjective nature of classifying adhesion in this way.

6.2.3.2 Force Pull-Off Testing

Figure 6-9 shows the effect of varying the Tween 80 concentration on PEDOT:PSS adhesion to glass, PP and PET substrates for drop cast films. It should first be noted that there are data point missing. In the case of the polymer substrates, only samples containing more than 0.93 wt% are shown due to unsuitable films being formed at lower concentrations (section 6.2.2). For the films on glass the missing measurements are due to experimental error causing the films to break during loading into the machine.

When considering films on glass, the addition of low surfactant concentrations causes a significant reduction in adhesion. For pristine PEDOT:PSS, the stress required to remove the film was 0.137 MPa which decreased to 0.016 MPa at 0.93 wt% Tween 80. As surfactant concentration increases further, there appears to be a slight increase in the adhesion up to 0.099 MPa at 3.46 wt%. Similar to wettability results (section 6.2.1 & 4.5.2), the decrease in adhesion at low surfactant concentrations can initially be explained by the Tween 80 interacting with the polar groups in PEDOT:PSS.[23,43-46] The reduces the availability of potential interactions with glass, causing adhesion to fall. However, the cause of the increase in adhesion at higher surfactant concentrations is uncertain. An explanation could be that once the PEDOT:PSS – surfactant interaction is saturated, the excess Tween 80 provides free hydroxyl groups with which the glass can interact, causing adhesion to increase.[10,18,19]

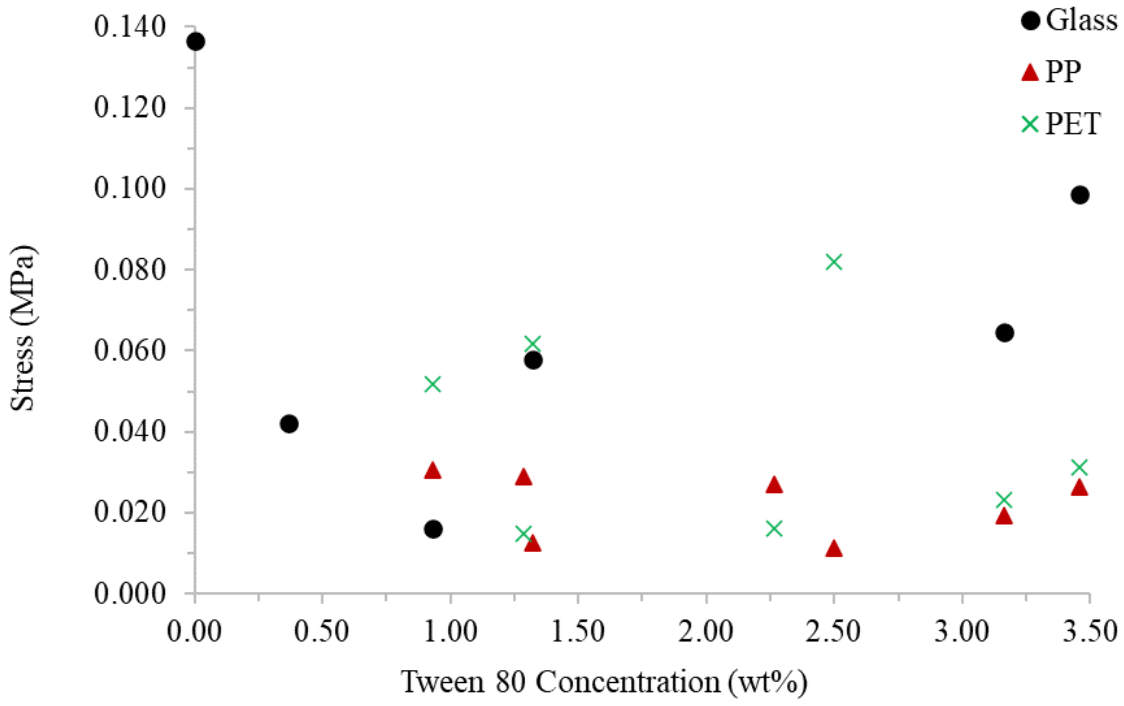

Figure 6-9: Pull-off stress (MPa) applied to remove PEDOT:PSS/Tween 80 films with differing surfactant concentrations (wt%) from substrates of glass (black circle), PP (red triangle), and PET (green cross)

For both PP and PET, coherent films were formed at 0.93 wt% and above providing an initial suggestion that adhesion is improved. However, the increase in Tween 80 concentration does not further enhance the adhesion to PP by any significant amount, with the results all lying between 0.015 and 0.030 MPa. Furthermore, although there is overlap in these results with glass and PET, PP shows comparatively low pull off stress more consistently compared to the other substrates. On PET, the data shows large amounts of scatter with the greatest stress being 0.082 MPa at 2.50 wt% and the lowest 0.015 MPa at 1.29 wt%, making it difficult to identify a consistent trend. However, while this variation seems large, the actual values are relatively small, and it could be said that, overall, there is no substantial change in the adhesion to a PET substrate for films containing 0.93 – 3.46 wt% Tween 80. In addition, compared to pristine PEDOT:PSS on glass, the adhesion to PET is still significantly lower, regardless of Tween 80

concentration. Despite this, when Tween 80 is present the adhesion results of glass and PET are comparable.

The results show that pristine PEDOT:PSS has superior adhesive properties on glass compared to polymeric substrates. This was evident by no coherent films being formed on PP or PET. The addition of Tween 80 to PEDOT:PSS caused adhesion to worsen on glass at low concentrations followed by a slight increase above 3 wt%, mirroring the contact angle data (section 6.2.1). The initial worsening was attributed to the Tween 80 interaction with the polar functional groups of PEDOT:PSS, reducing availability for interaction with glass.[23,43-46] However, at higher concentrations the polar groups in the excess surfactant act as points of electrostatic interaction.[10,18,19] Adhesion was improved on PP and PET, as deduced by the formation of films suitable for testing, however, this only occurred at and above 0.93 wt% surfactant concentration. However, adhesion to PP remained low regardless of further Tween 80 addition. Whilst the result for PET were variable, some pull-off stresses were comparable to that of PEDOT:PSS/Tween 80 films on glass.

6.3 PEDOT:PSS/Tween 80 on PDA Coated Substrates

The addition of Tween 80 to PEDOT:PSS has been shown to be somewhat beneficial to wettability, film quality and adhesion (section 6.2). The effect of implementing a PDA primer on substrates of glass, PP and PET on these properties was assessed for PEDOT:PSS/Tween 80 samples.

6.3.1 PEDOT:PSS/Tween 80 Solution Wettability on PDA Coated Substrates

Figure 6-10 shows how a PDA primer on glass alters the contact angle of PEDOT:PSS/Tween 80 solutions containing varying surfactant concentrations. It is clear that

the presence of the PDA coating causes the contact angle of each formulation to increase whilst still following a similar trend. A maximum contact angle of 42 ° was obtained at a concentration of 0.93 wt% on a glass/PDA substrate. This then decreases and is lowest at 3.16 wt% with a measurement of 31 °. As previously discussed (section 6.1.1), the higher contact angles are linked to the surface energy of PDA being lower than glass. When applied as a primer it will cause a greater discrepancy between the surface energies of the substrate and the solutions leading to an increase in the contact angles.[7,29,32] This decrease in wettability may contribute to the drop in adhesion (section 6.3.3) due to decreased solution spreading leading to reduced interaction with the substrate.[10,18,19]

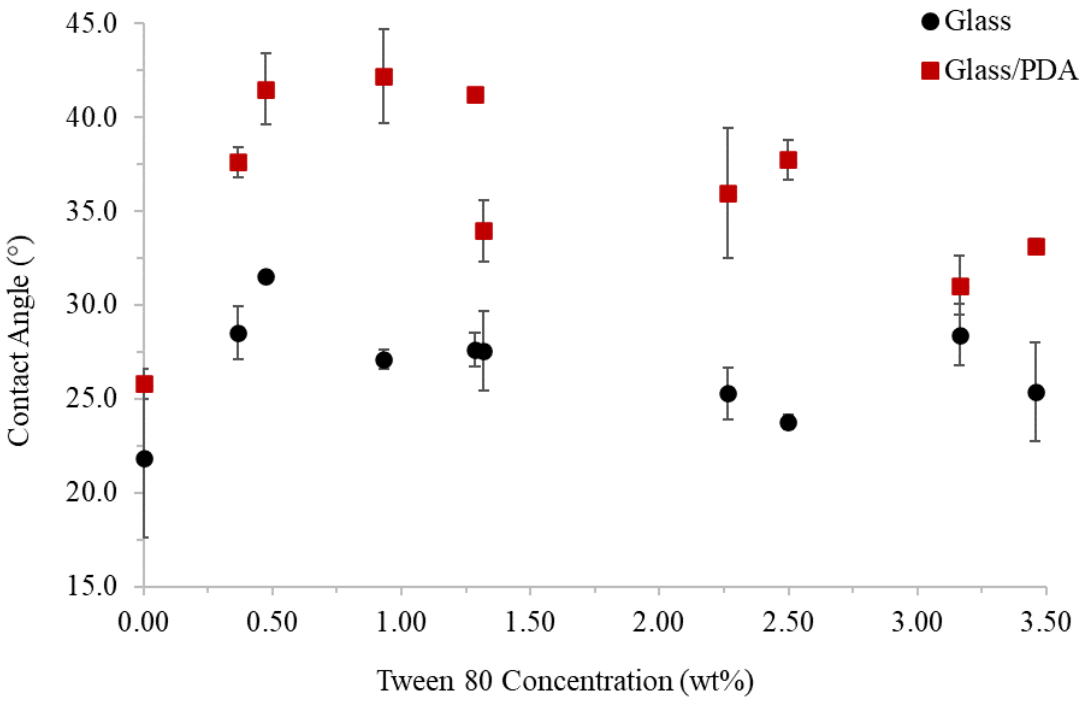

Figure 6-10: Contact angle (°) of droplets of PEDOT:PSS/Tween 80 solutions for differing surfactant concentrations (wt%) on a glass substrate without (black circle) and with (red square) a PDA primer layer present. Error bars show data range

The contact angle data for increasing Tween 80 concentration was the same for PP and PP/PDA substrates (Figure 6-11). The exception to this is pristine PEDOT:PSS which shows a significantly lower contact angle when PDA is present, as already established (section 6.1.1). The lowest contact angle recorded for a PP/PDA substrate was 43 ° at 3.16 wt%, with PP showing a similar result of 42 ° at the same concentration.

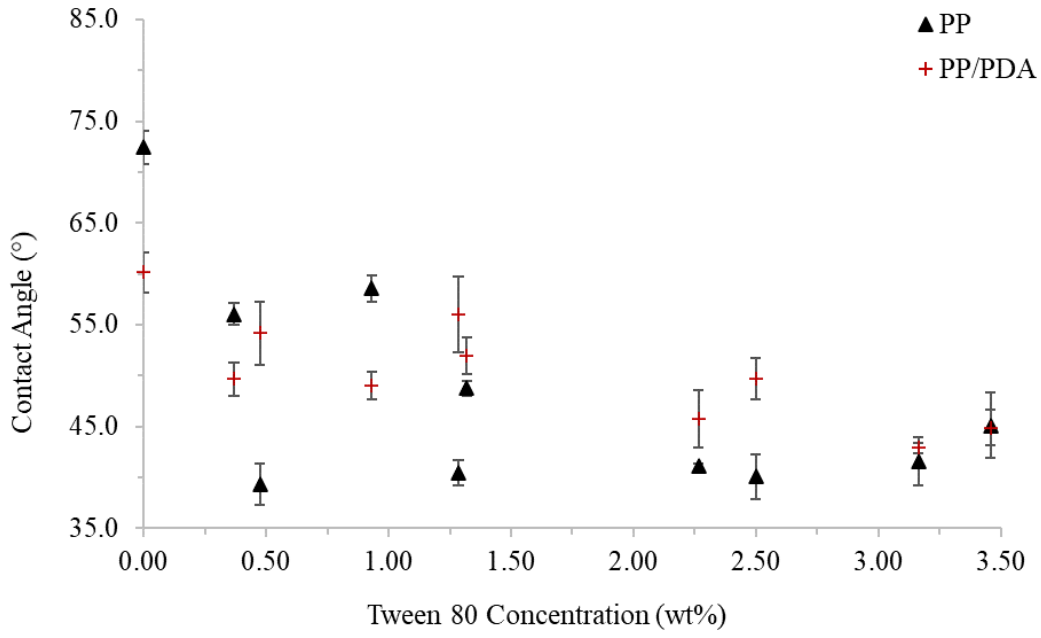

Figure 6-11: Contact angle (°) of droplets of PEDOT:PSS/Tween 80 solutions for differing surfactant concentrations (wt%) on a PP substrate without (black triangle) and with (red plus) a PDA primer layer present. Error bars show data range

Finally, in the case of PET (Figure 6-12), a similar phenomenon to glass occurs whereby coating with PDA results in the same overall trend but at elevated contact angles. However, unlike glass, this is only true for concentrations up to 1.32 wt%, above which the results become comparable regardless of the PDA primer. It appears that the presence of Tween 80 at these higher concentrations is mitigating the increase seen for pristine PEDOT:PSS when a PDA primer is applied.

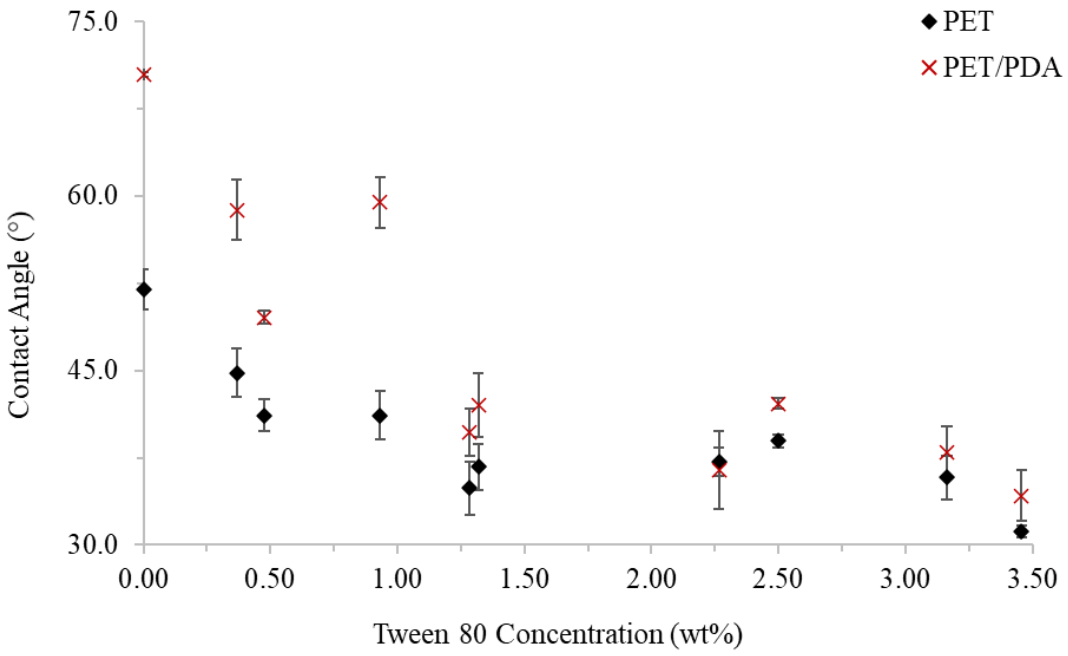

Figure 6-12: Contact angle (°) of droplets of PEDOT:PSS/Tween 80 solutions for differing surfactant concentrations (wt%) on a PET substrate without (black diamond) and with (red cross) a PDA primer layer present. Error bars show data range

6.3.2 PEDOT:PSS/Tween 80 Film Quality on PDA Coated Substrates

As has been the case throughout, the quality of dip and drop cast PEDOT:PSS/Tween 80 films on glass were good regardless of PDA application. The quality of the dip cast samples on PP and PET substrates with a PDA primer can be seen in Figure 6-13 and 6-14, respectively. For all surfactant concentrations, coherent films were formed with no quality issues. Previously when no PDA was applied (section 6.2.2), coherent films were only formed at concentrations above 0.47 wt% on PP and between 1.29 to 2.50 wt% on PET. This shows PDA improved film quality on these polymeric substrates.

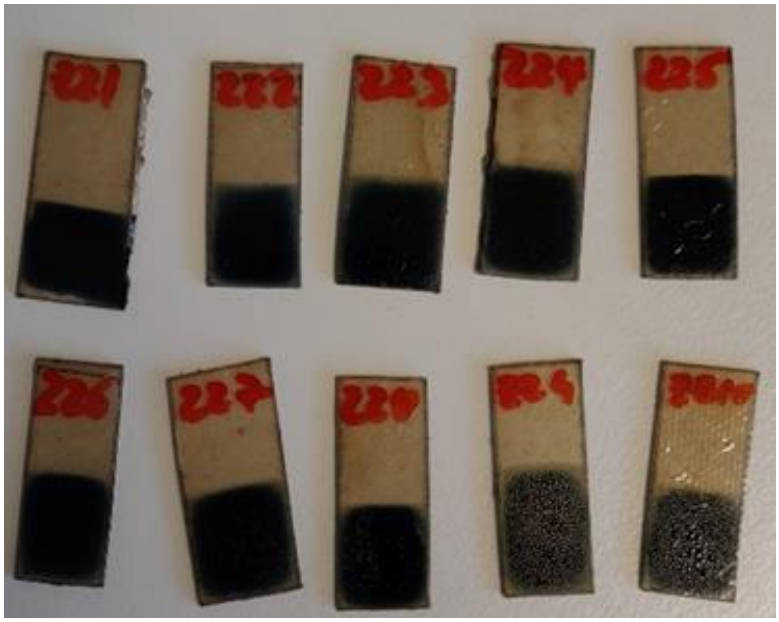

Figure 6-13: PEDOT:PSS/Tween 80 dip cast film samples on PP/PDA substrates used for adhesion scratch testing. Surfactant concentration increases with increasing sample number

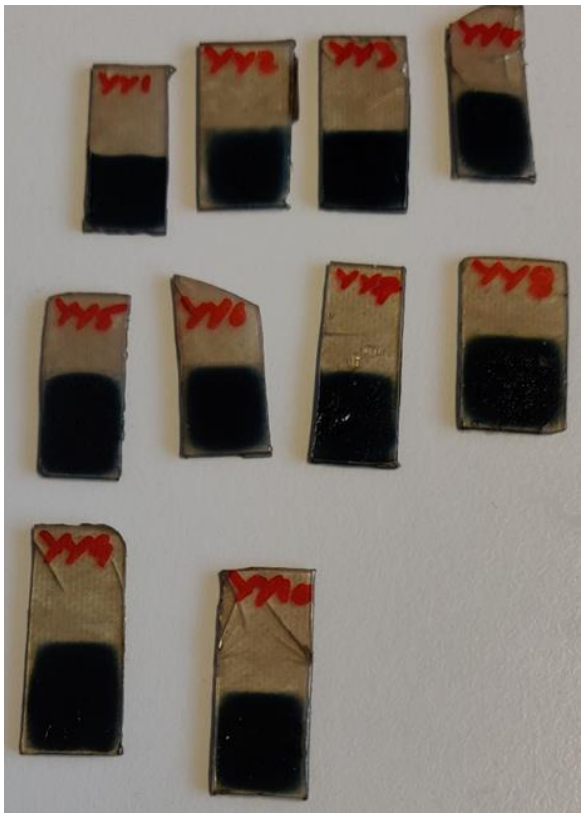

Figure 6-14: PEDOT:PSS/Tween 80 dip cast film samples on PET/PDA substrates used for adhesion scratch testing. Surfactant concentration increases with increasing sample number

The outcome of drop casting on PP and PET substrates with a PDA primer can be seen in Figure 6-15 and 6-16, respectively. Unlike dip casting, signs of cracking still appear when PDA is present. As seen with no PDA primer (section 6.2.2), this occurs at surfactant concentrations of 0.47 wt% and below (numbered 3 - 1) for PP/PDA and 0.37 wt% and below for PET/PDA. This suggests that Tween 80 is needed to resolve issues of cracking on drop cast samples.

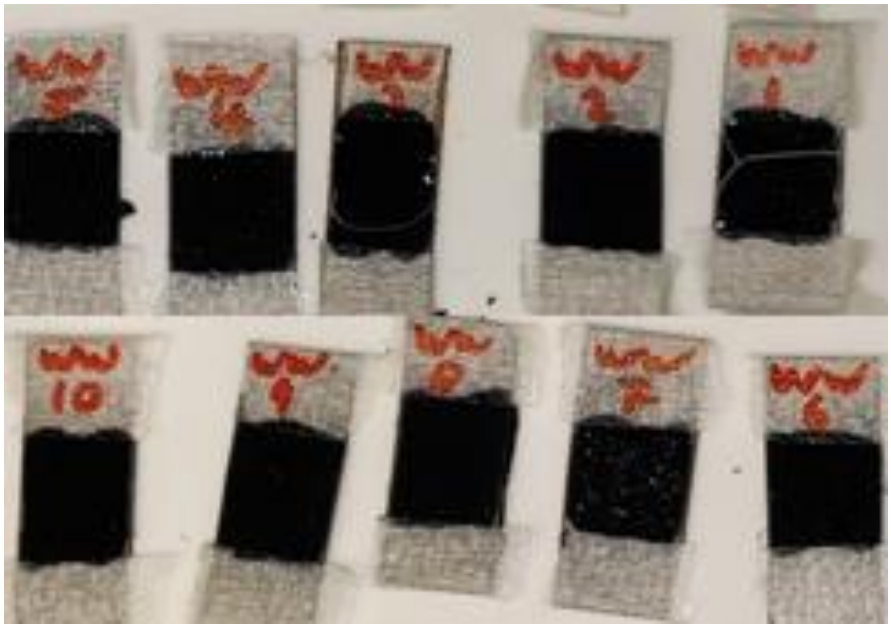

Figure 6-15: PEDOT:PSS/Tween 80 drop cast film samples on PP/PDA substrates used for force pull-off testing. Surfactant concentration increases with increasing sample number

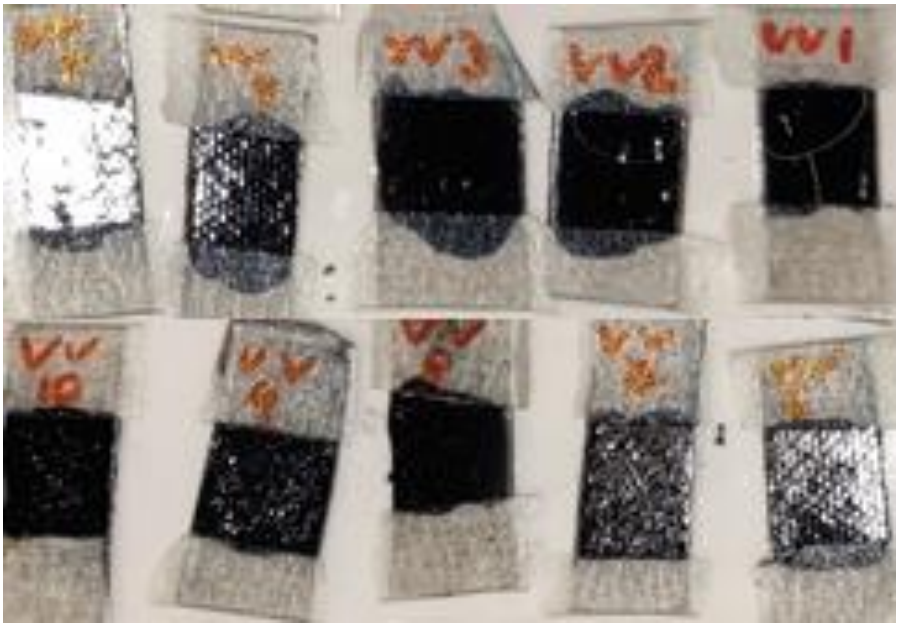

Figure 6-16: PEDOT:PSS/Tween 80 drop cast film samples on PET/PDA substrates used for force pull-off testing. Surfactant concentration increases with increasing sample number

The use of a PDA primer has shown to be effective at improving film quality for dip cast samples for all Tween 80 concentrations on polymeric substrates. As previously discussed, (section 6.1.1), this is likely due to PDA increasing the available polar functional groups.[13,14,20] PDA more readily interacts with PEDOT:PSS in solution and causes preferential deposition of the polymer compared to PP or PET with no PDA coating. However, the use of PDA does not stop the films from cracking at low Tween 80 concentrations following drop casting. As previously discussed (section 6.2.2), this could be linked to films shrinkage, which is mitigated by the plasticising effect of the surfactant.[41] Furthermore, the issue of excess Tween 80 above 2 wt% causing a waxy film surface is still an issue for both casting methods (section 6.2.2) on substrates primed with PDA.

6.3.3 PEDOT:PSS/Tween 80 Adhesion on PDA Coated Substrates

As before, scratch tape and force pull-off testing were performed to assess the adhesion of PEDOT:PSS/Tween 80 films on PDA coated substrates. Films that were cracked or incoherent from the film quality analysis were removed from the testing batch. Results from section 6.2.3 are shown again for comparison to substrates without a PDA coating.

6.3.3.1 Scratch Tape Testing

The data presented in Table 6-3 shows the awarded scratch test classification for dip cast films of varying Tween 80 concentrations on substrates with and without a PDA primer. As previously seen, the results for pristine PEDOT:PSS show an improvement for all substrates coated in PDA. This presented as a substantial decrease in film removal on glass and the capability of film formation on polymer substrates (section 6.1.3). However, the results for glass/PDA show a drop in the classification awarded once Tween 80 is added in low concentrations. This shows that the surfactant initially makes the adhesion worse which is likely due to it interacting with polar groups in the PEDOT:PSS meaning there is less interaction with the PDA.[23,43-46] At 0.93 wt% adhesion appears to increase with less film being removed, which may be an effect of excess surfactant acting as a barrier between the tape and the film. However, at the same concentration on glass with no primer, a classification of 0B was given showing an improvement in adhesion when PDA is present. Samples containing 1.29, 2.27, 2.50, 3.16 and 3.46 wt% Tween 80 were all awarded 5B classification meaning no film was removed. This shows an improvement caused by the PDA primer since only 2.27 and 2.50 wt% were awarded a 5B classification when no PDA was present. Furthermore, films at the highest concentrations were not damaged during cross hatching, unlike when no PDA was applied, also showing an advantage of the primer. These improvements are likely due to the increased availability of polar groups with which PEDOT:PSS/Tween 80 can interact, improving adhesion.[10,13,14,18-20]

Table 6-3: Scratch tape test classification PEDOT:PSS/Tween 80 films on varying substrates. Not applicable (N/A) results given where films were not coherently formed after casting or were significantly damaged during scoring meaning testing could not be completed. Each classification represents percentage removed as follows: 5B, 0%; 4B, <5%; 3B, 5 – 15%; 2B, 15 – 35%; 1B, 35 – 65%; 0B, >65%

Tween 80 Concentration (wt%)	**Substrate**					
	Glass		PP		PET	
	No PDA	PDA	No PDA	PDA	No PDA	PDA
0.00	0B	4B	N/A	0B	N/A	0B
0.37	0B	0B	N/A	0B	N/A	0B
0.47	0B	0B	0B	0B	N/A	0B
0.93	0B	3B	0B	0B	N/A	0B
1.29	4B	5B	0B	0B	N/A	0B
1.32	2B	4B	0B	0B	0B	0B
2.27	5B	5B	1B	2B	0B	4B
2.50	5B	5B	0B	2B	0B	3B
3.16	1B	5B	1B	2B	N/A	5B
3.46	0B	5B	2B	2B	N/A	5B

The results for PP show that classifications from 0.47 to 1.32 wt% do not vary, regardless of PDA application. However, the increase in film quality at 0.00 and 0.37 wt%, as well as awarding a 2B classification above 2.27 wt%, shows an improvement in adhesion caused by the PDA primer. In the case of PET, the use of PDA allowed all films to form coherently. A 0B classification was given for films up to 1.32 wt% surfactant, with most of the sample being removed. Above this concentration, higher classifications were awarded with 2.27 and 2.50 wt% showing higher classifications when PDA was present.

Despite the reduction in adhesion caused by Tween 80, the use of PDA as a primer shows improved adhesion across all substrates. This was primarily seen through the higher classification awarded at surfactant concentrations above 1.32 wt%. Furthermore, on PP and PET there is an improvement seen through the production of coherent films for all surfactant

concentrations. As before (section 6.2.3), the excess Tween 80 is likely interfering with the adhesion of the tape to the film. Despite this, situations where higher classifications were awarded for greater surfactant concentrations still provide evidence of the improved adhesion caused by PDA.

6.3.3.2 Force Pull Off Testing

Force pull-off testing was performed on drop cast PEDOT:PSS/Tween 80 films on glass, PET, and PP substrates with and without a PDA primer layer. The data seen in Figure 6-17 shows the effect of varying the Tween 80 concentration on adhesion to glass and glass/PDA substrates. It is clear that for pristine PEDOT:PSS, the application of PDA significantly increases adhesion on glass from 0.137 to 0.275 MPa, however, in the latter case the film was not removed so the final pull-off stress is likely higher (section 6.1.3). As was the case with no PDA primer (section 6.2.3), the addition of Tween 80 causes the pull-off stress to substantially decrease. Results drop to 0.052 MPa at a concentration of 0.37 wt% surfactant for glass/PDA which is very close to the 0.042 MPa achieved at the same concentration on glass. For a concentration of 0.93 wt%, the pull off stress required is greater for glass/PDA than when no primer is applied, however the film was not fully removed. Regardless, this is still evidence to suggest that PDA is improving adhesion at this concentration, although the degree to which this is occurring cannot be accurately commented on. For greater concentrations of Tween 80 the trends for glass and glass/PDA are very similar initially suggesting the primer is not improving adhesion. On the other hand, films were not being removed when PDA was present at concentrations of 0.93 wt% and above, which could be an indication that adhesion was better with the primer. However, further comment on the accuracy or extent of this cannot be made.

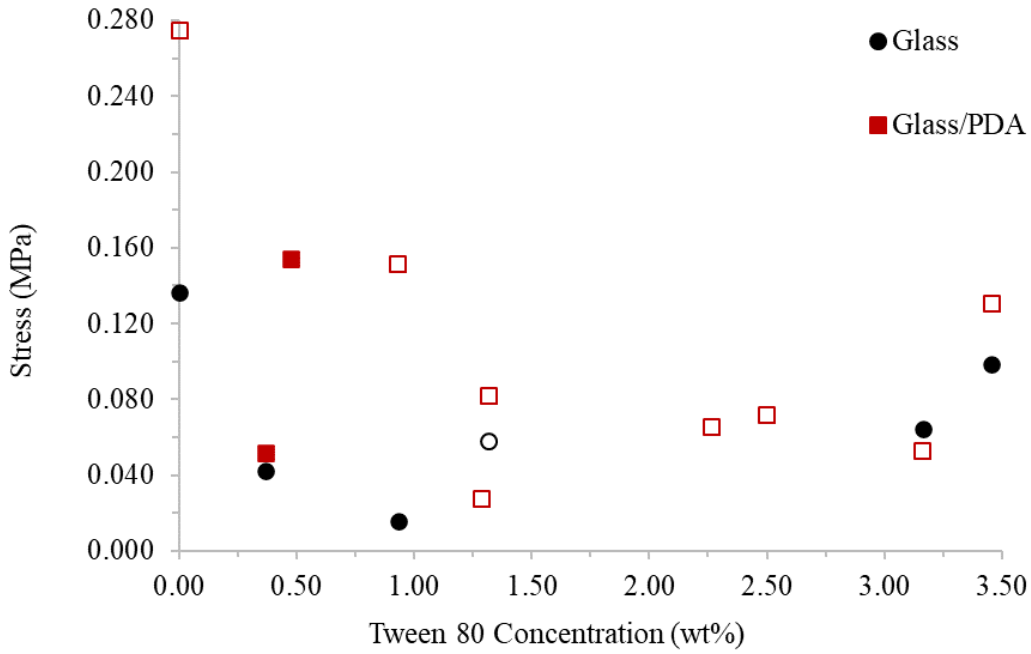

Figure 6-17: Pull-off stress (MPa) applied to remove PEDOT:PSS/Tween 80 films with differing surfactant concentrations (wt%) from a glass substrate without (black circles) and with (red squares) a PDA primer coating. Hollow shapes indicate films that were not removed

The application of a PDA primer to PP shows no noticeable improvement in force pull-off stress across all surfactant concentrations (Figure 6-18). Furthermore, PP/PDA adhesion shows consistently lower results (0.015 to 0.030 MPa) compared to glass and PET when PDA is present. It is also worth noting that all of the films were removed from the substrate, regardless of the potential for excess surfactant interfering with adhesive bond strength.

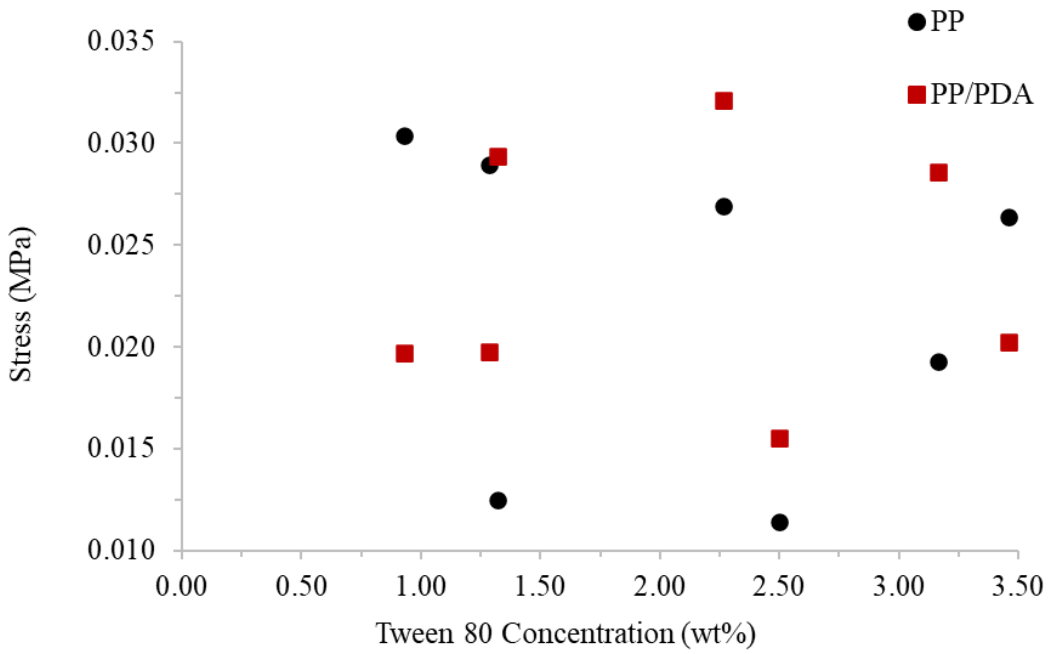

Figure 6-18: Pull-off stress (MPa) applied to remove PEDOT:PSS/Tween 80 films with differing surfactant concentrations (wt%) from a PP substrate without (black circles) and with (red squares) a PDA primer coating.

In the case of PET/PDA substrates (Figure 6-19), a coherent film was produced at 0.37 wt% which was not the case on PET alone. Furthermore, samples at 1.29 and 2.27 wt% gave results of 0.091 and 0.118 MPa, respectively, which are noticeably greater than any result attained on PET without PDA. These observations show evidence of improved adhesion when using PDA as a primer for PET. However, there is still a large amount of variation in the data, once again making trend identification difficult. Furthermore, a larger number of samples were not removed from the substrate (indicated by a hollow data point) meaning complete comparison of this data could not be made. However, given that no film removal is the worst case scenario, this still show that adhesion marginally improved with PDA application.

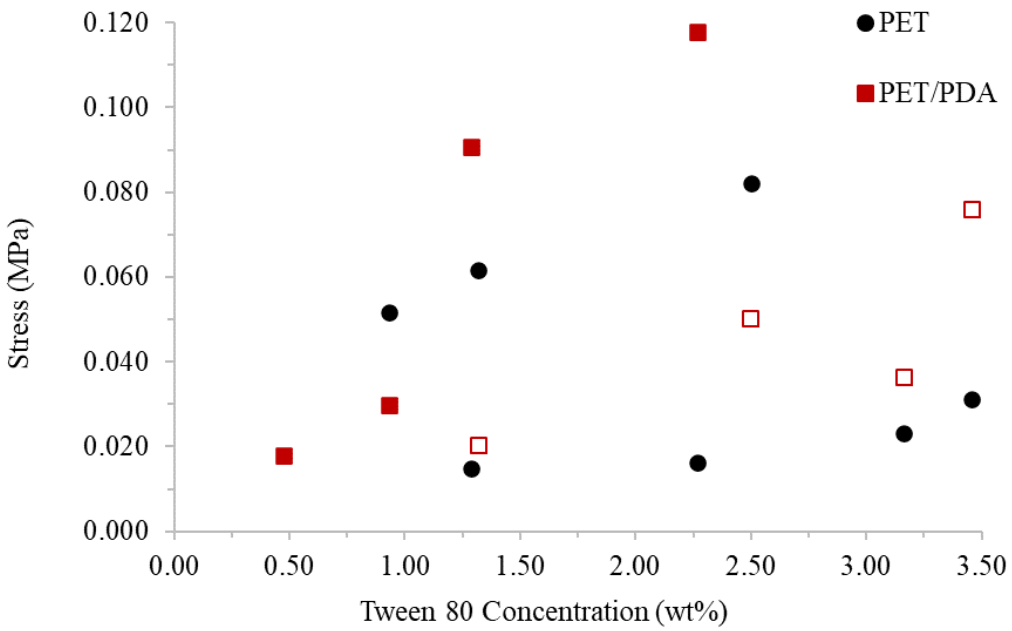

Figure 6-19: Pull-off stress (MPa) applied to remove PEDOT:PSS/Tween 80 films with differing surfactant concentrations (wt%) from a PET substrate without (black circles) and with (red squares) a PDA primer coating. Hollow shapes indicate films that were not removed

The adhesion data shows that, in general, the addition of PDA improves adhesion for all substrates when Tween 80 is present. The addition of PDA on glass only showed improvement in pull off data for low surfactant concentrations, but above 1.32 wt% there was no difference when the primer was present. However, the scratch test data showed adhesion increased for these higher concentrations. Although PDA did not appear to alter the pull off results on PP, improvement in film quality at low surfactant concentrations and the increase in awarded scratch test classification for concentrations above 2.27 wt% shows enhanced adhesion with the primer present. Similarly, PET showed the greatest adhesion when PDA was applied, and Tween 80 was added. In the pull off data this was particularly prominent for a concentration of 2.27 wt% which showed the greatest stress result for any PET/PDA sample. There was also evidence of this improvement with enhanced film quality, particularly dip cast samples

(section 6.2.2), and higher scratch test classifications achieved at higher surfactant concentrations.

6.4 Sheet Resistivity of PEDOT:PSS/Tween 80 Films on Varying Substrates

The sheet resistivities of PEDOT:PSS/Tween 80 dip cast films on varying substrates were analysed to determine if a PDA primer negatively impacted conductivity. During the annealing of the PEDOT:PSS/Tween 80 films on polymeric substrates, samples were found to either crack or lift off the substrate. Furthermore, it was suspected that annealing was melting or altering the structure of the polymer materials, therefore, the annealing stage was omitted. Instead, films were left at room temperature for 24 hours to allow drying and equilibration to take place. Figure 6-20 shows how removing the annealing phase impacts sheet resistivity (note, while annealed samples on a polymer substrate were produced, the film quality was of a low standard). The data initially shows that the sheet resistivity of annealed films on both glass and PP/PDA are very similar. On both substrates with no annealing, the sheet resistivity is higher at low surfactant concentrations since excess water removal and chain reorganisation will not occur (sections 4.3.2 & 3.3.1). However, above 1.50 wt% on glass the sheet resistivity is comparable regardless of annealing condition. For example, the film containing 3.46 wt% surfactant produced a resistivity of 61 $\Omega\square^{-1}$ when annealed, and 48 $\Omega\square^{-1}$ with no annealing. This could be related to the higher concentrations of Tween 80 displacing greater amounts of bound water from the samples. However, this is speculative and would require further investigation.

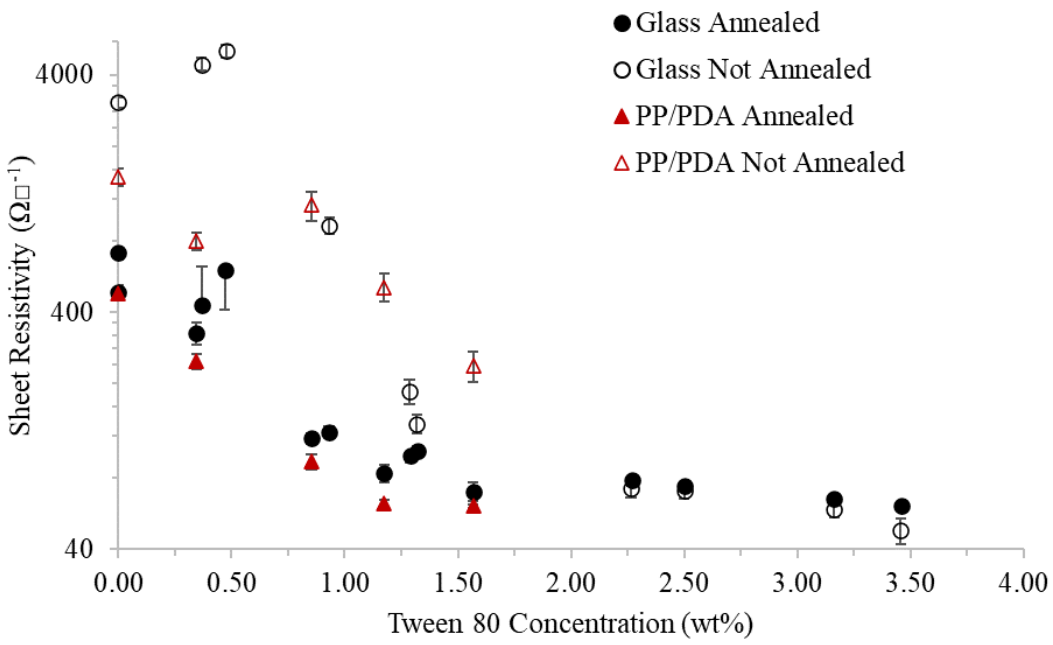

Figure 6-20: Sheet resistivity (Ω□-1) of PEDOT:PSS films with varying surfactant concentration (wt%) on glass (black circle) and PP/PDA (red triangle) substrates, with (solid shapes) and without (hollow shapes) annealing. Samples that were not annealed were left to dry and equilibrate for 24 hours at room temperature in atmospheric conditions. Error bars indicate ± 1 SD

Figure 6-21 shows the variation in sheet resistivity of PEDOT:PSS/Tween 80 samples for varying surfactant concentrations on a glass substrate with and without a PDA primer. As expected, the sheet resistivity for pristine PEDOT:PSS on glass is higher than observed in section 4.4.1 due to the lack of annealing, giving a measurement of 3065 $\Omega\square^{-1}$. However, the trend is comparable, with the addition of Tween 80 causing an initial increase in the sheet resistivity followed by a subsequent decrease. The sheet resistivity of PEDOT:PSS on glass/PDA is 3013 $\Omega\square^{-1}$, which is comparable to glass without PDA. Furthermore, the trend remains the same with an initial increase seen at low surfactant concentrations, a plateau above 1.32 wt% and the lowest resistivity of 47 $\Omega\square^{-1}$ being achieved at a concentration of 3.46 wt%. Across all concentrations of Tween 80 there is no observable difference in the sheet resistivity with the addition of the PDA primer.

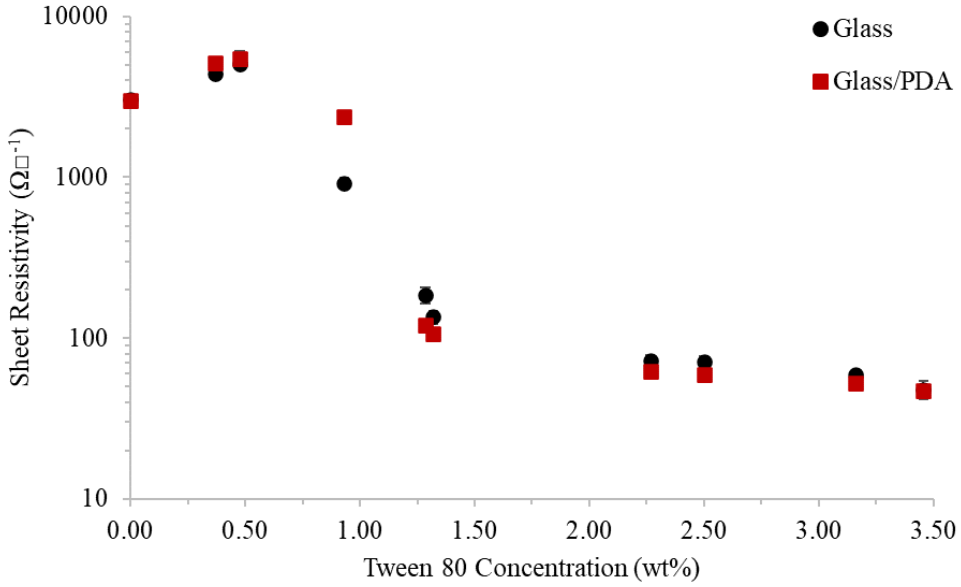

Figure 6-21: Sheet resistivity ($\Omega\square^{-1}$) of PEDOT:PSS films with varying surfactant concentration (wt%) on a glass substrate without (black circle) and with (red square) a PDA primer. Note, samples were not annealed but were left to dry and equilibrate for 24 hours at room temperature in atmospheric conditions. Error bars indicate ± 1 SD

The data for a PP substrate (Figure 6-22) shows a similar trend in sheet resistivity with increasing Tween 80 concentration reducing resistivity. Pristine PEDOT:PSS with no PDA gave a result of 2056 $\Omega\square^{-1}$, which is the lowest seen across any substrate without annealing. However, as seen previously in the annealed samples (section 4.4.1), this is within the error observed for pristine PEDOT/PSS. At low Tween 80 concentrations there was an initial increase in sheet resistivity with a maximum of 3216 $\Omega\square^{-1}$ being reached at 0.47 wt%, which was seen on glass (Figure 6-21) (section 4.4.1). Further surfactant addition then causes resistivity to decrease, with the lowest measurement of 47 $\Omega\square^{-1}$ being achieved at 3.46 wt%. Whilst there is a higher degree of variation, the addition of the PDA follows the same trend. At zero and low concentrations of Tween 80 the PDA primer resulted in marginally higher sheet resistivities. The lowest sheet resistivity at 3.46 wt% was also slightly higher than any other substrate at 57 $\Omega\square^{-1}$, however, this is still within normal variation for these samples so can be considered comparable.

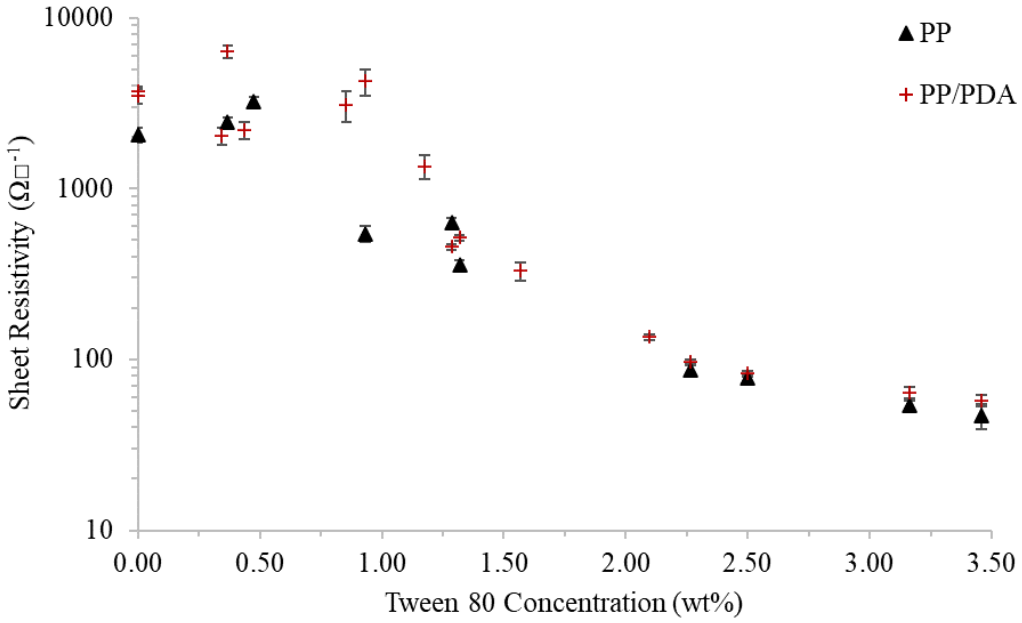

Figure 6-22: Sheet resistivity ($\Omega\square^{-1}$) of PEDOT:PSS films with varying surfactant concentration (wt%) on a PP substrate without (black triangle) and with (red plus) a PDA primer. Note, samples were not annealed but were left to dry and equilibrate for 24 hours at room temperature in atmospheric conditions. Error bars indicate ± 1 SD

Like the previous two substrates, PET without PDA (Figure 6-23) shows increasing surfactant concentration causes a decrease in sheet resistivity. The lowest resistivity measured at 3.46 wt% surfactant was 46 $\Omega\square^{-1}$ which is comparable to glass and PP at the same Tween 80 concentration. Due to the film not being coherently formed for pristine PEDOT:PSS no comparison could be made to when PDA was employed. Despite this, when Tween 80 was present no change in sheet resistivity was observed when PDA was applied.

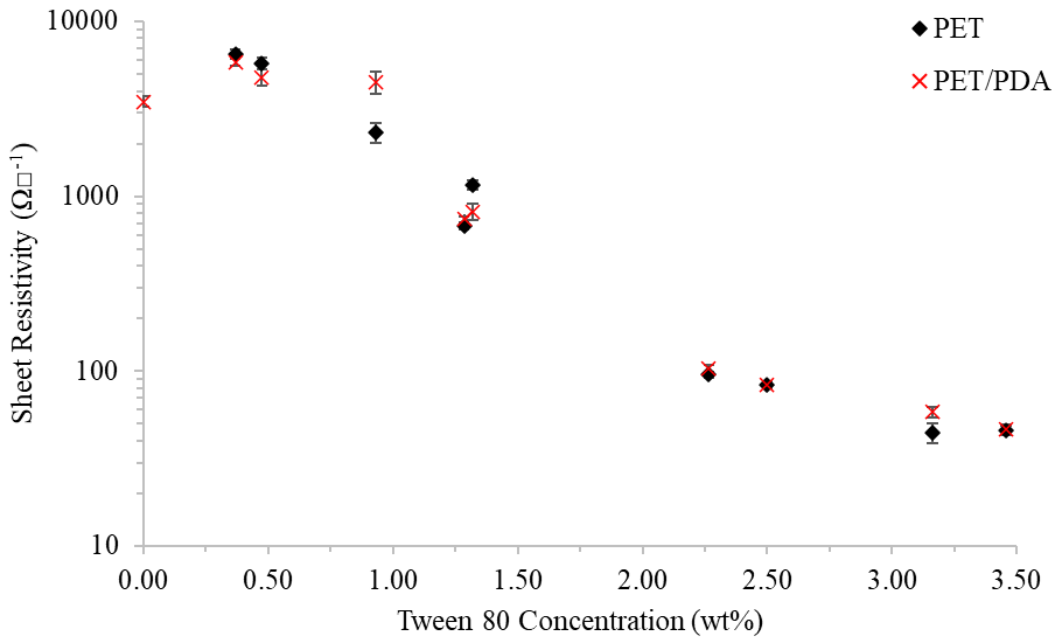

Figure 6-23: Sheet resistivity ($\Omega\square^{-1}$) of PEDOT:PSS films with varying surfactant concentration (wt%) on a PET substrate without (black diamond) and with (red cross) a PDA primer. Note, samples were not annealed but were left to dry and equilibrate for 24 hours at room temperature in atmospheric conditions. Error bars indicate ± 1 SD

Figure 6-24 shows that the overall trend across the three substrates with and without PDA is very similar for increasing Tween 80 concentration. The most noticeable difference is that for polymeric substrates, resistivity does not plateau until higher surfactant concentrations (above 2 wt%). It is unclear why the resistivity falls quicker on a glass substrate, but some hypotheses can be made. Firstly, wettability is worse on polymeric substrates due to their hydrophobic nature and given water will bond primarily to excess PSS this could reside more at the film surface. Therefore, a greater amount of Tween 80 would be needed to sufficiently improve wettability and prevent this movement of PSS. Secondly, the films on PP and PET are likely to be thinner due to reduced PEDOT:PSS deposition caused by poor wettability. A thinner film has been shown to result in increased sheet resistivity.[1,39,47-49] Therefore, Tween 80 could be improving wettability enough to equalise film thickness for all substrates, resulting in comparable resistivities at higher concentrations.

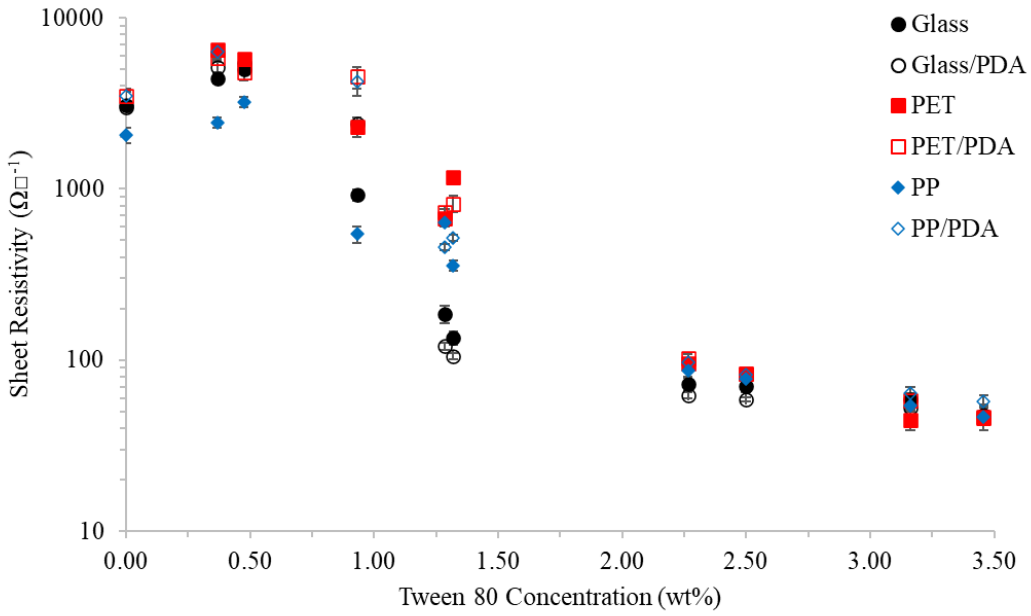

Figure 6-24: Sheet resistivity (Ω□-1) of PEDOT:PSS films with varying surfactant concentration (wt%) on glass (circle), PET (square) and PP (diamond) substrate without (hollow) and with (solid) a PDA primer layer. Note, samples were not annealed but were left to dry and equilibrate for 24 hours at room temperature in atmospheric conditions. Error bars indicate ± 1 SD

In general, the use of a PDA primer does not alter the sheet resistivity of PEDOT:PSS/Tween 80 films on any of the substrates used. While the results for PP/PDA where marginally higher at low surfactant concentrations, they were still comparable to PP.

6.5 Conclusion

This chapter assesses the wettability, adhesion, and sheet resistivity of PEDOT:PSS/Tween 80 films on glass, PET, and PP substrates, with and without a PDA primer layer. The initial focus on pristine PEDOT:PSS showed that the contact angle on glass was much lower than that of PET or PP, the latter showing the most inferior wettability of the three. This was due to the surface energy of glass being more closely matched to the surface tension of PEDOT:PSS solution, resulting in better wettability. Results then indicated that the presence of PDA increased the contact angle for glass and PET but decreased it for PP. The increase on glass was

attributed to the lower surface energy of PDA causing a greater discrepancy to PEDOT:PSS solution. On the other hand, the differences on the polymer substrates were attributed to the different orientations of the PDA molecule when adhering to the substrate. The film quality of pristine PEDOT:PSS on polymeric substrates was also shown to be poor for both dip and drop cast samples due to the poor wettability. This was dramatically improved for dip cast samples with the presence of PDA. However, cracking remained an issue on drop cast samples despite the PDA primer layer. Adhesion on PP and PET was also poor, but this could only be established due to incoherent or cracked films being formed. The PDA primer improved film quality of dip cast samples showing adhesion was enhanced, however, cracking was still an issue on drop cast samples. Furthermore, the extent of adhesion increase could not be measured. On the other hand, PDA on glass significant improved adhesion for pristine PEDOT:PSS films.

The effect of Tween 80 varied depending on the substrate. On glass, the wettability initially increased at low concentrations but subsequently decreased again above 1 wt%. This was likely due to the surfactant initially interacting with the excess PSS, reducing the PSS interaction with water. Once the PSS is saturated, the Tween 80 interacts with the water reducing the contact angle. In the case of PP and PET, the increase in Tween 80 concentration led to a continuous decrease in contact angle which was expected based on literature souces.[7,27,29,38-40] However, the improvement in wettability did not initially lead to an improvement in film quality on polymeric substrates. Quality on dip cast PP was only improved for concentrations above 0.47 wt% whilst coherent films were only produced for concentrations of 1.29 to 2.50 wt% on PET. Results for drop cast films were also poor at lower surfactant concentrations, with films containing 0.93 wt% and below showing signs of cracking. PEDOT:PSS adhesion to glass was negatively affected by the addition of Tween 80. However, the improvement in film quality was evidence of adhesion improvement on both polymer substrates, although pull off stress

remained low on PP regardless of surfactant concentration. There was some evidence of an upward trend on PET with increasing Tween 80 addition, however, data scatter made this hard to identify with certainty. There were also issues with leaching of Tween 80 from the films in concentrations of 1.29 wt% and above. This led to films being damaged when cross hatched in scratch testing and acted as a barrier to sufficient adhesion of the tape or adhesive in these testing methods.

When PDA was applied as a primer to these substrates, the trends in contact angle for increasing surfactant concentration did not vary greatly. This was most obvious for PP and PET. Whilst the trends for glass and glass/PDA were similar, there was an overall increase in the contact angles at each Tween 80 concentration. Film quality was improved across all dip cast samples when PDA was present on the polymer substrates. This was attributed to the PDA allowing preferential deposition of the PEDOT:PSS due to the increased availability of polar functional groups. However, cracking was still an issue on drop cast samples at lower Tween 80 concentrations due to shrinkage on setting. The PDA primer was then shown to improve adhesion across all substrates for all surfactant concentrations. An increase in awarded scratch test classification was seen for all substrates at concentrations above 1.32 wt% when PDA was applied. For glass, the pull of data only showed improvement at lower surfactant concentrations whilst PET showed a general overall improvement across all Tween 80 concentrations. The same increase in pull off data was not seen for PP samples. However, scratch test data and film quality improvement implied better adhesion on PP. Similar issues associated with excess Tween 80 were still present in these samples which may have interfered with the results.

Finally, sheet resistivity was shown to be higher for non-annealed samples, compared to annealed films, on glass and PP at surfactant concentrations below 2 wt%. Above this, there was no difference between annealed and unannealed samples on glass. It was established that

there was a difference in the resistivity trends between differing substrates. Whilst at Tween 80 concentrations above 2.27 wt% the resistivity is relatively similar, polymeric materials showed a more gradual decline in the resistivity to this point than glass. It was hypothesised that the hydrophobic nature of the polymer substrates and the affinity of water to PSS causes this insulating component to reside primarily at the surface. It was also suggested thinner films might be created on PP and PET due to issues with wettability which were mitigated at higher surfactant concentrations. For all substrates, the PDA coated material showed similar resistivity trends to when no PDA was present.

Overall, the use of PDA was shown to be effective in improving adhesion and the quality of films using dip and drop cast methods on glass, PET, and PP for PEDOT:PSS/Tween 80 samples. This was seen to be most effective for pristine PEDOT:PSS, however, it was established that the adhesion improvement on PP and PET did not elevate levels to that of glass. While Tween 80 did improve wettability and film quality, the improvement achieved by surfactant addition alone was not as substantial as PDA. Finally, PDA was shown to not interfere with the sheet resistivity of PEDOT:PSS/Tween 80 films, making it a suitable primer from this point of view.

6.6 References

1. Martin, B. D., Nikolov, N., Pollack, S. K., Saprigin, A., Shashidhar, R., Zhang, F. & Heiney, P. A. 2004. Hydroxylated secondary dopants for surface resistance enhancement in transparent poly(3,4- ethylenedioxythiophene)– poly(styrenesulfonate) thin films. *Synthetic Metals,* 142**,** 187-193.
2. Crawford, G. P. 2005. *Flexible flat panel displays,* Chichester, John Wiley & Sons, Ltd.
3. Lee, J.-H., Liu, D. N. & Wu, S.-T. 2008. *Introduction to flat panel displays,* Chichester, Wiley.
4. Wen, Y. & Xu, J. 2017. Scientific Importance of Water-Processable PEDOT–PSS and Preparation, Challenge and New Application in Sensors of Its Film Electrode: A Review. 55**,** 1121-1150.
5. Søndergaard, R., Hösel, M., Angmo, D., Larsen-Olsen, T. T. & Krebs, F. C. 2012. Roll-to-roll fabrication of polymer solar cells. *Materials Today,* 15**,** 36-49.
6. Kirchmeyer, S., Reuter, K. & Simpson, J. 2007. Poly(3,4-ethylene dioxythiophene) scientific importance, remarkable properties, and applications. *In:* Skotheim, T. & Reynolds, J. (eds.) *Handbook of conducting polymers.* 3rd ed. Boca Raton, London and New York: CRC press.
7. Oh, J. Y., Shin, M., Lee, J. B., Ahn, J. H., Baik, H. K. & Jeong, U. 2014. Effect of PEDOT nanofibril networks on the conductivity, flexibility, and coatability of PEDOT:PSS films. *ACS Applied Materials and Interfaces,* 6**,** 6954-6961.
8. Kishi, N., Kondo, Y., Kunieda, H., Hibi, S. & Sawada, Y. 2018. Enhancement of thermoelectric properties of PEDOT:PSS thin films by addition of anionic surfactants. *Journal of Materials Science: Materials in Electronics,* 29**,** 4030-4034.
9. Mustonen, T., Kordás, K., Saukko, S., Tóth, G., Penttilä, J. S., Helistö, P., Seppä, H. & Jantunen, H. 2007. Inkjet printing of transparent and conductive patterns of single-walled carbon nanotubes and PEDOT-PSS composites. *Physica Status Solidi (b),* 244**,** 4336-4340.
10. Awaja, F., Gilbert, M., Kelly, G., Fox, B. & Pigram, P. J. 2009. Adhesion of polymers. *Progress in polymer science,* 34**,** 948-968.
11. Koidis, C., Logothetidis, S., Kapnopoulos, C., Karagiannidis, P. G., Laskarakis, A. & Hastas, N. A. 2011. Substrate treatment and drying conditions effect on the properties of roll-to-roll gravure printed PEDOT:PSS thin films. *Materials Science & Engineering B,* 176**,** 1556-1561.
12. Leclercq, B., Sotton, M., Baszkin, A. & Ter-Minassian-Saraga, L. 1977. Surface modification of corona treated poly(ethylene terephthalate) film: adsorption and wettability studies. *Polymer,* 18**,** 675-680.
13. Lee, H., Dellatore, S. M., Miller, W. M. & Messersmith, P. B. 2007. Mussel-inspired surface chemistry for multifunctional coatings. *Science (New York, N.Y.),* 318**,** 426-430.
14. Della Vecchia, N. F., Avolio, R., Alfè, M., Errico, M. E., Napolitano, A. & d'Ischia, M. 2013. Building-Block Diversity in Polydopamine Underpins a Multifunctional Eumelanin-Type Platform Tunable Through a Quinone Control Point. *Advanced Functional Materials,* 23**,** 1331-1340.
15. Jia, Z., Li, H., Zhao, Y., Frazer, L., Qian, B., Borguet, E., Ren, F. & Dikin, D. A. 2017. Electrical and mechanical properties of poly(dopamine)-modified copper/reduced graphene oxide composites. *Journal of Materials Science,* 52**,** 11620-11629.
16. Ou, J., Pan, B., Chen, Y., Xie, C., Xue, M., Wang, F. & Li, W. 2015. Substrate-independent sequential deposition process to obtain the lotus effect based on mussel-inspired polydopamine. *Applied surface science,* 327**,** 149-153.

17. Chau, T. T., Bruckard, W. J., Koh, P. T. L. & Nguyen, A. V. 2009. A review of factors that affect contact angle and implications for flotation practice. *Advances in Colloid and Interface Science,* 150**,** 106-115.
18. Mittal, K. L. 1977. The role of the interface in adhesion phenomena. *Polymer Engineering and Science,* 17**,** 467-473.
19. Callister, W. D. 2000. Materials science and engineering: an introduction. 5th ed. New York; Chichester: Wiley.
20. Tyo, A., Welch, S., Hennenfent, M., Fooroshani, P. K., Lee, B. P. & Rajachar, R. 2019. Development and Characterization of an Antimicrobial Polydopamine Coating for Conservation of Humpback Whales. *Frontiers in Chemistry,* 7**,** 618-618.
21. Della Vecchia, N. F., Luchini, A., Napolitano, A., D'Errico, G., Vitiello, G., Szekely, N., d'Ischia, M. & Paduano, L. 2014. Tris Buffer Modulates Polydopamine Growth, Aggregation, and Paramagnetic Properties. *Langmuir,* 30**,** 9811-9818.
22. Gangopadhyay, R., Das, B. & Molla, M. R. 2014. How does PEDOT combine with PSS? Insights from structural studies. *RSC Advances,* 4**,** 43912-43920.
23. Lubianez, R. P., Kirchmeyer, S. & Gaiser, D. 2008. Advances in PEDOT: PSS conductive polymer dispersions.
24. Lang, U., Müller, E., Naujoks, N. & Dual, J. 2009. Microscopical Investigations of PEDOT:PSS Thin Films. *Advanced Functional Materials,* 19**,** 1215-1220.
25. Rhee, S. K. 1977. Surface energies of silicate glasses calculated from their wettability data. *Journal of materials science,* 12**,** 823-824.
26. Kinloch, A. J. 1987. *Adhesion and adhesives : science and technology,* London, Chapman and Hall.
27. Hoath, S. D., Hsiao, W.-K., Martin, G. D., Jung, S., Butler, S. A., Morrison, N. F., Harlen, O. G., Yang, L. S., Bain, C. D. & Hutchings, I. M. 2015. Oscillations of aqueous PEDOT:PSS fluid droplets and the properties of complex fluids in drop-on-demand inkjet printing. *Journal of Non-Newtonian Fluid Mechanics,* 223**,** 28-36.
28. Hoath, S. D., Jung, S., Hsiao, W.-K. & Hutchings, I. M. 2012. How PEDOT:PSS solutions produce satellite- free inkjets. *Organic Electronics,* 13**,** 3259-3262.
29. Kommeren, S., Coenen, M. J. J., Eggenhuisen, T. M., Slaats, T. W. L., Gorter, H. & Groen, P. 2018. Combining solvents and surfactants for inkjet printing PEDOT:PSS on P3HT/PCBM in organic solar cells. *Organic Electronics,* 61**,** 282-288.
30. Claussen, W. F. 1967. Surface Tension and Surface Structure of Water. *Science,* 156**,** 1226-1227.
31. Khattab, I. S., Bandarkar, F., Fakhree, M. A. A. & Jouyban, A. 2012. Density, viscosity, and surface tension of water+ethanol mixtures from 293 to 323K. *The Korean Journal of Chemical Engineering,* 29**,** 812-817.
32. Mallinson, D., Mullen, A. & Lamprou, D. 2018. Probing polydopamine adhesion to protein and polymer films: microscopic and spectroscopic evaluation. *Full Set - Includes `Journal of Materials Science Letters',* 53**,** 3198-3209.
33. Jia, L., Han, F., Wang, H., Zhu, C., Guo, Q., Li, J., Zhao, Z., Zhang, Q., Zhu, X. & Li, B. 2019. Polydopamine-assisted surface modification for orthopaedic implants. *Journal of Orthopaedic Translation,* 17**,** 82-95.
34. Kwon, I. S. & Bettinger, C. J. 2018. Polydopamine nanostructures as biomaterials for medical applications. *J. Mater. Chem. B,* 6**,** 6895-6903.
35. Woodall, J., Agúndez, M., Markwick-Kemper, A. J. & Millar, T. J. 2007. The UMIST database for astrochemistry 2006. *Astronomy and astrophysics (Berlin),* 466**,** 1197-1204.
36. McMurry, J. 2000. *Organic Chemistry,* Pacific Grove, CA, Brooks/Cole.

37. Henkel 2020. Technical Data Sheet - Loctite Super Glue Power Flex Gel.
38. Cho, C.-K., Hwang, W.-J., Eun, K., Choa, S.-H., Na, S.-I. & Kim, H.-K. 2011. Mechanical flexibility of transparent PEDOT:PSS electrodes prepared by gravure printing for flexible organic solar cells. *Solar Energy Materials & Solar Cells,* 95**,** 3269-3276.
39. Yoshioka, Y. & Jabbour, G. 2006. Desktop inkjet printer as a tool to print conducting polymers. *Synth. Met.,* 156**,** 779-783.
40. Eom, S. H., Senthilarasu, S., Uthirakumar, P., Yoon, S. C., Lim, J., Lee, C., Lim, H. S., Lee, J. & Lee, S.-H. 2009. Polymer solar cells based on inkjet-printed PEDOT:PSS layer. *Organic Electronics,* 10**,** 536-542.
41. Yoon, S. S. & Khang, D. 2016. Roles of Nonionic Surfactant Additives in PEDOT:PSS Thin Films. *J. Phys. Chem. C,* 120**,** 29525-29532.
42. Romyen, N., Thongyai, S., Praserthdam, P. & Wacharawichanant, S. 2017. Effect of Surfactant Addition During Polymerization on Properties of PEDOT:PSS for Electronic Applications. *Journal of Electronic Materials,* 46**,** 6709-6716.
43. Mengistie, D. A., Wang, P.-c. & Chu, C.-w. 2013. Effect of molecular weight of additives on the conductivity of PEDOT:PSS and efficiency for ITO-free organic solar cells. *Journal of Materials Chemistry A,* 1**,** 9907-9915.
44. Kim, S., Cho, S., Lee, S. J., Lee, G., Kong, M., Moon, S., Myoung, J.-M. & Jeong, U. 2017. Boosting up the electrical performance of low-grade PEDOT:PSS by optimizing non-ionic surfactants. *Nanoscale,* 9**,** 16079-16085.
45. Ouyang, J., Xu, Q., Chu, C.-W., Yang, Y., Li, G. & Shinar, J. 2004. On the mechanism of conductivity enhancement in poly(3,4- ethylenedioxythiophene): poly(styrene sulfonate) film through solvent treatment. *Polymer,* 45**,** 8443-8450.
46. Zotti, G., Zecchin, S., Schiavon, G., Louwet, F., Groenendaal, L., Crispin, X., Osikowicz, W., Salaneck, W. & Fahlman, M. 2003. Electrochemical and XPS studies toward the role of monomeric and polymeric sulfonate counterions in the synthesis, composition, and properties of poly(3,4- ethylenedioxythiophene). *Macromolecules,* 36**,** 3337-3344.
47. Alemu, D., Wei, H.-y., Ho, K.-c. & Chu, C.-w. 2012. Highly conductive PEDOT:PSS electrode by simple film treatment with methanol for ITO-free polymer solar cells. *Energy Environ. Sci.,* 5**,** 9662-9671.
48. Kim, Y. H., Sachse, C., Machala, M. L., May, C., Müller-Meskamp, L. & Leo, K. 2011. Highly Conductive PEDOT:PSS Electrode with Optimized Solvent and Thermal Post-Treatment for ITO-Free Organic Solar Cells. *Advanced Functional Materials,* 21**,** 1076-1081.
49. Mengistie, D. A., Ibrahem, M. A., Wang, P.-C. & Chu, C.-W. 2014. Highly conductive PEDOT:PSS treated with formic acid for ITO-free polymer solar cells. *ACS applied materials & interfaces,* 6**,** 2292-2299.

Chapter 7: Conclusions

The overall aims of this project were to optimise processing parameters, enhance conductivity and improve polymeric substrate adhesion of PEDOT:PSS. There was also focus on the thermal and solution properties of the system, as well as an intention to establish the mechanisms causing conductivity enhancement for each method implemented. Whilst most of these targets were met, some questions remain, which have the potential to be explored further in the future (Chapter 8). This section contains a summary of the main conclusions that can be draw from each chapter throughout this work.

Chapter 3 focused on pristine PEDOT:PSS with regards to thermal properties, moisture kinetics and optimal processing conditions. It was found that multiple heating runs did not identify any major thermal transitions, however, suggestion of a T_g caused by the softening of the PSS phase was identified at 140 °C. PEDOT:PSS atmospheric moisture uptake after annealing was shown to be rapid and resulted in a significant mass increase. However, the impact of this on sheet resistivity was minimal, removing the need for close environmental control or sample encapsulation. Finally, a maximum annealing temperature of 220 °C was established, above which degradation would become problematic. However, heating to 140 °C for 40 minutes was sufficient to fully anneal pristine PEDOT:PSS, removing the need for higher temperatures and greater times.

The aim in Chapter 4 was to assess the effect of the non-ionic surfactant Tween 80 on the thermal, film and solution properties of PEDOT:PSS. Major degradation was shown to occur at a substantially lower temperature when Tween 80 was present (160 °C) compared to pristine PEDOT:PSS (250 °C). It was hypothesised that this could be linked to the formation of acids as the surfactant breaks down. Despite this, annealing could still take place at 140 °C, but a time of 60 minutes was needed to achieve the lowest resistivity. The sheet resistivity, and

conductivity, of PEDOT:PSS were significantly improved with the addition of Tween 80, showing its potential as a conductivity enhancing agent. Improvement was most prominent up to 1 wt% surfactant in solution, above which only marginal reductions in sheet and bulk resistivity were seen. This was the case for both dip and drop cast samples. AFM and XRD analysis showed that Tween 80 led to the separation of PEDOT and PSS, as well as allowing for chain alignment to occur. This meant superior conducting pathways were formed and it was suspected a benzoid to quinoid structural change occurred in PEDOT, although this was not detected by methods used in this study. However, excess surfactant resulted in negative effects on film quality. Lastly, Tween 80 caused an increase in viscosity but a decrease in surface tension up to 1 wt%. Whilst the rise in viscosity may be considered detrimental, the reduction in surface tension would lead to greater wettability and film quality on polymer substrates.

The use of three alternative conductivity enhancement methods were assessed in Chapter 5, namely: multiple dip casting, MEK solvent addition, and solvent washing. Multiple dip casting dramatically improved the sheet resistivity of pristine PEDOT:PSS, causing consecutively lower measurements for each layer added, following previous literature findings. This was attributed to multiple possible factors including PSS removal from and additional annealing of subsurface layers, and the hypothesis that PEDOT:PSS solution will interact differently with a layer of PEDOT:PSS compared to glass. The multiple dip method resulted in the lowest sheet resistivity being recorded within this work when 5 layers were applied. Furthermore, the addition of Tween 80 limited the effectiveness of this method. However, it could not be determined whether the resistivity decrease would translate to an improved conductivity due to limitations with using a 4-point probe measurement. Furthermore, no evidence could be found that structural changes had occurred due to the application of multiple layers. It was also shown

to have significant drawbacks, including reduced film quality and unsuitability in bulk manufacturing processes.

The addition of MEK to PEDOT:PSS caused sheet resistivity to increase rather than decrease. It was also shown that PEDOT:PSS/Tween 80/MEK films produced a higher resistivity than PEDOT:PSS/Tween 80 films with no MEK. This showed that MEK was not a suitable additive for conductivity enhancement. Finally, solvent washing with methanol, ethanol and MEK all caused a decrease in sheet resistivity of pristine PEDOT:PSS films, with methanol causing the largest decrease and MEK producing the smallest. Structural analysis did not show any signs of chain alignment or a benzoid to quinoid shift meaning the improvement in sheet resistivity was due to PSS removal. This was confirmed by FTIR analysis of each solvent wash showing evidence of PSS present after washing. The addition of Tween 80 caused the effectiveness of washing to diminish and it was theorised this was due to the surfactant acting as a barrier to PSS removal. XRD analysis showed no chain alignment after washing PEDOT:PSS/Tween 80 films, suggesting that the long range order seen with Tween 80 addition occurs in the excess PSS chains.

To finish, Chapter 6 evaluated the use of PDA as a primer layer on polymeric substrates to improve PEDOT:PSS wettability and adhesion. It was initially shown that pristine PEDOT:PSS had low contact angle measurements on glass, with greater contact angles on PET and PP indicating poorer wetting on polymer substrates. Coating these materials in a PDA primer led to improved wettability on PP but reduced wetting on glass and PET. It was thought that the PDA molecule orientates differently depending on the substrate, leading to this variety in results. Film quality was also improved on the polymer substrates for both dip and drop cast films, however, cracking remained an issue on drop cast films regardless of PDA presence. PDA significantly increase in the adhesion of PEDOT:PSS on glass when assessed via scratch

tape and force pull off testing. The same could not be quantified for the polymer substrates due to issues of film quality. Tween 80 was shown to continuously improve wettability on PET and PP (without PDA) at greater concentrations. However, film quality only improved above 0.47 wt% for dip cast films, and between 1.29 to 2.50 wt% for drop cast samples. Furthermore, the addition of the surfactant caused a decrease in adhesion of PEDOT:PSS to glass. This was likely due to a reduction in available functional groups within PEDOT:PSS when Tween 80 was added. Therefore, there was a decrease in the electrostatic interactions between the PEDOT:PSS and glass. Alternatively, adhesion was deemed to have improved on polymeric substrates with surfactant addition, mainly due to the successful formation of coherent films. More substantial conclusions could not be drawn from the adhesion data due to scatter in the results and issues relating to the surfactant leaching out of the films interfering with the testing methods.

The application of a PDA primer did not significantly alter the contact angle for increasing surfactant concentrations on PET and PP. However, an overall increase in contact angle was seen across all surfactant concentrations when PDA was applied to glass. There was also an improvement in film quality for all Tween 80 concentrations with PDA present, although cracking was still an issue at low concentrations on drop cast samples. The benefits of adhesion on glass caused by priming with PDA were reduced when Tween 80 was added to PEDOT:PSS. However, PDA still showed comparatively greater adhesion at each Tween 80 concentration across all substrates. Finally, the presence of PDA did not negatively affect sheet resistivity. The trend of decreasing resistivity for increasing surfactant concentration was also seen across all substrates. However, a difference between glass and polymeric substrates was apparent, with a higher surfactant concentration of 2.27 wt% (compared to 1 wt% on glass) being needed before a plateau was achieved in the resistivity results.

Overall, the lowest PEDOT:PSS sheet resistivity in this study was obtained by applying 5 layers of pristine PEDOT:PSS to a glass substrate using the multiple dip casing method (16.75 $\Omega\square^{-1}$). However, the effect on conductivity could not be measured and it was established that this would be an impractical technique to implement on a bulk manufacturing scale. The greatest conductivity achieved in this study was obtained by washing pristine PEDOT:PSS with methanol (68.4 Scm^{-1}). Again, this is not a feasible approach to implement for bulk manufacturing given the volatility and the negative environmental impact of this solvent. Therefore, Tween 80 was shown to be a good, non-hazardous alternative to enhance the conductivity of PEDOT:PSS, with a solution addition of 1.40 wt% resulting in a measurement of 26.8 Scm^{-1}. This surfactant was also shown to have beneficial effects on solution properties resulting in superior wettability, film quality and adhesion on polymer substrates, making this method more suitable for processes such as R2R and IJP. Additionally, priming with PDA showed potential as a method to enhance PEDOT:PSS affinity to polymer substrates, with film quality and adhesion improving when implemented.

Chapter 8: Future Works

This chapter contains a description of possible future work that could follow on from the work presented in this document. This is grouped by the relevant results and discussion chapters, with a final paragraph on potential work further outside the scope of this project.

Firstly, the water kinetics of PEDOT:PSS could be better understood when considering films rather than a sample in a DSC pan. Even though this was evaluated in this study, tighter control of film sample environment and moisture removal without heat would provide a clearer understanding of moisture uptake. This could be achieved through the use of an environmental chamber at varying humidities and would also provide an opportunity to more closely assess how this impacts sheet resistivity/conductivity. It was also thought that heat was required to fully remove bound water from PEDOT:PSS. This could be confirmed through further use of the vacuum oven at a greater variety of temperatures and hold times. There is also scope for further optimisation of annealing conditions given this was only assessed in 10 °C and 10 minute intervals.

Although it was determined that the addition of Tween 80 caused an earlier onset of degradation in PEDOT:PSS, the reasoning for this was unclear and there is opportunity for further investigation. For example, TGA experiments could have been performed under inert argon to establish if degradation was oxidative. Additionally, FTIR could be performed during degradation or XPS could be used to provide alternative insight into the degradation mechanisms. It was also discussed that there was a saturation level for surfactant addition around 1 wt% which could be studied in more depth. This could be achieved using optical analysis to better identify when excess Tween 80 appears on the film surface. There is also availability for FTIR, Raman and XRD to be used during surface scanning, meaning areas of Tween 80, PEDOT and PSS could more accurately be identified. In this work, the mechanisms

behind the improvement in conductivity were analysed with XRD, AFM and Raman techniques. However, there is scope for deeper analysis using all of these methods. Firstly, only select surfactant concentrations were assessed using these techniques. Analysing a greater range of Tween 80 concentrations would more accurately identify the concentration at which structural changes occur. Whilst higher resolution AFM could not be done in this study, it has been previously used to show the appearance of 'nano-fibrils' with certain additives. Similarly, Raman was limited and may be used to identify a benzoid to quinoid shift within the material if greater analysis through curve deconvolution is performed. Samples could also be assessed with XPS or nuclear magnetic resonance spectroscopy to provide additional insight. The properties of PEDOT:PSS/Tween 80 solution could also be analysed in greater detail through the use of alternative methods to provide comparison to results seen in this study. For example, a mobile surface analyser could be used for surface energy and oscillating drop testing could measure viscosity.

Multiple dip casting was shown to improve pristine PEDOT:PSS sheet resistivity, but the cause for this was unknown. A more detailed analysis of this method could take place to identify why these improvements were seen. This could be performed though compositional surface analysis, with AFM, Raman, FTIR and energy dispersive x-ray spectroscopy (EDS), of each layer applied. Cross-sectional analysis of the layers via SEM would also provide understanding of how adjacent layers were interacting. These techniques may also be used to assess why the addition of Tween 80 hinders resistivity decrease for multiple dip samples. Optical and SEM could also be implemented to examine the film quality more closely. Solvent washing is a well-established method of improving PEDOT:PSS conductivity but the combination of Tween 80 addition and methanol washing did not appear to have the same compounding improvement as previously seen with Triton X-100 addition. Alternative solvents, such as

concentrated acids (e.g., H_2SO_4, TFMS) could be tested to see whether the desired compounding improvement can be achieved when Tween 80 is added. Washing with water has also rarely been done so the effectiveness of this could be tested. Surface scanning using Raman, FTIR, AFM and EDS could also be performed on PEDOT:PSS/Tween 80 washed samples to analyse whether the separated PSS regions are removed from the film.

There is a large scope for further assessment of the use of PDA as a primer layer for PEDOT:PSS adhesion improvement. This could initially be through testing a greater range of substrate materials to see where it is most effective. The polymerisation route of PDA could also be altered, for example with different buffers, to examine if that has an effect on wettability/adhesion. Additionally, measurements of contact angle and adhesion could be done though more accurate methods that remove human error. In the case of contact angle this could be using an automated measurement system, and for adhesion the use of standardised aluminium stubs and adhesion tester.

There are other areas that could be explored that are more loosely related to the scope of this project. For example, Tween 80 was the main additive used throughout, however, Tween 20, 40 and 60 could be tested as alternatives since they all have varying molecular weights and structures. Furthermore, the 4-point probe was used as the main technique to measure resistivity, and conductivity was calculated from this measurement. However, there are alternative methods to assess electrical properties, such as current – voltage characteristics, 2-point probe measurements, and dielectric analysis. Finally, the two film casting methods used in this study were representative of bulk manufacturing ink deposition. Considering an optimum Tween 80 concentration has now been identified, the suitability of this composition could now be tested in bulk processes such as IJP or gravure printing.